THE

PHYSICAL REVIEW

A JOURNAL OF EXPERIMENTAL AND THEORETICAL PHYSICS

PUBLISHED BY

THE

AMERICAN PHYSICAL SOCIETY

THE AMERICAN PHYSICAL SOCIETY

OFFICERS OF THE SOCIETY

[illegible]	Ernest G. Gale	University of Chicago, Chicago, Ill.
[illegible]	W. F. G. Swann	Bartol Research Foundation, Philadelphia, Pa.
[illegible]	W. L. Severinghaus	Columbia University, New York City
[illegible]	G. B. Pegram	Columbia University, New York City
[illegible]	John T. Tate	University of Minnesota, Minneapolis, Minn.
[illegible] Secretary for [illegible] Coast:	L. B. Loeb	University of California, Berkeley, Calif.

THE PHYSICAL REVIEW

[illegible]ished by the American Physical Society at 450 Ahnaip St., Menasha, Wis. [illegible]ative office: University of Minnesota, Minneapolis, Minn. Two volumes annually, [illegible] issues per volume.

[illegible] series. From July 1, 1893, to January 1, 1913, the REVIEW was conducted by Ed[illegible] L. Nichols, Ernest Merritt and Frederick Bedell, with the financial support of Cor[illegible] University. The first four volumes were issued annually; subsequent volumes, semi[illegible]ly; thirty-five volumes in all.

[illegible]d series. On January 1, 1913, the REVIEW was transferred to the American [illegible]l Society as announced on the first page of the new series which was then begun. [illegible] then it has been conducted by a Board of Editors elected by the Society. Semi[illegible]l volumes begin in January and July. Beginning July 1, 1929, the REVIEW will [illegible]ed semi-monthly instead of monthly as heretofore.

[illegible]ubscribers are referred to page 2 of the advertisements for further information.

[illegible]l Subscription, throughout the Postal Union, $10.00 in advance.

[illegible]gle copies of current volume, $1.60.

[illegible]l Index, 1899-1920, $4.00, in advance.

[illegible] Volumes, $6.00 per volume; Back Numbers, $1.00 per copy for issues prior to [illegible], 1929 (Vols. 1-33), $.60 per copy for issues subsequent thereto. Postage is free [illegible]ittance accompanies order; otherwise postage is extra. No bound volumes can be [illegible]. The REVIEW offers to purchase a limited number of First Series, Vol. 1, No. 1 [illegible] each); Second Series, Vol. 7, No. 1, January 1916; Vol. 7, No. 2, February [illegible] Vol. 7, No. 4, April 1916; and Vol. 7, No. 5, May 1916 (at $2.00 each).

[illegible]dvertisements. Rates will be supplied by the Editor on request. Copy for each num[illegible] must be received at Minneapolis two weeks prior to the dates of issue; old copy is [illegible] until new copy is received. Send electrotypes direct to the printers, George Banta [illegible]ishing Co., Menasha, Wis.

[illegible]nt of ten percent is allowed subscription agencies and members of the American [illegible]l Society.

[illegible]Changes of address and Complaints of failure to receive the REVIEW, in the case of [illegible]rs of the Physical Society, should be addressed to the Treasurer; in the case of [illegible] subscribers to 450 Ahnaip St., Menasha, Wis.; or to the Editor. New copies can [illegible] sent free in response to complaint of non-delivery only if notice of non-delivery is [illegible]ed within three months of date of issue.

[illegible]ditorial Correspondence should be addressed to the PHYSICAL REVIEW, University of [illegible]sota, Minneapolis, Minn.

Entered at the postoffice at Menasha, Wis., as second class matter.
[illegible]ation for mailing at special rate of postage provided for in section 1103, Act of October 3, 1917, authorized September 6, 1926.

Second Series *July 1, 1929* *Vol. 34, No. 1*

THE

PHYSICAL REVIEW

FINE STRUCTURE IN THE COMPTON EFFECT

By Bergen Davis and Harris Purks
Physics Laboratories, Columbia University

(Received April 29, 1929)

Abstract

This is a continuation of two crystal analyses of fine structure in scattered radiation. The displaced scattered radiation from carbon (pure graphite) and beryllium was investigated. A special x-ray tube was constructed with the scattering element near the target. The tube was mounted so that the scattering angle θ was large. The tube operated at 3200 watts.

Fine structure in the displaced scattered radiation from carbon.—The angle of scattering θ was 155°. The displaced radiation has fine structure as follows going toward long wave-lengths: A relatively strong line 0.0421A from Mo $K\alpha_1$ position, and three weaker lines at 0.0012A, 0.002A and 0.0109A from the strong line. These agree closely with fine structure lines previously found by Bergen Davis and D. P. Mitchell. The two pictures are alike, but the displaced one is shifted 0.0421 from the undisplaced. The displacement is less than is to be expected from $d\lambda = 0.0243 (1-\cos\theta)$. Our results give $d\lambda = 0.022 (1-\cos\theta)$. This is 9 percent less than is to be expected from theory. Errors could not be so great as this.

Fine structure in the displaced scattered radiation from beryllium.—Displaced scattering investigated at $\theta = 163°$. A strong main line was found at $0.0446A = 0.0228 (1-\cos\theta)$ from Mo $K\alpha_1$ position. A line at 0.0051A toward the *long wave-lengths* from this main line. This displacement is near the value to be expected from Be K energy level. A weak line at 0.0009A toward short wave-lengths from main line. These two lines were found by D. P. Mitchell in the undisplaced scattering from beryllium and were ascribed to the K and L_1 energy levels of Be. The L_1 line, however, was shifted 0.00058A, which is much less than the 0.0009A found here in the displaced spectrum.

THIS is a continuation of an investigation of fine structure of scattered radiation by means of the double x-ray spectrometer. Structure in the undisplaced scattered radiation from carbon (graphite) has been previously reported by Bergen Davis and D. P. Mitchell.[1] These latter experiments have been extended by D. P. Mitchell[2] to the undisplaced scattered radition from beryllium and aluminum.

An investigation of the *displaced* scattered radiation (Compton effect) is reported here. The double x-ray spectrometer as an instrument of high

[1] Bergen Davis and D. P. Mitchell, Phys. Rev. **32**, 331 (1928); Phys. Rev. **31**, 1119 (1928).
[2] D. P. Mitchell, Phys. Rev. June 1928.

resolving power has been previously described.[3] The scattering elements used were carbon (graphite) and beryllium. A special x-ray tube was constructed. A standard water-cooled molybdenum target was cut away at one side as shown in Figure 1. The scattering element S was placed with its front face about 1.7 cm from the center of target spot b. A special cathode constructed having a short linear filament. The housing of this filament was of such shape that it directed a uniformly distributed stream of electrons over the area of the target spot. This target spot was square in shape and about 6 mm on each edge. The x-ray tube was so mounted with respect to the slit system, that the angle of scattering θ should be large. The displacement to be expected is $d\lambda=(h/mc)(1-\cos\theta)$. The dimensions of the target spot and the scattering give a considerable divergence in the values of θ. However, since the variation of the cosine at large angles is small, it was found that angle $\theta=155°$ gave sufficient resolving power to separate the spectral lines in the case of carbon. When beryllium was the scattering element, the x-ray tube was set so that $\theta=163°$, but even at this large angle the nearest spectral line was not completely resolved. Care was also taken to mount the tube so that the divergence of the rays in the vertical plane should not be greater than the divergence in the horizontal plane.

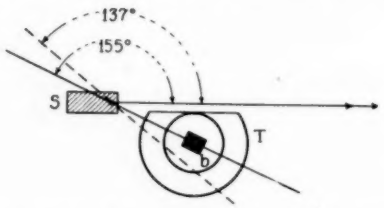

Fig. 1. Arrangement of x-ray tube target and scattering block.

The displaced scattered radiation (Compton effect) is quite weak even when observed from a single crystal. The energy observed in these experiments was very much smaller. The radiation was divided into separate spectral lines and the reflection was from two crystals. The x-ray tube was driven at as great power as safety would permit. The rate of dissipation of energy at the target was 3000 to 3200 watts (75 to 80 milliamperes at 40,000 volts). This great power caused the target spot to become incandescent on the surface even though it was water-cooled. Also one could hear the water boil as it passed through the target.

TABLE I.

Carbon Displacement from Mo $K\alpha_1$		Beryllium Displacement from Mo $K\alpha_1$	
$K\alpha_1'$	0.0421A	$K\alpha_1'$	0.0446A
CL_{111}'	0.0421+0.0012	—	—
CL_1'	0.0421+0.002	Be L_1'	0.0446−0.0009
CK'	0.0421+0.0109	Be K'	0.0446+0.0051
$0.0421=0.0221\,(1-\cos 155°)$		$0.0446=0.0228\,(1-\cos 163°)$	

[3] Bergen Davis and Harris Purks, Bulletin Nat. Acad. Sc. Vol. 13. June 1927.

The results obtained are given in Table I and in the figures. The lines of the undisplaced radiation are designated by subscripts (L_1, L_{III} etc.), the corresponding lines of the displaced radiation are designated by primes (L_1', L_{III}' etc.). The displaced scattered radiation from carbon has four lines as shown in Figure 2, a relatively strong line $K\alpha_1'$, and three weaker

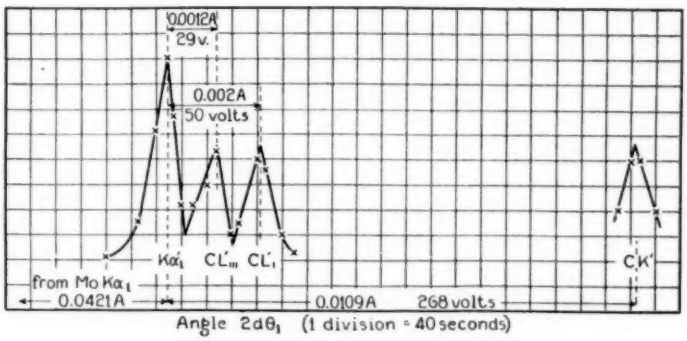

Fig. 2. Fine structure in the Compton effect from carbon.

lines CL_1', CL_{III}' and CK'. The shift of these three lines from the $K\alpha_1'$ is closely the same as the values previously found for the undisplaced scattered radiation. The spectrum of the displaced is a duplicate of that of the undisplaced. The shift, however, of the one spectrum from the other is not quite so great as is to be expected by the relation $d\lambda = h/mc(1-\cos\theta)$(1), in which h/mc has the value 0.0243. The shift of the spectra is better represented by $d\lambda = 0.0221\ (1-\cos\theta)$. The shift is less than the expected value by about 9 percent. This difference is too great to be accounted for by error in measurement of the angle θ. The tube should have been set at 137° instead of 155° to give the observed displacement.

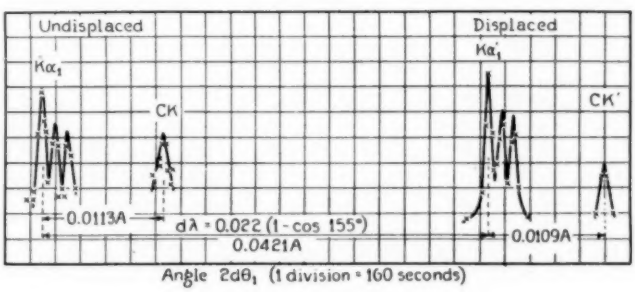

Fig. 3. Complete spectrum, scattered radiation from carbon.

This angle 137° is represented by the dotted line in Fig. 1. It will readily be seen that the difference is too great to arise from error in tube setting. Also the divergence effect due to size of target spot and size of scattering element, (Eq. (1)) would have been so great at 137° that the separate L lines would not have been resolved. The conclusion must be drawn that the constant h/mc does not completely represent the phenomena.

The complete spectrum of the scattered radiation from carbon is shown in Figure 3. The two spectral pictures are quite alike. The shift of the CK' line (0.0109A = 268 volts) from $K\alpha'_1$ is less than the shift of CK line (0.0113A = 279 volts) from the $K\alpha_1$. The shift (0.0109A = 268 volts) is less than the K energy level of carbon (280 volts). This latter shortage in the displacement of the CK' line may have the same physical cause as the shortage in the displacement of the whole spectral group.*

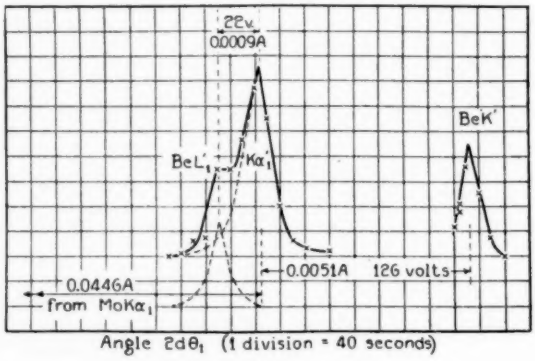

Fig. 4. Fine structure in the Compton effect from beryllium.

The results for beryllium are given in the Table I and in Figures 4 and 5. A relatively strong line $K\alpha_1'$ at 0.0446A from $K\alpha_1$ position, a weak line Be K' 0.0051A toward *long* wave-lengths from $K\alpha_1'$ and a weak line 0.0009A toward *short* wave-lengths from $K\alpha'_1$. This last line corresponds to the B L_1 found by D. P. Mitchell[2] in the undisplaced scattered radiation from beryllium. The Be K' line at 0.0051A corresponds to the Be K line in the undisplaced radiation as found by Mitchell. It is to be ascribed to the K energy level of beryllium. The shift of the displaced spectrum is 0.0446A = 0.0228

* It is perhaps worth while to refer here to some recent experiments of Ehrenberg on scattered radiation from graphite.[4] He used the single crystal photographic method and his results were negative. No lines were observed. His scattering element was Acheson graphite. He suggests that our fine structure might be due to impurities. We would say that the scattering elements used for data in table [1] for Experiment No. 2 was Acheson graphite. That used for Experiment No. 1 was a pure graphite obtained from General Electric Co. The great separation of the α_1 and α_2 lines in the Ehrenberg spectrogram indicates that the slits were very narrow. Our own previous experience with the photographic method and the experiments of P. A. Ross on the Compton effect indicate that it is difficult to observe scattered radiation with such narrow slits. The undisplaced scattering is of about the same intensity as the displaced. It would require many hundreds, perhaps thousands of hours exposure to register fine structure in scattered radiation on a film with such narrow slits. The intensity of the real scattered radiation is of a different order of magnitude than that observed by Ehrenberg. Graphite is a powdered crystal. We would suggest that the lines observed by Ehrenberg are higher order reflections from those minute crystals that are properly oriented for such reflection. A few years ago this experiment was made in our laboratory. Finely powdered calcite was formed into a placque. This was found to give quite strong reflection no matter at what angle the rays impinged on the placque.

[4] W. Ehrenberg, Zeits. f. Physik **53**, 234 (1929).

$(1-\cos 163°)$ from the undisplaced. The constant 0.0228 is less in this case also than h/mc as expected from theory. A most significant point about the two spectra is that the $K\alpha_1$ line is absent or very weak in the undisplaced, but is relatively strong in the displaced radiation. Attention is also directed

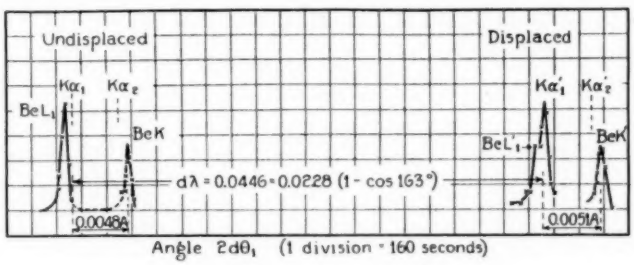

Fig. 5. Complete spectrum, scattered radiation from beryllium.

to the fact that the shift of Be L_1' (-0.0009A) from Be $K\alpha_1'$ is considerably greater than the shift of Be L_1 (-0.00058A) from the $K\alpha_1$ position on the undisplaced spectrum. The possibility of this type of fine structure has been suggested by Compton.[5] The expression for the displaced scattered radiation proposed by him is

$$d\lambda=\frac{\lambda^2}{\lambda_s-\lambda}+\frac{h}{mc}(1-\cos\theta).$$

This is the same as the fine structure found in these experiments, with the exception that the agreement with the constant $h/mc=0.0243$ is not exact.

Discussion. These experiments together with others give important information as to the possible modes of interaction of photons, electrons, and atoms. (*a*) A photon may lift an electron from an atomic energy level and give it kinetic energy expressed by $h\nu=\frac{1}{2}mv^2+Ve$, where Ve is the energy level from which the electron originated. The photon as such disappears. This is the photoelectric effect. (*b*) The photon may lift an electron from an energy level to the atomic limit and then escape without imparting either momentum or kinetic energy to the electron. This is represented by the relation $h\nu'=h\nu-Ve$. This is the mode of production of the fine structure in the undisplaced scattered radiation. There is one exception found by D. P. Mitchell[2] in the case of the L_1 level of beryllium. In this instance $h\nu'=h\nu+Ve$. The photon finds the electron already in a higher energy state near the atomic limit. When the two part company the potential energy of the electron is *added* to that of the photon. (*c*) The photon may lift an electron to a higher energy level at or near the atomic limit and then impart to it both energy and momentum in the manner proposed by Compton. This is the origin of the fine structure in the displaced spectrum. The $K\alpha_1'$ line in the case of beryllium is relatively strong. This occupies the position in the displaced spectrum that should arise from scattering from a free or slightly

[5] A. H. Compton, Phys. Rev. **24,** Aug., 1924.

bound electron. Also there is no spectral line on the *long wave-length side* of $K\alpha_1$ or $K\alpha_1'$ in either the displaced or the undisplaced spectrum ascribable to the Be L_1 energy level, but there is a line in both spectra on the *short wave-length side*. This indicates that the normal condition of the beryllium atom is a state of excitation in which those electrons that belong normally in the L_1 energy levels occupy positions at or near the atomic limit. Their energy of position is added to the photon at moment of scattering. (*d*) The photon may scatter from a free or nearly free electron after the manner proposed by Compton. This is indicated by the relatively strong lines at $K\alpha_1'$ position in the displaced spectra of both carbon and beryllium. (*e*) The photon of the wave-length here used probably does not scatter from an atomic nucleus. The $K\alpha_1$ line is absent or very weak in the undisplaced radiation from beryllium. It is present in the case of carbon and also in the case of aluminum (see D. P. Mitchell).[5] The number of nuclei per cc is about the same for beryllium as for carbon and aluminum. The number of bound electrons, however, in beryllium is small, since the two L_1 electrons appear to be in higher energy levels. It is greater in the case of elements of higher atomic number. The undisplaced scattered radiation decreases with atomic number and practically disappears in the case of scattering from lithium, as has previously been found by single crystal experiments. On the other hand it increases in intensity with increase of atomic number and hence with number of bound electrons. The undisplaced $K\alpha_1$ must be scattered from a large mass, since the loss of energy is negligibly small. The scattering in this case is probably from the whole group of electrons bound to the nucleus. The nucleus without electrons does not scatter radiation of the wave-length here used. It is probable, however, that hard radiation such as gamma-rays and cosmic rays may react with the concentrated field or wave pattern of a nucleus.

We wish to acknowledge our obligations to W. C. Beller for assistance in operation and control of x-ray equipment during this investigation.

EXPERIMENTAL EVIDENCE FOR THE FILLING OF ELECTRON LEVELS FROM THE RELATIVE INTENSITY OF X-RAY SPECTRUM LINES

By Samuel K. Allison
University of California, Berkeley

(Received, April 8, 1929)

Abstract

According to the accepted theory of the periodic system electrons first enter the 5_3 orbits at 57 La; only one electron remaining in these orbits until 72 Hf from whence the orbits fill up to 10 electrons at 79 Au. The $L\beta_5$ line is double, representing the transitions 5_{32}, $5_{33} \rightarrow 2_{22}$. In a previous paper the author found that this line was much more intense (about 37 times for $L\beta_5$ alone) in the uranium than in the tungsten L series. This paper reports intensity measurements involving this line in 76 Os, 77 Ir, 78 Pt, 79 Au, 81 Tl, 82 Pb, 83 Bi. It is shown that experimental difficulties due to deposition of tungsten on the targets from the filaments may be avoided by keeping high vacua in the tubes. A curve showing the intensity ratio β_5/β_1 as a function of the atomic number rises with increasing atomic number and takes an upward jump between 78 Pt and 79 Au. This indicates that the first element in which 10 electrons occupy the 5_3 orbits in an approximately undisturbed condition in the solid state is 79 Au. The curve is similar to one obtained in the region about 46 Pd for the lines $L\gamma_1$ and $L\beta_2$ by Jönsson.

INTRODUCTION. In a previous paper[1] the author found that the relative intensity of the line $L\beta_5$ ($O_{V}O_{IV} \rightarrow L_{III}$) to the line $L\beta_1$ ($M_{IV} \rightarrow L_{II}$) was 6.4/40.5 or 16/100 for uranium (92) when the excitation voltage was 52.8 kilovolts. The same ratio was measured in tungsten (74) by Allison and Armstrong[2] at 31.7 kilovolts and found to be 0.47/100. The relative intensity of these lines depends on the excitation voltage used, but the voltage 52.8 kilovolts for uranium is comparable to the voltage 31.7 for tungsten, since in each case the ratio of the voltage used to the average critical excitation voltage for the L-series is nearly the same. The average critical excitation voltage[3] for the uranium L-series is $(21.2+20.8+17.1)/3$ or 19.7 kilovolts, and the ratio 52.8/19.7 is 2.7. The average critical excitation voltage for the tungsten L-series is $(12.1+11.5+10.2)/3$ or 11.3, and the ratio 31.7/11.3 is 2.8.

Jönsson[4] has measured the ratio in question for tungsten at 20 kv and finds 0.2/40.8 or 0.49/100. If this ratio is corrected to 32 kv by the usual method[4] it is found to be 0.43/100 in agreement with the value of Allison and Armstrong.

[1] S. K. Allison, Phys. Rev. **32,** 1 (1928).

[2] Allison and Armstrong, Phys. Rev. **26,** 714 (1925).

[3] This method of computing an "average critical excitation voltage" is of course not of any general significance. It is only used to obtain a first approximation to comparable voltages in cases where the tube voltage is from 2 to 3 times that of the group of critical excitation voltages in consideration.

[4] Jönsson, Zeits. f. Physik **36,** 426 (1926).

There is no doubt, therefore, that the intensity ratio β_5/β_1 in uranium is about 37 times as great as it is in tungsten at comparable voltages. This increase is undoubtedly due largely to the fact that between tungsten (74) and uranium (92) the $O_{IV}O_V$ levels, which are the outer levels concerned in the line $L\beta_5$, are filling with electrons. It therefore seemed worth while to trace this process through as many elements in the intervening region of the periodic system as possible. The present report concerns experiments performed to determine the ratio β_5/β_1 at comparable voltages in 76 Os, 77 Ir, 78 Pt, 79 Au, 81 Tl, 82 Pb, 83 Bi. It was expected that a curve similar to that found by Jönsson[5] for the lines $L\beta_2$, $L\gamma_1$ in the vicinity of palladium (46) would be found. By consulting the energy level diagram it is seen that the line $L\gamma_6$, $(O_{IV}\rightarrow L_{II})$ also involves the O-levels in question. Due to the fact that in the region of the periodic system under consideration the line $L\gamma_6$ lies very close to other lines and sometimes in coincidence with them, no attempt was made to investigate this line.

Deposition of tungsten on the target. Siegbahn[6] has called attention to the fact that after a few minutes of operation, the x-ray tubes used by him give the tungsten spectrum strongly, even if the target material is not tungsten. This is due to the deposition of tungsten on the anticathode from the filament. If this were to take place in the present experiments, the results would be very untrustworthy for two reasons, (1) the possible interference of the tungsten lines with those of the target element, (2) the fact that the spectrum of the target element would have to pass through a layer of tungsten of unknown thickness and an absorption correction of unknown amount would enter.

It does not seem practicable to use oxide-coated filaments at the high voltages required as they rapidly become stripped of their coating by the positive ion bombardment to which they are subjected. Accordingly before beginning the measurements, some rather qualitative experiments were carried out on the deposition of tungsten on the target.[7] In the first place, it can be shown that this deposition cannot be due to thermal evaporation of the tungsten due to its vapor pressure at the filament temperatures used. The thermal evaporation of tungsten has been investigated by Langmuir.[8] In Table V of his paper he gives the grams per square centimeter per second evaporated from a tungsten surface at various temperatures between 2000°K and 5110°K. In making a rough calculation of the order of magnitude of the effect to be expected from thermal evaporation, these data have been combined with Table I of a paper by W. D. Coolidge[9] showing the electron current obtainable from a standard tungsten filament in an x-ray tube as a function of the temperature. Table I of this paper contains the results of cal-

[5] Jönsson, Zeits. f. Physik **41**, 221 (1927).

[6] The Spectroscopy of X-rays. Oxford Univ. Press, 1925, p. 36.

[7] Acknowledgement is hereby made to Professor K. T. Compton and Professor Bergen Davis for valuable information on this point.

[8] Langmuir, Phys. Rev. **2**, 329 (1913).

[9] Coolidge, Phys. Rev. **2**, 409 (1913).

culations on the thermal evaporation. The dimensions of the tungsten filament considered are 3.34 cm long; 0.216 mm diameter. It is assumed that the evaporated tungsten is evenly distributed over a spherical surface surrounding the filament and 3 cm in radius, corresponding to a filament-target distance of 3 cm.

TABLE I. *Order of magnitude of thickness of films of tungsten deposited on the target of the x-ray tube by thermal evaporation.*

Electron current (milliamperes)	Temperature of filament (°K)	Thickness of film deposited per hour (cm)
5.7	2055	3×10^{-13}
9.7	2074	4×10^{-13}
13.8	2090	5×10^{-13}
21.8	2116	1.6×10^{-12}
36.2	2240	2.1×10^{-11}

Table I shows that with a voltage saturation current of 36 milliamperes a run of a thousand hours would be required to deposit a film one atom thick through thermal evaporation alone.

The transportation of tungsten from filament to target must therefore be due to chemical action of residual gas. Water vapor is particularly active in this manner, oxidizing the tungsten to the more volatile oxide at the filament. This vaporizes off, deposits on the relatively cool target, and may be reduced to tungsten again by the hydrogen in the water vapor or by electronic bombardment. It is possible to calculate the maximum thickness of tungsten which could be deposited per hour by this method as a function of the residual gas pressure. If we assume that the number of atoms of the residual gas hitting a square centimeter of surface of the filament in terms of n, the number of atoms per cc and c, their velocity, is given by the ordinary kinetic theory expression $\frac{1}{4}nc$, and that every atom which hits the hot tungsten takes away a tungsten atom we can calculate the values of Table II. The calculations are carried out for the same dimensions of fila-

TABLE II. *Maximum thickness of tungsten deposited on target as a function of the pressure of residual gas.*

Pressure of residual gas (mm of mercury)	Maximum thickness of tungsten deposited per hour (cm)
10^{-3}	4×10^{-6}
10^{-4}	4×10^{-7}
10^{-5}	4×10^{-8}
10^{-6}	4×10^{-9}

ment and filament-target distances as those of Table I. From this we see that if the tube is at all "gassy" the deposition of tungsten by this process may be considerable. This is believed to be the case in Siegbahn's metal tubes where the presence of large metal surfaces makes high vacua difficult to obtain.

In the present experiments special precautions were taken to keep the pressure low. The x-ray tube was of the same general type as that shown in a previous paper,[10] but the target, which in the previous work was sealed in with cement, was sealed directly to glass with a Housekeeper seal, and the tube was cut open when target replacement was necessary. During the process of pumping out the tube was flushed with hydrogen occasionally while an induction coil was maintaining a gaseous discharge with the filament cold. This was an attempt to make the residual gas as far as possible hydrogen which presumably would be inactive in transporting tungsten.

Finally the spectra obtained from the tubes were examined for the tungsten lines. In some cases no evidence at all for the presence of the lines could be obtained Figure 1 shows the most intense tungsten spectrum obtained

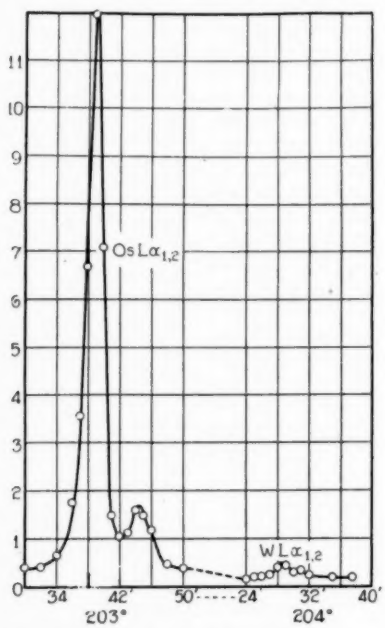

Fig. 1. Ordinates are rates of deflection of the electrometer in millimeters per second.

in all the experiments. The target was a button of metallic osmium. The relative intensity of W $L\alpha_1$ to Os $L\alpha_1$ is 1/39. An estimate of the thickness of the tungsten film in this case can be obtained by an expression due to D. L. Webster.[11] This expression is

$$\Delta x = (2V\beta/bn)(V - V_0)$$

in which the symbols have the following meanings: Δx is the thickness of the film over the osmium, V is the voltage used in kilovolts, 32 kv; β is the ratio W $L\alpha_1$/Os $L\alpha_1$ or 1/39; b is Whiddington's constant for tungsten in kv/cm^2 or 7.6×10^6; n is 1.8; V_0 is the critical excitation voltage in kv or 10.4.

[10] S. K. Allison, Phys. Rev. **30**, 245 (1927).

[11] Webster, Clark, Yeatman, Hansen, Proc. Nat. Acad. Sci. U. S. A. **14**, 679 (1928).

Putting these values in the equation one finds that the thickness of the film is about 1.3×10^{-6} cm. The applicability of this equation to this case is based on the facts (1) that osmium and tungsten are very near together in the periodic system and (2) the film was quite thin compared to the mean depth of penetration of the cathode rays. The effects due to the production of fluorescence radiation in the target itself have been neglected. Webster has shown these to be about 35 percent of the line intensity. These results show that with reasonable precautions to keep the pressure low in the x-ray tube the error from tungsten films on the surface of the target may be made inappreciably small.

Experimental procedure. The experimental arrangements were as described in the previous paper on uranium[1] with small changes. In all the experiments the x-ray beam was limited by two molybdenum-jawed slits 42 cm apart and each of width 0.020 cm. The angular width of the beam incident on the crystal was therefore about 3.3 minutes of arc. The radiation passed through two mica windows, one on the x-ray tube and one on the ionization chamber. The total thickness of mica traversed was 0.003 cm. The distance in air travelled by the rays was 60 cm. The ionization chamber was 64 cm long, 4 cm in diameter, and filled with methyl iodide vapor to a pressure of about 24 cm of mercury. All the experiments were performed with a current of 5.5 milliamperes through the x-ray tube. The intensities were taken as proportional to the maximum length of the ordinate of the curve representing the line above the base line due to scattered and reflected general radiation. The intensities were measured at some convenient voltage nearly 2.7 times the average critical excitation voltage for the L-series as defined above and then corrected to this voltage on the assumption that the intensities of the lines obey the empirical law

$$I=k(V-V_0)^{1.8}$$

where I is the intensity of the line at voltage V, V_0 is the critical excitation voltage, k is a constant depending on the line in question. These corrections and the absorption corrections were very small since the lines measured were all in the $L\beta$ group and did not differ greatly in wave-length.

Osmium. The target was a button of metallic osmium 1 cm in diameter and 1 mm thick. The voltage used was 32.5 kv which is 2.7 times the average of the excitation voltages of the osmium L-series, therefore no voltage correction was necessary. The values given are in each case the averages of three separate determinations. (See Fig. 3).

TABLE III. *Osmium (76).*

Line	Observed intensity	Correction for absorption	Relative intensity at 32.5 kv
β_4	7.2	1.01	7.3
β_1	100	1.00	100
β_3	12	0.99	12
β_2	47	0.99	47
β_6	1.5	0.99	1.5

Iridium. The target was a button of metallic iridium 1 cm in diameter and 0.025 cm thick. The voltage used was 33.2 kv which is 2.7 times the average of the L critical excitation voltages for iridium. The β_2 and β_3 lines were not entirely separated with the broad beam used.

TABLE IV. *Iridium* (77).

Line	Observed intensity	Correction for absorption	Intensity at 33.2 kv
β_4	8.1	1.00	8.1
β_1	100	1.00	100
β_2	45	0.99	45
β_5	2.5	0.99	2.5

Platinum. The target was a plate of chemically pure platinum 1 cm square and 0.005 cm thick. The osmium $L\beta_1$ and iridium $L\alpha_1$ lines were searched for and not found. The voltage used was 34.0 kv which is 2.6 times the average of the L critical excitation voltages. No voltage correction was made. Jönsson[4] has investigated the platinum L-series at 20 kv but did not measure the line $L\beta_5$ of primary importance to this research. The lines β_2 and β_3 are coincident in platinum, also β_4 and β_6. Four determinations of β_5/β_1 were made, giving the values 2.80, 2.87, 2.82, 2.92 to 100 respectively.

TABLE V. *Platinum* (78).

Line	Observed intensity	Correction for absorption	Intensity at 34 kv.
β_1	100	1.00	100
β_5	2.85	0.98	2.8

Gold. The target was a gold plate about 12 mm square. The voltage used was 34 kv. The voltage required for comparison with the other metals was 36 kv, and the observed intensities were corrected to this value. The lines β_2 and β_3 were not separated.

TABLE VI. *Gold* (79).

Line	Observed intensity	Correction for voltage	Correction for absorption	Intensity at 36 kv
β_4	7.8	1.00	1.01	7.9
β_1	100	1.00	1.00	100
β_5	5.3	0.99	1.00	5.3

Thallium. Metallic thallium of spectroscopic purity was used as a solder and flowed onto the copper target. The spectrum was examined for Pb $L\beta_1$ but nothing was found. The voltage used was 34 kv. The comparison voltage was 38.7. Since β_1 and β_2 were not separated with the wide slits used, β_4 was taken as the standard of comparison.

TABLE VII. *Thallium (81).*

Line	Observed intensity	Correction for voltage	Correction for absorption	Intensity at 38.7 kv
β_6	50	0.96	1.00	48
β_4	100	1.00	1.00	100
β_5	96	0.96	0.98	90

Lead. Metallic lead was used as a solder and flowed on to the copper target. The voltage used was 34 kv. The voltage for comparison was 39.6 kv. β_1 and β_2 are practically coincident.

TABLE VIII. *Lead (82).*

Line	Observed intensity	Correction for voltage	Correction for absorption	Intensity at 39.6 kv
β_6	45	0.95	1.01	43
β_4	100	1.00	1.00	100
β_3	138	1.00	0.99	137
β_5	106	0.95	0.99	100

Bismuth. Metallic bismuth was used as a solder and flowed on to the copper target. The voltage used was 34 kv. The voltage for comparison was 40.9 kv. β_1 and β_2 were not separated.

TABLE IX. *Bismuth (83).*

Line	Observed intensity	Correction for voltage	Correction for absorption	Intensity at 40.9 kv
β_4	100	1.00	1.00	100
β_3	149	1.00	0.99	148
β_5	131	0.94	0.98	121

Treatment of Results. The object of the experiments was to study the relative intensity of the line $L\beta_5$ to that of some line involving orbits deep in the atom as a function of atomic number throughout the region between tungsten and uranium. It seemed advisable to take as a reference line $L\beta_1$, since this is a strong line near $L\beta_5$ in wave-length which makes absorption corrections unimportant. A difficulty arises, however, in the elements thallium, lead, and bismuth, where the lines $L\beta_1$ and $L\beta_2$ lie so close together that they were not separated in the experiments. In order to calculate the intensity ratio β_5/β_1 in this region the ratio β_5/β_4 is used, and the assumption made that the ratio β_4/β_1 remains independent of atomic number. This assumption is reasonable because the ratio β_4/β_1 is within the experimental error the same in Os (76), Ir (77), Au (79) and U (92) and there is no apparent reason for a deviation in the intervening region. It is therefore assumed that for Tl (81), Pb (82), Bi (83) the ratio β_4/β_1 is 8/100 and the ratio β_5/β_1 then calculated from the observations. Further support to this assumption is given by the fact that it leads to a ratio β_6/β_1 in these elements the same as in uranium, and that the points given by it lie on reasonably smooth curves.

Figure 2 shows the behaviour of the weaker β-lines in this region. For tungsten the old values of Allison and Armstrong are used, although it is known that they are somewhat vitiated by absorption in the target. The points for the line β_3 are erratic and for no apparent reason. It is hoped that

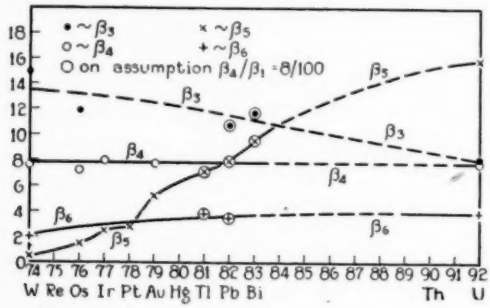

Fig. 2. Ordinates are the ratio of the intensity of the line in question to that of β_1 in percent. Dotted portions are less certain than full line portions.

experiments to be carried out in this laboratory in the near future will give more reliable results.

The chief interest lies in the upward trend of the line $L\beta_5$ and the discontinuity in its rise between platinum and gold. The reality of this break of

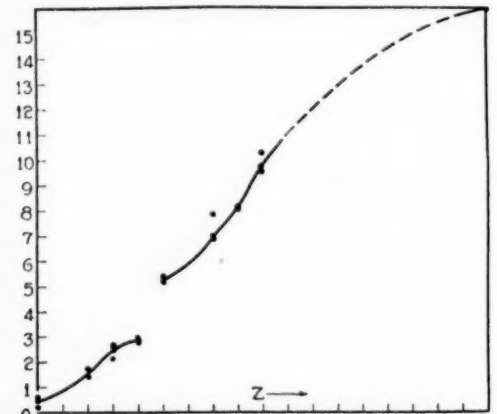

Fig. 3

course depends on the experimental error within which the ordinates can be determined. In Fig. 3 the curve for β_5 is plotted on a somewhat larger scale, and all the points measured (the values in Tables III-IX are averages)

are shown. In the same figure is a table of possible electron configurations for outer orbits in the elements in question. It is important to note that the existence of the break between platinum and gold is independent of any assumption about the ratio β_4/β_1 as this only effects Tl, Pb, and Bi.

Discussion of Results. The curve of Fig. 3 is qualitatively similar to those obtained by Jönsson for the lines $L\beta_2$, $L\gamma_1$ (N_{IV} $N_V \rightarrow L_{II}L_{III}$) in the region around palladium (46) where the N_{IV} N_V levels are filling with electrons. In that region the break occurred between Pd and Ag which is analogous to Pt and Au in the present case. The rise of intensity of an x-ray line with atomic number can be described therefore with some confidence. The line does not suddenly appear when electrons first enter the orbit in question, but usually before this in the periodic system. For instance the line $K\gamma$ (Siegbahn; $K\beta_2$) (N_{II} $N_{III} \rightarrow K$) is observed[12] as a semi-optical line as far down as vanadium (23) whereas electrons do not exist in these N-orbits in the normal state until gallium (31). Whether or not there is an upward jump when electrons first enter the orbit in question in the normal state has not been experimentally settled. It would seem difficult to do so since the total intensity is so low in this region. The relative intensity then increases up to the point where the level is filled. Here there is a sudden upward jump, but the full intensity in not reached at this point and a further increase with atomic number takes place. It must be remembered that there are some lines which apparently decrease in intensity with increasing atomic number, namely γ_4, γ_5, β_3 in the L-series.

The curve in Fig. 3 corresponds well with the optical data. McClennan and McClay[13] have found that the lowest term of the Pt arc spectrum is ^3F which makes the outer electron configuration different from Pd and similar to Ni. This means 8 electrons in the 5_3 orbits of Pt and 10 in the same orbits in Au, and the filling of these orbits at this point.

In the case of palladium, the conditions are somewhat different.[14] The arc spectrum of palladium has been investigated by McClennan and Smith.[15] They have found that the lowest term is $^1S_0$ corresponding to 10 electrons in the 4_3 orbits. There are, however, other energy levels lying near this such as ^3D whose energy difference is of the order of 0.9 volt-electrons from $^1S_0$. It is thus seen that Pd may be regarded as a rare gas with very small resonance potentials. At first thought it might seem that the optical data demand a break in the $L\gamma_1$ or $L\beta_2$ curve between rhodium (45) and palladium (46), whereas Jönsson[5] found the break between Pd and Ag (47). This discrepancy is considered to be due to the fact that the optical data deal with

[12] Allison and Armstrong, Phys. Rev. **26,** 714 (1925), see Fig. 3, p. 722.

[13] McClennan and McClay, Trans. Roy. Soc. Canada **20,** 201 (1926). Professor Shenstone has recently informed the author that the lowest term as assigned by McClennan and McClay to the platinum atom is probably incorrect, and that there are 9 electrons in the 5_3 and 1 in the 6_1 levels. It is clear however that the intensity data in this paper are not directly connected with electron configurations in the lowest levels of gaseous atoms.

[14] S. K. Allison, Phys. Rev. **32,** 1 (1928), see footnote p. 8.

[15] McClennan and Smith, Proc. Roy. Soc. **A112,** 110 (1926).

isolated atoms in a gas; the x-ray data with atoms under van der Waals' forces in solids. This view would predict also that the intensity of the criti-

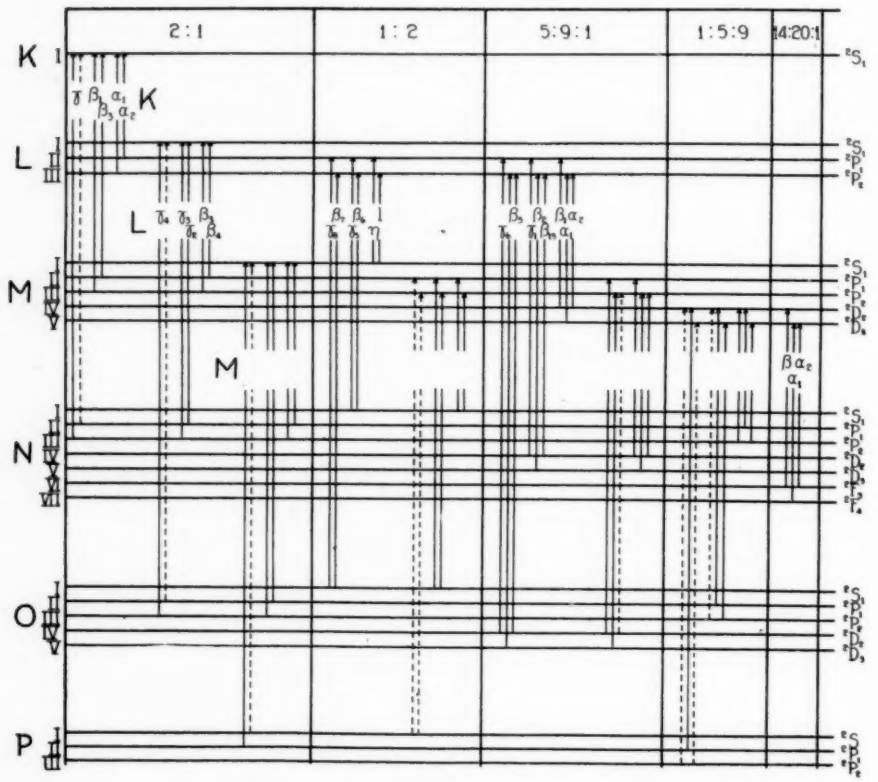

Fig. 4. Term diagram for x-rays showing lines in the *K*, *L* and *M*-series. Numbers at the top of each division represent relative intensities according to the Burger-Dorgelo rules. Dotted lines are ones not yet measured. There is an error in the similar diagram published in the previous paper on uranium.

cal line on the high atomic number side of the break should vary greatly with the state of chemical combination of the atom.

THE VECTOR COUPLING IN THE NICKEL-, PALLADIUM-, AND PLATINUM-LIKE SPECTRA

By J. E. Mack[1]
Palmer Physical Laboratory, Princeton University

(Received April 8, 1929)

Abstract

Spectroscopic data.—The $5d^9 6s$ and $5d^9 6p$ configurations are identified among the known levels of Pt I, and partly identified in Tl IV and Pb V. The lines observed in the condensed spark discharge of thallium λ868 to λ1070 and lead λ477 to λ1280 are listed.

Vector coupling.—The relative energies, line intensities, and g-values of the levels of the $d^9 s$ and $d^9 p$ configurations of the sequences Ni I-Ge V, Pd I-Sn V, and Pt I-Pb V show a gradual transition from LS or Russell-Saunders coupling to jj coupling with increasing atomic number and increasing net charge. In the "pure" jj coupling the levels are arranged in groups (two in $d^9 s$ and four in $d^9 p$). The positions of the $d^9 p$ groups observed for Hg III, Tl IV, and Pb V agree well quantitatively with the positions independently calculated for jj coupling with the aid of the Sommerfeld regular doublet law. In the $d^9 p$ configuration of Tl IV and Pb V, only levels built upon $d^9\ {}^2D_{5/2}$ are observed in spite of the fact that the $d^9_{3/2} + p_{1/2}$ levels are more stable than the $d^9_{5/2} + p_{3/2}$ levels.

Correlation of levels, with varying principal quantum number and varying nuclear charge.—In several cases among the spectra under consideration, levels of the same J-value cross when relative energy in a configuration is plotted against nuclear charge in an isoelectronic sequence. These levels, except in one case, happened to be recognizable on both sides of the "crossings" on account of their approximately normal intensities. But in general, correlation of levels and crossing or non-crossing in spectral series or isoelectronic sequences appears to be without meaning, for it necessitates considering quantum numbers or nuclear charges as continuous variables.

I. Introduction

MOST of the progress made thus far in the classification of complicated atomic spectra, has been made among spectra of the "normal" or Russell-Saunders type.[2] Roughly speaking, the normal type is characteristic of all atoms except those "near the right-hand edge" or "near the bottom" of the periodic table—that is, of all atoms except those with nearly enough equivalent outer electrons to form a complete Pauli shell, or with high atomic number.

Platinum is the extreme case "in the lower right-hand corner" of the periodic table. The platinum-like spectra[3] are by no means completely known; but sufficient progress has been made in their classification to lend

[1] National Research Fellow.

[2] That is, spectra which satisfy approximately Landé's interval formula and g formula (A. Landé, Zeits. f. Physik **15**, 189 (1923)) and Russell's intensity formula (H. N. Russell, Nat. Acad. Sci. Proc. **11**, 314 (1925)).

[3] That is, the spectra of the isoelectronic sequence Pt I, $Z=78$; Au II, $Z=79$; etc.

interest to a study of them from the viewpoint of the vector model and a comparison with the analogous nickel-like and palladium-like spectra. Such a study is the main object of this paper; but certain new spectroscopic data pertinent to the study will be presented first.

II. Data*

This paper will be confined largely to a consideration of the structure of atomic states wherein the outer electrons occur in configurations of nine d electrons and one s or p electron. The $3d^9 4s$, $3d^9 4p$ and $4d^9 5s$, $4d^9 5p$ configurations are already known for five spectra in each sequence.[4] The relative values of the levels arising from the $5d^9 6s$ and $5d^9 6p$ configurations are

* The work of numerial calculation for this paper has been materially lightened by the use of a calculating machine secured by this laboratory through the generosity of the Carnegie Corporation.

[4] Spectroscopic data from the following sources were used in the preparation of this paper (l means list of lines; c, list of levels; i, interpreted list of levels; z, Zeeman effect data):

Cr V i: R. C. Gibbs and H. E. White, Phys. Rev. **33,** 538 (1929).

Co I i: M. A. Catalán, Zeits. f. Physik **47,** 89 (1927); H. N. Russell, unpublished data.

Ni I i: K. Bechert and L. A. Sommer, Ann. d. Physik **77,** 351 (1925); z, O. Luttig (Peterko's data) Ann. d. Physik **38,** 43 (1912); *intensities*, quantitative measurements, F. Bouma, diss. Utrecht, and material about to be published in Dutch, obtained through the courtesy of Professor Ornstein.

Ni II i: A. G. Shenstone, Phys. Rev. **30,** 255 (1927); R. J. Lang, Phys. Rev. **31,** 773 (1928).

Cu I i: A. G. Shenstone, Phys. Rev. **28,** 449 (1926).

[a]Cu II i z: A. G. Shenstone, Phys. Rev. **29,** 380 (1927).

Cu III i: R. C. Gibbs and Alice M. Vieweg, Phys. Rev. **33,** 1092 (1929).

Zn II, Cd II i: G. v. Salis, Ann. d. Physik **76,** 145 (1925).

Zn III i: O. Laporte and R. J. Lang, Phys. Rev. **30,** 378 (1927).

[b]Zn III, Ga IV, Ge V i: J. E. Mack, O. Laporte, and R. J. Lang, Phys. Rev. **31,** 748 (1928).

[c]Cu-, Hg-, Au-like sequences i; Ga, Ge, Cd, In, Hg, Tl, Pb l: J. A. Carroll, Roy. Soc. Trans. **A225,** 357 (1925).

As VI (The paper of P. Pattabhiramiah and A. S. Rao, Zeits. f. Physik **53,** 587 (1929), has been consulted but its results have not been incorporated in this paper. A criticism is expected to appear shortly).

Pd I c: J. C. McLennan and H. G. Smith, Roy. Soc. Proc. **A112,** 110 (1926); i: Privately communicated by A. G. Shenstone; z: C. S. Beals, Roy. Soc. Proc. **A109,** 369 (1925) (g-values calculated by A. G. Shenstone).

Ag II i z: A. G. Shenstone, Phys. Rev. **31,** 317 (1928); and private communication.

[d]Cd III, In IV i: R. C. Gibbs and H. E. White, Phys. Rev. **31,** 773 (1928).

In III, Sn IV, Sb V i: R. J. Lang, Nat. Acad. Sci. Proc. **13,** 341 (1927).

Sn V i: R. C. Gibbs and H. E. White, Nat. Acad. Sci. Proc. **14,** 143 (1928).

[e]Pt, Au l: F. Exner and E. Haschek (Kayser's "Handbuch der Spektroscopie," vol. 6).

Pt l: W. F. Meggers, U. S. Bur. Stds. Sci. Papers **20,** 19 (1925).

Pt I c: J. C. McLennan and A. B. McLay, Roy. Soc. Canada Trans. **20,** 1 (1926); i: W. F. Meggers and O. Laporte (including Snyder's data), Phys. Rev. **28,** 642 (1926); cz: A. C. Haussmann, Astrophys. J. **66,** 333 (1927);

[f]ls: A. G. Shenstone and J. J. Livingood, unpublished data.

Au I i: J. C. McLennan and A. B. McLay, Roy. Soc. Proc. **112,** 95 (1926).

Au II i: J. C. McLennan and A. B. McLay, Roy. Soc. Canada Trans. **22,** 103 (1928).

Hg II i: F. Paschen, Preus. Akad. Sitzungsber. p. 536 (1928).

Hg III i: J. C. McLennan, A. B. McLay, and M. F. Crawford, Roy. Soc. Canada Trans. **22,** 247 (1928);

[g]i: R. J. Lang and J. E. Mack, unpublished data.

Hg l: T. Lyman, Astrophys. J. **38,** 282 (1913); G. Déjardin. Ann. de Physique **8,** 424 (1927).

collected in Table I. The conventional notation[5] has a significance somewhat more limited here than in cases of normal coupling; the discussion at the end of this paper should be consulted for its exact meaning.

TABLE I. *The $5d^96s$ and $5d^96p$ energy levels of the platinum-like spectra. The $5d^96s$ levels are listed according to energy values; the $5d^96p$ levels, according to J-values. The numbers after the values of the Pt I levels, are the arbitrary symbols assigned to these levels by Haussmann.*

		Pt I		Au II	Hg III	Tl IV	Pb V
$5d^96s$	$^3D_3$	0		0	0	0	0
	$^3D_2$	775.9		2601.5	3179	3588	3944
	$^3D_1$	10132.0		12726.7	15556	18865	
	$^1D_2$	13496.3		14582.0	18235	21681	25234
$5d^96p$	$^3F_4$	37590.7	7	57455.7	75143	92617	110296
	$^3F_3$	34122.1	3	49964.2	62777	74783	86370
	$^3D_3$	40970.1	15	59752.1	78750	97217	115744
	$^1F_3$	49286.1	33	70660.8	(89637)		
	$^3P_2$	32620.0	1	48014.0	60699	72582	84043
	$^3D_2$	38815.9	10	58138.8	75698		
	$^3F_2$	44444.4	21	61620.5	78077	95285	113130
	$^1D_2$	51286.9	37	71526.0	91736		
	$^3P_1$	41802.7	16	58364.5	(75756)		
	$^1P_1$	49544.5	34	66620.2	83704	100233	?117075
	$^3D_1$	50055.3	36	70668.0	(93626)		
	$^3P_0$	46433.9	26	67574.5			

Several investigators have recently extended the wave-number system of Pt I, which was developed about thirty years ago by Snyder. Meggers and Laporte assigned the lowest levels to the configuration $5d^96s$, and the subsequent Zeeman effect work of Haussmann has confirmed their assignment. Mr. J. J. Livingood and Professor Shenstone have kindly put their unpublished data on the Zeeman effect in the platinum arc spectrum, at my disposal; this aid, and the wealth of material now available for comparison with other spectra, have made it possible to identify the $5d^96s$ and $5d^96p$ levels of Pt I.

In the palladium atom, the levels of the configuration d^9p are a good deal more stable than any other "odd" levels of the spectrum. In platinum, as in nickel, the levels of this configuration are sprinkled among those of the rich configuration d^8sp, which completely overlap it; but, as we shall see below, in platinum the usual criteria for sorting levels have almost completely broken down. Fortunately, three guides—first, the expectation of a fair degree of smoothness in the relative behavior of the energy levels in the isoelectronic sequence; second, the g-sum rule for the behavior of the levels in a weak magnetic field; the third, the relative intensities of the transitions $5d^86s^2 \leftarrow 5d^86s6p$, $5d^96s \leftarrow 5d^86s6p$, $5d^96s \leftarrow 5d^96p$ (one electron jump) and

[5] The orbital, spin, and total angular momenta of an atomic system as a whole are designated by capital letters L, S, J in accordance with a recommendation of the committee on spectroscopic notation, Phys. Rev. **33**, 900 (1929).

$5d^86s^2 \leftarrow 5d^96p$ (two electron jump)—were sufficient to allow the $5d^96p$ levels to be sorted from the others, with quite a high degree of certainty. The numbers after the values of the Pt I levels in Table I are the arbitrary numerical symbols used by Haussmann.

The levels of Au II were discovered and classified by McLennan and McLay. This classification was especially useful in the study of the d^9p

TABLE II. *Energy levels and lines of triply ionized thallium, Tl IV.*

			$(5d^9_{5/2}6s)_3$ or $5d^96s^3D_3$ 0	$(5d^9_{5/2}6s)_2$ or $5d^96s^3D_2$ 3588	$(5d^9_{3/2}6s)_1$ or $5d^96s^3D_1$ 18865	$(5d^9_{3/2}6s)_2$ or $5d^96s^1D_2$ 21681
$(5d^9_{5/2}6p_{1/2})_2$ or $5d^96p^3P_2$		72582	72582(7) 0	68995(5)+1	53717(3) 0	50901(3) 0
$(5d^9_{5/2}6p_{1/2})_3$	$^3F_3$	74783	74784(4)+1	71195(8) 0		53101(5)−1
$(5d^9_{5/2}6p_{3/2})_4$	$^3F_4$	92617	92617(6) 0			
$(5d^9_{5/2}6p_{3/2})_2$	$^3F_2$	95285	95285(2) 0	91684(4)−13	76423(2)+3	73606(5)+2
$(5d^9_{5/2}6p_{3/2})_3$	$^3D_3$	97217	97224(4)+7	93623(4)−6		75542(1C?)+6
$(5d^9_{5/2}6p_{3/2})_1$	$^1P_1$	100233		96643(3)−2	—	78553(3)+1

levels, which again in Au II are considerably more stable than any other "odd" levels.

McLennan, McLay, and Crawford have recently published a classification of Hg III. Most of their levels are confirmed by an independent investigation by Lang and Mack; but three (shown in parentheses in Table I)

TABLE III. *Classified lines of triply ionized thallium, Tl IV.*

Carroll			This investigation		
λ	ν	Int.	ν	Int.	Designation
1028.55	97224	4	97219	6	$d^9s^3D_3-d^9p^3D_3$
1034.74	96643	3	96655	4	$^3D_2-\ ^1P_1$
1049.48	95285	2	95277	5	$^3D_3-\ ^3F_2$
1068.11	93623	4	93624	5	$^3D_2-\ ^3D_3$
1079.71	92617	6	92622	6	$^3D_3-\ ^3F_4$
1090.70	91684	4	91689	5	$^3D_2-\ ^3F_2$
1273.03	78553	3	78557	6	$^1D_2-\ ^1P_1$
1308.50	76423	2	76426	4	$^3D_1-\ ^3F_2$
1323.76	75542	1 C?	75542	6	$^1D_2-\ ^3D_3$
1337.19	74784	4	74781	7	$^3D_2-\ ^3F_3$
1358.58	73606	5	73603	7	$^1D_2-\ ^3F_2$
1377.75	72582	7	72579	7	$^3D_3-\ ^3P_2$
1404.60	71195	8	71191	7	$^3D_2-\ ^3F_3$
1449.37	68995	5			$^3D_2-\ ^3P_2$
1861.6	53717	3			$^3D_1-\ ^3P_2$
1883.2	53101	5			$^1D_2-\ ^3F_3$
1964.6	50901	3			$^1D_2-\ ^3P_2$

C? Possibly due to carbon.

were derived from lines which are classified elsewhere or show such great wave-length discrepancies that they can not be treated with the same certainty as the others. An attempt to find $d^9p\ ^3P_1, ^3P_0, ^1F_3, ^3D_1$ and higher levels in Hg III has been, thus far, unsuccessful.

The condensed spark spectra of thallium and lead were photographed on the University of Michigan's one meter, 15,000 lines/inch grating spectro-

graph; the generous cooperation of Professor Sawyer made this part of the investigation possible. For thallium, the data are in good agreement with Carroll's in the region of overlapping; since Carroll measured his lines in several orders, his values are used. For lead, the new values are preferred in the region of overlapping.

TABLE IV. *Lines of the condensed spark discharge between thallium electrodes (supplimentary to Carroll's λ>1000).*

Carroll λ	This investigation λ	ν	Int.		Carroll λ	This investigation λ	ν	Int.	
	868.99	115076	2			955.88	104616	0	
	872.06	114661	0			956.8	10452	0	
	874.87	114303	1			958.36	104345	5	
	879.68	113678	0			958.69	104309	5	
	903.77	110648	3	C		959.73	104196	2	
	904.13	110604	5	C		960.16	104149	3	
	908.31	110095	1			960.85	104075	1	
	909.43	109959	4			962.00	103950	4	
	910.35	109848	2			962.87	103856	1	
	911.70	109685	2			964.75	103654	2	
	912.74	109560	3			965.45	103579	3	
	916.93	109060	4			966.60	103455	2	
	917.31	109014	5			966.85	103429	5	
	919.73	108728	2			967.51	103358	1	
	921.6	10851	0			968.55	103247	4	
	922.42	108410	1			970.39	103051	3	
	924.40	108178	1			974.69	102597	0	
	925.34	108068	1			976.00	102459	2	
	926.29	107958	2		977.02	977.03	102351	8	C977.031
	928.01	107757	3			979.38	102123	0	
	929.80	107550	1			989.57	101054	2	
	930.80	107435	5		993.66	993.73	100631	5	
	931.15	107394	1		995.5	995.57	100445	2	
	931.88	107310	1			1001.50	99850	0	
	932.32	107260	1			1002.25	99776	0	
	933.11	107168	4			1005.41	99462	0	
	933.69	107102	3			1006.17	99387	0	
	934.70	106986	4			1010.35	98976	2*d*	C
	935.61	106882	4			1022.9	9776	0	
	936.87	106738	5			1025.85	97480	1	
	937.62	106653	2			1030.07	97081	0	
	938.91	106506	1		1031.7	1031.85	96913	2	
	940.17	106394	3			1035.42	96579	0	
	940.59	106316	2		1036.60	1036.52	96477	4	C?
	941.54	106209	2			1036.92	96439	3	C?
	941.99	106158	1		1053.5	1053.50	94922	2	
	944.17	105913	?0		1054.80	1055.01	94786	0	
	944.45	105820	?0		1058.2	1058.21	94499	1	
	945.81	105729	2		1059.9	1059.98	94341	0*d*	
	948.28	105454	?0			1066.69	93748	1	
	948.82	105394	?0			1069.93	93464	0	
	950.09	105253	4						
	951.50	105097	1						
	952.24	105016	1						
	953.57	104869	2						
	954.57	104759	6						

?0 Existence of line uncertain.
C Carbon.
d Diffuse.

Tables II and V show the wave-number schemes for Tl IV and Pb V, respectively. The alternative notation for the levels is explained on page 33. For each line, two numbers are given: the intensity, in parentheses, and

the difference $\nu_{obs}-\nu_{calc}$ between the observed frequency of the line and the frequency calculated from the values assigned to the levels. The frequencies

TABLE V. *Energy levels and lines of quadruply ionized lead, Pb V.*

			$(5d^9_{5/2}6s)_3$ or $5d^96s^3D_3$ 0	$(5d^9_{5/2}6s)_2$ or $5d^96s^3D_2$ 3944	$(5d^9_{3/2}6s)_2$ or $5d^96s^1D_2$ 25234
$(5d^9_{5/2}6p_{1/2})_2$ or $5d^96p^3P_2$		84043	84044(6)+1	80097(3)−2	58813(00 Carroll)+4
$(5d^9_{5/2}6p_{1/2})_3$	$^3F_3$	86370	86368(8)−2	82427(6)+1	61136(00 Carroll) 0
$(5d^9_{5/2}6p_{3/2})_4$	$^3F_4$	110296	110296(8) 0		
$(5d^9_{5/2}6p_{3/2})_2$	$^3F_2$	113130	113128(x)−2	109192(6)+6	87892(8)−4
$(5d^9_{5/2}6p_{3/2})_3$	$^3D_3$	115744	115748(7)+4	111796(6)−4	90510(1) 0
$(5d^9_{5/2}6p_{3/2})_1$	$^1P_1$	?117075		113128(5−x)−3	91843(4)+2

? Existence of level uncertain.

of the four thallium lines $d^9s^3D_3$, $^3D_2-d^9p^3F_2$, $^3D_3$ derived from Carroll's measurements, show relatively high discrepancies; but a careful remeasurement of the intervals has verified this classification.

TABLE VI. *Classified lines of quadruply ionized lead, Pb V.*

Carroll λ	Int.	This investigation λ	ν	Int.	Designation
864.0	5	863.95	115748	7	$d^9s^3D_3-d^9p^3D_3$
883.9	4	883.95	113128	5	$^3D_3-\ ^3F_2$
					$^3D_2-\ ^?P_1$
894.4	4	894.49	111796	6	$^3D_2-\ ^3D_3$
906.7	7	906.65	110296	8	$^3D_3-\ ^3F_4$
915.9	3	915.82	109192	6	$^3D_3-\ ^3F_2$
1088.9	2	1088.82	91843	4	$^1D_2-\ ^?P_1$
1104.8	00	1104.85	90510	1	$^1D_2-\ ^3D_3$
1137.8	5*d*	1137.76	87892	8	$^1D_2-\ ^3F_2$
1158.0	8	1157.83	86368	8	$^3D_3-\ ^3F_3$
1190.1	7	1189.85	84044	6	$^3D_3-\ ^3P_2$
1213.4	5	1213.20	82427	6	$^3D_2-\ ^3F_3$
1248.6	2	1248.49	80097	3	$^3D_2-\ ^3P_2$
1635.7	00				$^1D_2-\ ^3F_3$
1700.3	00				$^1D_2-\ ^3P_2$

d Diffuse.

Tables III and VI are lists of the newly classified lines.

Table IV is a list of the lines observed in the condensed spark spectrum of thallium, in the region λ868 to λ1070, supplementary to Carroll's list. For the lines not listed, the present measurements are in agreement with Carroll's, with an average discrepancy of 0.04A. Table VII, for lead in the region $\lambda < 1280$ is similar except that here all the lines in the region are listed. Hydrogen λ1215.680 and Bowen and Ingram's lines[6] were used as standards. Since it was necessary to extrapolate from λ833, the shorter wave-lengths in the thallium list may be in error by as much as 0.3A in absolute value. The probable random error is about 0.05A.

[6] I. S. Bowen and S. B. Ingram, Phys. Rev. **28**, 444 (1926).

TABLE VII. *Lines of the condensed spark discharge between lead electrodes.*

Carroll λ	Carroll Int.	This investigation λ	This investigation ν	This investigation Int.	This investigation Assignment
		474.81	210610	3	
		477.75	209314	2	
		495.92	201645	4	
		497.8	20090	?0	
		499.39	200244	4	
		514.49	194367	2	
		529.5	18886	1	
		541.11	184805	1	
		542.31	184396	3	
		569.77	175509	4	
		572.36	174715	3	
		648.22	154279	2*d*	
		652.56	153243	3*pd*	
		653.46	153032	?0	
		655.82	152439	3	
		689.8	14498	0	
		694.35	144020	1	
		703.63	142120	2	0? 703 blend
		706.06	141631	0	
		707.39	141365	1	
		708.97	141050	2	
		717.05	139460	1	
		718.07	139262	2	
		719.17	139049	1	
		721.46	138608	1	
		728.59	137251	4	
		739.49	135228	1	
		741.89	134791	4	
		749.09	133495	3*p*	
		752.6	13288	1*p*?	
		754.93	132463	4	
		755.73	132322	3	
		760.9	13142	0	
		762.85	131087	1	
		764.57	130792	2	
		765.74	130593	1	
767.5	0	767.38	130314	6	
		769.48	129958	4	
		771.28	129655	5	
		772.51	129448	2	
		775.58	128936	3	
		781.3	12798	2*p*	
		782.14	127854	4	
		783.40	127649	2	
786.48	1				
787.73	2	787.74	126945	4	0 787.716
790.21	3	790.21	126549	1	0 790.205
		795.35	125731	4	
796.58	0	796.8	12550	1*d*	0? 796.665
		798.79	125189	0*d*	
		799.76	125076	1*d*	
		800.37	124942	1*d*	
802.07	1	802.03	124684	5	
		802.96	124539	0	
804.8	00?	804.55	124293	1	
806.3	00?	806.09	124056	2	
		807.12	123897	0	
		808.40	123701	2	
		809.59	123519	3	
		811.8	12319	?1	
		812.58	123065	4	
		813.26	122962	2	
815.91	1	815.76	122585	3ν	
		816.96	122405	3	
		818.15	122227	2	
819.5	0	819.25	122063	3	
		821.32	121728	0	
		822.86	121527	1	
		826.1	12105	?0	
826.9	0	826.72	120960	3	
827.8	0	827.63	120827	2	
		828.63	120681	3	
829.32	0	829.28	120587	2	
830.3	0	830.10	120467	6	
834 group		832.7	12009	1*d*	0 832 blend
834.5	3	834.46	119838	4	0 834.459
835.4	3	835.4	11970	1	0 835 blend
		836.03	119613	0	
		838.42	119272	1*d*	
		839.6	11911	?0*d*	
		840.99	118908	5	
		842.33	118718	2*d*	
		842.81	118651	1*d*	
		844.84	118366	4ν	
		845.96	118209	4	
		847.8	11795	0	
849.6	00	849.57	117707	6	
852.1	00	851.98	117374	2	
		853.07	117224	2	
		854.46	117033	0	
854.9	00?	854.81	116985	?0	
857.8	0	857.63	116600	6	
		858.91	116427	1	
		860.6	11620	?0	
862.5	0	862.36	115961	5	
864.0	5	863.95	115748	7	Pb V
		865.4	11555	0	
		867.16	115319	0	
		867.94	115215	0	
870.5	3	870.44	114884	5	
		872.57	114604	2	
		879.9	11364	0*d*	
883.9	4	883.95	113128	5	Pb V
885.0	1	884.98	112997	6	
		887.3	11271	1	
888.5	3	888.41	112561	5	
890.8	4	890.78	112261	7	Pb IV?
894.4	4	894.49	111796	6	Pb V
		896.10	111595	5	
903.6	3	903.7	11065	?0	C
		904.17	110599	4	C
		904.74	110529	0	
906.7	7	906.65	110296	8	Pb V
908.5	0	908.54	110067	5	
		915.08	109280	0	
915.9	3	915.82	109192	6	Pb V
916.8	0				
918.1	1*d*	917.96	108937	6	
920.4	3	920.32	108658	5	
		920.95	108584	1	
922.5	4	922.48	108403	10	Pb IV?
923.4	1	923.52	108281	2	
924.5	0	924.59	108156	3	
		926.32	107954	4	
927.7	3	927.70	107794	6	
		930.50	107469	1	
932.3	3	932.23	107270	7	
933.7	0*d*	933.8	10708	?0	
937.2	2*d*	937.10	106712	5	
		940.74	106299	1	
944.6	00?				
946.4	00?				
		953.00	104932	4	
954.4	5	954.34	104784	6	
955.5	00?	955.33	104676	3	
		959.01	104274	2	
		960.93	104066	5	
		967.15	103396	4*d*	
970.3	0?	970.28	103063	1	
		974.27	102641	2*d*	
977.0	4	977.03	102351	8	C 977.031
		978.4	10221	0	
		979.47	102096	2	
981.2	0	981.07	101930	6	
		982.20	101812	1	
		989.15	101097	3	
		991.43	100864	2	
995.8	2	995.74	100428	8	
		997.0	10030	1	
		1002.9	9971	0	
1005.5	1	1005.56	99447	7	
		1007.7	9924	0	
		1009.5	9906	1	
		1011.05	98907	2*d*	
1012.5	00	1012.45	98770	3	
1021.4	00				
1022.2	00	10. 96	97842	0	
		1024.30	97628	2	

? (before intensity) Existence of line uncertain.
d Diffuse.
p Pair.
ν Diffuse toward shorter wave-lengths.

TABLE VII. (continued)

Carroll λ	Carroll Int.	This investigation λ	This investigation ν	This investigation Int.	Assignment
1028.7	10	1028.57	97222	8	Pb IV?
1030.5	3	1030.36	97054	6	
		1032.04	96896	2	
		1036.3	9650	0	
		1037.02	96430	2	
1041.3	3*d*	1041.10	96052	4*d*	
		1044.3	9576	2*d*	
1048.9	12	1048.84	95344	12	
1051.4	0				
1052.3	2	1052.21	95038	5	
		1053.8	9490	0	
		1056.43	94658	3	
		1059.3	9440	1	
1060.6	0	1060.63	94284	5	
1062.8	1*d*	1062.63	94106	0*d*	
1068.0	00				
1069.2	4	1069.07	93539	8	
		1070.83	93386	0	
1072.1	1	1072.05	93279	6	
1073.1	1	1073.1	9319	0	
1074.7	3	1074.63	93055	7	
1076.8	3	1076.72	92875	4	
		1079.81	92600	3	
1080.8	0	1080.85	92520	3	
		1082.51	92378	2	
		1084.12	92241	3	
1087.6	1	1087.34	91968	2	
1088.9	2	1088.82	91843	4	Pb V?
1090.1	0	1089.90	91752	1	
1094.3	00	1094.1	9140	1*d*	
1096.5	1*d*	1096.47	91202	2	
		1097.34	91129	0	
1098.4	0*d*	1098.37	91044	6	
		1098.7	9102	0	
1099.2	1*d*				
		1100.46	90871	2	
1103.6	0*d*	1103.7	9061	6*d*	
1104.8	00	1104.85	90510	1	
1105.6	00				
1108.7	1	1108.40	90220	5	
		1109.69	90115	3	
		1111.43	89974	1	
		1112.89	89856	0	
1115.0	2	1114.93	89692	7	
1116.2	4	1116.09	89598	7	
1117.4	0				
1118.9	00?	1118.60	89397	3	
1119.9	00	1119.56	89321	4	
		1121.19	89191	3	
1123.7	3	1123.45	89012	3	
1131.9	00				
1133.2	2	1133.09	88254	5	
1137.8	5*d*	1137.76	87892	8	Pb V
1142.9	1	1142.86	87500	6	
1145.0	3	1144.83	87349	6	
		1146.6	8722	0	
1148.3	0	1148.17	87095	4	
		1150.8	8690	0	
		1155.88	86514	2	
1158.0	8	1157.83	86368	8	Pb V
1165.1	4	1164.96	86840	8	
1167.0	4	1166.89	86698	8	
		1170.75	86415	1	
		1171.68	85347	2	
		1174.93	85111	2	C 1174.922
1176.0	00	1175.66	85059	4	C blend
		1176.32	85011	2	C 1176.359
		1178.47	84856	1	
1185.6	6	1185.37	84362	6	
1190.1	7	1189.85	84044	6	Pb V
1197.8	2	1197.68	83495	5	
1199.5	0				
1203.6	3	1203.4	8310	7	
1206.6	0	1206.61	82877	3	
1213.4	5	1213.20	82427	6	
		1214.21	82358	?1	
1215.8	2	1215	plate broken here		H 1215.680
1231.3	1	1231.15	81225	5*d*	
1233.6	3	1233.53	81068	5	
		1247.39	80167	0	C 1247.391
1248.6	2	1248.49	80097	3	Pb V
1250.6	4	1250.36	79977	6	
		1258.19	79479	?0	
		1260.94	79306	2	
		1264.52	79081	1*d*	
1266.9	1	1266.64	78949	7	
1274.6	0	1274.45	78465	5	
		1275.53	78399	2	
1279.5	3	1279.31	78167	6	

TABLE VIII. *Regular doublet screening numbers, $Z-Z_{eff}$, for shells lacking one d electron.*

Spectrum		I		II		III		IV		V	X-rays
$3d^9$	^2D 27 Co I, etc.	*1232.45a*		*1507*		*2070*					
		13.398	−0.299	13.697	0.182	13.515					
		−0.295		0.181		0.145					
$3d^9 4s$	^3D 28 Ni I, etc.	*1508.29*		*2069.7*		*2754*		*3575*		*4536*	
		13.693	0.177	13.516	0.146	13.370	0.121	13.249	0.088	13.161	
		0.127		0.094							
$3d^9 4s^2$	^2D 29 Cu I, etc.	*2042.9*		*2719.06*							
		13.566	0.144	13.422							
$3d^9 4s^2 4p^6$....											13.0
$4d^9$	^2D 45 Rh I, etc.	*2348.1*		*3539*							
		25.171	1.141	24.030							
		1.115		0.457							
$4d^9 5s$	^3D 46 Pd I, etc.	*3529.8*		*4574.8*		*5766.1*		*7108*		*8620*	
		24.056	0.483	23.573	0.395	23.178	0.333	22.845	0.293	22.552	
				0.252							
$4d^9 5s^2$	^2D 47 Ag I, etc.			*5634.8*							
				23.321							
$4d^9 5s^2 5p^6$....											24
$5d^9$	^2D 77 Ir I, etc.										
$5d^9 6s$	^3D 78 Pt I, etc.	*10132.0*		*12726.7*		*15556*		*18865*		(*22.6 · 10³*)	
		44.215	0.982	43.233	0.841	42.392	0.857	41.535		(40.7)	
		0.660		0.532							
$5d^9 6s^2$	^2D 79 Au I, etc.	*12274*		*15038*							
		43.555	0.854	42.701							

a Possibly belongs to the configuration d^7s^2
( ) Extrapolated.

Table VIII is an extension of a table started by Laporte[7] when he applied the regular doublet law of x-ray spectroscopy (below, Eq. (3)) to d^9 doublets in the optical region. The doublet or triplet separation, and the screening number, are given for every spectrum with a configuration d^9, d^9s, or d^9s^2. The corresponding x-ray $M_{32}M_{33}$ and $N_{32}N_{33}$ screening numbers are included. The regularity of the separations is now recognized as a special case of Goudsmit's Γ sum rule.[8] Separations are given in italic, screening numbers in ordinary light face, and screening number differences in bold face type.

The slight increase in screening which occurs with the addition of an s electron (except in the case of Ni II, where the decrease is about as large as the probable error) becomes increasingly important with increasing atomic number. The addition of a second outer s electron to form a stable shell, has naturally more effect on the screening than the addition of the first. This property has often been observed in connection with the first order screening, that is with absolute term values; here we see it influencing the separations.

The downward slope of the screening number in an isoelectronic sequence also, becomes considerably greater as we go down in the periodic table; this fact, combined with the great magnitude of the separations themselves, made the predictions in the platinum-like sequence crude compared with those for the lighter atoms.

TABLE IX. *Mean distances (centroid distances) between configurations: d^9s-d^9p and $d^{10}s-d^{10}p$.*

Spectrum	I		II		III		IV		V
$3f^94s-3f^94p$ Ni I, etc.	28740		46705		63247		79459		95550
		17965	**1423**	*16542*	**330**	*16212*	**121**	*16091*	
$3d^{10}4s-3d^{10}4p$ Cu I, etc.	30700		49063		66313		83169		99875
		18363	**1113**	*17250*	**394**	*16856*	**150**	*16706*	
$4f^95s-4f^95p$ Pd I, etc.	28913		43879		57677		71067		84305
		14966	**1168**	*13798*	**408**	*13390*	**152**	*13238*	
$4d^{10}5s-4d^{10}5p$ Ag I, etc.	30165		45790		60080		73894		87557
		15625	**1335**	*14290*	**476**	*13814*	**151**	*13663*	
$5f^96s-5f^96p$ Pt I, etc.	36836		54308		(70600)		(86600)		(102500)
		17472		(*16300*)		(*16000*)		(*15900*)	
$5d^{10}6s-5d^{10}6p$ Au I, etc.	39902		57571		74032		90190		
		17669	**1208**	*16461*	**303**	*16158*			

( ) Extrapolated.

Table IX shows the progress of the "irregular doublet" separation $s-p$ for atomic systems built upon the ion configurations d^9 and d.[10] The centroid (with each level assigned the weight $2j+1$) is taken as the best representative energy value for the configuration. The regularity of the other sequences indicates that the extrapolated values for Hg III, Tl IV, and Pb V are probably correct within about 200 units. First differences are in italic, and second differences in bold face type.

The spectra of the systems built upon the ion d^9 are very much like those built upon d^{10}, so far as the mean differences $s-p$ are concerned. The distance is about the same for Ni I as for Pd I; but its slope with increasing

[7] O. Laporte, Phys. Rev. **29**, 650 (1927).
[8] S. Goudsmit, Phys. Rev. **31**, 946 (1928).

nuclear charge is much greater in the first sequence than in the second. For Pt I the distance is more than one-fourth greater than for Ni I and Pd I, and the initial slope is almost as great in the third sequence as in the first; so the separation in Pb V is about ten percent greater than in Ge V and twenty percent greater than in Sn V.

III. The Vector Coupling

The absolute energy of an atom with a given net nuclear charge and a given electronic configuration may be determined approximately by certain well-known laws which apply quite independently of whether the spectrum is of the normal type.[4b] The special interest attached to the spectra we are considering lies in the relative behavior of the levels within each configuration. Naturally our study is based on the fundamental work of Goudsmit[9] and Uhlenbeck,[10] who pointed out the significance of the departures from the normal type, from the viewpoint of the vector model, using the $2p^5 3s$ and $2p^5 3p$ configurations of neon as an example. The configurations $d^9 s$ and $d^9 p$ are in fact close analogues of the famous example. The nickel-like spectra $3d^9 4s$, $3d^9 4p$ have already been treated in detail, under Professor Laporte's direction.[4b] We can now study the relative trends in fifteen spectra, in three closely analogous sequences.

First, however, let us glance at two theoretical "pure" coupling schemes.[10] In the normal, Russell-Saunders, or LS coupling scheme

$$(l_1 l_2)(s_1 s_2) = (LS) = J \tag{1}$$

the atom is characterized by a constant or "quantized" resultant orbital angular momentum L and a constant angular momentum of electronic spin S. The subscripts 1 and 2 refer to the ion and the added electron, respectively. In the jj coupling scheme

$$(l_1 s_1)(l_2 s_2) = (j_1 j_2) = J \tag{2}$$

the ion (that is, the whole system except the most loosely bound electron) is characterized by a total angular momentum j_1; and the electron by a total angular momentum j_2.

There are three criteria for the empirical study of the vector coupling in a complex spectrum: (a) relative energy values, (b) behavior in a magnetic field, and (c) line intensities. The spectra in our sequences will be compared among themselves and with these "pure" cases, with respect to these properties.

(*a*) *Relative energy values.* Figures 1, 2, and 3 show the relative positions of the levels in each configuration. Unit distance for each spectrum is taken to be the total separation of the $d^9 s\ ^3D$ (Table VIII). The zero of the figure, for each configuration, is arbitrarily chosen at the centroid.

The LS equation (1) yields, of course, normal triplets and singlets. The separations within a triplet are proportional to the higher j-values (Landé's

[9] S. Goudsmit, Zeits. f. Physik **32**, 794 (1925).
[10] S. Goudsmit and G. E. Uhlenbeck, Zeits. f. Physik **35**, 618 (1926).
[11] S. Goudsmit and C. J. Humphreys, Phys. Rev. **31**, 960 (1928).

rule[2]); the relative separations of the several d^9p triplets might be determined, with the use of one more empirical constant (Goudsmit's rule[11]). But the theory can not yet tell us the distance between multiplets; it can only say, that the distances between certain of them are large compared with the unit chosen in the figures. Due to this incompleteness of the theory it would be impossible to show the LS case in the figures.

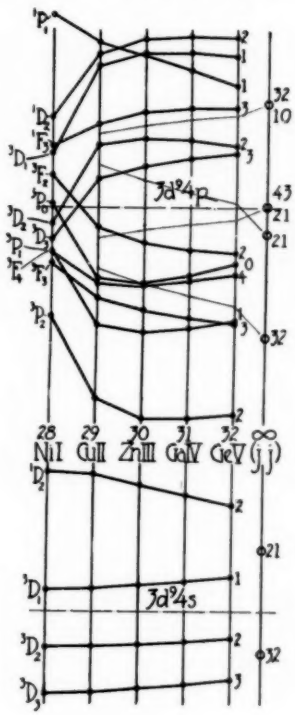

Fig. 1.

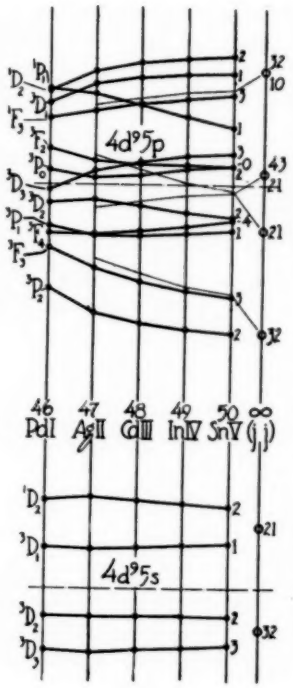

Fig. 2.

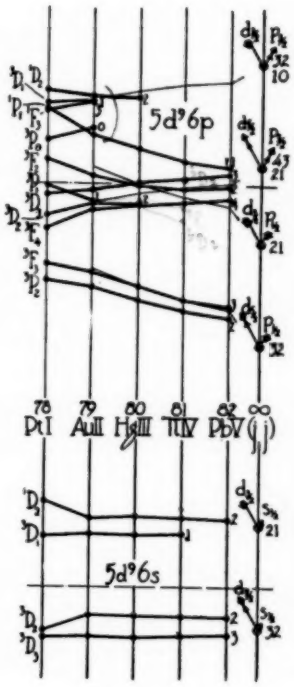

Fig. 3.

Relative positions of the levels in each configuration.

In the jj case, Eq. (2), on the other hand, we have definite knowledge of the gross structure of each configuration, at the expense of exact knowledge of the fine structure. This definite knowledge of the gross structure is given by the Sommerfeld regular doublet law

$$\Delta\nu = \frac{\alpha^2 R Z_{eff}^4}{n^3 l(l+1)} \cdot \tag{3}$$

The d^9s configuration splits into two groups; the duplicity arises from the doublet nature of the ion d^9. The d^9p configuration splits into four groups, due to the doublet nature of both d^9 and p.[12]

We can easily determine the interval between the states arising in the case of jj coupling from the two values $j_1 = 5/2$ and $j_1 = 3/2$ of the ion d^9 or

[12] It was supposed in a previous paper (4b) that the separation due to the p electron would be negligible, in this asymptotic case. The authors of that paper are indebted to Professor Goudsmit for pointing out this error.

minus d doublet, provided j_2 be kept constant. This interval is the same for both configurations d^9s and d^9p (neglecting a slight difference in screening). It is simply the total separation of the $d^9s\ ^3D$ (unity, in the figure); this is the special case of the Γ sum rule, mentioned in connection with Table VIII.

The calculation of the interval between $j_2=1/2$ and $j_2=3/2$ (with j_1 kept constant) for d^9p is a little more complicated. We shall consider two cases: large net charge, and small net charge. As the nuclear charge increases in a given sequence, the system approaches asymptotically a condition in which we may neglect the penetration of the p orbit and the difference between Z_{eff} for the p separation and Z_{eff} for the d separation. Then the ratio of the p separation to the minus d separation (cancelling the numerators on the right-hand side of Eq. (3)) is

$3^3\cdot 2\cdot 3/4^3\cdot 1\cdot 2=1.27$ for the nickel-like spectra,
$4^3\cdot 2\cdot 3/5^3\cdot 1\cdot 2=1.54$ for the palladium-like spectra, and
$5^3\cdot 2\cdot 3/6^3\cdot 1\cdot 2=1.74$ for the platinum-like spectra.

The relative positions of the several groups of levels for this case, are plotted in the figures, in the columns labeled "∞_{jj}".

Where the net charge for the outer part of the orbit under consideration is small compared with the Z_{eff} of Eq. (3), as it is for the p separations of all our spectra, we must use the modification of (3) introduced by Landé for penetrating orbits:

$$\Delta\nu=\frac{\alpha^2 R Z_{\text{inner}}^2\, Z_{\text{outer}}^2}{n_{\text{eff}}^3 l(l+1)}\,. \tag{4}$$

We can calculate the separation for the d^9p configurations of the spark spectra of our sequences, by comparison with the principal doublet $d^{10}p\ ^2P$ separation, for the copper-, silver-, and gold-like spectra of the same atoms. It is not even necessary to calculate any new screening numbers. The effect of the tenth d electron, on the inner effective charge Z_{inner} may be neglected; while the outer effective charge Z_{outer} is given by the roman numeral which designates the spectrum. The following table gives the (configuration centroid) values of n_{eff} for the added p electron, calculated from the first two members of the s series, uncorrected:

d^9p	Ni I	1.87	Cu II	2.13				
$d^{10}p$			Cu I	1.82	Zn II 2.11	Ga III 2.31	Ge IV 2.46	As V 2.58
	Pd I	1.83	Ag II	2.17				
			Ag I	1.83	Cd II 2.16	In III 2.41	Sn IV 2.58	Sb V 2.74
	Pt I	1.72	Au II	2.11				
			Au I	1.73	Hg II 2.10	Tl III (2.40)	Pb IV(2.60)	Bi V (2.77)

The numbers in parentheses are extrapolations. Whenever this approximate n_{eff} is known for a d^9p configuration, it is almost the same as for the corresponding $d^{10}p$ configuration with the same net charge. We may use this fact in extrapolating the values of n_{eff} for the d^9p configurations. The errors due to the crudity of this approximation will tend to cancel out in the ratio, which is all that is needed for our purposes. Let us consider an example. For Hg II $d^{10}p$ the p separation is 9123. For Hg III it will be, by Eq. (4),

$9123 \cdot 3^2 \cdot 2.10^3/2^2 \cdot 2.40^3 = 15720$. The approximate positions of the four groups into which the d^9p configurations would fall for the *jj* coupling case, calculated in this way, are shown by the light lines in the figures, connected with their respective "∞_{jj}" groups. It will be noticed that these calculations are completely independent of the empirical d^9p separation data.

Among empirical data, the comparison of energy values is the most accurately measurable of the three criteria for the study of coupling; it is also generally the first to indicate a breaking away from normal coupling. The figures show hardly any indication of similarity to normal spectra, even for Ni I, the most nearly normal of all; but we shall see below, that the Zeeman effect and line intensity data clearly show the *LS* character of several of these spectra.

Many of the levels show certain trends with increasing nuclear charge in an isoelectronic sequence, and the same trends with constant net charge but "passing down the column" in the periodic table; that is, Figs. 2 and 3 act something like successive extrapolations to the right, of Fig. 1. This behavior is most easily apparent in the simpler configuration d^9s. A table started earlier[4b] can be extended now, showing numerically the progress of the distance $d^9s\ {}^3D_2 - {}^3D_3$ in the figures; the values are:

LS coupling:	0.600				
Ni I, Cu II, etc.:	0.448	0.444	0.428	0.407	0.384
Pd I, Ag II, etc.:	0.337	0.345	0.330	0.309	0.287
Pt I, Au II, etc.:	0.077	0.204	0.204	0.190	0.170
jj coupling:	0.000				

Though the trend is not monotonically downward the tendency is unmistakable.

There is an anomalous break in the $d^9s\ {}^3D_2$, ${}^1D_2$ curves at Pt I. This is the only exception to a regularity that persists among all the other known triplet-singlet configurations (except where the triplet separation is quite small). But the present assignment of d^9s levels in Pt I can not be avoided without making the anomaly much worse.

The d^9p levels show a decided tendency among the more highly ionized members of the palladium-like sequence, to form four groups. The grouping there agrees with the calculated *jj* grouping except that the levels $J=4$ and $J=0$ are too low. Although the data for the platinum-like sequence unfortunately are incomplete, the indications are that the configuration has arrived at a state of more nearly pure *jj* coupling. Toward the right-hand side of Fig. 3 both of the well-developed groups $J=2, 3$ and $J=4, 2, 3, 1$, are relatively much more concentrated than in Fig. 2, and here the quantitative agreement of the energies with the values independently calculated for the *jj* coupling (light lines in the figures) is quite satisfactory.

(*b*) *Behavior in a magnetic field.* Table X shows all the *g*-values available for our spectra, together with those calculated for the "pure" *LS* and *jj* cases:

$$g_{LS}=\frac{L}{J}g_L\cos(LJ)+\frac{S}{J}g_S\cos(SJ)=\frac{3J(J+1)+S(S+1)-L(L+1)}{2J(J+1)}$$

and

$$g_{jj}=\frac{j_1}{J}g_{j_1}\cos(j_1J)+\frac{j_2}{J}g_{j_2}\cos(j_2J)$$

$$=g_{j_1}\frac{J(J+1)+j_1(j_1+1)-j_2(j_2+1)}{2J(J+1)}+g_{j_2}\frac{J(J+1)+j_2(j_2+1)-j_1(j_1+1)}{2J(J+1)}.$$

TABLE X. *Zeeman effect data.*

Calculated *LS* coupling		Observed g-values					Calculated *jj* coupling		
structure	g_{LS}	Ni I	Cu II	Pd I	Ag II	Pt I	g_{jj}	J	structure
$d^9p\ ^1F_3$	1.00		1.1	1.09	1.10	1.2	$1.07=\frac{16}{15}$	3	$-d_{3/2}+p_{3/2}$
$^1D_2$	1.00		*n*	1.17	1.20	1.1	$1.07=\frac{16}{15}$	2	
$^3D_1$	0.50		*n*	0.85	0.52	0.87	$1.07=\frac{16}{15}$	1	
$^3P_0$	0/0						0/0	0	
$^3F_4$	1.25		*n*	1.25	1.26	1.2	$1.25=\frac{5}{4}$	4	$-d_{3/2}+p_{3/2}$
$^3D_3$	1.33		1.0	1.33	1.25	1.12	$1.24=\frac{223}{180}$	3	
$^3F_2$	0.67		*n*	0.7	0.92	1.2	$1.21=\frac{109}{90}$	2	
$^1P_1$	1.00	1.00	*n*	0.80	1.00	1.24	$1.10=\frac{11}{10}$	1	
$^3D_2$	1.17		*n*	1.00	0.87	0.8	$0.77=\frac{23}{30}$	2	$-d_{3/2}+p_{1/2}$
$^3P_1$	1.50		*n*	1.42	1.50	0.9	$0.83=\frac{5}{6}$	1	
$^3F_3$	1.08		*n*	1.1	1.08	1.21	$1.11=\frac{10}{9}$	3	$-d_{5/2}+p_{1/2}$
$^3P_2$	1.50		*n*	1.50	1.50	1.39	$1.29=\frac{58}{45}$	2	
$d^9s\ ^1D_2$	1.00		*n*	1.00	1.03	1.17	$1.10=\frac{11}{10}$	2	$-d_{3/2}+s_{1/2}$
$^3D_1$	0.50		*n*	0.50	0.50	0.50	$0.50=\frac{1}{2}$	1	
$^3D_2$	1.17		*n*	1.15	1.13	1.01	$1.07=\frac{16}{15}$	2	$-d_{5/2}+s_{1/2}$
$^3D_3$	1.33		*n*	1.33	1.33	1.3	$1.33=\frac{4}{3}$	3	

n Normal, within probable error of 0.1.

The empirical values were derived in a few cases from blends, by Russell and Shenstone's method;[13] but usually from resolved patterns. The largest

TABLE XI. *Intensities.*

																	$3d4s$	$^3D_3$	$^3D_2$	$^3D_1$	$^1D_2$			
																		Cr V						
																	$3d4p\,^5F_4$	8						
																	$^3F_3$	0	7		—			
																	$^3F_2$	—	0	6	—			
																	$^3D_3$	7	1		—			
																	$^3D_2$	3	5	1	—			
																	$^3D_1$		2	4	—			
																	$^3P_2$	7	5	—	—			
																	$^3P_1$		5	3	—			
																	$^3P_0$			3				
																	$^1F_3$	—	—		7			
																	$^1D_2$	—	0	0	6			
																	$^1P_1$		—	—	3			
d^9s	$^3D_3$	$^3D_2$	$^3D_1$	$^1D_2$	$^3D_3$	$^3D_2$	D_1	$^1D_2$	$^3D_3$	$^3D_2$	D_1	$^1D_2$	$^3D_3$	$^3D_2$	$^3D_1$	$^1D_2$									
		Ni I				Cu II				Zn III				Ga IV[4b]					Ge V[4c]					
$3d^94s\,^3F_4$	9.5				10				8				8					7						
$^3F_3$	6.6	8.6		7.8	4	10		6	4	5		4	5	8		2		5	5		0			
$^3F_2$	0.9	5.2	9.1	2.7	3	4	8	0	4*c*	5	5	2	1	5	8	0		—	4	5	0			
$^3D_3$	6.6	6.4		6.5	8	—		9	4	—		5	5	0		8		5	0		0			
$^3D_2$	0.7	10.0	5.2	5.0	1	8	3	7	1	4	4*c*	4	0	5	3	6		—	6	3	5			
$^3D_1$		0.1	8.8	0.2		2	7	4		3	3	4*c*		2	5	2			2	4	0			
$^3P_2$	10.0	5.3	1.0	0.4	10	5	2	7	5	3	2	2	8	1	0	1		6	0	0	0			
$^3P_1$		8.6	6.7	1.0		8	5	2		5	4	4		5	2	1			8*c*	1	4			
$^3P_0$			7.0				5				4				3					5				
$^1F_3$	5.0	5.5		12.4	7	6		6	4	3		5	5	5		9*c*		6	5		5			
$^1D_2$	0.3	1.3	0.2	9.3	2	2	5	5	3	4	4	4	1	3	4	5		2	3	4	8			
$^1P_1$		4.0	1.7	10.6		1	1	5		2	3	5		0	2	6			—	1	4			
		Pd I				Ag II				Cd III[4d]				In IV[4d]					Sn V					
$4d^95p\,^3F_4$	10				10				8				8					8						
$^3F_3$	5	10		2	7	9		8	6	8		4	3	5		1		3	6		2			
$^3F_2$	—	0	5	2	—	5	7	8	1?	5	5	5	1	4	3	2		0	5	2	4			
$^3D_3$	10	3		2	8	5		8	6	4		5	5	4		—		6	2?		2			
$^3D_2$	1	5	2	2	1	8	8	1	1?	4	6	3	1	4	4	2		?	6	5	4			
$^3D_1$		2	3	2		2	6	0		4	5	2		2	4	2			3	4	1			
$^3P_2$	20	1	0	2	10	3	2	3	8	2	1?	2	6	?	—	3		8	?	—	1			
$^3P_1$		10	1	1		8	6	6		6	3	3		4	1	1			5	2	3			
$^3P_0$			3				7				4				4					4				
$^1F_3$	1	3		5	2	4		8	3	4		6	2	3		6		2	4		6			
$^1D_2$	1	2	3	2	1	2	4	6	2	3	4	6	1	1	3	5		—	1	5	5			
$^1P_1$		0	3	2		2	1	8		2	4	5		2	3	5			2	2	3			
		Pt I[4c,f]				Au II				Hg III[4g]				Tl IV					Pb V					
$5d^96p\,^3F_4$	10				10				10				6					8						
$^3F_3$	7	10		—	8	9		6	8	8		3	4	8		5		8	6		0			
$^3F_2$	0	1	3	2	1	2	7	6	9	6	8	7	2	4	2	5		5*c*	6		8			
$^3D_3$	1	2*c*		3*c*	9	7		4	8	9		4	4	4		1*c*		7	6		1			
$^3D_2$	—	3	3	1	4	9	7	1	5	8	6	6												
$^3D_1$		0	1	1		4	7	2																
$^3P_2$	17	3	1	1	10	7*c*	2	6	8	7	0	3	7	5	3	3		6	3		0			
$^3P_1$		1	3	—		7	2	7																
$^3P_0$			1				6																	
$^1F_3$	0	2		1	2	3		9																
$^1D_2$	0?	0	1	1	4	6	6	7	1	5	2	8												
$^1P_1$		—	0	1		6	3	8		6	5	6		3	—	3			?5*c*		?4			

— Permitted line missing.
c Line also classified elsewhere.
? (before intensity) Existence of level uncertain.
? (elsewhere) Existence of line uncertain.

probable errors (depending on blends) are about 0.1, but for most levels the probable errors are in the neighborhood of 0.03. In the interesting cases

[13] A. G. Shenstone, article forthcoming in Phil. Mag.

of multiply ionized atoms the lines lie in the ultra-violet, generally beyond the reach of present day Zeeman-effect technique.

If only the g-values were considered, clearly the designations $^3D_2$ and $^1D_2$ of the d^9s configuration of Pt I would have to be interchanged. Similarly in the case of several of the d^9p levels the g's pass somewhat beyond the asymptotically expected values. Marked transient disturbances, too, occur in the intermediate coupling cases of Cu II $J=3$ and Pd I $J=1$. But for the rest, there appears to be a trend toward the g_{jj} values.

(*c*) *Line intensities.* The evaluation of relative intensities is especially difficult for the heavy atoms, because of the large separations of related levels. For Pt I, for instance, the transition $d^9s \leftarrow d^9p$ extends from the green to the edge of the Schumann region; one "multiplet" $^3D-{}^3D$ covers the range from λ3485 to λ2028.

Table XI shows the relative intensities in our spectra, along with those for Cr V $3d4s-3d4p$, which is inserted as an example of a normal-type complex spectrum for a many times ionized atom. The intensities for some spectra have been multiplied by a factor so that the numbers for the several spectra are of the same order of magnitude.

Where the lists of several investigators are available for the lines of an element, even the best show wide disagreements in intensity, particularly in the Schumann region. For instance, the two available lists give the following intensities for the "multiplet diagonals" $^3D_3-{}^3F_4$, $^3D_2-{}^3F_3$, etc., of In IV:

Gibbs and White:	15, 10, 6; 10, 8, 7; 12, 7, 7
Carroll:	5, 6, 3; 5, –, 4; 2, 5, 3.

(The dash, –, indicates that the line $^3D_2$–$^3D_2$ is missing in Carroll's list, although it lies in the region reported by him.) It is impossible then in the present state of our knowledge of intensities, to distinguish between two influences: the crudity of the data, which has introduced spurious apparent changes; and actual changes in the character of the levels, which probably have influenced the relative intensities.

But at least we can say that in only three of our spectra, Ni I, Pd I, and Ag II, is the evidence of the intensities sufficient for the unambiguous assignment of complete names (including multiplicities and L-values) to the levels in these spectra. As examples of the ambiguities, the cases of $^3D_3$ and $^1F_3$ in the nickel-like spectra and $^3F_2$ and $^3D_2$ in the palladium-like spectra are instructive.

IV. Discussion

Significance of the jj coupling. Three kinds of terms contributing toward the total energy, play important rôles in the relative separations of the levels of a configuration: first, the mutual spin interaction energy term[14]

[14] From the viewpoint of this vector model discussion it is immaterial whether the terms discussed are interaction terms in a strict sense, or not. Large $(s_i s_k)$ interaction, for instance, means here simply that levels whose vector pictures differ only in the resultant of s_i and s have greatly different energies.

whose importance in normal spectra is represented by the close coupling or association of the spins $(s_i s_k)$ in Eq. (1); second, the mutual orbital interaction $(l_i l_k)$, which shares the importance of $(s_i s_k)$ in Eq.(1); third, the orbit-spin interaction $(l_i s_i)$, which determines the multiplet separations or more generally the Goudsmit γ's.[8] This last term is small for normal coupling, but becomes predominant in the case of *jj* coupling, Eq. (2). (The small $(l_i s_k)_{k \neq i}$ term may be neglected except for extremely light atoms.[15])

We were able to solve quantitatively for the asymptotic behavior of the separations in the *jj* case, because the predominant $(l_i s_i)$ contribution (the $\Delta\nu$ of Eq. (3)) is given by the solution of the one body problem. There is no such quantitatively useful theoretical expression yet for the $(l_i l_k)$ or $(s_i s_k)$ terms. It is an old empirical fact, that the $(s_i s_k)$ term (the "triplet-singlet distance") depends only slightly upon the atomic number, so that we were prepared to find the $(s_i s_k)$ interaction small compared with the fourth-power dependence of the $(l_i s_i)$ term for the more highly ionized members of an isoelectronic sequence, as well as for the heavier members of a column in the periodic table. The *jj*-like behavior of Tl IV and Pb V gives us the new empirical fact that here the $(l_i l_k)$ term also is small compared with the $(l_i s_i)$ term.

Non-occurrence of certain expected levels. Possibly the fact that only the levels built upon the lower level $d^9\ ^2D_{5/2}$ have been found for the d^9p configuration of the spectra shown toward the right in Fig. 3, in spite of the stability of the missing $d^9\ ^2D_{3/2}+p\ ^2P_{1/2}$ levels, indicates a relatively high probability for levels built upon the more stable state of the ion. This is analogous to the occurrence of only the lower levels in the configuration $6p6d$ of Pb I; though the latter case is complicated by the relatively low ionizing potential of Pb I.

Naming the levels, and coordination of levels. The conventional notation, which has been used here, assigns an electronic configuration and quantum numbers J, L, and S to each level; that is, it is exactly suited to the description of normal spectra. We have seen that although the configuration and J-value are quite definite, for some of the levels in our spectra all the criteria for the assignment of L and S have broken down; there is no evidence that these symbols retain any meaning, in these cases. If we are to endow the symbols with a meaning, we must postulate that L and S would assume the assigned values, if the level were traced through a continuous change of coupling to the normal. In many of our cases it would be more natural to use a notation based on j_1 and j_2 (Table X, last two columns). Such a notation is used as an alternative, in Tables II and V.

The comparison of one spectrum with others in its column of the periodic table, and especially with others in its isoelectronic sequence, is a means frequently used in the naming of energy levels; it is only by this means that the levels newly named in this paper, could have been named according to the usual notation. The fact that levels of the same name are approaching

[15] W. Heisenberg, Zeits. f. Physik **39**, 499 (1926).

the same grouping in both Figs. 2 and 3 (for instance: $^3P_2$, $^3F_3 \sim d^9_{5/2}\, p_{1/2}$) is worth noting but probably not very important, as it might naturally have been expected from our extrapolative way of choosing the names.

The problem of naming levels is closely related to that of coordination. Hund[16] has recently advanced the conjecture that except where symmetry considerations demand it, levels do not cross each other. Figures 1 and 2 show three instances of levels with the same J, crossing: $^3D_2$ and $^3F_2$ near Ni I, and $^3D_1$ and $^1P_1$ near Zn III and again near Ag II.[17] But in order that the idea of "crossing" in general have meaning, it is necessary to identify a level at two points, between which it is "to cross" or "not to cross" another. We must treat the energy as a function of a continuous parameter. In questions of spectral series it is the dependence upon principal quantum number which is at issue; and in isoelectronic sequences, dependence upon electric charge. But the discreteness of quantum numbers lies at the very root of quantum mechanics; therefore it appears that coordination of levels to series limits, in general, is without physical meaning. Likewise there can be little serious doubt that the discreteness of electric charge is as deeply founded, although the present-day equations contain Ze as a continuous parameter. It is therefore doubtful whether the giving of "normal" names to levels has any meaning except in special cases.

Note added to proof, May, 1929. Professor Hund explains that the crossing of levels is never in disagreement with his conjecture, when supported by experimental evidence such as that of the intensities here; for, any such experimental evidence reveals a symmetry property of the system. The non-crossing conjecture may best be treated, then, simply as a convention for naming levels where experiment does not distinguish sharply in character between them.

Note added June 27, 1929. K. R. Rao, Phys. Soc. London Proc. *41*, 361 (1929) has classified Tl IV independently, using Carroll's data. Rao gives sixteen levels, of which six agree with six of the ten in this paper. Rao's $d^9s\,^3D_1 = 18614$ makes Table VIII look better ($s = 41.666$) than at present, but its existence depends largely upon that of the unverified levels above 100,000. Figure 3 of this paper decides in favor 92617 (Rao's alternative) for $d^9p\,^3F_4$.

[16] F. Hund, Zeits. f. Physik **52**, 601 (1928).

[17] Of course it would have been possible to connect the levels in the figures so that no two lines connecting levels with the same J, should cross. But these "crossing" levels, on the whole, retain nearly normal intensities, and the evidence of the intensities as well as the naturally expected curve smoothness, is in favor of crossing. (But for $d^9p\,^3D_1$, $^1P_1$ the nearly equal intensities in Zn III and nearly equal intensities and g-values in Pd I are interesting. The naming of Pd I $d^9p\ ^3D_1$, $^1P_1$ is almost purely arbitrary.) On the other hand, Shenstone (4a, 13) has shown that if relative energy is plotted against total quantum number in any known d^9, s series, these criteria of intensities, g-values, and smoothness (in this case, fitting a Rydberg-Ritz formula) indicate non-crossing.

STUDIES ON THE SPECTRA OF Cu I, Cu II, AND Mn II By MEANS OF A VACUUM TUNGSTEN FURNACE

By O. S. Duffendack and J. G. Black
University of Michigan

(Received March 25, 1929)

Abstract

New design of a high temperature vacuum tungsten or molybdenum furnace. A high temperature vacuum tungsten furnace for the study of the spectra of elements having high boiling points is described.

Absorption spectrum of Cu.—All previously observed absorption lines of Cu in the range of the quartz spectrograph were observed and in addition six new lines from the $3d^9 4s$ level as follows 2618.381, 2824.375, 2882.81, 2961.177, 3010.840, 3194.103. CuH bands were also observed in absorption.

Excitation of Cu I spectrum by resonance absorption.—Light from the furnace walls excited Cu atoms to the ^2P state with the subsequent emission of 3247, 3274, 5106, 5700, 5782. With the walls somewhat cooler these lines were brought out when the vapor was exposed to intense radiation from the outside.

Excitation of Cu II and Mn II spectra by collisions of second kind with rare gas ions.—A-Cu mixtures at 25 volts failed to develop the Cu II spectrum. From Ne-Cu mixtures at 25 volts the lines from the $3d^9 5s$ state were much stronger than those from $3d^9 4p$. Theory shows that in A-Mn, Ne-Mn, and He-Mn mixtures the spectrum of Mn II should be excited to the extent of 64800, 113400 and 138500 wavenumbers respectively. The strong $(3d^5 4p)^7P - (3d^5 4d)^7D$ multiplet should be excited in Ne-Mn mixtures but not in A-Mn. This was verified experimentally. An analysis, similar to that of Russell, of the Mn II spectrum is given.

THE purpose of the work described here was to develop a high temperature vacuum furnace for the study of the atomic spectra of the elements having high boiling points and to demonstrate the adaptability of the furnace to these studies by using it to secure new information regarding such elements in a variety of ways.

In the analysis of the spectra of the elements, each group offers difficulties peculiar to itself and the chief difficulty with the more refractory elements is that of obtaining them in the vapor state under controllable conditions. From time to time various types of furnaces have been designed for this purpose. Thus King[1], in 1907, described a furnace which consisted of a thin horizontal tube of graphite, heated by a current of about 1500 amperes and enclosed in a chamber which could be evacuated to a few millimeters of mercury. Zumstein[2] did considerable work on absorption spectra by using a horizontal tube of carbon mounted under a ventilating hood and heated by a blast from a large oxyacetylene blow-torch. He made no attempt at evacuation. The metal was vaporized in air at atmospheric pressure

[1] King, Astrophys. J. **28**, 300 (1908).
[2] Zumstein, Phys. Rev. **27**, 562 (1926).

unless the oxidation was too great, in which case a stream of nitrogen or hydrogen or illuminating gas was passed through the tube. McLennan and McLay[3] also worked on absorption spectra and used a furnace consisting of a horizontal carbon tube which acted as the upper electrode of a carbon arc, the lower electrode being touched to the center of the upper and an arc maintained between them.

Duffendack[4] used a tungsten furnace in studying the critical potentials of atomic hydrogen. A large percentage of dissociation of H_2 was obtained thermally in such a furnace. It consisted of a thin horizontal tube of tungsten clamped between heavy water-cooled leads and heated by an electric current. It was enclosed in a vacuum chamber. A similar furnace has been used by Olmstead and Compton.[5] The furnace used in the present experiment was very similar to that used by Duffendack.

Apparatus

A diagram of the apparatus is shown in Fig. 1. A sheet of tungsten or molybdenum about 0.001 inch thick was rolled into a cylinder about 2 cm in diameter and 9 cm long. This is shown as *C* in the drawing. It is clamped horizontally between two heavy water-cooled copper rods and heated by a large current from the low voltage transformer shown at the bottom of the

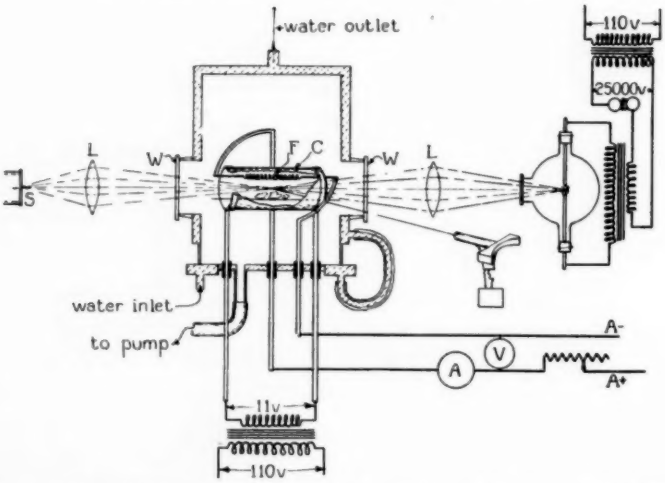

Fig. 1. Tungsten furnace mounted in a water-cooled vacuum chamber.

figure. The rods extend upward through collars in the base of the large chamber shown and are insulated from this base plate by thick collars of Pyrex tubing sealed on with deKhotinsky cement. The tungsten cylinder is so adjusted that its axis is in line with the centers of the two quartz windows *W*. These windows are sealed on with cement.

[3] McLennan and McLay, Trans. Roy. Soc. Can. Sec. **III.** 89 (1925).
[4] Duffendack, Phys. Rev. **20,** 665 (1922).
[5] Olmstead and Compton, Phys. Rev. **22,** 559 (1923).

Extending through the cylinder near the top is shown a tungsten filament of 12 mil wire with a few turns at the center. This filament serves as the hot cathode for the low voltage arc studies; electrons being accelerated from it to the trough which holds the metal. This trough is supported by two other water-cooled leads, insulated from the base, and of the same size as those supporting the furnace.

A water-cooled vacuum chamber surrounds the furnace and is sealed to the base plate with a laboratory wax known as "Picein." The inside of the water-cooled chamber is made of a tube of seamless cooper 6″ in diameter, 7″ high and 3/16″ thick. The bottom and top are of pure copper plate and the top is soldered on. The inside of the cylinder is heavily nickel-plated as an increased precaution against diffusion of gases and water vapor through the walls. The reason for using copper is that brass is porous to water vapor. The outer water jacket is made of brass. A circular hollow brass collar is soldered to the base plate just below the point at which the chamber is cemented to the base and cold water circulating through this prevents the Picein from softening.

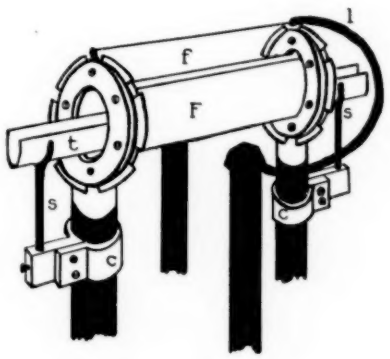

Fig. 2. Details of mounting of tungsten furnace.

Through the cylindrical furnace near the base may be seen a horizontal trough on which rests the metal to be studied. This trough is supported by insulated arms not shown in the figure and is grounded to the base plate. It is made of a strip of 5 mil molybdenum or tungsten about 1.5 cm wide and 10 cm long, bent into the shape of a trough. The details of this may be seen in Fig. 2. When the furnace is used for a low voltage arc discharge this trough is held at a positive potential with respect to the filament and serves as the anode.

In the absorption work on copper, a few grams of copper selected from Baker's Analyzed Chemicals were placed in the trough, the chamber was placed on and sealed and the system pumped out thoroughly. The furnace was then heated and the absorption spectrum taken in the usual manner.

The pumping system was of the usual type, consisting of a two-stage mercury vapor condensation pump backed by a Hyvac oil pump. A McLeod gauge was used to read the pressure and a pair of mercury cut-offs facilitated

letting in gases when desired. A small pressure of hydrogen was used to decrease the diffusion of metal vapor to the windows and helium, neon, and argon were used in the work of ionization and excitation by positive ions. Absorbable impurities in the helium and neon were removed by an activated cocoanut charcoal trap immersed in liquid air. To purify the argon a "getter" consisting of a bundle of sticks of misch metal was used.

The method of mounting the furnace tube is important. It is obvious from a glance at Fig. 2 how the ends of the cylinder of tungsten were split and flared into a fan shape so as to permit clamping with the soft steel clamps shown. Some trouble was experienced by the condensation of copper on these clamps. The current which flowed through this cylinder varied from 150 to 375 amperes, depending upon the temperature desired. When it was necessary to be very careful of the temperature it was measured with an optical pyrometer. Such was the case in the work on the excitation of the copper spectrum by photoelectric action. When the furnace cylinder burned or melted in two, about one hour's time was required for replacing it and getting the vacuum pumps into operation again.

The continuous light for the absorption experiments was furnished by a Tesla spark between tungsten electrodes in distilled water. This gave a beautiful continuous spectrum from the red to 2240A.

Absorption Studies on Copper

The first attempt at an adaptation of the furnace to a problem of atomic physics was in a study of the absorption spectrum of copper vapor. Copper was chosen because of its relatively high boiling point and because we could use it to compare the furnace with others which had been used in absorption studies on the same element. The classification of these lines by Shenstone[6] was used in the interpretation of the results.

The normal state of Cu I is a ^2S state. Taking this as zero we find next metastable $^2D_3$ and $^2D_2$ states at 11202.5 and 13245.4 cm^{-1} respectively while ^2P levels come at 30543.1 and 30782.8 cm^{-1}. The chief interest for our absorption work lies in the ^2D levels. It should be remembered that in absorption by "cold" vapors only lines from the normal state are absorbed, since all of the atoms are in this state. If the temperature of the vapor is increased however, higher energy states will be occupied and absorption may be obtained from these states.

All the absorption lines of copper which have been observed from the normal state had been obtained previous to the work of Zumstein. He was able to obtain nine absorption lines from the $(3d^9 4s)^2D$ state, using the temperature obtainable with the oxyacetylene blow-torch. He was also able to absorb the bands of copper-hydride by passing a stream of hydrogen through the vapor.

Using the tungsten furnace described here we were readily able to obtain all the previously observed absorbed lines within the range of a quartz spectrograph and in addition six new lines from the $3d^9 4s$ level, as follows:—

[6] Shenstone, Phys. Rev. **28,** 449 (1928).

2618.381, 2824.375, 2882.81, 2961.177, 3010.840, 3194.103. There also appeared a nice absorption of the copper-hydride bands.

Excitation of the Cu I Spectrum by Absorption of Resonance Radiation

We next attempted to excite the emission spectrum of Cu I by the absorption of resonance radiation. The necessity of attempting to excite the copper spectrum in this manner arose when we obtained certain Cu I lines in *emission* while trying to get the 5700, 5782 lines in absorption.

Since we were using a temperature close to the melting point of tungsten in order thermally to obtain a large number of metastable copper atoms, the furnace wall was emitting light whose short wave-length limit was about 2500A. We were thus subjecting a large number of atoms to radiation of resonance wave-length. These atoms were thus excited to the ^2P, state and any lines representing transitions from this state to the 1^2S or ^2D should appear in emission. We were thus able to obtain the lines 3247, 3274, 5106, 5700, 5782 in emission.

The fact that these lines appear thus in emission probably explains the difficulty encountered by Zumstein in absorbing the 5106, 5700, and 5782 lines, because there were probably as many electron transfers from ^2P down to ^2D as from the ^2D up to ^2P. With special effort he obtained 5106 as a narrow line but could not get 5700 and 5782. The line 5106 was obtained as a narrow, sharp absorption in our work, but the 5700 and 5782 lines failed to appear.

Reflections upon the theory of impacts of the second kind lead to interesting modifications which might be made in absorption experiments. For instance, it is theoretically possible that the hydrogen which we used to reduce the diffusion of the metal vapor inside of our furnace was able at the higher temperatures to increase the populations of the ^2P levels by collisions in which the atomic hydrogen excited the copper to the ^2P state. Such an action has been observed by Mohler[7] in the excitation of metallic spectra by atomic hydrogen. This would account for some of the radiation which registered as 5106, 5700 and 5782.

To return to the discussion of the present experiment—the walls of the furnace had been very hot during the absorption experiments and it was necessary to cool them so as to make sure that they were not emitting the resonance lines of copper while at the same time keeping them hot enough to furnish a supply of copper vapor. Maintaining them at such a temperature we photographed the spectrum emitted by the vapor when no resonance radiation was allowed to enter the vapor and on the same plate we took an exposure when an intense beam of continuous radiation entered the vapor from a direction at right angles to the optical axis of the collimator of the spectrograph. In the first case we obtained no evidence whatever of the emission of copper lines while in the second case there appeared strong lines at the wave-lengths mentioned above, 3247, 3274, 5106, 5700, 5782. Precau-

[7] Mohler, Phys. Rev. **29**, 419 (1927).

tions were taken to keep the total power input into the furnace slightly lower in the second case than in the first in order to be sure that the vapor which was not illuminated had fully as high a temperature as the illuminated, and for the same reason the temperature of the furnace as registered on an optical pyrometer was kept slightly lower in the second case.

Excitation of the Cu II Spectrum by Positive Rare Gas Ions

We next applied the furnace in a test of simultaneous ionization and excitation by positive ions. It has recently been demonstrated by Smyth and Harnwell[8] and Hogness and Lunn[9] that a positive ion of one ionizing potential may, upon collision with a neutral atom or molecule, rob it of an electron, provided its ionization potential is lower. They used the method of Dempster's positive-ray analysis.

At the same time Duffendack and Smith [10] were performing an experiment which involved the ionization by contact with positive ions and which dealt with the disposal of the excess energy at such collisions. They showed that positive helium ions could, upon contact with CO molecules, ionize them, and spend the residual energy in exciting the ion formed. They were thus able to excite the bands of CO^+. Their experiment differed from the others in that they were concerned with the excess energy at collision and showed that the excess energy after ionization went to excite the ion formed.

It was thought advisable to make a test of this type of energy transfer in metallic vapors, which are monatomic. Since the first spark spectrum of copper had been analyzed,[11] the method was tried in copper-helium, copper-neon and copper-argon mixtures.

The excess energy made available in the reaction

$$He^+ + Cu = Cu^+ + He \text{ is } 24.5 - 7.8 = 16.7 \text{ volts}$$
$$Ne^+ + Cu = Cu^+ + Ne \text{ is } 21.4 - 7.8 = 12.6 \text{ volts}$$
$$A^+ + Cu = Cu^+ + A \text{ is } 15.4 - 7.8 = 7.7 \text{ volts}$$

Reference to the energy levels of Cu II, Fig. 3, will show that helium ions should be able to excite any levels in the *Cu II* spectrum which are below 135270 wave-numbers. Neon ions should excite any levels below 110160 wave-numbers and should show the lines from the $3d^9 4p$ configuration. Argon should, however, only be able to reach 61560 wave-numbers and the lines from the $3d^9 4p$ levels should not be developed in this type of mixture. Such was found to be the case, and thus the conclusion of Duffendack and Smith that the excess energy went into excitation of the spark spectrum was confirmed in the case of monatomic molecules.

As for the experimental work, this consisted in outgassing the system and then introducing 3 millimeters of argon. The filament was next lighted

[8] Smyth and Harnwell, Nature Jan. 15, (1927).
[9] Hogness and Lunn, Phys. Rev. **30,** 26 (1927) See also a succeeding article in this journal.
[10] Duffendack and Smith, Nature **119,** 743 (1927).
[11] Shenstone, Phys. Rev. **29,** 380 (1927).

and then the furnace, so that after a few seconds a mixture of rare gas and copper vapor filled the furnace tube.

An accelerating potential difference of 25 volts was then applied between the trough and filament and the spectrum examined by means of a pocket spectroscope. When the currents had been adjusted for the desired intensity of the copper lines, a photograph was taken in a mixture of argon and copper. The system was again exhausted and outgassed and a photograph placed on the same plate, with the same conditions, except that neon and copper were used.

The argon-copper mixture failed to develop the lines of the Cu II spectrum while the neon-copper mixture showed a strong development of the spark lines.

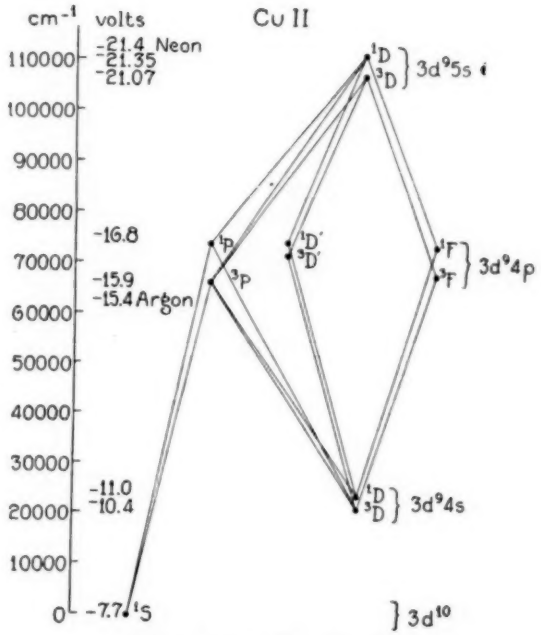

Fig. 3. Energy levels of Cu^+

In the excitation of Cu II by neon ions the lines from the $3d^9 5s$ state were relatively much stronger than those from the $3d^9 4p$. Reference to Fig. 3 will show that this $3d^9 5s$ state is just below the ionizing potential of neon, while the $3d^9 4p$ level is just below 16.7 volts, which is an important excited state of neon. The strong development of the lines from the $3d^9 5s$ state can be attributed to the fact that this level is practically resonant with the normal ionized state of neon. The weakness of the lines from the $3d^9 4p$ state which is resonant with the 16.6 volt excited state of neon is, however, somewhat unexpected, especially in the light of the work of Duffendack and Smith described in a succeeding paper. We had the opportunity to discuss this matter with Professor J. Franck, and he suggested that the weakness of these lines is probably due to the quenching action of hydrogen

on this state of neon. The ionizing potential of H_2 is also practically resonant with this state of neon and Duffendack and Smith showed in their experiments that hydrogen does have a marked quenching action on this state of neon. Since the furnace chamber could not be outgassed and hydrocarbon vapors may be expected from the cements used, the presence of hydrogen in the neon can readily be explained.

Excitation of the Spectrum of Mn II

We next excited the spectrum of Mn II by the same method as was used on Cu II. The excess energy after contact ionizations by argon, neon and helium ions is 8, 14, 17.1 volts respectively and these are able therefore to excite the Mn II spectrum to the extent of 64800, 113400, 138500 wave numbers respectively. Reference to Fig. 4 will show that argon ions should

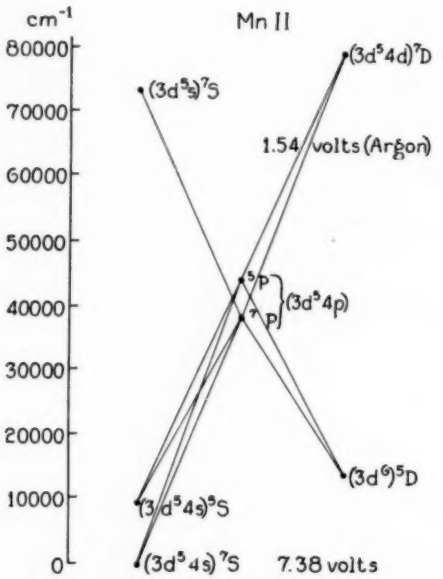

Fig. 4. Energy levels of Mn^+.

develop the lower important terms, while neon ions should develop all the main terms in the spectrum while the second spark spectrum should be entirely absent. An interesting consequence of this is that the strong $(3d^5 4p)$ $^7P - (3d^5 4d)$ ^7D multiplet should not be developed by argon ions, but should easily be developed by neon ions. This was tested by taking two successive exposures on the same plate, one using argon ions and the other neon. The neon ions gave a strong development of the nine lines but the argon failed to develop them.

In 1923 Catalan[12] discovered four multiplets in the spectrum of Mn II which we have recently identified[13] as the strongest multiplets of a septet

[12] Catalan, Phil. Trans. Roy. Soc. **223A** (1923).
[13] Black and Duffendack, Science **66**, 401 (1927).

and quintet system. The relative positions of the two systems were estimated from computations of convergences of two series in Mn I furnished us by Dr. O. Laporte, and intercombination lines which fixed the relative positions of the system were easily found.

The term scheme for the Mn II spectrum as far as we were able to analyze it is given graphically in Fig. 4. The same analysis was made independently by Russell.[14] Since he has published the classification of the lines, it is not necessary to reprint them here. He located a $(3d^5 5s)^7S$ level at 74555.98 cm^{-1} and although the three lines which located it by combinations with $(3d^5 4p)^7P$ fit excellently, we are inclined to doubt its correctness; for two of the lines, namely 2762.3 and 2796.3, were developed by argon ions whereas this ^7S level is above the ionization potential of argon. In all other respects his analysis is identical with ours.

A considerable number of unclassified lines in Mn II in the region between 2600A and 3100A, 38500 and 32400 wave-numbers, are intensified in argon while many equally intense spark lines fail to appear in the spectrum excited in the argon- manganese vapor mixtures. It would seem that these lines are due to transitions between other terms of the configurations indicated in Fig. 4, and since the lines are excited in the argon mixture they must come from terms lying below 64800 wave-numbers from the normal state of the manganese ion. Therefore these lines are probably due to transitions from unknown terms of the $3d^5 4p$ state to the terms of the $3d^5 4s$ and $3d^6$ states. It is hoped that a classification of these lines may be possible soon in order to check this hypothesis.

[14] H. N. Russell, Astrophys. J. **66**, 292 (1927).

ON THE ABSORPTION SPECTRUM OF HYDROGEN CHLORIDE

By Charles F. Meyer and Aaron A. Levin
University of Michigan

(Received, April 29, 1929)

Abstract

The *fundamental band* and the *harmonic band* of hydrogen chloride have been measured with narrow slits. The lines of the *fundamental* as previously measured, have been resolved, each into two lines arising from the existence of the isotopes Cl_{35} and Cl_{37}. The relative intensities of the lines in the two series are in accord with the accepted ratio for the abundance of the isotopes. In the *harmonic*, a slight separation of the lines arising from the isotopes had been previously achieved by Randall and Imes. In the present work the degree of separation is greatly enchanced. Wave-number and intensity determinations for the two series of lines in each band are submitted. Figures are given representing the bands in the new form. The ratio of the intensities of the fundamental and harmonic bands, as experimentally determined, is found to be in good agreement with the computed value.

THE vibration-rotation spectrum of hydrogen chloride consists principally of a fundamental band at 3.46μ and a harmonic at 1.76μ. The work of Randall and Imes[1] demonstrated that the principal lines in the harmonic are accompanied by faint companions, which were interpreted by Loomis,[2] and Kratzer,[3] independently as arising from the existence of the isotope Cl_{37} in combination with hydrogen, the principal lines arising from the more abundant Cl_{35}. The suggested interpretation was supported by good agreement between observed and computed values of the separation of the principal lines and the companions. The companion lines were barely evident in the experimental curve, but their reality seemed established through the fact that a companion was indicated for nearly every principal line, and the success of the above mentioned hypothesis added further weight to the evidence.

In the fundamental band, companions were not observed, but there was no reason for believing that they did not exist. The failure to find them was presumably due to less favorable experimental conditions as determined by the spacing of the grating used, in relation to the expected separation. Subsequent investigators obtained in one case slight evidence,[4] and in another case indirect evidence[5] for the existence of the companions, but the companions were in no way separated from the principal lines.

[1] Randall and Imes, Phys. Rev. **15,** 152 (1920); also Imes, Astrophys. J. **50,** 251 (1919).
[2] F. W. Loomis, Astrophys. J. **52,** 248 (1920).
[3] A. Kratzer, Zeits. f. Physik **3,** 460 (1920).
[4] W. F. Colby and C. F. Meyer, Astrophys. J. **53,** 300 (1921).
[5] E. C. Kemble and D. G. Bourgin, Nature **117,** 789 (1926); also D. G. Bourgin, Phys. Rev., 29, 794 (1927).

The performance of a new spectrometer, described elsewhere,[6] led to the belief that the separation in the fundamental might now be achieved. Preliminary trials at once demonstrated the existence of the companions, and by narrowing the slits to the extreme, the principal and companion lines were separated to a degree which exceeded the most optimistic expectations. The slits were narrowed to 0.25 mm, and as the focal length of the spectrometer is 1 m, the spectral range included by the slit is about one-fourth of that of the older work in which slits of 0.5 mm were usually employed with a focal length of 0.5 m.

In Fig. 1 are shown several of the curves which have been obtained. The abscissae represent settings of the grating circle. These were made at every fifteen seconds of arc, as indicated by the plotted points. The ordinates represent percent of absorption, correction being made for the diminution of energy by the rock-salt windows of the cell.

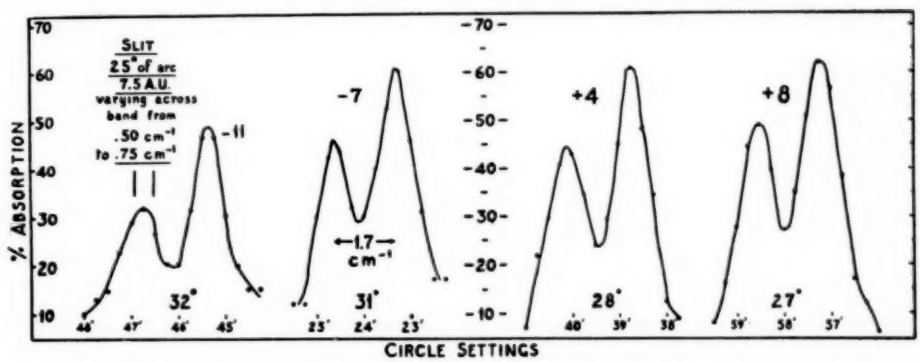

Fig. 1. Doublet structure of lines of the fundamental band. The right hand member of each doublet is due to HCl_{35}; the left hand member is due to HCl_{37}.

When the lines are separated to the degree which is here represented they no longer have the appearance of a *principal* line and a *faint* companion, but rather that of a *major* and a *minor* component of a pair. The ratio of the abundance of the isotopes Cl_{35} to Cl_{37} is about 3:1 and it is surprising to find that the maxima of absorption attained by the two components, as measured, should differ by so little as they do. However, the relation existing between measured maximum of absorption and true intensity of a line is an involved one, and it is not to be concluded that an anomaly is in evidence. A direct experimental comparison of the intensities was made by determining the absorption curve for one line (+4) first with a cell 1 mm in length, and then with a cell 3 mm in length. In Fig. 2 the left hand curve represents the result in the first instance, and the right hand curve represents the result in the second instance. As is to be expected the maximum of absorption attained by the major component in the first case is approximately equal to the maximum attained by the minor component in the second case.[7] The

[6] A. A. Levin and C. F. Meyer, J.O.S.A. & R.S.I. **16**, 137 (1928).

[7] See also note on relative intensities by D. M. Dennison in the last section of this article.

points near the maxima in question were determined with more than ordinary care. Each final, plotted, point represents the mean position of three or four original points obtained in measuring back and forth across the line. Each original point represents the percentage of absorption calculated from eight galvanometer deflections taken with the cell in the beam, and eight with the cell out of the beam.

The primary object of the present investigation was to furnish measurements of the positions of the lines when separated as above shown and a secondary object was to furnish measurements of the intensities. It is important for the development of the theory of the vibrating rotating dipole, that the laws of both spacing and intensity be determined as accurately as possible. The older measurements, which showed the lines as composite, could not reveal these laws as closely as might be desired. It is believed that

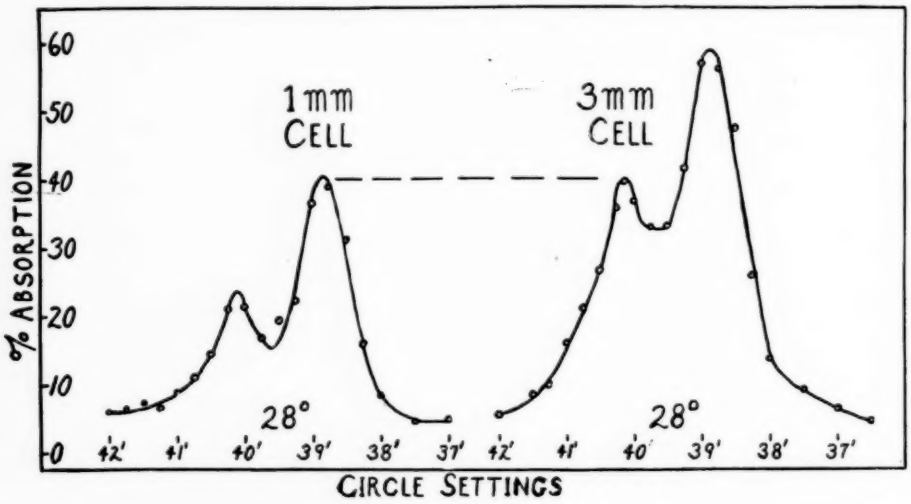

Fig. 2. Comparison of intensities of major and minor components.

the present work presents greatly improved data in regard to spacing. As for intensity, it is a necessary consequence of the use of narrower slits that the total available energy is reduced, and that the errors in absorption percentages are increased. Therefore the percentages will not be as accurately given as in some previous work.[5] Nevertheless, because of the very fact that the slit width is so much narrower, and because the lines are separated into their components, it is believed that the measurements of intensity will also have value.

Calibration etc.

A grating of 7200 lines per inch (2835 per cm), ruled by E. F. Barker, was used for work on the fundamental. One of 15,000 lines per inch (5900 per cm), by J. A. Anderson, was used for the harmonic. Both were calibrated by means of the 1.014μ mercury line for which the exact wave-length was taken as 10,139.8A. in air at the temperature and pressure of the experiment,

about 23°C and 74 cm. The wave-numbers for the HCl lines have been reduced to vacuum by taking $n-1$ equal to $25.\times10^{-5}$ in the region of the fundamental, and equal to $26.\times10^{-5}$ in the region of the harmonic, n being the index of refraction for air.[8]

Much attention has been given in the present investigation to reducing error, and it is believed that the wave-number determinations are more accurate than previous ones in infra-red absorption measurements. The greater sharpness of the lines when measured with narrow slits, and the comparative freedom from overlapping should also contribute materially toward achieving this result. In the past, independent sets of determinations made by different observers, working with different apparatus, have usually shown minor discrepancies which indicated systematic error. It is hoped that such error has been decidedly reduced, but positive claims to this effect cannot be made and the authors do not wish to insist on high *absolute* accuracy for the measurements. The *relative* accuracy of the wave-number determinations should however be distinctly greater than that of previous determinations, and moreover the *law of spacing* should appear with much improvement because the series of lines arising from the two isotopes are now determined separately.

The Fundamental Band

In the work on the fundamental it was not feasible to follow the usual procedure of measuring the entire band with a fixed cell length and gas content. It was desired to measure twelve lines in each branch of the band. The variation in intensity among these is so great that no one amount of

Table I. *Fundamental band, observed wave-numbers, cm^{-1}, vacuum.*

Line No.	Major Comp.	Minor Comp.	Diff.	Line No.	Major Comp.	Minor Comp.	Diff.
−12	2599.00	2597.43	1.57	1	2906.25	2904.16	2.09
−11	2625.74	2624.03	1.71	2	25.78	23.69	2.09
−10	51.97	50.36	1.61	3	44.81	42.71	2.10
−9	77.73	75.90	1.83	4	63.24	61.08	2.16
−8	2703.06	2701.29	1.77	5	80.90	78.68	2.22
−7	27.75	26.01	1.74	6	97.78	95.66	2.12
−6	52.03	50.31	1.72	7	3014.29	3012.16	2.13
−5	75.79	73.77	2.02	8	29.96	27.69	2.27
−4	98.78	96.88	1.90	9	44.88	42.62	2.26
−3	2821.49	2819.51	1.98	10	59.07	56.84	2.23
−2	43.56	41.59	1.97	11	72.76	70.51	2.25
−1	65.09	62.99	2.10	12	85.62	83.28	2.34

gas will do for all. In the more intense lines the major and minor components will overlap considerably while the fainter lines will show insufficient absorption for proper measurement. Consequently, a set of position measurements was first made, with varying amounts of hydrogen chloride in the beam, the quantity being adjusted until the line or lines which were shortly to be measured exerted a proper amount of absorption. Air remained in

[8] F. Paschen, Ann. d. Phys. **27,** 537 (1908); **29,** 625 (1909); **38,** 717 (1910).

the cell admixed with the hydrogen chloride, the pressure of the mixture being atmospheric. The separation of the components in this set of measurements was throughout about as complete as shown for the lines of Fig. 1. Had the separation been less complete, it would have been necessary to make a correction for the position of each component due to the influence of its neighbor. As it was, such a correction was deemed unnecessary. The wave-numbers for the above mentioned series of measurements are given in Table I as are likewise the separations between the major and minor components.

Subsequently the first six lines in each branch of the band were measured with a cell of fixed length of 3 mm, filled with hydrogen choloride at atmos-

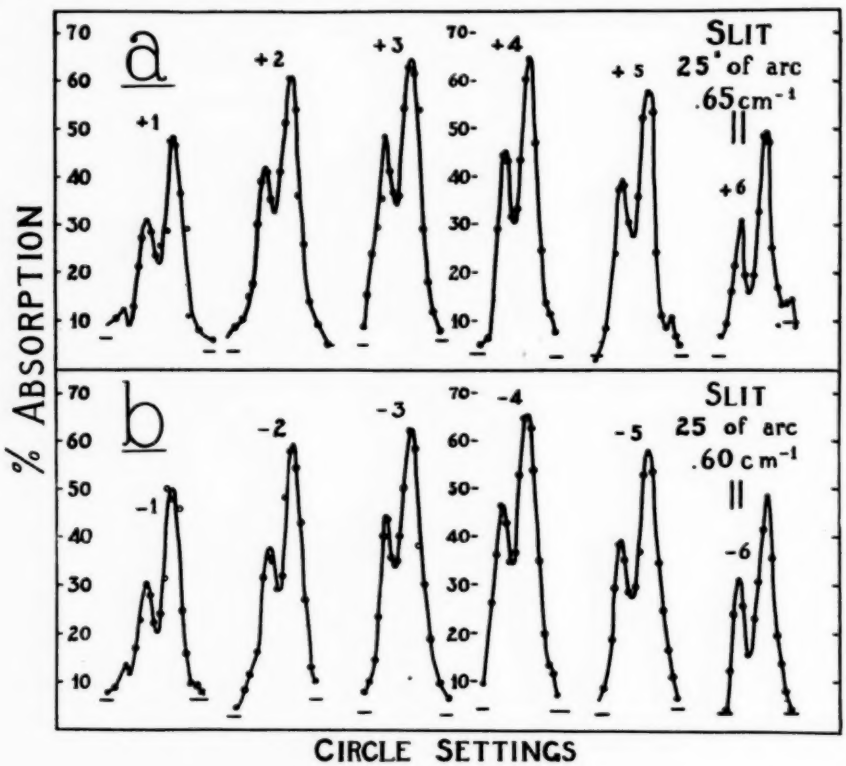

Fig. 3. Individual lines of the fundamental band.

pheric pressure. The curves obtained are given in Fig. 3. They are submitted because of such interest as they may have in regard to intensity of absorption. In plotting them, correction was of course made for the diminution of energy due to the windows of the cell. At the base of the curve for each pair of lines, short horizontal marks indicate the height of the absorption curve in the intervening regions between the pairs of lines. These intervening regions were explored throughout, but with large intervals between successive settings of the grating. The curve rises and falls irregularly in the region between the lines due to the observational error of individual determinations of percentage of absorption. The range of variation is usually two or

three and sometimes as high as five percent. The separation between the major and minor components is not so complete in the curves of Fig. 3 as in those of which examples are given in Fig. 1. The difference is attributed to some slight change in the condition of the spectrometer which is not under control, perhaps a slight distortion in the large mirror or the grating which impaired the definition, or perhaps a refusal on the part of the slit to assume always the same width for the same setting of the micrometer head. Several months intervened between the two sets of observations.

It was deemed desirable to depict the *entire* band in its new form with the lines due to the isotopes separated. When the drawing of the figure was undertaken it became evident that the representation could not be made in the usual manner of an absorption *curve*, but would have to be shown as a "silhouette" of the absorption *area*. This is necessitated by the extreme

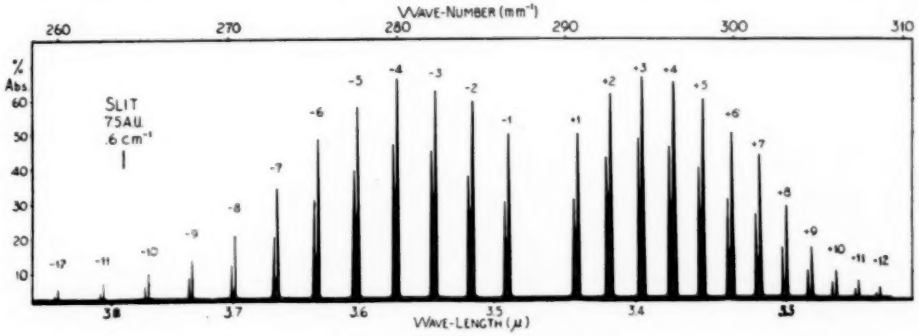

Fig. 4. The fundamental band.

narrowness of the lines in relation to the width of the region which must be depicted. The band is represented in Fig. 4. The first six lines in each branch are shown in accordance with the intensity measurements made with the 3 mm cell, and the intensities of the remaining six lines in each branch are estimated. The regions intervening between the pairs of lines have been smoothed out. If they had not been, the figure would have presented a confused appearance, as was demonstrated by a preliminary drawing.

The Harmonic Band

In the work on the harmonic a cell 30 cm in length was employed which was fitted with plate glass windows. The cell was as long as the arrangement of the apparatus permitted. It contained hydrogen chloride at a pressure of about 60 cm, and with this was admixed air to atmospheric pressure. The amount of gas which was present was such that the more intense lines of the band exerted about the maximum of absorption which was consistent with having good separation between the components. As many lines were measured in each branch of the band as could be measured with this amount of gas, namely, eight in the P branch and nine in the R branch. The wave-numbers and separations for these are given in Table II, and the absorption

curves for the individual lines are shown in Fig. 5. Short horizontal marks again indicate the height of the curve in the regions intervening between the lines. These regions were explored throughout. To the right of line −8 is shown a section of the curve which intervenes between lines −8 and −7.

TABLE II. *Harmonic band, observed wave-numbers, cm^{-1}, vacuum.*

Line No.	Major Comp.	Minor Comp.	Diff.	Line No.	Major Comp.	Minor Comp.	Diff.
−8	5468.55	5464.67	3.88	1	5687.81	5683.91	3.90
−7	96.97	93.12	3.85	2	5706.21	5702.01	4.20
−6	5525.04	5521.23	3.81	3	23.29	19.42	3.87
−5	51.68	47.74	3.94	4	39.29	35.26	4.03
−4	77.25	73.40	3.85	5	53.88	49.69	4.19
−3	5602.05	97.98	4.07	6	67.50	63.28	4.22
−2	24.81	5620.92	3.89	7	79.54	75.40	4.14
−1	47.03	43.10	3.93	8	90.54	86.28	4.26
				9	99.94	96.04	3.90

The irregularities here are typical, and this section is shown by way of example. Repetition of the measurements in some of the intervening regions indicated that the irregularities arose purely from accidental errors, due of course to the accidental disturbances of the galvanometer.

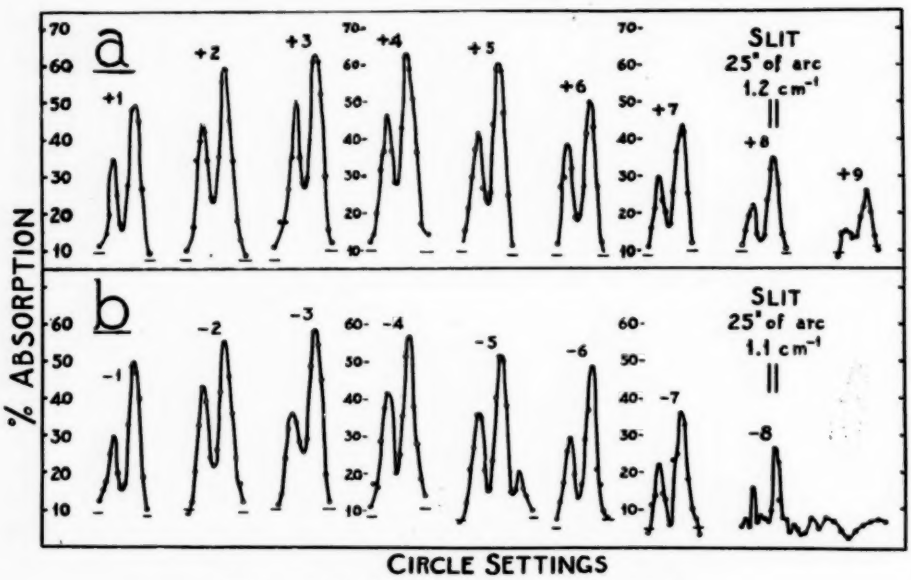

Fig. 5. Individual lines of the harmonic band.

It will be noted that the degree of separation of the major and minor components of the harmonic, as shown in Fig. 5 is about the same as that for the first series of measurements on the fundamental, Fig. 1. In point of time the observations on the harmonic succeeded those of the first series on the fundamental. Those of the second series on the fundamental were made later,

and those in connection with Fig. 2 were made last and these show the greatest impairment of definition.

In Fig. 6 the harmonic is shown in "silhouetted" form. The representation is according to measurement in regard to all of the lines. The intervening regions between the lines are smoothed out.

The separation between neighboring pairs of lines in the harmonic, when expressed in wave-numbers, is the same as the separation between corresponding neighbors in the fundamental. But the separation between the major and minor component of one pair in the harmonic is twice as great as the separation between the components of the corresponding pair in the fundamental. Consequently the harmonic presents a more crowded or fuller appearance than does the fundamental. Comparison of Figs. 4 and 6 elucidates the effect.

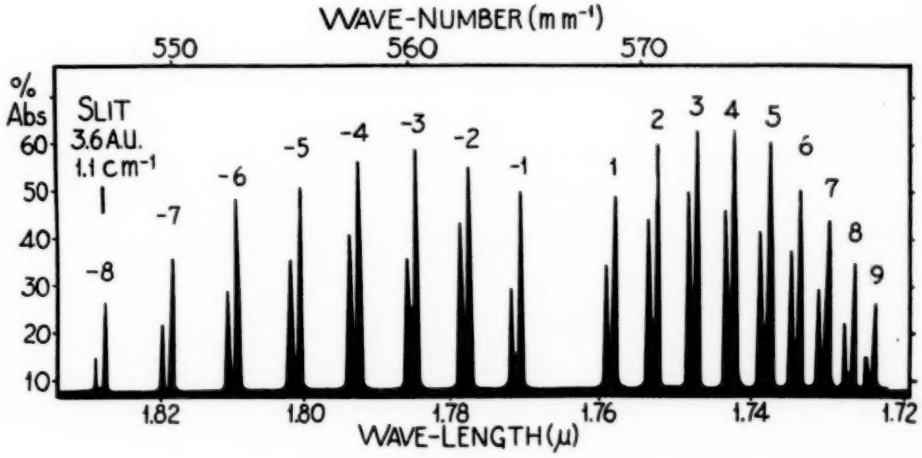

Fig. 6. The harmonic band.

In this investigation the problem of separating the components due to the isotopes was found to be much the same in the two bands. The grating which was used in the harmonic was of about twice the finensss of the one which was used in the fundamental. The separation of the components in seconds of arc on the grating circle was practically the same in the two cases. The slit width used for both bands was 0.25 mm. The available energy was greater in the region of the fundamental, perhaps because of more favorable concentration by the grating. Observations were easier in the fundamental, though they had been considered more difficult.

The Line Intensities

The authors wish to acknowledge their indebtedness to Professor D. M. Dennison for the following numerical computations and remarks.

The intensities of the HCl lines as shown in the foregoing curves were examined in three ways: (*a*) the relative intensity of a line and its isotope companion; (*b*) the intensities of the stronger components in a band

(i. e. lines +1, +2, +3, etc); and (*c*) the relative intensity of corresponding lines in the fundamental and harmonic bands.

Under (*a*) the computation was carried out for several lines in the fundamental band of which the line −6 may be taken as representative. The observed ratio of the areas under the absorption curves of the major and minor components has the value $\rho=2.2$. This ratio may be computed theoretically[9] by substituting the known constants of the HCl molecule and the slit width of the spectrometer and assuming that Cl_{35} is 3.3 times as abundant as Cl_{37}. The ratio thus obtained between the areas is $\rho=2.1$ in good agreement with the observed ratio.

(*b*) The comparison of the stronger components in a band was carried out sufficiently to show that the observed intensities agree within the experimental error with the theoretical formula for band line intensities. The work by Kemble and Bourgin[5], which was performed with the express purpose of determining these line intensities, leads to results which are certainly more accurate than those which could be obtained from the present data.

(*c*) We may, however, compare the intensities of corresponding lines of the fundamental and first harmonic with greater precision then has been attained heretofore. Examination of several representative lines shows that the ratio of the intensities of the two bands I_2^0/I_1^0 lies between 0.017 and 0.025, the experimental error being rather large. This value of I_2^0/I_1^0 may also be given through the use of the wave mechanical solution of the perturbed oscillator in terms of the derivatives of the force function.

$$I_2^0/I_1^0=(\phi'''/6\phi'')^2(h/2\pi^2\mu\nu_0).$$

Substituting the appropriate values of the constants (see the paper following by W. F. Colby), we obtain as a theoretical value $I_2^0/I_1^0=0.0197$. It is interesting to notice that the ratio as given by the older quantum theory and the correspondence principle[10] was twice as great, namely, .039. and lies distinctly outside the range of the experimental values.

[9] D. M. Dennison, Phys. Rev. **31**, 503 (1928), see Eq. (13).
[10] D. M. Dennison, Phil. Mag. **1**, 195 (1926).

ANALYSIS OF THE HCl BANDS

By W. F. Colby
University of Michigan

(Received April 29, 1929)

Abstract

Wave-numbers for the two isotopes of hydrogen chloride in the bands at 3.5μ and 1.76μ have been fitted to formulae cubic in the rotational quantum number. From these formulae the constants of the molecule have been determined in accordance with the energy expression for the rotating dipole as derived by means of wave mechanics.

THE separation of the isotope components of the HCl infra-red bands and the accurate measurement of their positions as reported by Meyer and Levin in the preceding paper in this periodical have made it possible to test the success of formulae derived with the help of the new wave mechanics. In a recent paper,[1] Fues has discussed the case of the rotating vibrating dipole and has obtained an energy expression in the following form:

$$E=A+h\nu_0(n+\tfrac{1}{2})[1-B(j+\tfrac{1}{2})^2] + (h^2/8\pi^2J)(j+\tfrac{1}{2})^2[1-k^2(j+\tfrac{1}{2})^2]-(h^2/8\pi^2J)(n+\tfrac{1}{2})^2C \quad (1)$$

n is the vibrational quantum number and j the rotational. B, C, ν_0 and k^2 contain constants of the force function but are independent of j and n. J is the moment of inertia of the molecule about an axis normal to the nuclear line. The entrance of the factors $(n+\frac{1}{2})$ and $(j+\frac{1}{2})$ throughout in place of n and j of the Kratzer formula gives a new interpretation to the experimental results.

The transitions involved in these bands are for n, $0\rightarrow\Delta n$ for j, $j\rightarrow j\pm 1$ where $\Delta n=1$ for the fundamental and $\Delta n=2$ for the harmonic. For both of these bands the initial values of j in the positive branch begin with zero and for the negative branch with 1. It is more convenient however not to use initial values of j in numbering the lines but rather to number them on both sides starting with 1. This formulation allows one to write a single formula for both branches. We then have

$$\nu=\nu_0\Delta n-\tfrac{1}{4}\nu_0B\Delta n-(h/8\pi^2J)C(\Delta n^2+\Delta n) + (-\nu_0B-\nu_0B\Delta n+(2h/8\pi^2J)-(h/8\pi^2J)k^2)j - \nu_0B\Delta nj^2-(h/8\pi^2J)4k^2j^3$$

where j is the number of the line from the center of the band positive for the positive branch and negative for the negative. It has been possible

[1] Fues, Ann. d. Physik **80**, 367 (1926).

to fit the wave-numbers determined by Meyer and Levin very successfully to this cubic formula. The following four equations give the constants thus determined.

Fundamental

Major isotope component: $\nu = 2885.88 + 20.562j - 0.3030j^2 - 0.0020j^3$

Minor isotope component: $\nu = 2883.84 + 20.536j - 0.3022j^2 - 0.0020j^3$

Harmonic

Major: $\nu = 5667.96 + 20.291j - 0.6028j^2 - 0.0025j^3$

Minor: $\nu = 5663.97 + 20.259j - 0.6029j^2 - 0.0022j^3$

Tables I and II give the wave-numbers computed from these equations and the differences ($\Delta\nu$) between them and the observed values. It will be noticed that these differences lie satisfactorily within experimental error.

TABLE I. *Calculated frequencies of fundamental.*

j	Major Component	$\Delta\nu$	Minor Component	$\Delta\nu$	j	Major Component	$\Delta\nu$	Minor Component	$\Delta\nu$
−12	2598.98	0.02	2597.40	0.03	1	2906.14	0.11	2904.07	0.09
−11	2625.72	.02	2624.08	−.05	2	2925.78	0.00	2923.68	.01
−10	2651.98	−.01	2650.29	.07	3	2944.79	.02	2942.67	.04
−9	2677.75	−.02	2676.02	−.12	4	2963.16	.08	2961.01	.07
−8	2703.03	.03	2701.25	.04	5	2980.87	.03	2978.70	−.02
−7	2727.79	−.04	2725.97	.04	6	2997.91	−.13	2995.73	−.07
−6	2752.04	−.01	2750.18	.13	7	3014.28	.01	3012.08	.08
−5	2775.75	.04	2773.85	−.08	8	3029.96	0.00	3027.74	−.05
−4	2798.92	−.14	2796.99	−.11	9	3044.93	−.05	3042.69	−.07
−3	2821.52	−.03	2819.56	−.05	10	3059.19	−.12	3056.93	−.09
−2	2843.56	0.00	2841.57	.02	11	3072.73	.03	3070.45	.06
−1	2865.02	.07	2863.00	−.01	12	3085.52	.10	3083.23	.05

TABLE II. *Calculated frequencies of harmonic.*

j	Major Component	$\Delta\nu$	Minor Component	$\Delta\nu$	j	Major Component	$\Delta\nu$	Minor Component	$\Delta\nu$
−8	5468.33	0.22	5464.44	0.23	1	5687.65	.16	5683.63	.28
−7	5497.24	−.27	5493.37	−.25	2	5706.11	.10	5702.06	−.05
−6	5525.05	−.01	5521.19	.04	3	5723.34	−.05	5719.26	.16
−5	5551.75	−.07	5547.88	−.14	4	5739.32	−.03	5735.22	.04
−4	5577.31	−.06	5573.43	−.03	5	5754.04	−.16	5749.92	−.23
−3	5601.73	.32	5597.83	.15	6	5767.47	.03	5763.35	−.07
−2	5624.99	−.17	5621.06	−.14	7	5779.61	−.07	5775.49	−.09
−1	5647.07	−.04	5643.11	−.01	8	5790.44	.10	5786.34	−.06
					9	5799.94	0.00	5795.87	.17

In the energy Eq. (1) the constants B, C and k^2 have been used to replace somewhat inconvenient combinations of the constants of the force function which we are now in a position to evaluate from the empirical data for these four bands. In Kratzer's original paper the potential energy of the molecule was developed in the form

$$\phi = \phi_0 - (2\pi\nu_0)^2 J\{1/\rho - 1/(2\rho^2) + c_3\xi^3 + c_4\xi^4 + \cdots\}$$

where $\rho = r/r_0$, the ratio of the distance between nuclei to the equilibrium distance. $\xi = \rho - 1$. ν_0 is the frequency of vibration for infinitesimal amplitude. In terms of the above constants

$$k = (h/4\pi^2\nu_0 J) \; ; \quad B = (3/2)k^2(1+2c_3) \; ; \quad C = 3+15c_3+(15/2)c_3^2+3c_4.$$

The constants ν_0 and J are easily found from the band data. To determine ν_0 both fundamental and harmonic band must be used. The two values for the two isotopes are given in the following table. Their ratio is satisfactorily equal to the inverse ratio of the square roots of the reduced masses. This is shown in the later computation of ϕ''. Four values of J may be obtained, one for each band. With the help of the relation $J = \mu r_0^2$, r_0 has been computed and found to agree surprisingly well for the two isotopes. The small variation from fundamental to harmonic is typical of all the constants. It may be partly due to the fact that the harmonic has fewer lines and therefore less reliable constants. More probably it indicates that the energy expression is a closer approximation for the fundamental for which the amplitude of vibration is smaller. The value of k may be found directly from the coefficient of j^3. This however is the least reliable of the coefficients. It has also been computed from the formula given above involving J and ν_0. The latter values agree closely and do not differ much from the mean of the values found from the cubic term. The values of c_3 and c_4 have been calculated using the more satisfactory determination of k^2. They are sensitive to small variations of the other constants but these relative variations are not important in the calculation of the derivatives of the force function. The constants are given in the following table.

TABLE III.

	Fundamental Major	Harmonic Major	Fundamental Minor	Harmonic Minor
$(h/8\pi^2 J)/(1/3\cdot 10^{10})$	10.5843	10.5980	10.5703	10.5817
$J\cdot 10^{40}$	2.6126	2.6092	2.6161	2.6132
$r_0\cdot 10^8$	1.2765	1.2757	1.2764	1.2757
$\nu_0(1/3\cdot 10^{10})$	2989.36		2987.28	
C	4.8848		4.8894	
$k^2\cdot 10^5$ (cubic term)	4.7499	5.8808	4.8107	5.1669
$k^2\cdot 10^5$ $(k = h/4\pi^2\nu_0 J)$	5.0146	5.0276	5.0082	5.0193
c_3	0.17370	0.16845	0.17342	0.17015
c_4	−0.31633	−0.28942	−0.31249	−0.30000

Writing

$$\phi = \phi_0 + \frac{1}{2}\phi_0''(r-r_0)^2 + \frac{1}{3!}\phi_0'''(r-r_0)^3 + \frac{1}{4!}\phi_0^{IV}(r-r_0)^4 + \cdots$$

and comparing with Kratzer's energy function, we have

$$\frac{1}{2}\phi'' = \frac{(2\pi\nu_0)^2 J}{2r_0^2} = 2\pi^2\nu_0^2\mu$$

$$\frac{1}{3!}\phi''' = -(1+c_3)\frac{(2\pi\nu_0)^2 J}{r_0^3}$$

$$\frac{1}{4!}\phi^{IV} = \frac{3-2c_4}{2}\,\frac{(2\pi\nu_0)^2 J}{r_0^4}.$$

The derivatives of ϕ have been computed from these equations and are given in the following table.

TABLE IV.

	Fundamental Major	Harmonic Major	Fundamental Minor	Harmonic Minor
$\frac{1}{2}\phi''10^{-6}$	2.5454		2.5457	
$\frac{1}{3!}\phi'''10^{-13}$	−4.6809	−4.6628	−4.6806	−4.6701
$\frac{1}{4!}\phi^{IV}10^{-21}$	5.6745	5.5835	5.6641	5.6313

The agreement of all the constants bears witness both to the high precision of this experimental work and to the success of the present theory of the rotating dipole.

DIATOMIC MOLECULES ACCORDING TO THE WAVE MECHANICS. II. VIBRATIONAL LEVELS

By Philip M. Morse
Palmer Physical Laboratory, Princeton University

(Received April 8, 1929)

Abstract

An exact solution is obtained for the Schroedinger equation representing the motions of the nuclei in a diatomic molecule, when the potential energy function is assumed to be of a form similar to those required by Heitler and London and others. The allowed vibrational energy levels are found to be given by the formula $E(n)=E_e+h\omega_0(n+1/2)-h\omega_0 x(n+1/2)^2$, which is known to express the experimental values quite accurately. The empirical law relating the normal molecular separation r_0 and the classical vibration frequency ω_0 is shown to be $r_0^3\omega_0=K$ to within a probable error of 4 percent, where K is the same constant for all diatomic molecules and for all electronic levels. By means of this law, and by means of the solution above, the experimental data for many of the electronic levels of various molecules are analyzed and a table of constants is obtained from which the potential energy curves can be plotted. The changes in the above mentioned vibrational levels due to molecular rotation are found to agree with the Kratzer formula to the first approximation.

Introduction

THE wave equation for the nuclear motion[1] of a diatomic mocluele of nuclear masses M_1 and M_2 and charges Z_1 and Z_2, is approximately

$$\nabla^2\psi+\frac{8\pi^2\mu}{h^2}[W-(e^2Z_1Z_2/r)+V_e(r)]\psi=0 \qquad (1)$$

where $\mu=M_1M_2/(M_1+M_2)$, r is the distance between the nuclei, θ and ϕ the usual orientation angles measured from the center of gravity, and $V_e(r)$ the electronic energy calculated by considering the two nuclei as fixed in space a distance r apart.

The combination of the energy of repulsion and the electronic energy can be considered as a nuclear potential energy

$$E(r)=(e^2Z_1Z_2/r)-V_e(r).$$

The wave function Ψ can be considered as a product of three factors $\Psi=N\cdot\Phi(\phi)\cdot\Theta(\theta)\cdot R(r)/r$, where it can be shown that

$$\Phi=e^{ig\phi}$$

$$\Theta=\sin^g\theta\cdot P_j^g(\cos\theta)$$

where g and j are integers. The normalizing factor N is adjusted so that $\int\Psi\cdot\bar{\Psi}\,dv=1$.

When these functions have been substituted in the general equation an equation for R results,

[1] Born and Oppenheimer, Ann. d. Physik **84**, 457 (1927).

$$\frac{d^2R}{dr^2}+\frac{j(j+1)R}{r^2}+\frac{8\pi^2\mu}{h^2}[W-E(r)]R=0. \tag{2}$$

Since we are primarily interested in vibrational levels, j is set equal to zero.

The function $E(r)$ is a complicated function of r and of the electronic quantum numbers, and is not known accurately for any molecule, so it is useless to try to substitute the actual expression for E in the equation. It is possible, however, to assume some functional form for E which gives curves of approximately the same shape as the actual curves, and whose constants can be carried through the calculations to the end and then adjusted to conform to the experimental data.

The forms for E which have been used are, among others, the two series[2] $a/r+b/r^2+c(r-r_0)^3+\cdots$, and $b'(r-r_0)^2+c'\ (r-r_0)^3+\cdots$.
These series give a general equation for the allowed energy levels

$$W=-D+h\omega_0[(n+\tfrac{1}{2})-x(n+\tfrac{1}{2})^2+K_3(n+\tfrac{1}{2})^3+\cdots] \tag{3a}$$

where the constants ω_0, x, K, $\cdots$, are functions of a, b, c, etc., and so if W is known empirically, E can be determined.

There are several objections to such series forms for E. In the first place the effect of all the terms in $(r\text{-}r_0)$ to the power 3 or over (which terms are not always small) must be computed by perturbation methods, thus adding another approximation to a list already long. In the second place the series for E determined from the known values of ω_0, x, K_3, etc., does not converge for large values of r, and so the series is only applicable over a restricted range of r.

In the third place the experimental data show that constants $K_3\cdots$, are very much smaller than ω_0 or x, whereas the general series for E do not show that any such peculiarities should exist. In other words these series are too general.

We must search, then, for a form for E which will satisfy the following requirements: (1), It should come asymptotically to a finite value as $r\to\infty$; (2), It should have its only minimum point at $r=r_0$; (3), It should become infinity at $r=0$ (this need not be exactly true, however, the results are practically the same if E becomes very large at $r=0$); (4), It should exactly give the allowed energy levels as the finite polynomial.

$$W(n)=-D+h\omega_0[(n+\tfrac{1}{2})-x(n+\tfrac{1}{2})^2]. \tag{3}$$

The very small correction term coefficients $K_3\cdots$, can then be determined by perturbation methods with a reasonable expectation that these methods on such small quantities will give fairly accurate results.

A form will be chosen for E which satisfies requirements 1 and 2 exactly, and 3 approximately, and the problem will then be to show that the chosen form satisfies requirement 4.

A Solution of the Problem

The function which it is proposed to use here is the simple one

$$E(r)=De^{-2a(r-r_0)}-2De^{-a(r-r_0)}. \tag{4}$$

[2] E. Fues, Ann. d. Physik **80**, 367 (1926).

This function has a minimum of $-D$ at $r=r_0$, comes asymptotically to zero at $r=\infty$ and in general gives curves of a very similar form to the few potential energy curves which have been calculated theoretically.[3,4,5] The only portion where it does not fit these curves is at $r=0$, where it should be infinity. But it will be seen that for the values of D and a used to fit the data $E(r)$ is between $100D$ and $10000D$ at $r=0$, a value so large that, as far as its effect on the energy levels and wave function goes, it is as good as infinity.

The frequency of classical small vibrations about r_0 is

$$\omega_0=(a/2\pi)(2D/\mu)^{1/2}. \tag{5}$$

If this form of E is substituted in Eq. (3), j set equal to zero, and the transformation $u=(r-r_0)$ made, then

$$\frac{d^2R}{du^2}+\frac{8\pi^2\mu}{h^2}[W-De^{-2au}+2De^{-au}]R=0. \tag{6}$$

The boundary conditions are now set that R must be finite, single valued and continuous in the range $-\infty \leqq u \leqq +\infty$. It will be found that for some allowed solutions in this case $r\Psi$ will not be zero at $r=0$. But in every case $r\Psi$ will be extremely small, and since the point $r=0$ is some distance outside the important interval where $W>E$ this discrepancy will not affect the values of the energy levels.

In other words, since we have admittedly not used the correct form for E, and since we presumably could not find the true solution for R anyway, we must content ourselves with a solution which deviates from the correct solution in a portion which has little effect on the values of the allowed energies, especially since this deviation is very small.

Make a second transformation, letting $y=e^{-au}$. Then

$$\frac{d^2R}{dy^2}+\frac{1}{y}\frac{dR}{dy}+\frac{8\pi^2\mu}{a^2h^2}\left[\frac{W}{y^2}+\frac{2D}{y}-D\right]R=0 \tag{7}$$

where now R must be finite, continuous and single valued over the range $\infty \geqq y \geqq 0$. Let $R=e^{-dy}\cdot(2dy)^{b/2}\cdot F(y)$. Then if

$$d=2\pi(2\mu D)^{1/2}/ah \tag{8}$$

$$W=-a^2h^2b^2/32\pi^2\mu \tag{9}$$

and if $z=2dy$, then the equation becomes

$$z(d^2F/dz^2)+(b+1-z)(dF/dz)+\left(\frac{8\pi^2\mu D}{a^2dh^2}-b/2-1/2\right)F=0. \tag{10}$$

The solution of this equation is a finite polynomial[6] if $(8\pi^2\mu D/a^2h^2d-b/2-1/2)=n$, an integer greater than zero. That is

$$b=4\pi(2\mu D)^{1/2}/ah-1-2n=k-1-2n \tag{11}$$

[3] O. Burrau, Klg. Danske. Vid. Selskab. **7,** 14 (1927).
[4] Heitler and London, Zeits. f. Physik **44,** 455 (1927).
[5] Morse and Stueckelberg, Phys. Rev. **33,** 907 (1929).
[6] Schroedinger Ann. d. Physik **80,** 483 (1926).

where k $(=4\pi(2\mu D)^{1/2}/ah)$ must be greater than unity to have a discrete energy spectrum. The positive values of b are the only ones for which R is finite over the range $0\leqq z\leqq\infty$. This means that n can have any integral value in the range $0\leqq 2n\leqq(k-1)$.

The solutions for F are the generalized Laguerre polynomials

$$F=L^{b}_{n+b}(z)=\frac{d^{b}}{dz^{b}}\left[e^{z}\cdot\frac{d^{n+b}}{dz^{n+b}}(z^{n+b}e^{-z})\right].$$

Usually both superscript and subscript-minus-superscript are taken to be integers, although the superscript need not be integral. Here b is a fraction, and fractional differentiation must be used to obtain the polynomial from the definition above. The polynomial can be obtained by the use of the recursion formula obtained directly from Eq. (10) without evoking the use of fractional differentiation, but it is felt desirable to use the general definition for the sake of uniformity. Such differentiation does not vitiate the general formulas of integration etc., which have been developed for these polynomials, as long as n is an integer.

The formulas needed for fractional differentiation are given here for convenience.

$$\frac{d^{b}(z^{a})}{dz^{b}}=\frac{\Gamma(a+1)}{\Gamma(a-b+1)}z^{a-b}\ ;\quad\frac{d^{b}(e^{-z})}{dz^{b}}=e^{i\pi b}\cdot e^{-z}.$$

The application of this to the definition of F results in

$$L^{b}_{n+b}(z)=e^{i\pi(k-n-1)}\frac{\Gamma(k-n)}{n!}\left[x^{n}-(k-n-1)nx^{n-1}+\frac{(k-n-1)(k-n-2)n(n-1)x^{n-2}}{2!}\cdots\right]$$

The normalizing integral

$$\int_{0}^{\infty}z^{b-1}\cdot e^{-z}\cdot L^{b}_{n+b}(z)\cdot L^{b}_{m+b}(z)\cdot dz=N_{nm}$$

$$=\begin{cases}0 & (\text{if } n\neq m)\\ [\Gamma(k-n)]^{2}\sum_{s=0}^{n}\dfrac{\Gamma(k-2n+s-1)}{\Gamma(s-1)} & (\text{if } n=m)\end{cases}\quad(12)$$

so that the complete wave function R for the nuclear vibration is

$$(2da/N_{nn})^{1/2}\cdot e^{-de^{-a(r-r_0)}}\cdot[2de^{-a(r-r_0)}]^{(k-2n-1)/2}\cdot L^{k-2n-1}_{k-n-1}[2de^{-a(r-r_0)}]$$

The square of this, times the perturbing energy, is to be multiplied by dr as a "volume element" and the integral taken from zero to infinity to obtain the perturbation energy.

The allowed energy levels are obtained from Eqs. (9) and (11)

$$\begin{aligned}W(n)&=-a^{2}h^{2}(k-1-2n)^{2}/32\pi^{2}\mu\\&=-D+\frac{ah}{2\pi}(n+1/2)(2D/\mu)^{1/2}-a^{2}h^{2}(n+1/2)^{2}/8\pi^{2}\mu\qquad(13)\\&=-D+h\omega_{0}(n+1/2)-(h^{2}\omega_{0}^{2}/4D)(n+1/2)^{2}\end{aligned}$$

from Eq. (5). As has been noted before, n takes on all integral values from zero to $(k-1)/2$. This is the first case noted of a Schroedinger equation giving a finite number of discrete energy levels.

Equation (13) is of the form of empirical Eq. (3), and it therefore is of the form which we set out to obtain. Since this equation expresses the empirical data so well in most cases, therefore the potential energy E, as given by Eq. (4), must have the same shape as the real potential energy throughout the range where Eq. (13) is a valid representation of the actual energy levels.

Thus if the lists of spectroscopically determined molecular constants give r_0 in Angstrom units and ω_0 and $\omega_0 x$ in wave-numbers, D is found in wave-numbers by the equation

$$D=\omega_0^2/4\omega_0 x \tag{15}$$

and the coefficient a is found by the relation

$$a=(8\pi^2 c\mu\omega_0 x/h)^{1/2}=0.2454(M\omega_0 x)^{1/2} \tag{16}$$

where $M=M_1M_2/(M_1+M_2)$, M_1 and M_2 being the atomic weights of the two nuclei in terms of oxygen 16.

With r_0 known and D and a determined, the potential energy curve corresponding to the data is given by Eq. (4), where E is in wave-numbers if r is in Angstrom units.

An Empirical Law for r_0

When the available lists of molecular constants were examined it was found that in many cases ω_0 and $\omega_0 x$ were known but r_0 was not known. Several writers[7] have made use of a relation $r_0^2\omega_0=$constant to obtain the unknown r_0's, but deviations from this relation are quite large.[8]

To find what law obtained, if any, between r_0 and ω_0, 21 cases were taken from Birge's table[9] where r_0 and ω_0 were both known. An equation, $\log\omega_0-p\log r_0=\log K$ was assumed, and the data were subjected to a least squares analysis. The most probable values of the constants were found to be $p=2.95$ and $K=2975$. If p be taken to be 3 then the equation becomes

$$r_0^3\omega_0=3000\text{A}^3/\text{cm} \tag{17}$$

to within a probable error of ± 120 and a maximum deviation of 420. This is about due to the probable error of the recorded values of r_0, for if these values had a probable error of 1.3 percent, then r_0^3 would be given to a probable error of 4 percent.

[7] Birge, Phys. Rev. **25**, 240 (1925). Mecke, Zeits. f. Physik **32**, 823 (1925).

[8] Since this paper has been sent to the editor, Professor Birge has kindly brought to the writer's notice the fact that the equation $r_0^2\omega_0=C_m$, where C_m has a different value for each molecule, is a better fit for some data than Eq. (17). In other words, the slope of the curve $\log r_0$ plotted against $\log\omega_0$ is nearer two for each individual molecule, but the slope of the band representing all molecules is nearer three, as given by Eq. (17). However, at least one value of r_0 must be known for a molecule before C_m can be known. Therefore Eq. (17) presents the only means of obtaining a value for r_0 for a molecule when no empirical value of r_0 for that molecule is available; and so it is useful, even if the probable error of the value so obtained were rather larger than the above least squares analysis would indicate.

[9] Mulliken, Phys. Rev. **32**, 206 (1928) and Birge, Int. Crit. Tables, Vol. V, 411, (1929).

TABLE I.[10]

No.	Mol.	State	A wave-nos.	D wave-nos.	a	r_0 obs. A units	r_0 calc. A units	reference
1	BeO	$^1\Sigma$	41600	42300	2.12	1.33	1.27	(14)
2	BeO	$^1\Sigma$	72200	51700	1.76	1.36	1.30	(14)
3	BO	$^2\Sigma$	74200	75100	2.14	1.21	1.17	(9)
4	BO	$^2\Pi$	59800	36800	2.04	1.36	1.34	(9)
5	BO	$^2\Sigma$	82500	40000	1.99	1.31	1.33	(9)
6	AlO	—	33100	33600	2.06	1.62	1.46	(15)
7	AlO	—	70000	49800	1.51	1.66	1.52	(15)
8	C_2	$^3\Pi$	55900	56700	2.14	1.31	1.23	(9)
9	C_2	$^3\Pi$	49100	40600	2.65	1.27	1.19	(9)
10	CN	$^2\Sigma$	75600	76600	2.32	1.17	1.14	(9)
11	CN	$^2\Pi_i$	68700	55200	2.30	—	1.20	(9)
12	CN	$^2\Sigma$	78600	53900	2.88	1.15	1.12	(9)
13	CO	$^1\Sigma$	90500	91600	2.29	1.15	1.12	(9)
14	CO	$^3\Pi$	99200	51600	2.45	—	1.20	(9)
15	CO	$^3\Sigma$?	94900	38300	1.93	—	1.37	(9)
16	CO	$^1\Pi$	96700	32600	2.67	1.24	1.26	(9)
17	CO	$^1\Sigma$	108800	28800	4.55	1.12	1.12	(9)
18	CO	$^1\Pi$	145000	46300	2.86	—	1.16	(9)
19	CO^+	$^2\Sigma$	193100	79200	2.91	1.11	1.11	(9)
20	CO^+	$^2\Pi_i$	177300	42700	2.42	1.25	1.25	(9)
21	CO^+	$^2\Sigma$	189100	29600	3.17	1.17	1.21	(9)
22	F_2	$^1\Sigma$	33600	34200	2.39	1.4	1.37	(9)
23	F_2	$^1\Sigma$	24800	1420	3.21	—	2.11	(9)
24	H_2	$1^1\Sigma$	38000	40100	1.85	.76	.89	(11)
25	H_2	$2^1\Sigma$	116900	27600	.69	1.31	1.31	(16)
26	H_2	$2^3\Pi$	112000	19500	1.48	.97	1.08	(11)
27	H_2	$2^3\Sigma$	118200	24600	1.44	1.08	1.05	(11)
28	H_2	(C)	119200	21300	1.41	1.06	1.08	(11)
29	H_2	$3^3\Pi$	131500	21200	1.37	1.14	1.09	(11)
30	H_2	$3^1\Pi$	225000	114500	.61	—	1.08	(11)
31	H_2	$4^3\Pi$	136500	20400	1.38	1.14	1.10	(11)
32	H_2	$5^3\Pi$	140400	21800	1.32	1.17	1.10	(11)
33	H_2	$6^3\Pi$	143000	23000	1.28	1.17	1.11	(11)
34	H_2^+	—	143700	20600	1.36	1.06	1.11	(11)
35	I_2	—	19100	19200	1.50	2.66	2.41	(13)
36	I_2	—	20300	4770	1.80	3.01	2.86	(13)
37	N_2	$^1\Sigma$	94300	95500	2.56	—	1.09	(9)
38	N_2	$^3\Sigma$?	103200	37600	2.42	—	1.28	(9)
39	N_2	$^1\Pi$	119100	51000	2.41	—	1.21	(9)
40	N_2	$^3\Pi_u$	126000	51200	2.46	1.21	1.21	(9)
41	N_2	$^3\Pi_u$	150300	46100	3.31	1.15	1.14	(9)
42	N_2^+	$^2\Sigma$	202800	67000	2.62	1.12	1.11	(9)
43	N_2^+	$^2\Sigma$	224500	62900	3.10	1.08	1.08	(9)
44	NO	$^2\Pi_u$	61300	62200	2.55	1.15	1.16	(9)
45	NO	$^2\Sigma$	149200	106200	2.42	1.07	1.09	(9)
46	NO	$^2\Pi_u$	80300	35400	1.82	1.42	1.43	(9)
47	NO	—	102100	50000	3.49	—	1.09	(9)
48	O_2	$^3\Sigma$	53000	53800	2.34	1.21	1.24	(9)
49	O_2	$^1\Sigma$?	54500	42100	2.39	1.23	1.29	(9)
50	O_2	$^3\Sigma$	59000	10100	2.44	1.61	1.62	(9)
51	O_2^+	$^2\Pi$	164400	56100	2.82	—	1.16	(9)
52	O_2^+	$^2\Pi$	165400	14300	2.57	—	1.50	(9)
53	O_2^+	—	174800	23800	2.31	—	1.43	(9)
54	O_2^+	—	187700	19700	2.93	—	1.37	(9)
55	SiN	—	49400	50000	1.92	1.57	1.38	(12)
56	SiN	—	38200	14500	3.15	1.58	1.43	(12)

[10] It will be noticed that the molecules for which r_0 calc. differs markedly from r_0 obs. are the least symmetric molecules in the list [ie., $M_1M_2/(M_1+M_2)$ differs considerably from $(M_1+M_2)/4$]. Professor R. S. Mulliken has kindly suggested to the writer that perhaps the rule enunciated in Eq. (17) above only holds accurately for molecules where M_1 is about equal to M_2. Certainly the calculated values of r_0 for the perfectly symmetric molecules O_2, H_2 and N_2 give the most consistent check with the experimental values. To apply the rule to very unsymmetric molecules it may be necessary to introduce an "unsymmetry factor" of the type $[4M_1M_2/(M_1+M_2)^2]^{1/4}$ into the term $r_0^3\omega_0$. Curiously enough, those levels for which the above rule is not satisfactory are the ones whose vibrational levels fit Eq. (13) least satisfactorily.

Since six different neutral molecules and two different molecular ions were used in the analysis, it would appear that K is independent of molecular weight, of the electronic state, and of the net charge on the molecule. An independent check of this rule is discussed in the following paper.

Results

A table is given from which the potential energy curves can be plotted by means of the equation

$$E=A+De^{-2a(r-r_0)}-2De^{-a(r-r_0)} \tag{18}$$

r_0 is given in Angstrom units and D, ω_0 and $\omega_0 x$ are given in wave-numbers. The values of r_0 in the column marked r_0 calc. were calculated from ω_0 by means of rule (17). The striking agreement between these values and the experimental values is to be noted. A is given so that all curves of neutral molecule and ion are reckoned from the lowest vibration level of the lowest electronic state of the neutral molecule. Figure 1 shows the levels for N_2 and N_2^+ plotted from these data.

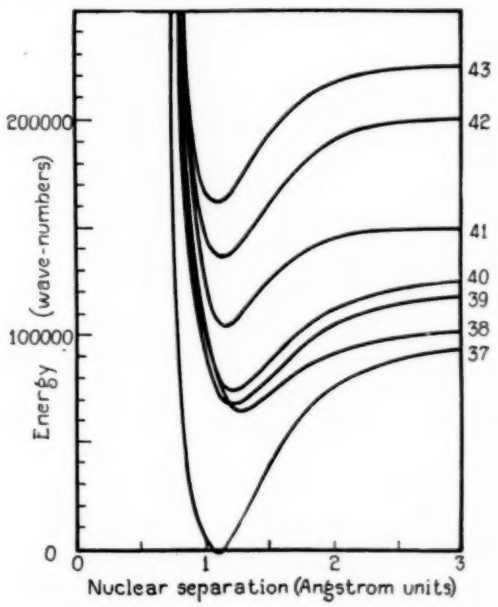

Fig. 1. Potential energy curves for nitrogen. Energy in wave-number and nuclear separation in Angstrom units. Numbers on curves refer to Table I.

Rotational Levels

When the rotational quantum number j is different from zero, the potential energy E in Eq. (4) is increased by an amount $E_j=j(j+1)h^2/8\pi^2\mu r_0^2$. Inasmuch as this increase only affects the wave function to an appreciable

[11] Birge, Proc. Nat. Acad. **14,** 12 (1928).
[12] Jenkins and Laszlo, Proc. Roy. Soc. **A122,** 103 (1929).
[13] Birge, Molecular Spectra in Gases, N. R. C. Bull. **57,** 230 (1927).
[14] Rosenthal and Jenkins, Phys. Rev. **33,** 163 (1929).
[15] Pomeroy, Phys. Rev. **29,** 57 (1927).
[16] Hyman and Birge, Nature **123,** 277 (1929).

extent in the region near $r=r_0$ (where $W>E$), it can be expanded about this point,

$$E_j=\frac{h^2j(j+1)}{8\pi^2\mu r_0^2}\left[1-2\frac{(r-r_0)}{r_0}+3\frac{(r-r_0)^2}{r_0^2}-\cdots\right].$$

In the range where E_j has any appreciable effect, $r-r_0$ is small compared to r_0, and since $h^2j(j+1)/8\pi^2\mu r_0^2$, (which can be called R) is small compared to E for the usual values of j, this expansion can be added to the expansion for E, giving for the first two terms

$$E+E_j=-D+R-R^2/Da^2r_0^2+a^2(D-R)(r-r_0-R/r_0a^2D)^2$$

plus terms in higher powers of $(r-r_0)$.

These two terms can be considered as the first two terms of the expansion of

$$E+E_j=(D-R+R^2/Da^2r_0^2)e^{-2a(r-r_0-R/r_0a^2D)}$$
$$-2(D-R+R^2/Da^2r_0^2)e^{-a(r-r_0-R/r_0a^2D)} \qquad (19)$$

indicating that to the first approximation D has decreased to $D-R+R^2/r_0^2a^2D$ and that r_0 has increased to r_0+R/r_0a^2D. The resultant energy levels will be, to the first approximation

$$\begin{aligned}W(n,j)&=-D+R+(ah/2\pi)(n+\tfrac{1}{2})\left(\frac{2D-2R}{\mu}\right)^{1/2}\\&\quad-a^2h^2(n+\tfrac{1}{2})^2/8\pi^2\mu-R^2/Da^2r_0^2\\&=-D+h\omega_0(n+\tfrac{1}{2})[1-h\omega_0(n+\tfrac{1}{2})/4D-h^2j(j+1)/16\pi^2D\mu r_0^2] \qquad (20)\\&\quad+(h^2j(j+1)/8\pi^2\mu r_0^2)[1-h^2j(j+1)/16\pi^4\mu^2r_0^4\omega_0^2].\end{aligned}$$

This agrees with the general Kratzer[17] formula to the first approximation. (i.e., as far as the above expansion is written).

The energy levels required by Eqs. (13) or (20) agree quite well with the experimentally determined levels for most molecules up to quite high values of n. In other words the $\Delta W(n)$ curve is a straight line for a considerable distance as n is increased. This indicates that the potential energy is effectively that given by Eq. (4) for a large range of r.

However there are some electronic states, usually the normal levels of the molecules, whose $\Delta W(n)$ curves are not straight lines, and therefore whose potential energy curves deviate somewhat from the form given by Eq. (4). This is not surprising, however, for the potential energies of initial states have usually much deeper minima than the rest, and would be expected to deviate most markedly from the standard form.

Such deviations from the straight line ΔW curve can be considered as due to an additional term in the potential energy of the form $E'=B/r+C/r^2+\cdots$, where B and C etc., are very small compared to D. This perturbation can be dealt with in the same manner as E_j has been dealt with, and the values of $B, C, \cdots$, can be found by comparing the resulting formula for $\Delta W(n)$ with the data.

In most cases, however, the $\Delta W(n)$ curve deviates so little from the straight line that such a calculation is not necessary.

[17] Kratzer, Zeits. f. Physik **3**, 289 (1920).

SIMULTANEOUS IONIZATION AND DISSOCIATION OF OXYGEN AND INTENSITIES OF THE ULTRA-VIOLET O_2^+ BANDS

By E. C. G. Stueckelberg
Palmer Physical Laboratory, Princeton University

(Received April 8, 1929)

Abstract

Observations by Hogness and Lunn, Smyth and Stueckelberg, showing that O^+ is formed from the neutral molecule by a single impact of about 20 volts, are explained from the potential energy curves of the molecule and ion. These have been obtained from a method given by P. M. Morse, and from the empirical law $r_0^3\omega_0 = 3000\text{A cm}^{-1}$. The intensities of the ultra-violet O_2^+ bands have been calculated from the same curves and are in good agreement with experiment.

DIFFERENT observers[1] have found ionization potentials between 13.5 and 15.5 volts corresponding to the formation of stable O_2^+. Mackay[2] was the only observer who found two distinct ionization potentials, at 12.6 and 16.1 volts. Above 20 volts Hogness and Lunn[3] found O^+ ions as products of single impacts. Smyth and Stueckelberg[4] confirmed this result and found in addition, that neon ions (having an energy of 21.6 volts) react with neutral O_2 molecules in collisions of the second kind, forming O^+. The conclusion is, therefore, that the potential at which O^+ is formed from O_2 lies between 20 and 21.6 volts.

These facts have been compared with the scheme of potential energy curves for the different states of O_2 and O_2^+. The data for these curves have been obtained from the tables of Birge[5] and of Mulliken.[6] The calculation has not been done by a power series in $(r-r_0)$ as usual, but by a method given by Morse in the foregoing paper.[7] The equilibrium separation (r_0) is not known experimentally for the O_2^+ levels, because the rotation structure has not yet been analysed. The values of r_0 for these states have been obtained by an empirical law which relates ω_0 and r_0, also described in the paper by Morse.

Applying the principle of Franck concerning the most probable transitions between electronic states in molecules[8] to the curves of Fig. 1 we see that the following reactions may be expected: at 13.5 volts: $O_2 \rightarrow O_2^+$ (in the normal state of O_2^+); at higher voltages transitions to the excited stages of

[1] Franck u. Jordan, Anregung v. Quantensprungen p. 273.
[2] Mackay, Phys. Rev. **24**, 319 (1924).
[3] Hogness and Lunn, Phys. Rev. **27**, 732 (1926).
[4] Smyth and Stueckelberg, Phys. Rev. **32**, 779 (1928).
[5] Birge, Molecular Spectra in Gases, p. 232.
[6] R. S. Mulliken, Phys. Rev. **32**, 186 and 761 (1928).
[7] P. M. Morse, Phys. Rev. **34**, 57 (1929).
[8] J. Franck, Trans. Far. Soc. **21**, part 3 (1925).

O_2^+ will occur, such as at 20 volts: $O_2 \rightarrow O_2^{+\prime}$ (in a higher vibrational state of the electronic state labelled with Π?); at 20.3 volts: $O_2 \rightarrow O + O^+$. The most probable transition reaches this upper $^2\Pi$ state at its dissociation limit. The $O_2^{+\prime}$ will therefore immediately dissociate into O and O^+.

Comparing these values with the observed data the formation of 0^+ as a primary product at 20.3 volts agrees with the observed facts, but we have no good explanation for the different values for the ionization potential forming stable O_2^+.

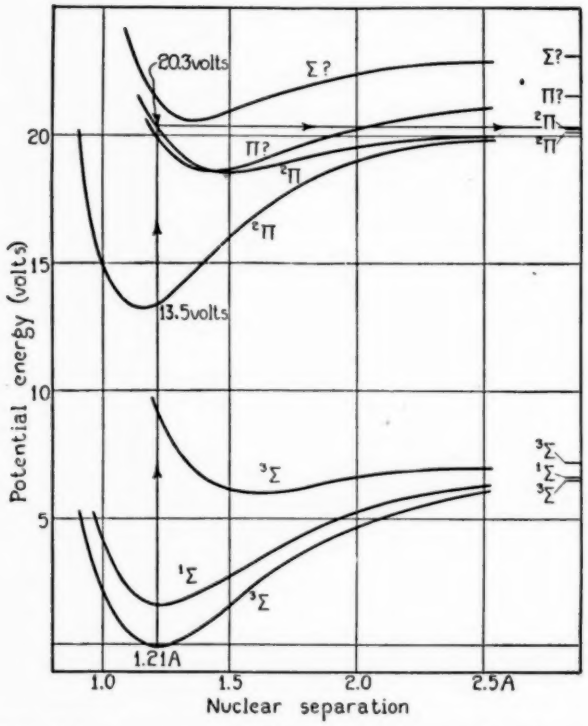

Fig. 1. Potential energy curves for O_2 and O_2^+. Energy in volts and nuclear separation in Angstrom units.

Taking into account the inexactness of the Franck principle, as suggested from quantum mechanics by Condon,[9] we expect that below 20.3 volts a considerable number of O_2^+ is formed with a vibrational energy near dissociation. We expect therefore that besides the O^+, formed by a primary process, there will occur some secondary O^+. In the experiments mentioned above there has not been found any evidence of this. This may suggest that the r_0 of this state is a little too small.

The relative value of the r_0 in this state with respect to the normal state of the O_2^+ can be checked by calculating the intensities of the transitions between these states. This has been done by a method given by Condon.[10]

[9] E. U. Condon, Phys. Rev. **32,** 858 (1928).
[10] E. U. Condon, Phys. Rev. **28,** 1182 (1926).

Figure 2 shows the two potential energy curves on larger scale and the vibration levels associated with them. Taking as the most probable transition

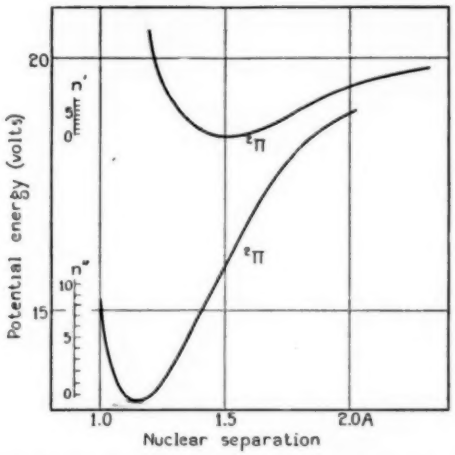

Fig. 2. Potential energy curves and vibration levels for $^2\Pi \rightarrow {}^2\Pi$ bands (ultra-violet O_2^+ bands). Energy in volts, nuclear separation in Angstrom units.

the one which leaves position and momentum of the nuclei unchanged during the transition we obtain the curve in Fig. 3. The observed bands as found by Johnson[11] are marked with crosses. As the centre of gravity of the ob-

	$\Delta\nu$	1810	1777	1744	1712	1679	1646	1613		
$\Delta\nu$	n'' \ n'	3	4	5	6	7	8	9	10	
871	0				×	×	×	×	×	
844	1				×	×	×	×		
817	2			×	×	×	×	×		
789	3		×	×	×	×	×			
762	4	×	×	×	×					
734	5	×	×	×						
707	6	×	×							
680	7	×	×							
	8	×	×							

Fig. 3. Bandheads observed by Johnson marked by ×, and curve of maximum intensity as calculated from Fig. 2.

served bands coincides with the calculated curve, we have an additional confirmation for the chosen values of r_0, and therewith for the potential of 20.3 volts.

[11] R. C. Johnson, Proc. Roy. Soc. **105A**, 683 (1924).

SIMULTANEOUS IONIZATION AND EXCITATION OF DIATOMIC MOLECULES BY IMPACTS WITH POSITIVE IONS AND EXCITED ATOMS

By O. S. Duffendack and H. L. Smith
University of Michigan

(Received March 25, 1929)

Abstract

A study of mixtures of helium, neon, and argon with carbon monoxide and nitrogen is made wherein it is demonstrated that impacts occur between a rare gas ion and a diatomic molecule leading to ionization and excitation of the latter. It is also shown that impacts of the second kind between excited helium and neon atoms and neutral carbon monoxide molecules, resulting in the simultaneous ionization and excitation of the latter, are possible. Experiments are described which show the effectiveness of either type of impact to be greatest when the energy difference is the least. These impacts are shown to explain several previously observed but unexplained effects in similar mixtures in glow dicharges. Two new bands in the Baldet-Johnson band system due to ionized carbon monoxide with edges at λ4454.95, 4458.94, 4480.24, 4485.00; and 4494.30, 4498.31, 4519.89, 4524.89 are reported and six new edges and a new band at λ3413.14, 3414.60; 3584.20, 3600.75; 4116.69, 4348.08; 5856.30, 5860.37, 5900.21, 5905.85 in the comet-tail system. The wave-lengths of the heads of all bands of these two systems observed in this investigation have been measured and an analysis of the systems is given. From a study of the intensity distribution of the negative band systems of carbon monoxide excited in He-CO and Ne-CO mixtures, the following deductions relative to the degree of excitation of the CO-ion in the two mixtures are made: In Ne-CO mixtures there are many more CO-ions in the 16.8 volt state than in the 20 volt state, but in He-CO mixtures the reverse is true. A study of the intensities of the individual comet-tail bands excited in He-CO and in Ne-CO mixtures under the same conditions shows that the exciting processes in He-CO mixtures are more effective in exciting the higher vibrational states of the comet-tail bands than they are in Ne-CO mixtures. The spectrum of carbon dioxide recently observed and reported by Fox, Duffendack and Barker has been shown to be due to the carbon dioxide ion.

EVERY now and then some unusual and interesting effect observed in an electrical discharge through a mixture of gases at low pressure is reported. The conditions under which most of the effects have been noted were those of the ordinary glow discharge. One of the most interesting of these effects is the modification of the spectra of the components of the mixture.

A series of investigations on the effect of helium, neon, and argon on certain diatomic gases has been conducted by Merton and Johnson;[1] Johnson;[2,3] Johnson and Cameron;[4] and Cameron.[5] The results of these investigations are summarized clearly in the Table I taken from Cameron's paper.

[1] Merton and Johnson, Proc. Roy. Soc. **A103,** 383 (1923).
[2] Johnson, Phil. Mag. **48,** 1069 (1924).
[3] Johnson, Proc. Roy. Soc. **A108,** 343 (1925).
[4] Johnson and Cameron, Proc. Roy. Soc. **A106,** 195 (1924).
[5] Cameron, Phil. Mag. **1,** 405 (1926).

TABLE I. *Summary of the observed effects of rare gases on the spectra of diatomic gases.*

System	Emitter	In helium	In neon	In argon
Comet-tail bands	CC^+	strong	less strong	absent
Associated bands (Baldet-Johnson)	CO^+	fairly strong	weak	absent
Negative carbon bands (1st negatives)	CO^+	very strong	moderately strong	very weak
Carbon arc lines	C	present	absent	absent
Negative nitrogen bands	N_2^+	strong	strong	absent
Nitrogen arc lines	N	present	present in part	absent
Triplet system	C	present	present	present
Ultra-violet oxygen bands	O_2^+	weak	weak	absent
Negative oxygen bands	O_2^+	fairly strong	very weak	absent
Oxygen O I	O	present	present	present
Oxygen O II	O^+	?	strong members present	absent

TYPES OF IMPACTS

The foregoing examples of mixture effects, together with many others not mentioned, make a systematic spectroscopic study of electrical discharges in gas mixtures desirable. It is the purpose of this investigation to make such a spectroscopic study, with a simple discharge, in order to demonstrate types of impacts which will explain many of the afore-mentioned effects.

Most of the mixture effects mentioned in the beginning have been observed in glow discharges. This type of discharge is unsatisfactory if an explanation of the observed effects is sought on the basis of impacts, because of the complexity of the phenomena occurring in the discharge. A type of discharge must be chosen wherein the conditions under which the discharge takes place are rather easily controlled. The low voltage arc meets this requirement.

Another most important reason for using the low voltage arc is that it permits the use of two filaments or hot cathodes, separately controlled both as far as electron emission and electron speeds are concerned. The use of such an auxiliary filament in the present investigation has aided materially in demonstrating the types of impacts just discussed above.

APPARATUS

A cross section of the discharge tube together with side and end views of the filaments and the plate is shown in Figure 1.

The discharge tube was made of Pyrex glass throughout. The stoppers S_1 and S_2 and the quartz window W were sealed in with hard deKhotinsky cement and the joints water-cooled to prevent softening when the tube was hot. The side tubes A and B were placed diametrically opposite to avoid reflection from the glass wall at the back of the tube. The filaments were made by winding five turns of 12 mil tungsten wire about another of the same diameter used as an arbor. These spirals were welded to the 100 mil tungsten leads. The U shaped tungsten plate P was placed about 8 mm from

the filaments. The entire tube was placed in an electrically heated oven so that it could be thoroughly outgassed.

The circuit used was similar in many respects to the low voltage arc circuit. The important differences were that the two filaments F_1 and F_2 were on separate circuits, and by means of a potential divider, it was possible

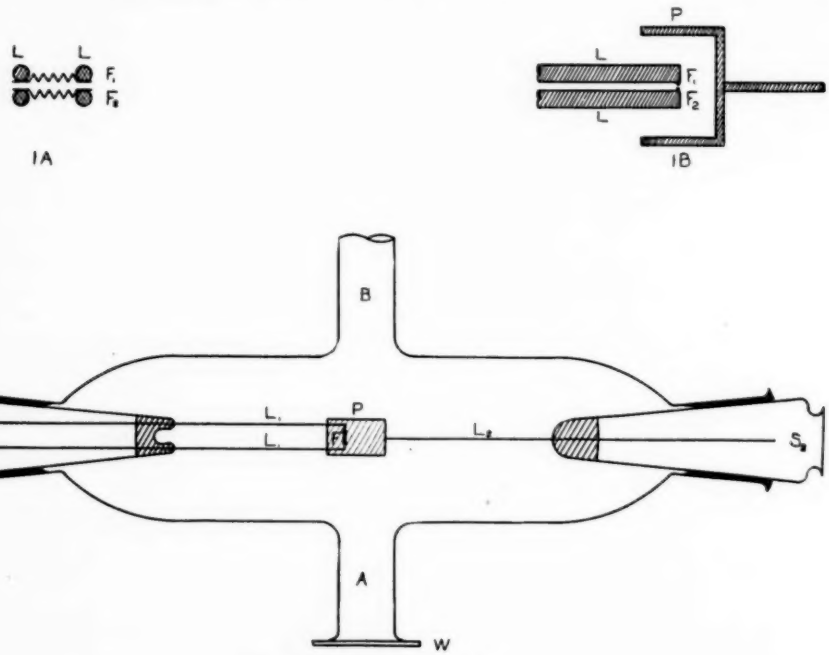

Fig. 1. The discharge tube.

to apply a smaller potential difference between F_2 and the plate than between F_1 and the plate. The necessary voltage for the filament and the plate circuits was supplied by storage cells.

The usual apparatus for purifying, circulating, and storing the gases used was employed in conjunction with the discharge tube. The entire system was exhausted by a single stage mercury diffusion pump backed by a Cenco-Hyvac oil pump.

Manipulation of the Apparatus

In evacuating the system preparatory to the admission of gas, the usual methods of pumping, and baking out of the discharge tube and charcoal traps were employed.

The helium was obtained from the Bureau of Mines at Washington, D. C. Impurities were removed by circulating the gas several times through charcoal traps at liquid air temperatures. Magnesium discharge tubes were also operated during this time to aid in purifying the gas.

The neon came from the Linde Air Products Company. This was admitted to the system and circulated through charcoal traps as in the case of helium. The neon was found to be very pure.

The argon was obtained from the Nela Research Laboratory at Cleveland. This gas was known to contain nitrogen. A calcium arc purifier was used successfully in removing the nitrogen from the argon.

The carbon monoxide was prepared outside the system by heating chemically pure oxalic acid crystals in the presence of concentrated sulphuric acid. This yields carbon monoxide with some carbon dioxide and water vapor. The mixture was passed through a wash bottle containing a concentrated solution of potassium hydroxide to remove the CO_2. The remaining gas was passed over phosphorus pentoxide to remove the water. Any water vapor and carbon dioxide not removed at this time was condensed in the liquid air traps. The dried gas was allowed to flow into an evacuated bulb which filled up to atmospheric pressure. This bulb was sealed on to the system and the gas admitted through a stop-cock as desired.

In producing mixtures of a rare and a diatomic gas the rare gas was admitted first to the required pressure and the diatomic gas added very slowly and the two allowed to mix for some time.

Mixtures of the Rare Gases with Carbon Monoxide and with Nitrogen

The spectra of carbon monoxide excited by electron impacts[6] have recently been investigated in this laboratory. Nine band systems are now known. Six of these originate in the neutral molecule and the remaining three in the ionized molecule. The names of the bands and their respective excitation potentials are given in the accompanying energy level diagram.

Comparative runs were made, using mixtures of each of the rare gases with first, carbon monoxide and later nitrogen, under the same conditions. There were five important variable factors to be considered, namely: partial pressures of the rare gas and the diatomic gas, total gas pressure, potential difference between electrodes, current density, and region of the arc photographed.

After a considerable number of trials with total gas pressures ranging from 0.5 mm to 10 mm and with partial pressures of CO varying from one half to one fiftieth of the total, an optimum total pressure was found at 2.4 mm, with a partial pressure for the CO at 0.2 mm. Under these conditions an arc current of 40 milliamperes could be maintained under a potential difference of from 23 to 25 volts.

A region of the discharge about 4 mm from the filament was focussed on the slit of the spectrograph. It is in this region that the greatest concentration of positive ions produced by direct electron impacts is to be expected. Spectrograms made with the Hilger E2 quartz spectrograph under the above conditions showed in the He-CO mixture a beautiful development of the three band systems of CO, to the practical exclusion of the bands due to the neutral molecule. In the Ne-CO mixtures the first negative bands were present, but weak, the comet-tail bands were fairly strong, and the Baldet-

[6] Duffendack and Fox, Astrophys. J. **65**, 214 (1927).

Johnson bands absent. In the A-CO mixtures all of the band systems due to the ionized molecule were entirely absent.

Simultaneous Ionization and Excitation of Molecules by Positive Ions

In order to account for the development of the band systems of ionized CO in He-CO and Ne-CO mixtures the following three possible processes must be considered: (1) Direct electron impacts, (2) Impacts of the second kind with excited rare gas atoms, (3) Impacts by slow positive ions.

1. *Direct electron impacts.* The simultaneous ionization and excitation might be due to direct electron impacts as Duffendack and Fox[6] have shown to be possible.

That this process is not operative was shown by taking two spectrograms with an He-CO mixture in the tube. In the first, the applied potential difference between the cathode and the plate was 24.7 volts. The second filament was hot but no potential difference was applied between it and the plate. The arc current was 40 milliamperes. In the second, a voltage greater than the excitation potential of the first negative bands, 20 volts, but less than the ionization potential of helium, 24.5 volts, was applied between the auxiliary filament and the plate. The arc current was then 120 milliamperes. The current from the auxiliary filament being now twice as great as from the cathode, the possibility of excitation of the negative bands by direct electron impact was thereby increased threefold, while the concentration of helium ions was increased very little. The intensity of the first negative bands in the second case was not noticeably greater than in the first. It is to be concluded then that under the above conditions the CO molecule is not ionized and excited by direct electron impacts.

2. *Impacts of the second kind with excited rare gas atoms.* The helium spectrum is made up of singlets and triplets. The singlet series belongs to parhelium and the triplet series to orthohelium. The lowest term of parhelium is a 1^1S term corresponding to the normal helium atom; the lowest term of orthohelium is a 2^3S corresponding to an energy of 19.8 volts. The 2^1S term corresponds to an energy of 20.5 volts. The neon atom has its lowest excited state at 16.6 volts.

From the accompanying energy level diagram for carbon monoxide, Fig. 2, it is to be noted that the 19.8 volt level of orthohelium and the 16.6 volt level of neon almost exactly coincide with the minimum excitation potentials of the first negative and comet-tail bands respectively. Hence it is to be expected that in He-CO and Ne-CO mixtures, collisions of the second kind may occur between the excited rare gas atoms and the CO molecules, wherein the latter are simultaneously ionized and excited. The small energy difference of 0.2 to 0.3 of a volt may be expected to come out of the relative kinetic energy of translation of the two colliding molecules, as Franck has shown to be possible. However a study of the first negative bands excited in He-CO mixtures and the comet-tail bands excited in Ne-CO mixtures shows an absorption of energy in the vibrational states of 0.8 volt and 0.7 volt re-

spectively, thus increasing the total energy necessary to excite the band system in the one case to 20.8 volts and in the other to 17.5 volts. While these values increase the amount of energy to come out of translational energy to rather large values, still the possibility of simultaneous ionization and excitation of CO molecules by excited He and Ne atoms must be considered.

When nitrogen is substituted for carbon monoxide the situation is somewhat changed, since the excitation potential of the negative band system of nitrogen, which is less than the ionizing potential of neon, lies far enough above the strong radiating potentials of neon to preclude the simultaneous ionization and excitation of nitrogen molecules by excited neon atoms. However, spectrograms taken with Ne-N_2 mixtures in the discharge tube under the same conditions used for Ne-CO mixtures showed a strong development of the negative bands of nitrogen. As a result it must be concluded that the appearance of the negative bands is not due to collisions of the second kind between excited rare gas molecules and the molecules of N_2, but that the N_2 molecule is ionized by contact with the neon ion.

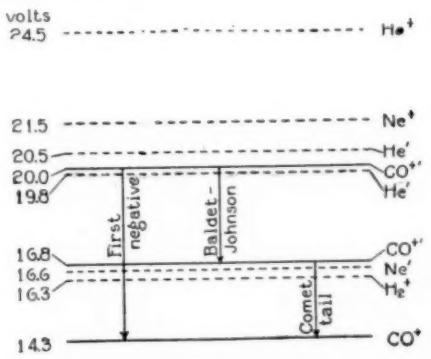

Fig. 2. Energy levels of H_2, Ne, He, and CO^+.

In case both positive ions and excited atoms are present, each possessing sufficient energy to ionize a neutral molecule, then it is to be expected that both types of impacts will occur. Presumably that impact will be most effective wherein the energies are most nearly the same.

3. *Impacts by slow positive ions.* The results of the preceding considerations indicate that the rare gas ion is an effective agent in producing the bands of the ionized diatomic molecule. If the rare gas ion is effective in exciting the negative bands, two possibilities suggest themselves, namely: 1. The rare gas ion upon contact with the molecule might ionize and excite the latter simultaneously, or 2. The excitation of the molecule-ion by direct electron impact might follow as a later event after the molecule had been ionized by the rare gas ion.

That this latter process was not operative was demonstrated by introducing into the discharge, electrons from the auxiliary filament at a voltage sufficiently great to excite the CO ions on collision. Here again the electron current from this filament was twice as great as from the cathode, the total

current being 120 milliamperes. *However, no increase in the intensity of the negative bands was observed.* On the other hand, the electrons from the auxiliary filament were effective in developing the bands due to the neutral CO molecule, especially the third positive bands. These bands, not present in the original discharge, appeared with moderate intensity in the discharge with the auxiliary filament in operation, when the difference of potential between the auxiliary filament and the plate was equal to their excitation potential. In mixtures containing nitrogen the second positive bands of nitrogen were present even though the auxiliary filament was not used, but their intensities increased enormously when the voltage of the auxiliary filament reached their excitation potential. This suggests a new method for determining the excitation potentials of positive bands and arc lines.

Simultaneous Ionization and Excitation of Monatomic Molecules by Positive Ions

In some recent experiments by Duffendack and Black, as outlined in a preceding paper, it is demonstrated that positive ions of high ionization potential may simultaneously ionize and excite monatomic molecules. In neon-copper mixtures those lines originating in levels lying between 21.0 and 21.4 volts were greatly enhanced due to the fact that these levels are in resonance with the neon ion at 21.5 volts.

The reaction may be written:

$$Ne^{+}+Cu \rightarrow Cu^{+\prime}+Ne$$

The failure of the excited neon atoms, 16.6 volts, strongly to excite the Cu^{+} levels lying between 15.9 and 16.8 volts is probably due, as suggested by Professor J. Franck, to the presence of molecular hydrogen, which, with an ionization potential of 16.3 volts, quenched the excited neon atoms.

The reaction may be written:

$$Ne'+H_2 \rightarrow H_2^{+}+Ne+e$$

Impacts by Slow Positive Ions vs. Impacts by Excited Atoms

Since in a discharge through a He-CO mixture there are He ions and excited He atoms, it is important to determine, at least in an approximate way, which is more effective in exciting the bands of CO, the He ion or the excited He atoms. A similar statement may be made for Ne-CO mixtures. Professor J. Franck has suggested that by adding hydrogen it should be qualitatively possible to say which is more effective in exciting a given band system, a positive ion or an excited atom.

The following table shows the possible reactions in mixtures of He-CO-H_2 and Ne-CO-H_2, listed presumably in the order of their probabilities. It is assumed that the probability of the impact is greatest when the energy difference is the least. The energy values of the various components may be obtained from the accompanying energy level diagram, Fig. 2.

The experimental work was carried out as follows:—Hydrogen was prepared by the electrolysis of water carefully dried over P_2O_5 and de-oxidized

by being in contact with a hot tungsten filament in the presence of P_2O_5 for several hours. Helium was introduced into the system to a pressure of 2 mm, then CO was added until the total pressure was 2.2 mm. With a plate voltage of 26 volts and an arc current of 40 m. a., a spectrogram was made in 30 minutes with a Hilger E2 spectrograph. A second exposure was made

TABLE II. *Possible reactions in He-CO-H_2 and Ne-CO-H_2 mixtures.*

Reactions	Energy difference (volts)
(a) $He'+CO\rightarrow CO_{20}^{+'}+He+e$	$-.2$ to .5
(b) $He'+CO\rightarrow CO_{16.8}^{+'}+He+e$	3.0 " 3.7
(c) $He'+H_2\rightarrow H_2^{+}+He+e$	3.5 " 4.2
(d) $He^{+}+CO\rightarrow CO_{20}^{+'}+He$	4.5
(e) $He^{+}+CO\rightarrow CO_{16.8}^{+'}+He$	7.7
(f) $He^{+}+H_2\rightarrow H_2^{+}+He$	8.2
(g) $Ne'+CO\rightarrow CO_{16.8}^{+'}+Ne+e$	$-.2$
(h) $Ne'+H_2\rightarrow H_2^{+}+Ne+e$	.3
(i) $Ne^{+}+CO\rightarrow CO_{20}^{+'}+Ne$	1.5
(j) $Ne^{+}+CO\rightarrow CO_{16.8}^{+'}+Ne$	4.7
(k) $Ne^{+}+H_2\rightarrow H_2^{+}+Ne$	5.2

with all conditions the same except that 0.01 mm of H_2 was added. In a third exposure the partial pressure of H_2 was 0.05 mm, and in a fourth hydrogen pressure was 0.1 mm, that is, there was one half as much hydrogen as carbon monoxide.

Next, two exposures were made with Ne-CO mixtures in the discharge tube, the first with no hydrogen present and the second with 0.1 mm of hydrogen added. The plate voltage was 25 volts and the arc current 40 m.a.

The results of these experiments are summed up in the following table:

TABLE III.

No.	Partial pressures (mm)				Intensities of the band systems		
	He	Ne	CO	H_2	First negative	Baldet-Johnson	Comet-tail
1	2		0.2	—	strong	strong	strong
2	2		0.2	0.01	"	"	"
3	2		0.2	0.05	weaker	weaker	much weaker
4	2		0.2	0.10	"	"	very weak
5		1.85	0.18	—	weak	absent	fairly strong
6		1.85	0.18	0.10	no change	"	very weak

The reduction in intensity of the comet-tail bands, as shown in No. 4 above, is presumably due to the fact that reactions (*b*) and (*c*) are about equally probable. The smaller reduction in intensity of the first negative and Baldet-Johnson bands indicates that reaction (*a*) is much more probable than (*c*) and that (*d*) is more probable than (*f*). The first negative and Baldet-Johnson bands are no doubt largely excited through reaction (*a*) and to a lesser degree through reaction (*d*).

The failure of the Baldet-Johnson bands to appear in Ne-CO mixtures may be due to the fact that the transition probability from the 20 volt level

of CO^+ to the normal level of the ion is greater than that to the 16.8 volt level. In Ne-CO mixtures the 20 volt level is reached through reaction (*i*) only, which does not seem to be extremely probable; since the first negative bands do not have a great intensity in these mixtures. Number 6 in Table III shows that the addition of hydrogen does not affect the intensity of the first negative bands, which indicates that reaction (*k*) is quite improbable. In Ne-CO mixtures there appears to be a greater reduction of intensity of the comet-tail bands when H_2 is added than there is in He-CO mixtures. This is probably due to the fact that the 16.8 volt of CO^+ is the final level for the Baldet-Johnson bands and the intitial level of the comet-tail bands, hence in He-CO mixtures where the Baldet-Johnson bands are strong the addition of H_2 can only effect the direct excitation of the 16.8 volt level while in Ne-CO mixtures the excitation of the 16.8 volt level is due almost entirely to a direct process (*g* in Table II), but since (*h*) may be expected to be equally probable, the addition of H_2 should greatly affect the intensity of the comet-tail bands. This is in agreement with the results shown in Table III.

Conclusion

The results of the fore-going experiments demonstrate conclusively two types of impacts, wherein a neutral molecule is simultaneously ionized and excited.

1. An ion of one kind may, upon collision with a molecule of another gas, ionize that molecule and excite the resulting molecule-ion to the degree that the work of ionization of the one exceeds that of the other. This means that an ion may rob a molecule of an electron, and at the same time give to the resulting ion the excess energy made available by its recombination with the electron over the amount needed to take that electron out of the molecule. Since the energies of excitation are quantized there is usually some energy to be accounted for, and this probably goes into increased kinetic energy of one or both particles involved in the collision.

2. An excited atom of one kind may, upon collision with a molecule of another gas, ionize that molecule and excite the resulting molecule-ion to the degree that the energy of excitation of the one exceeds the work of ionization of the other. In this process an electron is liberated and must take up its share of any excess energy as kinetic energy of translation.

It is also demonstrated that the effectiveness of these impacts in ionizing and exciting a molecule depends upon the energy difference between the states involved, that type of impact being most effective wherein the energy differences are the least.

There is no reason to believe that the method of excitation either by a positive ion or an excited molecule is limited to the ions or excited molecules of the rare gases or to multi-atomic molecules. The same processes may be expected to occur in any mixtures of gases or vapors and should find some application in the production of the first spark spectra of atomic ions to the exclusion of higher spark spectra or even of higher levels in the first spark spectra, and in the approximate determination of the excitation potentials of the spark lines.

Simultaneous Investigations

During the progress of this investigation two other investigations of a somewhat similar nature, but attacking the problem from a different standpoint were being carried on, one by Harnwell[7,8] at Princeton and the other by Hogness and Lunn[9] at the University of California.

It is very evident that, while the results of these two investigations are in harmony with those obtained by the writers, they are not as specific regarding the disposition of the energy in excess of that necessary to produce ionization.

Band Systems of Ionized Carbon Monoxide
The First Negative Bands

The appearance of the first negative bands of carbon monoxide when excited in the helium mixtures is different from that when the bands are excited by direct electron impacts. In the latter case the fine structure seems to be continuous right up to the head of the band, while in the former there is a break in the fine structure just back of the head which indicates an absence of transitions originating in low rotational states.

Baldet-Johnson and Comet-Tail Band Systems

Two bands in the Baldet-Johnson system, one comet-tail band and several band edges in this system not previously reported were observed in

Table IV. *Baldet-Johnson bands. n', initial vibrational levels; n'', final vibratinal levels.*

	n''	$n'=0$	1	2	3
Int.		7	5		
λ	0	3978.29	3729.88	3515.8	3331.9
ν		25129.3	26803.5	28434.9	30004.3
		1674.2	1631.4	1569.4	
$\Delta\nu$		1530.8			
Int.		5			
λ	1	4236.36			
ν		23598.5			
$\Delta\nu$		1504.7			
Int.		3	1		
λ	2	4524.89	4205.74		
ν		22093.8	23770.3		
		1676.5			
$\Delta\nu$			1480.0		
Int.			1		
λ	3		4485.00		
ν			22290.3		

[7] Smyth and Harnwell, Nature, Jan. 15, (1927); Harnwell, Phys. Rev. **29**, 683 (1927).
[8] Harnwell, Phys. Rev. **29**, 830 (1927).
[9] Hogness and Lunn, Phys. Rev. **30**, 26 (1927).

spectrograms of the helium-carbon monoxide mixture. The wave-lengths of all the bands of both systems found on the spectrograms taken with the Hilger E1 quartz spectrograph have been carefully measured by interpolation between lines of the iron comparison spectrum. The wave-lengths and wave-numbers of the band edges of both systems together with their intensities are given in Tables IV and V. The two new bands in the Baldet-Johnson system are both of longer wave-length than those previously reported, and two bands of short wave-length observed by Johnson were not observed by the writers.

TABLE V. *Comet-tail bands.*

n''	$n'=0$	1	2	3	4	5	6
0	Int 2	8	10	9	7	4	2
	λ 4879.72	4539.4	4248.66	3997.43	3777.86	3584.20	3413.14
	ν 20487.4	22023.2	23530.0	25009.2	26462.2	27892.3	29290.5
	$\Delta\nu$ 2180.1	1535.8 2183.6	1506.8 2183.1	1479.2	1453.0 2177.7	1430.1	1398.2
1	Int 2.5	3	4		1		
	λ 5460.83	5039.03	4682.20		4116.69		
	ν 18307.3	19839.6	21346.9		24284.5		
	$\Delta\nu$ 2154.3	1532.3 2154.0	1507.3				
2	Int 2.5	1					
	λ 6189.06	5652.75					
	ν 16153.0	17685.6					
		1532.6					
3	Int		00				
	λ		5856.3				
	ν		17071				

The addition of new bands to the Baldet-Johnson system aids in the analysis of the system. According to Birge,[10] these bands constitute a combination system between the initial states of the first negative and the comet-tail systems. The new Baldet-Johnson bands fit into the analysis made on this basis. The appearance of the bands excited in the various mixtures is in agreement with the above.

Not all the bands of the comet-tail system reported by Baldet[11] were observed either by Johnson or by the writers, in particular the band at λ5281A, corresponding to a wave-number 18,930 which in Baldet's analysis is taken as the 0—0 band. If this band is excluded and the band at λ4879.72A taken as the 0—0 band, as Birge has done, then both the comet-tail and the Baldet-Johnson band systems may be analyzed to include the new bands.

DEDUCTIONS FROM INTENSITY DISTRIBUTION OF NEGATIVE BANDS OF CO EXCITED IN HE-CO AND NE-CO MIXTURES

It is supposed that the CO ion possesses only two energy levels above the normal state, namely at 20 volts and at 16.8 volts, and that the CO ion

[10] Birge, Nature **117**, 230 (1926).
[11] Baldet, Comptes Rendus **180**, 272 (1925).

when once excited loses energy only by radiation. In He-CO mixtures all three band systems are strongly developed with almost equal intensity, the comet-tail bands the most strongly. Since the first negative and the Baldet-Johnson bands have the same initial level, there must have been many more CO ions in the 20 volt state than in the 16.8 volt state. In Ne-CO mixtures, the first negative bands are weak, the Baldet-Johnson bands absent and the comet-tail bands fairly strong. This indicates that in the Ne-CO mixtures there are many more CO ions in the 16.8 volt state than in the 20 volt state.

Vibrational States

The ratio of the intensity of a band excited in a Ne-CO mixture to the intensity of the same band excited in a He-CO mixture may be expected to be the same for all bands with a common initial level.

If one now takes the ratio of intensities of the individual comet-tail bands from the same initial level excited in He-CO and Ne-CO mixtures under the same conditions it is found that the ratio is approximately constant for a given value of n', but as one goes to larger values of n', the ratio decreases. This means that the exciting processes in He-CO mixtures are more effective in exciting the higher vibrational states of the comet-tail bands than they are in Ne-CO mixtures.

The Spectrum of Ionized Carbon Dioxide

Fox, Duffendack, and Barker[12] have recently devised a method for obtaining the spectrum of a gas while it flows continuously through the discharge tube. This method was applied to carbon dioxide and revealed a band spectrum not previously reported, which they assigned to the CO_2 molecule.

This same band spectrum has been obtained in He-CO-O_2, and Ne-CO-O_2 mixtures but not in A-CO-O_2 mixtures. A reduction in the total gas pressure during the exposure was noted in all cases which suggests a clean-up of the CO_2 molecules in the liquid air trap near the discharge tube. The failure of the spectrum to appear in A-CO-O_2 mixtures accompanied by the pressure reduction suggests that CO_2 molecules were formed but not excited.

Several runs were made using He-CO-O_2 and Ne-CO-O_2 mixtures with the auxiliary filament in use at voltages varying from 12 to 19 volts. No increase in the intensity of the bands was noted. This behavior suggests the simultaneous ionization and excitation of the CO_2 molecule by He and Ne ions, by excited He and Ne atoms or both. The immediate conclusion is that the so-called CO_2 bands are really due to ionized CO_2 molecules. In view of the fact that the bands appeared in neon but not in argon the excitation potential of the negative bands of CO_2 must lie between 15.4 and 21.5 volts, the ionization potentials of argon and neon respectively.

[12] Fox, Duffendack and Barker, Proc. Natl. Acad. Sci. **13**, 302 (1927).

The type of positive ion impact which has been demonstrated in this investigation obviously has very little effect on the number of charged carriers in the discharge tube since the process always results in the loss of a positive ion of one kind and a gain of one of another kind. If the newly formed ion has a different mobility than the ion instrumental in its formation a modification of the space charge may result as a secondary effect which may tend to change the value of the current through the tube. The ion formed in the impact while having the same charge will usually have a smaller energy than the ion making the impact, and since some of the energy of the latter is used in exciting the former, and since this energy of excitation is lost by radiation it is thus seen that more energy will be dissipated in the body of the gas than would otherwise be if the conditions were such that the impact could not occur. In this latter case more of the energy of the positive ions would be dissipated by recombination at the cathode where they are collected.

Ionizing impacts by excited molecules will, however, have an effect in cases of conduction of electricity through gases. These effects may be expected to appear in regions like the positive column of a glow discharge when an electric field must be maintained of sufficient intensity to produce ions by electron collisions in order to maintain a neutral space charge in the column. If ionization results from impacts with excited atoms a reduction of the intensity of the field may result and should be observed when a slight amount of a suitable gas or vapor is introduced into the discharge tube.

THE EFFECT OF TEMPERATURE ON THE ABSORPTION BANDS OF FUSED QUARTZ IN THE INFRA-RED

By W. A. Parlin
Johns Hopkins University

(Received March 30, 1929)

Abstract

The absorption bands of specimens of fused quartz, ranging in thickness from 2.0 mm for the 3μ region, to 4×10^{-4} mm for the 8μ region, were studied. In regions where sufficient energy was available, an echelette grating was used to give greater dispersion. Measurements were taken at room temperature and at 850°C. In accord with previous work, the absorption band in the region of anomalous dispersion at 9μ was found to shift toward longer wave-lengths with increasing temperature. With higher resolution, however, fine structure bands were found which did not shift with the temperature, but did undergo marked changes in intensity. Several sharp bands between 2 and 4μ were found to remain fixed as the temperature was changed. A broad band which proved to be double, was found at 12.5μ. These bands did not shift with temperature. In most cases, there was a marked change in intensity with temperature. It was found that inside the strong bands, the absorption was much less at high temperatures, while outside the bands, the reverse was the case.

Introduction

CONSIDERABLE work, extending over a period of more than a hundred years, has been done on the absorption of various substances. The study of temperature effects on the absorption bands has been almost equally extensive. The first observations of this kind were made by Brewster, who described a series of experiments in his Treatise on Optics, published in 1831. In these experiments, Brewster studied the effect on the transmission of various specimens of colored glass. These experiments at first appeared to give conflicting results, that is, in some cases an increase in the temperature caused an increase in the transmission, while in other cases, an increase in temperature made the glass opaque. In particular, Brewster found that blue glass when heated, transmitted first the yellow and finally the red, and as the glass cooled again, gradually cut off the red and yellow, transmitting only the blue. He found further that ruby glass when heated became practically opaque. Upon cooling, it again allowed the red to be transmitted.

These results, conflicting at the time, were later explained by the fact that the color of the glass was due to rather broad absorption bands which cut off one or more regions of the spectrum, and that these bands, or regions of absorption, shifted toward longer wave-lengths as the temperature was raised. Thus, if a broad band extends from the ultra-violet up through the yellow, heating the substance would cause the band to shift toward longer wave-lengths, finally cutting off all visible light. On the other hand, if there were no band in the near ultra-violet, but there was a band extending

from the red end of the spectrum down through the yellow, then an increase in temperature would shift the band toward the red and finally out into the infra-red, thereby increasing the transmission. This shifting of the absorption bands toward longer wave-lengths with increasing temperature, was definitely shown by Conroy in 1891. He was the first to study the absorption bands with a prism spectrometer.

Temperature also has a marked effect on the intensity of the absorption bands, and a corresponding effect on the width of the bands. As early as 1852, Schonbein observed that substances that were highly colored at room temperature, became nearly white at very low temperatures. For example, sulphur appears white at $-50°C$. Many other substances behave in the same manner. An explanation of this loss of color at low temperature was made by Becquerel in 1907, while studying the effect of temperature on the absorption bands of the rare earths. Becquerel found that with decreasing temperature, the bands shifted slightly toward shorter wave-lengths. This was in accord with the work of previous investigators. He also found that at low temperatures, the absorption bands became very narrow, in some cases the bands were less than one-tenth as wide as at room temperatures. The bands were also found to be correspondingly more intense at the low temperatures.

In recent years, considerable work has been done on the absorption bands in the infra-red. H. Rubens and G. Hertz[1] studied the effect of temperature on the reflection maxima of calcite and crystal quartz in the infra-red. They made measurements of room temperature and at the temperature of liquid air. In the case of calcite, they found no shift in the reflection maximum as the temperature was changed. In the case of quartz, however, they claimed a slight shift of the maxima toward shorter wave-lengths as the temperature was lowered. From the observed points shown on the curves that were published, the only result that can be observed is a slight change in the relative intensity of the two bands. The position of maximum intensity remained fixed. This is in accord with results published recently by A. H. Pfund[2] who made a study of the reflection maxima of various substances in the region of anomalous dispersion. Pfund found that the reflection maximum of calcite at 6.5μ showed slight if any shift when heated to 510°C. In the case of amorphous substances, Pfund observed that the reflection maxima of fused quartz and glass in the region of 9μ underwent a marked shift toward longer wave-lengths as the temperature was increased, the shift for fused quartz being approximately 0.4μ when the temperature was changed from 40°C to 1100°C. The reflection maxima for glass were found to shift approximately 0.2μ when the temperature was raised from 40°C to 450°C. Pfund also found that with all substances studied, there was a progressive decrease in the reflecting power with increasing temperature. It was thought of interest to study the absorption in this region, so, at his suggestion, the following work under greater dis-

[1] H. Rubens and G. Hertz, Berl. Ber. 256–274 (1912).
[2] A. H. Pfund, J.O.S.A. and R.S.I. **15**, 69–73 (1927).

persion, on the effect of temperature on the absorption of fused quartz in the regions from 2 to 12μ, was undertaken.

Apparatus

The arrangement of the apparatus is shown in Figure 1. A Nernst glower, *N*, was used as the source of infra-red radiation. It was mounted in a small metal box to protect it from air drafts. It was operated from a storage battery. Since no other instruments were connected to the storage battery, the glower would reach a steady state after about fifteen minutes, and would then remain steady for several hours. It was found, however, that when a new Nernst glower was mounted, it was necessary to operate it for about an hour before it would reach a steady state. It was also noted that

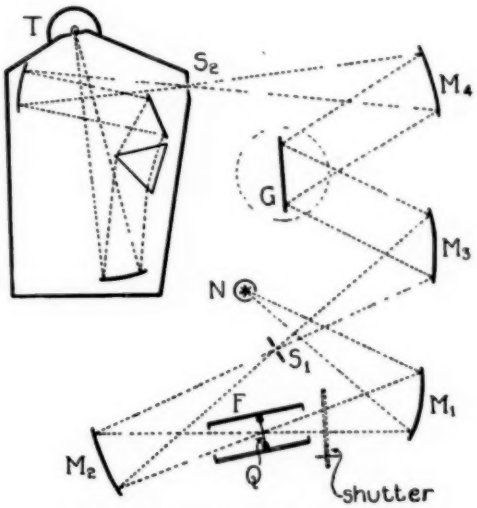

Fig. 1. Arrangement of apparatus.

shortly before a filament burned out it became unsteady. The radiation from the Nernst glower was focused by the mirror, M_1, on the specimen of quartz, *Q*, to be studied. This specimen of quartz was mounted in a steel frame which fitted tightly in the furnace, *F*. The furnace consisted of a clay tube, 4 cm in diameter, and 15 cm long, around which were wrapped several turns of Nichrome wire. The heating element was protected by a thick layer of asbestos. The ends of the furnace were still further protected by asbestos hoods to prevent convection currents as much as possible. The furnace had a rather large heat capacity, and was well insulated, requiring about 45 minutes to reach a steady state. The temperature of the furnace was measured by means of a thermocouple and galvanometer. After passing through the specimen of quartz, the radiation was focused by the mirror M_2 on the first slit S_1 of the grating spectrometer. The radiation is then made parallel by the mirror M_3 and directed on the echelette grating[3] *G*.

[3] Kindly loaned for this work by Dr. Wood.

The setting of the grating was made by observing the position of the image of a lamp filament reflected from a small mirror mounted on the axis of the grating. From the grating, the radiation was focused by mirror M_4 on the second slit of the grating spectrometer S_2. In order to prevent the overlapping of the various orders in the grating spectrum, a rock-salt spectrometer[4] was used. This consisted of a 60° rock-salt prism and mirror having a focal length of 30 cm, mounted according to Wadsworth. The second slit of the grating spectrometer was used for the first slit of the rock-salt spectrometer. Behind the second slit of the rock-salt spectrometer, was placed a compensating vacuum thermopile,[5] which in turn was connected to a D'Arsonval galvanometer having a period of about 5 seconds. To read the galvanometer deflections, a scale was mounted at a distance of 5 meters. The order of

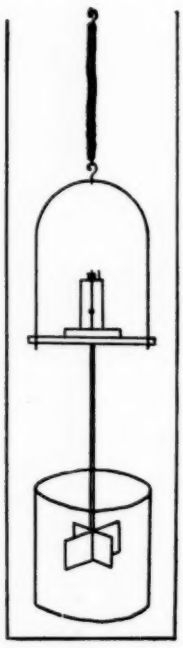

Fig. 2. Spring support for galvanometer.

the grating and prism spectrometers in the present investigation, is the reverse of that used by W. W. Sleator[6] at the University of Michigan. Sleator used a prism of small angle and some difficulty was had in preventing overlapping in the near infra-red. In the present work, a regular 60° prism was used, and any overlapping of orders was entirely eliminated. The only reason for changing the order of the two spectrometers was the fact that the rock-salt spectrometer with thermopile already in place, was kindly placed at my disposal by Dr. Pfund. The grating spectrometer and the

[4] Used by A. H. Pfund, J.O.S.A. & R.S.I. **15**, 69–73 (1927).
[5] A. H. Pfund, Phys. Zeits. **13**, 870 (1912).
[6] W. W. Sleator, Astrophys. J. **48**, 125 (1918).

rest of the apparatus were then constructed around it. The sensitivity of the vacuum thermopile was such that a candle at a meter's distance gave a deflection of 2000 mm.

One of the first difficulties to be overcome was the unsteadiness of the galvanometer deflection due to vibration of the building. Mounting the galvanometer on a wall bracket and resting the galvanometer on a thick felt pad cut down the vibration to some extent, but it was necessary to take readings between 12 and 4 o'clock in the morning. Finally, a spring suspension was used. The arrangement is clearly shown in Figure 2. The suspension consisted of a heavy platform supported by a long spring having a very slow period. A long rod having crossed vanes on its lower end, was rigidly attached to the base of the platform. The vanes were immersed in heavy oil to damp out any oscillation set up by air drafts. To prevent air drafts as much as possible, shields were built around the galvanometer and suspension. This arrangement was very steady, in fact, striking the wall near the galvanometer support a sharp blow with a hammer caused no change in the galvanometer deflection, and a deflection of 0.01 mm could have been detected. With the arrangement thus described, it was possible to take readings to less than 0.1 mm at a scale distance of 5 meters. To obtain these readings, a very narrow diffraction band from a lamp filament was focused on the scale of a micrometer eye-piece. The width of the image thus formed was about 0.05 mm.

Results

Considerable difficulty was encountered in obtaining films of quartz thin enough to be sufficiently transparent in the region of 9μ. Films having a thickness of 0.01 mm were absolutely opaque in this region. By using a very hot oxygen torch, it was possible to blow some thin quartz bulbs having a thickness of 1.5×10^{-3} mm. The thickness of the various specimens was determined by the channeled spectrum method.

With a film of quartz having a thickness of 1.5×10^{-3} mm, the curves shown in Figure 3 were obtained. The absorption was measured for temperatures of 25°, 780°, and 1100°C. As can be seen from the curves, the band is very broad and extremely deep, the transmission in the deepest part of the band being only 0.2 percent. As the temperature was increased, a progressive shift of the absorption region toward longer wave-lengths was observed. A marked increase in transmission was also observed at the higher temperatures, and a corresponding broadening of the band. The actual shift of the region of absorption was approximately 0.4μ.

A very interesting result appeared at about 9.45μ, namely a slight, transparent region which did not shift as the temperature was changed. This small transparent region was found in every set of observations, very decided in some cases, while in others it appeared as a sharp change in the inflection of the curves. This transparent region suggested the probability of a small band on either side which did not shift with temperature, but which did change their relative intensity with increasing temperature.

The problem was then to obtain very much thinner films of fused quartz. Several methods were tried without success. Some of the thinnest films were immersed in hydrofluoric acid. This was not satisfactory, for while it did make the films thinner, they were not of uniform thickness, and could not be used. The first method was again resorted to, and finally a bulb was blown thin enough to show Newton's colors. A small film from this was obtained having a thickness of only 4×10^{-4} mm, or about one-twentieth of the wave-length of light in the region to be studied. This specimen was many times more transparent, and gave much better results as shown in Figure

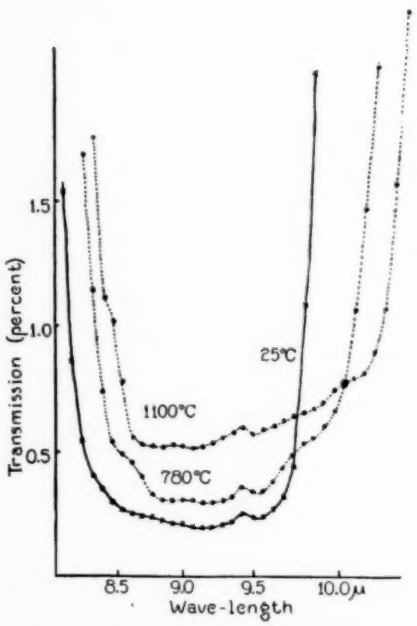

Fig. 3. Transmission of quartz film 1.5×10^{-3} mm thick.

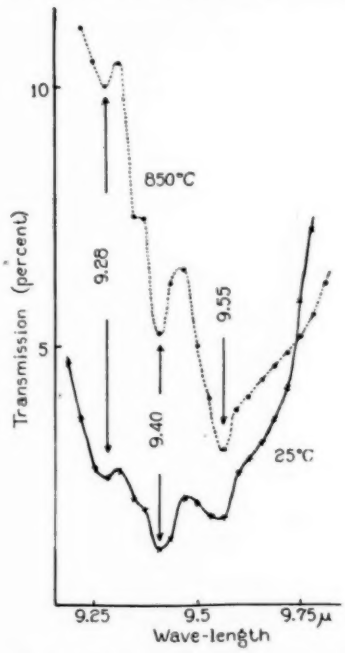

Fig. 4. Transmission of quartz film 4×10^{-4} mm thick.

4. Unfortunately this film was not quite large enough to take advantage of all the energy available but this was more than made up by its greater transparency. In this case measurements were made at 25° and 850°C. A marked increase in transmission at the higher temperatures was observed, as in the previous case. Distinct bands were found at 9.28, 9.40, and 9.55μ. A sharp bend in the curve for high temperature was observed at about 9.34μ which was not so pronounced at low temperature. The position of the maximum for all these bands remained fixed as the temperature was varied, which shows definitely that, while the region as a whole shifts toward longer wave-lengths with increasing temperature, the fine structure bands within the region remain fixed. Attention is called to the marked reversal of the relative intensity of the 9.40 and 9.55 μ bands. This change in the relative intensity of the fine structure bands with temperature is probably the cause of the apparent shift of the region as a whole. In all cases, two observations

were made with the specimen at room temperature, one before the high temperature readings were taken, and one afterwards. No permanent change in the absorption as a result of heating was observed, the two sets of data checking well within the range of experimental error.

A detailed study was next made of the absorption of fused quartz between 2 and 4μ. For this purpose, an echelette grating, having 2000 lines per inch and concentrating in the region of 3.5μ, was used. The effect of temperature on the absorption bands in this region is shown by the curves in Figure 5. The band at 2.71μ was very sharp, being slightly less intense at the high temperature and correspondingly broader. The position of the maximum remained fixed as the temperature was changed from 25°C to to 850°C. As before, low temperature readings were taken before and after the high temperature readings, and no permanent effect of the heating was

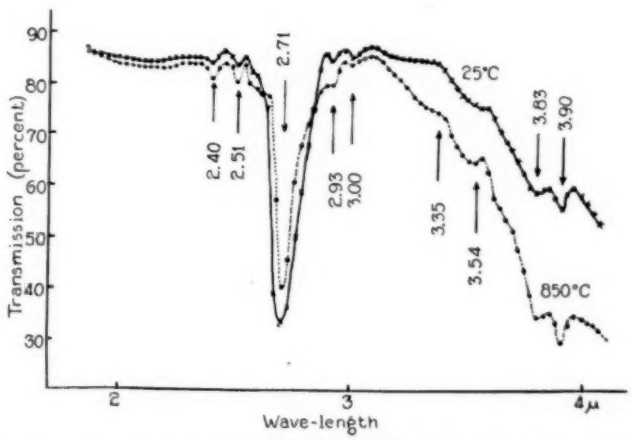

Fig. 5. Effect of temperature on the absorption bands of fused quartz in region of 3.5μ.

observed. Small bands at 3.83μ and 3.90μ did not shift with temperature, but there was a marked increase in absorption of the whole region with increasing temperature. The relative intensity of these two bands remained practically the same as the temperature was changed. A rather weak band was observed at 3.54μ, slightly more pronounced at the higher temperature. A sharp bend in the curves occurred at 3.35μ, and although there was a marked increase in the absorption at this point, the position of the bend was not changed as the temperature was raised. Small bands were found at 2.40μ and 2.51μ, the intensity of the bands being slightly greater at the high temperature, but remaining fixed in position. Two small bands were found at 2.93μ and 3.00μ. These bands were always present in the several sets of observations made, but there was a marked change in intensity of these bands in different observations, even at the same temperature. T. Dreish[7] has made a study of the absorption of fused quartz and crystal quartz in the 3μ region. He found bands for crystal quartz at 2.91μ and

[7] T. Dreish, Zeits. f. Physik **42,** 426–427 (1927).

3.02μ which correspond almost exactly to those mentioned in the present work at 2.93μ and 3.00μ. From this fact, and since fused quartz is a super-

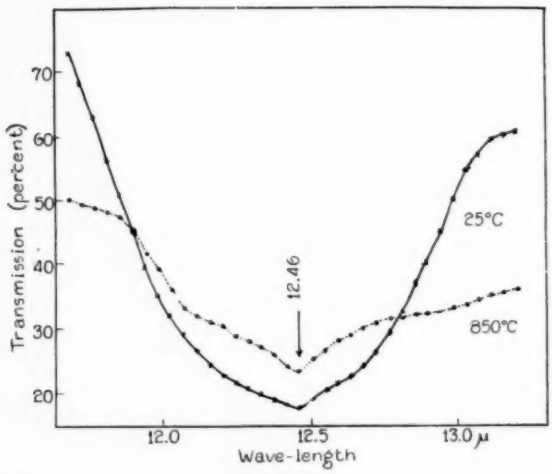

Fig. 6. Effect of temperature on the absorption bands of fused quartz in region of 12.5μ. Thickness of quartz 3×10^{-3} mm.

cooled form that reverts very slowly at low temperatures to the natural form, namely, crystal quartz, it was thought that there might be slight traces of crystalline structure present, which might be the explanation of these bands. The specimen was examined under a strong microscope with

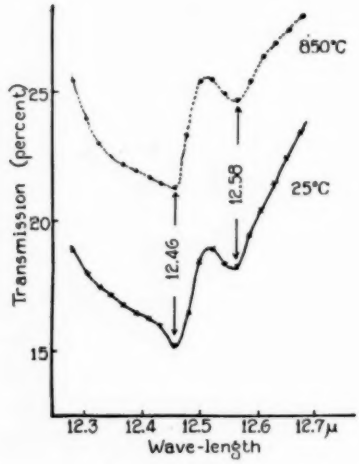

Fig. 7. Effect of temperature on the absorption bands of fused quartz in region of 12.5μ. Thickness of quartz 2×10^{-3} mm.

polarized light, and it was found to have a very slight structure. While these bands may thus be due to crystal quartz, it is possible that these bands

occur in both forms but with very great differences in the relative intensity in the amorphous and crystal form. E. K. Plyler[8] found a very slight band in crystal quartz which corresponds to the very intense band in fused quartz at 2.71μ.

A study was next made of the absorption of fused quartz in the region of 12μ. With a film of quartz of thickness 3×10^{-3} mm, the curves of Figure 6 were obtained. The absorption region is very broad, showing a maximum at 12.46μ. A thinner specimen, 2×10^{-3} mm, was then used. The band was clearly shown to be double as seen in Figure 7. Besides the band at 12.46, there was a band of less intensity at 12.58μ. The intensity of the absorption region was much less at the high temperature, 850°C. The relative intensity of the two bands did not change with the temperature, and the position of the maxima remained fixed, as in all the previous cases. A marked broadening of the band was observed at the high temperature.

Thus it appears that the individual fine structure bands do not change their position with temperature, although there is in some cases a relative change in the intensity of two neighboring bands which results in an apparent shift toward longer wave-lengths with increasing temperature for the unresolved band. In general, the bands are broader and correspondingly less intense at the higher temperature.

Discussion

As to the nature of these bands, it is evident that they must be due to vibrations within the molecule itself. It has been suggested by E. K. Plyler,[8] that the bands at 9μ, 12.5μ, 21μ, and 26μ are fundamental bands. This assumption is made on the basis of the great intensity of the bands, and on their position in the spectrum. In view of the results of the present work, however, it is possible that the fine structure bands at 9μ are, themselves, combination bands rather than fundamental bands. In the first place, temperature should not affect greatly the relative intensity of the fundamental bands. A fundamental band corresponds to an energy change of $\delta n=1$. This amount of energy is absorbed in a jump from the level $0\rightarrow1$, $1\rightarrow2$, or $2\rightarrow3$, etc. If the vibration were truly harmonic, the energy change, corresponding to a jump between any two consecutive energy levels, would be the same. But since the vibration is not exactly elastic, the energy, and accordingly the frequency, will be different in each case. The deviation from the true harmonic oscillator is a function of the temperature. Hence, a change in temperature would be expected to cause a change in the wave-length of the various bands. This effect, however, is of the same order of magnitude as the expansion of the substance with temperature, and is, therefore, too small to be detected with the present infra-red methods.

On the other hand the combination bands result, primarily, from the deviations from the true harmonic oscillator, due to coupling between the vibrators, and since this deviation depends on the temperature, one would

[8] E. K. Plyler, Phys. Rev. **33**, 48–51 (1929).

expect marked changes in the intensity of combination bands with temperature.

Referring again to Figure 4, it is observed that the intensity of the bands at room temperature is as much as 500 percent greater than at a temperature of 850°C. Furthermore, if the bands found by Pringsheim and Rosen[9] using the Raman method, at 38μ and 80μ, together with those previously found at 26μ and 2 =μ, and the two observed in the present work at 12.46μ and 12.58μ are used to calculate combination frequencies, the fine structure bands at 9μ appear as simple combinations of the bands of longer wave-length. If we denote the frequency corresponding to 12.46μ by ν_1, 12.58μ, by ν_2, 21μ by ν_3, 26μ by ν_4, 38μ by ν_5, and 80 by ν_6, the following results are obtained:

Combination	Wave-lengths	
	Calculated	Observed
$(2\nu_3+\nu_6)$	9.28μ	9.28μ
$(\nu_1+\nu_6)$	9.39μ	9.40μ
$(\nu_2+2\nu_6)$	9.57μ	9.55μ

Whether these bands at 9μ are combination bands or not, the fact still remains that the frequency of vibration is not appreciably altered by a large change in temperature, although the number of vibrators affected by coupling may vary in a marked manner as the temperature is changed, which results, in some cases, in the great variation in relative intensity of the combination bands with temperature.

An attempt to check the bands found in the region between 2μ and 4μ by the combination principle was made with the following results:

TABLE I. *Interpretation of bands between 2μ and 4μ as combinations.*

Combination	Wave-lengths		Combination	Wave-lengths	
	Calculated	Observed		Calculated	Observed
$(5\nu_1+\nu_6)$	2.42μ	2.40μ	$(4\nu_1+\nu_6)$	3.01μ	3.00μ
$(3\nu_1+2\nu_2)$	2.51μ	2.51μ	$(3\nu_3+4\nu_4)$	3.36μ	3.35μ
$(3\nu_1+3\nu_3)$	2.63μ	2.62μ	$(3\nu_3+3\nu_4+2\nu_6)$	3.52μ	3.54μ
$(4\nu_2+2\nu_6)$	2.71μ	2.71μ	$(3\nu_2+2\nu_6)$	3.80μ	3.83μ
$(4\nu_2+\nu_6)$	2.91μ	2.93μ	$(2\nu_1+2\nu_3)$	3.92μ	3.90μ

The damping, which results from the deviation from the simple harmonic oscillator, produces the well-known effect of broadening the absorption band. And as this damping is a direct function of the temperature, the broadening would be expected to increase with increasing temperature. This was found to be the case. The increased broadening of a band was always accompanied by a corresponding decrease in the intensity of the band. This was to be expected from the fact that the amount of energy absorbed in the whole band depends directly on the number of absorbing vibrators that are present, and, since this number is constant for fundamental bands (except for the small change due to expansion of the material), the amount

[9] Pringsheim and Rosen, Zeits. f. Physik **50**, 741–755 (1928).

of energy absorbed must be constant. Hence, when the band becomes broader, it must necessarily become correspondingly less intense.

While it is true that the frequency is not changed with temperature when the material has undergone no change of form, other than the slight thermal expansion, it is quite probable that where there are changes in the form of the substance with temperature, there will be a corresponding shift of the absorption bands. It is the intention to study this problem in the near future.

In conclusion, I wish to express may appreciation to Dr. Pfund, who suggested the present investigation and was a continuous source of help and inspiration throughout the progress of the work, and to Dr. Wood for the loan of gratings and for helpful suggestions from time to time. I also wish to thank Dr. Herzfeld for his help in discussing the results and his kindly interest in the work in general.

THE QUANTUM MECHANICS OF CHEMICAL REACTION*

By R. M. Langer[1]
Bureau of Standards, Washington, D. C.

(Received March 27, 1929)

Abstract

It is shown that the quantum mechanics is capable of describing processes which have all the aspects of certain chemical reactions. It turns out that a system may change from one configuration to another when a quantum level of the one configuration has the same energy as a quantum level of the other. Among such reactions mention is made and some discussion given of the large classes of molecular rearrangements, and decompositions, including radioactive disintegration. The dependence on pressure and temperature is slightly discussed and it is indicated that the present theory quite explains the necessity of the old "activation hypothesis" of Arrhenius. The old notions should, however, be modified to take into account that it is not sufficient to have at least the "activation energy" but the molecule must be in a particular state to react. Moreover when there are several "activated" states the rate of reaction from different ones may be very different indeed. Insight is gained into the nature of certain types of catalytic action including special wall catalyses. Some features of photochemical reactions are made clear by the theory.

THE quantum mechanics have been shown[2] capable of dealing with very general types of transition problems which were outside the scope of the old quantum theory. The methods developed have been used[3] in a great variety of important applications with such marked success that it may be hoped that any physical phenomenon will be susceptible to the same treatment.

With this optimistic point of view the problem of chemical change is approached. It is closely related to the problems already discussed and its importance justifies any serious effort even though much is left to be desired.

The treatment of the present article is not the only one possible but it has the advantage that it can be discussed in familiar chemical and mechanical terms. The chief result of this first paper is that it gives a plausible picture of a certain kind of chemical change. The reason for an "activation hypothesis" appears clearly but it seems that modifications are necessary in the form which this hypothesis has taken up to the present. It will be shown that reaction takes place not when the energy content of a molecule exceeds a certain critical value but rather when a molecule is in a particular

* Publication Approved by the Director of the Bureau of Standards of the U. S. Department of Commerce.

[1] National Research Fellow, Bureau of Standards.

[2] Especially in the hands of P. A. M. Dirac, Proc. Roy. Soc. **114,** 243 (1927); E. Schroedinger, Ann. d. Physik **83,** 956 (1927) and M. Born, Zeits. f. Physik **38,** 803 (1926).

[3] E.g., C. Fues, Zeits. f. Physik **43,** 726 (1927); G. Wentzel, Zeits. f. Physik **43,** 524 (1927); F. Hund, Zeits. f. Physik **40,** 742 (1927); Heitler and London, Zeits. f. Physik **44,** 455 (1927); Gamow, Zeits. f. Physik **51,** 204 (1928); Gurney and Condon, Phys. Rev. **33,** 127 (1929).

state whose energy is equal to that of some other physically distinguishable state. The chance that the change will take place depends of course on the interaction between parts of the system and this interaction is dependent not only on the forces involved but most essentially on the distances involved. For example, in the reaction $H+Cl_2 \rightarrow HCl+Cl$, the chlorine molecule might well have too much energy to favor the reaction. The energy required will at no stage be enough to separate the two chlorine atoms. When the molecule is in the right state the chance that a hydrogen atom remove one chlorine to form hydrochloric acid will go down exponentially with the distance between the chlorine molecule and the hydrogen atom.

At present it seems that these same features characterize practically all types of chemical reaction, and what is especially interesting, they may also govern the heretofore mysterious field of catalysis.

I. Introduction

Since the "activation hypothesis" of Arrhenius no important advance has been made in the understanding of the nature of chemical reaction. Arrhenius designed the hypothesis to interpret the most striking fact of chemical reactions, namely, their enormous temperature coefficient. The assumption is that only molecules having more energy than the average (activated molecules) actually undergo reaction. So nicely did this assumption lead to the observed change of reaction rate with temperature, and so difficult has it proved to provide an alternative explanation, that chemists almost without exception believe the "activation hypothesis" to be sound. Apart from the one success for which the hypothesis was invented, it has led only to difficulties. The existence of activated molecules has in general not been demonstrated experimentally.[4] Until within the last few years workers in chemical kinetics had been unable to imagine how molecules of the very high energy required by the "activation hypothesis" in the case of homogeneous unimolecular gas reactions could be supplied fast enough to account for the observed reaction rates. This question is by no means completely solved even now. Perhaps most disheartening was the failure of classical models in the matter of furnishing a convincing picture showing why a molecule was inert until it had a large excess of energy.

Nowadays this failure is easily understood. Classical mechanics could not even approximate the phenomena of chemistry because it did not include the principles which govern the forces between atoms. The "quantum resonance" has no direct counterpart in the older mechanics. Moreover, as will appear later, changes in configuration of a molecular system depend essentially on the very features of the problem which were quite immaterial in the classical theory, namely, the regions where the potential energy is greater than the total energy, and therefore inaccessible to a Newtonian system, which must have positive kinetic energy.

[4] See, however, M. Cantor, Wied. Ann. **62**, 482 (1897), also O. Wulf, Proc. National Acad. **12**, 129 (1926).

In the considerations which follow, the question might arise as to whether it is proper to assume, as we do, that atoms brought close enough together to interact chemically can be approximately described by the functions which describe them when they are alone. This assumption is justified by the success with which the "zero*th*" approximation has dealt with the homopolar bond. The work of Heitler and London has shown that in the main the phenomena of chemical combination are reproduced without consideration of higher order effects. The phenomena of chemical reaction should have less stringent requirements for presumably reaction takes place only when the binding between parts of the molecules is normally loose or is greatly loosened (compared with the normal state) by a large excess of internal energy. This state of affairs is very fortunate for the development of the quantum theory of chemistry, for the higher approximations are extremely complicated.

I. Qualitative Discussion of the Wave Equation

Whereas formerly the difficulty was to find any mechanism for a chemical reaction, the difficulty now is to decide which of many possible mechanisms is the actual one for a particular reaction. It is the chief purpose of this paper to describe a process which, with only slight modifications, will be applicable to many special types of reaction. The case in which the energy of activation, determined from the temperature coefficient, is greater than the energy of dissociation of the bond where reaction occurs is perhaps the most difficult but it will not be treated because it is not certain that such cases exist among chemical reactions. A possible treatment of this case has already been sketched[5] but it might be remarked here that the mention of certain reactions in the reference does not imply that these reactions are necessarily members of the class considered.

It will be desirable first to discuss the wave equation for a case of one degree of freedom from a point of view which is well known.[6] We may write it in the form

$$\frac{d^2\psi}{dx^2}+\frac{8\pi^2 m}{h^2}(E-V)\psi=0. \tag{1}$$

If $V(x)$ were constant this equation would have the simple solution

$$\psi=Ae^{\pm(2\pi i/h)[2m(E-V)]^{1/2}x}. \tag{2}$$

When V is not constant we may hope to approximate the solution by a similar form in which the amplitude and wave-length of oscillation or the decay constant (depending on the sign of $(E\text{-}V)$) are variable. The forms

$$\psi=\frac{e^{\pm(2\pi i/h)\int[2m(E-V)]^{1/2}dx}}{[2m(E-V)]^{1/4}} \tag{3}$$

[5] R. M. Langer, Phys. Rev. **33**, 290 (1929).

[6] H. A. Kramers, Zeits. f. Physik **39**, 828 (1926); G. Wentzel, Zeits. f. Physik **38**, 518 (1926).

have been shown capable of yielding a good approximation. For $(E\text{-}V)>0$ the solutions can be combined to give a real function

$$\psi=\frac{\cos\left\{(2\pi/h)\int[2m(E-V)]^{1/2}dx\right\}}{[2m(E-V)]^{1/4}} \tag{4}$$

and for $(E\text{-}V)<0$ the boundary conditions are satisfied by the solution

$$\psi=\frac{e^{+(2\pi i/h)\int[2m(E-V)]^{1/2}dx}}{[2m(E-V)]^{1/4}}. \tag{5}$$

Kramers has shown how the constant of integration can be chosen so that the solutions for the different regions will go continuously into one another through the singular points where $E-V=0$ in which (4) and (5) fail. The condition that this can be accomplished is approximately the old quantum condition on the energy, namely,

$$\oint p\,dx=2\int_{x_1}^{x_2}[2m(E-V)]^{1/2}dx=nh \tag{6}$$

where x_1 and x_2 are two successive points at which $E-V=0$. Between these two points there are n zeros of ψ_n.

It should be noticed that the amplitude of ψ is especially large (although it turns out to be finite) at x_1 and x_2. Moreover the exponential decay outside of the region x_1 to x_2 is so rapid that it will usually be permissible to use linear approximations for V and actually carry out the integration indicated in (5). For values of x even moderately remote from x_1 or x_2, ψ will be practically zero.

III. A System Capable of Chemical Reaction

The problem we wish to consider is the case in which there are more than two points at which $E-V=0$. For the sake of definiteness let us speak of a special but typical example—an atom A of free valence two is acted on by two heavy atoms, B and C, each with one free valence. Let the motion be restricted to one dimension.

According to present notions of chemical forces in the configuration

$$\dot{B}\qquad\dot{A}\qquad\dot{C}$$

the potential energy between B and A might be of the type shown in Fig. 1 by the dotted curve BA, that between C and A by the dotted curve AC (the potential energy at infinite separation is taken as zero). Then if we assume that all separations are large enough so that no other mutual potentials arise, and that the two mentioned are not appreciably changed, the potential energy of the system will be represented by the full curve BAC.

Under the circumstances a classical system could not undergo the reactions $BA+C\rightleftarrows B+AC$ unless the initial compound had almost the dis-

sociation energy over its normal state. However, we know many reactions which fit our case but which could not possibly depend on the molecules having such a large energy. We shall see that in quantum mechanics the reaction might proceed even for certain lower values of E.

First we shall inquire as to the allowed values of the energy of the composite system. For values of E less than the maximum of the curve BAC (and only such values are interesting here) condition (6) will be satisfied for almost the same energies that were characteristic for the curves BA and AC. The composite system has therefore all the levels of the two simple systems which could be formed from it by removal of either B or C. For a particular value of E, characteristic of one of these systems, the solution of the wave equation for one of the regions where (4) holds (namely, the one where (6) also holds) will be practically the same as though the corresponding simple system were alone. Condition (6) assures that this solution will go to the proper

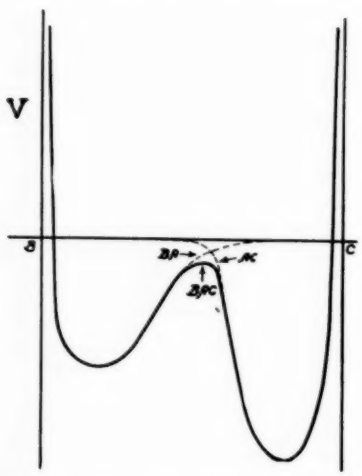

Fig. 1. Potential distribution for rearrangement reaction.

exponential form (5) just outside this region. The question now arises how shall this solution be prolonged into the other region where $(E-V)$ is positive. In general the condition (6) will not hold for this region and it will therefore be impossible to get a continuous function different from zero in this region which will satisfy the boundary requirements beyond it. We conclude that if (6) is not satisfied in each region separately the solutions for the composite system are approximately the solutions for the two component systems. In the special case in which the two component systems have an energy level in common, (6) is satisfied for each of the two regions and a continuous solution can be made up of a linear combination of those solutions for the separate systems which correspond to the common level. It is this coincidence which forms the basis for the present theory of chemical reaction.

The argument just outlined indicates that it will be possible to treat the problem by the methods used in perturbation theory although there is

no small quantity which can be considered as a perturbation potential. The point is that the problem can be formulated so that the matrix elements of the perturbation functions are small quantities.

We shall do this by the method of variation of constants[7] starting with the wave equation in the form

$$\Delta\Psi-\frac{8\pi^2m}{h^2}V\Psi-\frac{4\pi mi}{h}\dot{\Psi}=0. \tag{7}$$

The potential energy $V=V^{(1)}+V^{(2)}$ where $V^{(1)}$ is the potential between B and A, and $V^{(2)}$ that between A and C. The general solution of (7) is

$$\Psi=\Sigma_k C_k\psi_k e^{2\pi iE_kt/h} \tag{8}$$

where the functions ψ_k satisfy the equation

$$\Delta\psi_k+\frac{8\pi^2m}{h^2}(E_k-V)\psi_k=0 \tag{9}$$

for the appropriate energy E_k. For simplicity we shall always take the functions satisfying (9) to be real and to include a normalizing constant such that

$$\int|\psi_k|^2dx=1. \tag{10}$$

The equations

$$\Delta\psi^{(1)}-\frac{8\pi^2m}{h^2}V^{(1)}\psi^{(1)}-\frac{4\pi mi}{h}\dot{\psi}^{(1)}=0 \tag{11}$$

$$\Delta\psi^{(2)}-\frac{8\pi^2m}{h^2}V^{(2)}\psi^{(2)}-\frac{4\pi mi}{h}\dot{\psi}^{(2)}=0 \tag{12}$$

describe the component systems A with B, C at infinity and A with C, B at infinity, respectively. If the solutions of (11) are known functions

and those of (12)
$$\left.\begin{matrix}\psi_i^{(1)}e^{(2\pi i/h)E_it}\\ \psi_j^{(2)}e^{(2\pi i/h)E_it}\end{matrix}\right\} \tag{13}$$

we are led to expect that a zero'th approximation to (8) will be given by

$$\Psi_0=\sum_i C_i\psi_i^{(1)}e^{(2\pi i/h)E_it}+\sum_j\gamma_j\psi_j^{(2)}e^{(2\pi i/h)E_jt}. \tag{14}$$

To justify this we try for a better approximation by regarding the quantities C_i and γ_j as functions of the time instead of constants. Their derivatives will prove to be small and therefore (14) is a proper approximation. Substituting (14) in (7), considering C_i and γ_j functions of t and using (11) and (12) we can get for example

[7] P. A. M. Dirac, Proc. Roy. Soc. **112,** 674 (1926); E. Schroedinger, Ann. d. Physik **83,** 956 (1927). The method of breaking up the potential energy has also been used by F. Bloch, **Zeits. f. Physik 52,** 555 (1928).

$$-(4\pi mi/h)\Big(\sum_i \dot{C}_i\psi_i^{(1)}e^{(2\pi i/h)E_it}+\sum_j \dot{\gamma}_j\psi_j^{(2)}e^{(2\pi i/h)E_jt}\Big)$$

$$-(8\pi^2m/h^2)\Big[V^{(2)}\sum_i C_i\psi_i^{(1)}e^{(2\pi i/h)E_it}+V^{(1)}\sum_j \gamma_j\psi_j^{(2)}e^{(2\pi i/h)E_jt}\Big]=0$$

from which by multiplying by $\psi_{i'}^{(1)}$ and integrating

$$\dot{C}_{i'}=(2\pi i/h)\Big[\sum_i C_iV_{ii'}^{(2)}e^{(2\pi i/h)(E_i-E_{i'})t}+\sum_j \gamma_jV_{ji'}^{(2)}e^{(2\pi i/h)(E_j-E_{i'})t}\Big] \quad (15)$$

where

$$V_{ii'}^{(2)}=\int V^{(2)}\psi_i^{(1)}\psi_{i'}^{(1)}dx, \quad V_{ji'}^{(1)}=\int V^{(1)}\psi_j^{(2)}\psi_{i'}^{(1)}dx \quad (16)$$

similarly

$$\dot{\gamma}_{j'}=(2\pi i/h)\Big[\sum_i C_iV_{ij'}^{(2)}e^{(2\pi i/h)(E_i-E_{j'})t}+\sum_j \gamma_jV_{jj'}^{(1)}e^{(2\pi i/h)(E_j-E_{j'})t}\Big] \quad (17)$$

where

$$V_{ij'}^{(2)}=\int V^{(2)}\psi_i^{(1)}\psi_{j'}^{(2)}dx, \quad V_{jj'}^{(1)}=\int V^{(1)}\psi_j^{(2)}\psi_{j'}^{(2)}dx. \quad (18)$$

When it is considered that the functions $\psi_i^{(1)}$ diminish extremely rapidly in receding from the region where E_i-V is positive and corespondingly for $\psi_i^{(2)}$ it is seen that the quantities of (16) and (18) are very small, as they should be, to establish our procedure. In the integrations, besides using

$$\int \psi_i^{(1)}\psi_{i'}^{(1)}=0 \quad i\neq i' \quad (19)$$

$$\int \psi_j^{(2)}\psi_{j'}^{(2)}=0 \quad j\neq j' \quad (20)$$

we have used the fact that

$$\int \psi_i^{(1)}\psi_j^{(2)}dx\doteq 0 \quad (21)$$

and have therefore neglected $\dot{\gamma}_\gamma\int\psi_j^2\psi_{i'}^1dx$ and $\dot{C}_i\int\psi_i^1\psi_{j'}^2dx$ as being of second order. If the problem is to be completely and properly solved then the functions $\psi^{(1)}$ and $\psi^{(2)}$ would have to be really orthogonal and (21) would be exactly zero. It is believed. however, that the results then obtained would be qualitatively the same as those here given. Of course in cases where (21) does not hold, i.e., where the functions are not even approximately orthogonal, our method does not apply. This failure will occur only when $(E-V)$ near the maximum of V is fairly small which is a very special case of little importance in most problems.

If the $E_i's$ and $E_j's$ are all distinct we can integrate (15) and (17) by discarding all terms excepting the important one which has zero exponent and obtain a first approximation instead of (14)

$$\Psi_1(t) = \sum_i C_i^0 \psi_i^{(1)} e^{(2\pi i/h)(E_i + V_{ii}^{(2)})t} + \sum_j \gamma_j^0 \psi_j^{(2)} e^{(2\pi i/h)(E_j + V_{jj}^{(1)})t} \qquad (22)$$

If the system is initially in a particular state so that the constant coefficients in (22) are all zero except one, then that one state will persist with only a slight energy displacement (i.e., phase change) due to the presence of a third body. That is to say no appreciable reaction occurs and therefore the case of all different energy levels is of no special interest for us.

Something new arises when one of the $E_i's$ coincides with an E_j. Then there are two terms in (15) and (17) with zero exponents and which therefore may undergo a considerable variation in amplitude. For these two states we shall label the energies (E_i and E_j) E_1 and E_2 respectively, and the wave functions ($\psi_i^{(1)}$ and $\psi_j^{(2)}$) u and v[8] respectively. Then with $E_1 = E_2$, (15) and (17) reduce to

$$\dot{C} = (2\pi i/h)[CV_{uu}^{(2)} + \gamma V_{vu}^{(1)}] \quad \dot{\gamma} = (2\pi i/h)[CV_{uv}^{(2)} + \gamma V_{vv}^{(1)}] \qquad (23)$$

with

$$V_{uu}^{(2)} = \int V^{(2)} u^2 dx \quad V_{vu}^{(1)} = \int V^{(1)} vu dx$$
$$V_{uv}^{(2)} = \int V^{(2)} uv dx \quad V_{vv}^{(1)} = \int V^{(1)} v^2 dx \qquad (24)$$

Equations (23) are solved by the substitution

$$C = C^0 \exp[(2\pi i/h)\alpha t] \qquad \gamma = \gamma^0 \exp[(2\pi i/h)\alpha t]$$

The values of α are determined from

$$\begin{vmatrix} V_{uu}^{(2)} - \alpha & V_{vu}^{(1)} \\ V_{uv}^{(2)} & V_{vv}^{(1)} - \alpha \end{vmatrix} = 0 \qquad (25)$$

The roots are

$$\alpha_+ = \tfrac{1}{2}(V_{uu}^{(2)} + V_{vv}^{(1)}) + [(V_{uu}^{(2)} + V_{vv}^{(1)})^2/4 + V_{vu}^{(1)} V_{uv}^{(2)} - V_{uu}^{(2)} V_{vv}^{(1)}]^{1/2}$$
$$= \tfrac{1}{2}(V_{uu}^{(2)} + V_{vv}^{(1)}) + [(V_{uu}^{(2)} - V_{vv}^{(1)})^2/4 + V_{vu}^{(1)} V_{uv}^{(2)}]^{1/2} \qquad (26)$$

[8] There is an ambiguity of the sign of u with respect to the sign of v. Consequently $V_{vu}^{(1)}$ and $V_{uv}^{(2)}$ may be either positive or negative although their product is always positive. Correspondingly there are two linearly independent solutions for the composite system. For two similar component systems one is symmetrical, the other antisymmetrical, in the attracting centers B and C. The symmetrical and antisymmetrical solutions which appear in problems involving several degrees of freedom involve oscillations which play a part in certain chemical changes and will be considered elsewhere. F. Hund, (Zeits. f. Physik **40**, 742 (1927); also **43**, 805 (1927)) in discussing the wave equation, more particularly from the spectroscopic point of view, has emphasized the existence of solutions symmetric and antisymmetric in the coordinate, and has shown how in some cases these might describe a change in activity of a symmetrical optically active substance.

and

$$\alpha_-=\tfrac{1}{2}(V_{uu}^{(2)}+V_{vv}^{(1)})-[(V_{uu}^{(2)}-V_{vv}^{(1)})^2/4+V_{vu}^{(1)}V_{uv}^{(2)}]^{1/2}. \tag{27}$$

These are always real because $V_{vu}^{(1)}$ and $V_{uv}^{(2)}$ have the same sign. For these values of α (23) can be solved in the form

$$\begin{aligned} C&=C^{0+}e^{(2\pi i/h)\alpha_+^{(1)}t}+C^{0-}e^{(2\pi i/h)\alpha_-^{(1)}t}\\ \gamma&=\gamma^{0+}e^{(2\pi i/h)\alpha_+^{(1)}t}+\gamma^{0-}e^{(2\pi i/h)\alpha_-^{(1)}t} \end{aligned} \tag{28}$$

where the constants C^{0+}, γ^{0+} and C^{0-}, γ^{0-} satisfy the relations

$$\begin{aligned} C^{0+}&=V_{vu}^{(1)}\gamma^{0+}/(\alpha_+-V_{uu}^{(2)})=(\alpha_+-V_{vv}^{(1)})\gamma^{0+}/V_{uv}^{(2)}\\ &=\{(V_{uu}^{(2)}-V_{vv}^{(1)})/2+[(V_{uu}^{(2)}-V_{vv}^{(1)})^2/4+V_{vu}^{(1)}V_{uv}^{(2)}]^{1/2}\}\gamma^{0+}/V_{uv}^{(2)} \end{aligned}$$

and

$$\begin{aligned} C^{0-}&=V_{vu}^{(1)}\gamma^{0-}/(\alpha_--V_{uu}^{(2)})=(\alpha_--V_{vv}^{(1)})\gamma^{0-}/V_{uv}^{(2)}\\ &=\{(V_{uu}^{(2)}-V_{vv}^{(1)})/2-[(V_{uu}^{(2)}-V_{vv}^{(1)})^2/4+V_{vu}^{(1)}V_{uv}^{(2)}]^{1/2}\}\gamma^{0-}/V_{uv}^{(2)}. \end{aligned} \tag{29}$$

If the system is initially in any state other than u or v then it stays there as in the case of Eq. (22). Let us say, however, that the system is, for example, initially in state u. Then the first approximation to the wave function is

$$\Psi_1=Cue^{(2\pi i/h)E_1t}+\gamma ve^{(2\pi i/h)E_2t} \tag{30}$$

where C and γ are determined by the Eqs. (29) together with the initial conditions

$$\begin{aligned} |C^0|^2&=|C^{0+}+C^{0-}|^2=1\\ |\gamma^0|^2&=|\gamma^{0+}+\gamma^{0-}|^2=0. \end{aligned} \tag{31}$$

Writing $C^{0+}=|C^{0+}|e^{i\delta+}$, $C^{0-}=|C^{0-}|e^{i\delta-}$ the Eqs. (29) and (31) give $\delta^+-\delta^-=(2n+1)\pi$

$$\begin{aligned} |\gamma^{0+}|&=|\gamma^{0-}|=|V_{uv}^{(2)}|/(\alpha_++\alpha_-)\\ &=|V_{uv}^{(2)}|/2[(V_{uu}^{(2)}-V_{vv}^{(1)})^2/4+V_{vu}^{(1)}V_{uv}^{(2)}]^{1/2} \end{aligned} \tag{32}$$

Using Eqs. (26) to (32) and with the abbreviation

$$h\nu_q=[(V_{uu}^{(2)}-V_{vv}^{(1)})^2/4+V_{vu}^{(1)}V_{uv}^{(2)}]^{1/2} \tag{33}$$

Eq. (30) reduces to

$$\begin{aligned} \Psi_1=(1/2h\nu_q)\{&[(V_{uu}^{(2)}-V_{vv}^{(1)})\sin 2\pi\nu_qt+2h\nu_q\cos 2\pi\nu_qt]u\\ &+[2V_{uv}^{(2)}\sin 2\pi\nu_qt]v\}e^{(2\pi i/h)(E_1+(V_{uu}^{(2)}-V_{vv}^{(1)})/2)t+i\delta^+} \end{aligned} \tag{34}$$

This can also be written

$$\begin{aligned} \Psi_1=(1/h\nu_q)\{&[(h\nu_q)^2+(V_{uu}^{(2)}-V_{vv}^{(1)})^2/4]^{1/2}u\sin 2\pi(\nu_qt+\phi)\\ &+V_{uv}^{(2)}\cdot v\cdot\sin 2\pi\nu_qt\}e^{(2\pi i/h)(E+(V_{uu}^{(2)}-V_{vv}^{(1)})/2)t+i\delta^+} \end{aligned} \tag{35}$$

where $\tan 2\pi\phi=2h\nu_q/(V_{uu}^{(2)}-V_{vv}^{(1)})$

The coefficients of u and v in (35) inside the bracket are harmonic functions of the same period and amplitude. There is a phase displacement so that at one moment the coefficient of u is zero and at a time ϕ/ν_q later, that of v is zero. The frequency of this oscillation ν_q as defined in Eqs. (33) and (24) depends on the shape of the potential energy curve. Usually the equation $h\nu_q \doteq V_{vu}^{(1)} \doteq V_{uv}^{(2)}$ will hold approximately. Consideration of this shows that the rate of transfer from u to v depends on the height of the maximum of V above E and especially on the range of x over which V-E has large positive values. These quantities enter exponentially in ν_q which is therefore sensitive to slight changes in them.

IV. Application of Results to Chemistry

The valence properties attributed to the system previously used as an example had of course no practical significance. The calculation of the last section will apply to any case where the potential energy curve is of the type shown in Fig. 1. And even Fig. 1 is to be considered in a generalized way. The potential energy need not go up indefinitely high on two sides; it might become asymptotically horizontal on one side or on both. There need not even be two minima, although if there is only one a slight modification must be introduced in the calculation; this will be done elsewhere. The particular features which are really characteristic are that the equation $E_n - V = 0$ shall have more than two finite roots, and that E_n shall approximately satisfy Eq. (6) in at least two different regions.

A few remarks may be made about the assumption that the energy E_n should exactly match in the two regions. The problem can be solved even when this is only approximately fulfilled. No essential change results. When there is a continuous distribution of solutions in one region, one must integrate over all which nearly match the energy E_n and this also involves no change in principle. A question arises as to how often even an approximate match can be expected in molecular systems. First it should be pointed out that one of the characteristic features of infra-red spectroscopy is the ease with which it is possible to arrange all lines in a single or a very few series. The interpretation of this is that the different fundamentals have multiple relations between them which means that the energy match we require will be nearly satisfied quite often. Moreover, superposed on the vibration is the rotation spectrum so that each level is effectively broadened, especially when we consider that these rotations have long periods and are therefore easily subject to perturbation so that they may become practically continuous over considerable ranges. Of course when there is a large continuous range of energies or when the two component systems are exactly alike, there will be many different values of energy which match exactly.

We can describe the matter in more nearly chemical language. A system may be capable of existence in two geometrically different configurations. In each of these configurations it may have only certain motions characterized by the total energy. If one of the allowed energies of one configuration coincides with one of the other then according to Eq. (35) the system

will periodically change from one configuration to the other. If the configurations are physically distinguishable then this change can well be called a chemical reaction. It is important to notice that one configuration changes to the other not from the normal state but only when it is in the excited state of the first configuration. This is the theoretical foundation for the "activation hypothesis."

The rate at which the reaction proceeds depends on external conditions such as pressure, temperature, etc., as well as on the forces of the system itself, for these external conditions determine how many systems will be in a favorable state for reaction at any moment. Let us say that a system changes in a reaction from configuration I to configuration II, let us call the states of equal energy u for configuration I and v for II. Then among a large number N of states in configuration I a fraction f_u will be in the important state u. This fraction will depend on the temperature according to the Boltzmann law. The full Boltzmann quota will however not be reached unless the pressure is high enough so that the number of collisions raising molecules of configuration I to state u is large compared with the number which leave state u according to Eq. (35). The rate will therefore depend on the temperature in the way required by the "activation hypothesis" and will also diminish with the pressure in the manner already discussed in the study of unimolecular gas reactions.[9] There is still a further interesting possibility. According to the ordinary interpretations of the wave equation the fractional number of systems in state v will be given by the square of the coefficient of v in the solution (35) of the equation. In our case this is

$$\left| V_{uv}^{(2)} \right|^2 \sin^2 2\pi\nu_q t/(h\nu_q)^2. \tag{36}$$

If collisions played no part, the systems would pass back and forth between u and v, but actually they will tend to remove the systems from state v to other states of configuration II while on the whole they will scarcely affect the number of systems in state u which is nearly in equilibrium with other states of configuration I. Under ordinary conditions when this action of collisions is taken into account the expression (36) will be changed into one with linear initial dependence on the time so that the reaction will follow unimolecular exponential law. But if the pressure is low enough, that is, so that the time between collisions is long compared with the period $1/\nu_q$ in (36) the periodic feature will be important and the rate of reaction will be enormously diminished. Such an effect has been observed[10] and been interpreted in another way which may of course be the correct way.

V. Molecular Rearrangements

The process which has here been treated may not be clearly in evidence in some reactions because of preliminary or consequent steps in the reac-

[9] O. K. Rice and H. C. Ramsperger, Jour. Am. Chem. Soc. **49**, 1927, and **50**, 1928. See also L. S. Kassel, Jour. Phys. Chem. **32**, 1928.

If there is more than one pair of states u and v, then the most general dependence on pressure considered by these authors can be reproduced without taking on their special assumptions.

[10] Chariton and Z. Walta, Zeits. f. Physik **39**, 547 (1926); N. Semenoff, Zeits. f. Physik **46**, 109 (1927); **48**, 571 (1928); also G. Sprenger, Zeits. f. Physik. Chemie **136**, 49 (1928).

tions. Nevertheless there are cases where the existence of such a process has been fairly well established as a part of a chemical change. For example in the so-called Hofmann rearrangement one of the steps is the change

$$0=C-N= \rightarrow 0=C=N$$
$$\quad\;\; | \qquad\qquad\quad\;\; |$$
$$\quad\;\; R \qquad\qquad\quad\;\; R$$

A common rearrangement is from the "cis" to the "trans" configuration of a complicated molecule. This is represented diagrammatically in Fig. 2.

It is easy to picture in these rearrangements a potential energy curve of the type of Fig 1. The various types of photochemical behavior in these reactions are easily understood on the present theory. Consider for example

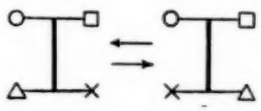

Fig. 2. Diagrammatic representation of the "cis" to "trans" reaction.

the case where the reaction of Fig. 2 can be made to go almost completely in one direction or another by illuminating with different wave-lengths. In the configuration I it might take $h\nu_u$ to raise the system to state u while in configuration II, it might require a different energy $h\nu_v$ to raise the system to state v. Illumination by frequency around ν_u will clearly tend to make the reaction go in one direction while frequencies around ν_v will push it in the other. If the values $h\nu_u$ and $h\nu_v$ are large compared with kT the reaction may be made to go almost to completion in either direction. Other types of photochemical reactions can be treated in a similar manner.

VI. Catalysis

The fundamental requirement that two configurations of a system must have a common energy level will of course not always be sufficiently met to permit appreciable reaction. A suggestion comes immediately from the quantum mechanical theory which may explain a very important type of catalysis. The curious thing about catalysts is that often without any very energetic interaction with a molecular system they have a great influence on the rate at which the system undergoes a change involving considerable energy. One might imagine that the catalyst have a fairly weak attraction—that of an induced dipole for example—on the molecule. The proximity of the catalyst will change the shape of the potential of Fig. 2 and even a small change may suffice to bring about an equality of energy in two configurations. The reaction then proceeds without affecting the catalyst. This perturbing influence may be a specific one where a particular substance affects another so as to match energy levels just accidentally. That substance may then catalyze only one type of reaction. Another substance may naturally have a strong field of force so that it will perturb almost anything. Moreover this perturbation may be variable, depending on the orientation or concen-

tration of molecules and so there will always be a match in energy level for some molecules. Such a substance will be a catalyst for many reactions. A solid body has a good chance of being of this type. The natural irregularity of the surface may provide the variability which is required for different reactions. We have evidence that a catalytic surface often is especially active in special "spots" and this is nicely in accord with our picture. On these spots, possibly with rapidly varying curvature, some molecules are sure to be perturbed just the right amount.

To be sure this theory does not preclude the existence of many totally different kinds of catalysis.

VII. The Racemization of Pinene

Since its investigation in vapour and liquid phase[11] the unimolecules transformation of pinene from a dextro to a laevo variety or vice versa has been of great interest to workers in chemical reaction theory. This reaction involving no change of heat content is carried out only through molecules having an average internal energy of about 40,000 cal. per gram mol.

This is a particularly simple case under our theory. The pinene molecule has the structure

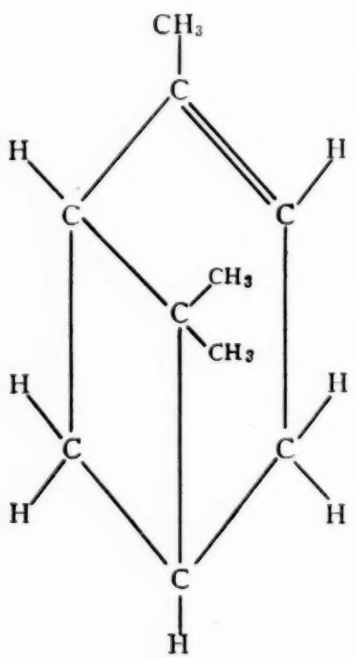

The reaction presumably involves a rearrangement of the central group from a position above the plane of the ring to a symmetrical configuration below it. Whether the motion is through the ring or around the corner carbon, the potential energy can be represented in a way of the type of Fig. 1 with

[11] D. Smith, Jour. Am. Chem. Soc. 49, 47 (1927).

the special feature that it is symmetrical to a line through the maximum of the potential. In this case all the energy levels in one configuration will be matched by levels in the other and so the reaction could proceed from any level. The rate at which the change takes place is extremely sensitive to the value of E since in the important part of (35) or (36) namely ν_q, there is a negative exponential factor involving $(V\text{-}E)$. The symmetry of the potential makes

$$V_{vv}^{(1)} = V_{uu}^{(2)} \quad \text{and} \quad V_{vu}^{(1)} = V_{uv}^{(2)}$$

so that ν_q reduces to

$$h\nu_q = V_{uv}^{(2)} = V_{vu}^{(1)} = \int_{-\infty}^{\infty} V^{(2)} uv dx. \tag{37}$$

The only values of x at which there is an appreciable contribution to the integral are those between which $E\text{-}V$ is negative. In this region u and v will be given by expressions of the form of Eq. (5). It can be shown from these that (37) will contain as an essential factor $\exp\left[(2\pi i/h)\int[2m(E\text{-}V)]^{1/2}dx\right]$ where the integral is taken over the range where $E-V<0$ and where V is the resultant potential energy function. The square of this expression determines the rate of conversion between u and v and we see why the change is faster for molecules of higher energy. On the other hand there are fewer molecules of higher energy so that the average energy of the reacting molecules is limited.

There is some possibility of computing numerical values for this reaction from the variation with pressure. We shall however in this paper avoid numerical comparison with data.

Other reactions of this type are known in liquid phase although not all appear to be as simple. In particular it is by no means necessary to have a symmetrical potential energy function. In fact the potential function is usually not symmetrical. This however is no complication in principle.

VIII. Decomposition

The straightforward breaking up of a molecular system is a very important class of reaction. Many of the homogeneous unimolecular gas reactions are of this type. A common feature of most of these reactions is that they involve the ejection of a part from a central position in a more or less symmetrical system. Notice for example the structures

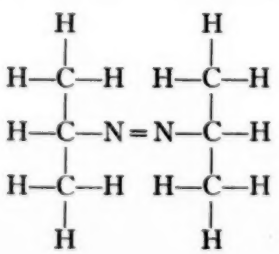

azoisopropane

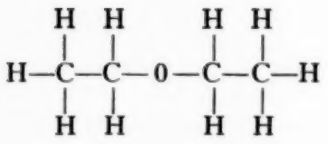

diethyl ether

It might be imagined that for small oscillations about the horizontal axis of symmetry the central part is attracted. If the amplitude becomes large the opposite parts of the molecule might attract each other directly and then repel the displaced central part. The potential energy curve would be of the type shown in Fig. 3. For every allowed positive value of the energy in the region with the minimum there is a continuous range of nearly equal values allowed in the outside region. A similar diagram holds for radioactive problems which therefore also come under the class here considered.[12]

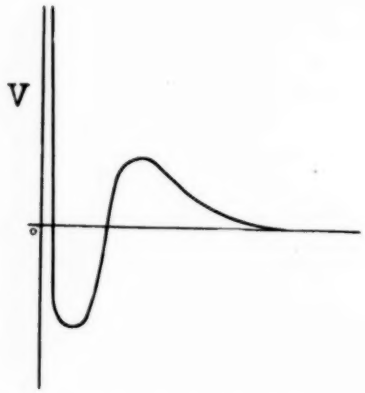

Fig. 3 Potential distribution for a decomposition.

The existence of a continuous range of energies requires a slight deviation from the development of Eq. (35). We shall go through with this without striving for completeness mathematically so that it must not be expected that our results will cover all cases satisfactorily.[13] The failure of the present treatment comes about just as in the case when there are two minima, namely, when E-V does not become a large negative quantity over a sufficient range near the maximum of V.

Under the conditions assumed, the solution to the wave equation must be written

$$\Psi(x) = \sum_i C_i \psi_i^{(1)}(x) e^{(2\pi i/h)E_i t} + \int \gamma(E) \psi^{(2)}(E, x) e^{(2\pi i/h)Et} dE \qquad (38)$$

[12] Radioactive disintegration has recently been treated by Gamow, Zeits. f. Physik **51**, 204 (1928), and by Gurney and Condon, Phys. Rev. **33**, 127 (1929).

[13] A similar treatment has already been given by J. R. Oppenheimer, Phys. Rev. **31**, 66 (1928).

where we normalize the orthogonal functions $\psi^{(2)}(E, x)$ so that

$$(\Delta E)^{-1}\int\int_{\Delta E}\psi^{(2)}(E,x)\psi^{(2)}(E,'x)dEdx=1 \tag{39}$$

provided $|E'-E| \ll \Delta E$ where ΔE is any arbitrary interval of energy, while the same integral is zero when $|E'-E| > \Delta E$. The condition

$$\int \psi_i{}^{(1)}(x)\psi^{(2)}(E,x)dx \doteq 0 \tag{40}$$

is still required.

We can now repeat the process used with Eq. (7) and find

$$\dot{C}_{i'}=(2\pi i/h)\left[\sum_i C_i V_{ii'}{}^{(2)}e^{(2\pi i/h)(E_i-E_{i'})t}+\int\gamma(E)V_{Ei'}{}^{(1)}e^{(2\pi i/h)(E-E_{i'})t}dE\right]$$

$$\dot{\gamma}(E')=(2\pi i/h)\left[\sum_i C_i V_{iE'}{}^{(2)}e^{(2\pi i/h)(E_i-E')t}+\int\gamma(E)V_{EE'}{}^{(1)}e^{(2\pi i/h)(E-E')t}dE\right] \tag{42}$$

where

$$\begin{aligned}
V_{ii'}{}^{(2)} &= \int V^{(2)}\psi_i{}^{(1)}\psi_{i'}{}^{(1)}dx \\
V_{Ei'}{}^{(1)} &= \int V^{(1)}\psi^{(2)}(E,x)\psi_{i'}{}^{(1)}(x)dx \\
V_{iE'}{}^{(2)} &= \int V^{(2)}\psi_i{}^{(1)}(x)\psi^{(2)}(E',x)dx \\
V_{EE'}{}^{(1)} &= \lim_{\Delta E'=0}(\Delta E')^{-1}\int dx\int_{\Delta E'}V^{(1)}\psi^{(2)}(E,x)\psi^{(2)}(E',x)dE.
\end{aligned} \tag{43}$$

As before we wish to have the system initially in state u so that we take

$$C_{i'}=|C^0|e^{i\delta}, \qquad \psi_{i'}{}^{(1)}=u, \quad |C^0|=1, \quad C_i{}^0=0 \quad \text{for} \quad i\neq i'$$
$$\gamma^0(E)=0, \qquad \psi^{(2)}(E',x)=v$$

Since the quantities (43) are small we can solve (41) and (42) with enough approximation for short intervals of time by putting for C and $\gamma(E)$ their initial values. The integrals then are

$$C=(2\pi i/h)\cdot C^0V_{uu}{}^{(2)}t+C^0 \tag{44}$$

$$\gamma(E')=C^0V_{uv}{}^{(2)}/(E_u-E')\cdot\left[e^{(2\pi i/h)(E_u-E')t}-1\right]. \tag{45}$$

The initial change in the fractional number of systems in states v is given by integrating the square of (45) over all energies E'. If N_u is the number of systems in state u

$$-\Delta N_u/N_u = \int |V_{uv}^{(2)}|^2/(E_u-E')^2 \cdot (2-2\cos\{(2\pi/h)(E_u-E')\Delta t\}dE'$$
$$= 4\int |V_{uv}^{(2)}|^2/(E_u-E')^2 \cdot \sin^2\{(\pi/h)(E_u-E')\Delta t\}dE'. \quad (46)$$

If we note that only values of E' near E_u contribute to the integral, and that $V_{uv}^{(2)}$ is a slowly varying function of E' we may write

$$\Delta N_u/N_u = -4|V_{uv}^{(2)}|^2 \int_{-\infty}^{\infty} \frac{\sin^2\{\pi/h(E_u-E')\Delta t\}\cdot dE'}{(E_u-E')^2}$$
$$= -4\pi/h \cdot |V_{uv}^{(2)}|^2 \Delta t \int_{-\infty}^{\infty} \frac{\sin^2 x}{x^2}dx \quad (47)$$
$$= -(4\pi^2/h)\cdot |V_{uv}^{(2)}|^2 \Delta t.$$

In integral form

$$N_u = N_u{}^0 e^{-(4\pi^2/h)|V_{uv}^{(2)}|^2 t} \quad (48)$$

showing the exponential decay characteristic of decomposition processes.

IX. Conclusion

The sketchy treatment of this paper is of course not sufficient to establish the theory proposed. It will be necessary to show numerical agreement with experiment. This will be attempted in a more concrete treatment to be published in the Bureau of Standards Journal of Research. Some special experiments which might test the point of view will be mentioned in future papers.

It should be emphasized that the analysis which has been presented applies not only to one-dimensional cases such as those mentioned in this article but, without appreciable change, can be made to describe similar problems from the point of view of electron coupling, or the very important reactions in which two parts of the system interchange positions. The fundamental requirement is simply that a molecular system be capable of existing in physically distinguishable states of equal energy. From this general point of view practically any type of chemical change can be treated in the manner of the present paper. The special problem in each case is to find the perturbing potential which acts on the reactants, making it possible for them to go over into the reaction products. This question will be further discussed elsewhere.

THE MOMENTUM DISTRIBUTION IN HYDROGEN-LIKE ATOMS

By Boris Podolsky* and Linus Pauling
University of California, Berkeley

(Received April 5, 1929)

Abstract

The probability density that an electron have certain momenta is given by the square of the absolute magnitude of a *momentum eigenfunction* $\Upsilon_{nlm}(P, \Theta, \Phi)$, in which P, Θ, and Φ are spatial polar coordinates of the total momentum vector referred to the same axes as the coordinates r, θ, and ϕ of the electron. The following general expression for these functions for a hydrogen-like atom is obtained:

$$\Upsilon_{nlm}(P,\Theta,\Phi)=\left\{\frac{1}{(2\pi)^{1/2}}e^{\pm im\Phi}\right\}\left\{\left(\frac{(2l+1)(l-m)!}{2(l+m)!}\right)^{1/2}P_l^m(\cos\Theta)\right\}$$
$$\left\{\frac{\pi 2^{2l+4}l!}{(\gamma h)^{3/2}}\left(\frac{n(n-l-1)!}{(n+l)!}\right)^{1/2}\frac{\zeta^l}{(\zeta^2+1)^{l+2}}C_{n-l-1}^{l+1}\left(\frac{\zeta^2-1}{\zeta^2+1}\right)\right\}$$

in which $\zeta=(2\pi/\gamma h)P$, with $\gamma=(4\pi^2\mu e^2Z/nh^2)=(Z/na_0)$. The probability $\Xi_{nl}(P)dP$ that the electron have a total momentum lying within the limits P and $P+dP$ is also evaluated, and it is shown that the root mean square of the total momentum is equal to the momentum of the electron in a circular Bohr orbit with the same total quantum number.

THE eigenfunctions $\Psi_{nlm}(r, \theta, \phi)$ which are obtained by solving the Schrödinger wave equation for a hydrogen atom are functions of the spatial polar coordinates r, θ, and ϕ of the electron relative to the nucleus. The interpretation which has been given them is that the square of the absolute magnitude of an eigenfunction represents the probability per unit volume that on experimental investigation a hydrogen atom in the state characterized by this eigenfunction will be found to have the configuration described by r, θ, and ϕ. Thus $|\Psi_{nlm}(r, \theta, \phi)|^2$ can be called the distribution function for the electron; the probability that the electron will be found in the elementary volume dV in the region given by certain values of the coordinates relative to the nucleus is $|\Psi_{nlm}(r, \theta, \phi)|^2 dV$.

In Dirac's transformation theory the eigenfunction $\Psi_{nlm}(r, \theta, \phi)$ is the transformation function from the cartesian coordinates of the electron to the quantum numbers, and may be represented by the symbol $(x, y, z/n, l, m)$. The transformation function from the momenta p_x, p_y, p_z to the quantum numbers n, l, m, which may similarly be given the symbol $(p_x, p_y, p_z/n, l, m)$, can also be used to give a distribution function, in this case in momentum space. If this transformation function is known for a given set of values of n, l, and m, then the probability that the electron have a total momentum lying in a given range can be easily calculated. The usefulness of this transformation function is indicated by one recent application.[1]

* National Research Fellow in Physics.

[1] J. W. M. DuMond, Phys. Rev. **33**, 643 (1929).

In this paper we are communicating a general expression for the transformation function from momenta to quantum numbers for a hydrogen-like atom. Weyl[2] has discussed another method of obtaining the momentum eigenfunctions as solutions of an integral equation, without, however, carrying out its application to the case of a hydrogen-like atom.[3]

2. The transformation function $(p_x, p_y, p_z/n, l, m)$ can be obtained from that $(x, y, z/n, l, m)$ by the equation[4]

$$(p_x,p_y,p_z/n,l,m) = h^{-3/2}\int_{-\infty}^{\infty}\int_{-\infty}^{\infty}\int_{-\infty}^{\infty} e^{-(2\pi i/h)(xp_x+yp_y+zp_z)}(x,y,z/n,l,m)\,dx\,dy\,dz. \quad (1)$$

Let us substitute for x, y, z the spherical polar coordinates given by the equations

$$\left.\begin{aligned} x &= r\sin\theta\cos\phi \\ y &= r\sin\theta\sin\phi \\ z &= r\cos\theta \end{aligned}\right\} \quad (2)$$

and write for p_x, p_y, p_z

$$\left.\begin{aligned} p_x &= P\sin\Theta\cos\Phi \\ p_y &= P\sin\Theta\sin\Phi \\ p_z &= P\cos\Theta. \end{aligned}\right\} \quad (3)$$

P then is equal in magnitude to the total momentum vector, and the angles Θ and Φ give the orientation of the momentum vector relative to the cartesian axes of coordinates. The function $(p_x, p_y, p_z/n,l,m)$ then becomes a function of P, Θ, and Φ, which we may call the *momentum eigenfunction* and give the symbol $\Upsilon_{nlm}(P, \Theta, \Phi)$. Eq. (1) is transformed into

$$\Upsilon_{nlm}(P,\Theta,\Phi) = h^{-3/2}\int_0^{\infty}\int_0^{\pi}\int_0^{2\pi} e^{-(2\pi i/h)[\sin\theta\sin\Theta\cos(\phi-\Phi)+\cos\theta\cos\Theta]rP}\cdot\Psi_{nlm}(r,\theta,\phi)r^2\sin\theta\,dr\,d\theta\,d\phi \quad (4)$$

with

$$\Psi_{nlm}(r,\theta,\phi) = \left\{\frac{1}{(2\pi)^{1/2}}e^{\pm im\phi}\right\}\left\{\left(\frac{(2l+1)(l-m)!}{2(l+m)!}\right)^{1/2}P_l^m(\cos\theta)\right\}$$
$$\left\{\frac{(2\gamma)^{l+1}}{(n+l)!}\left(\frac{\gamma(n-l-1)!}{n(n+l)!}\right)^{1/2}e^{-\gamma r}r^l L_{n+l}^{2l+1}(2\gamma r)\right\}, \quad (5)$$

in which $\gamma = 4\pi^2\mu e^2 Z/nh^2 = Z/na_0$.

[2] H. Weyl, Zeits. f. Physik. **46**, 1 (1928).

[3] On page 43 of his paper Weyl states that the momentum eigenfunctions are given in his dissertation, Math. Ann., **66**, 307–309, 317–324 (1908). We have, on attempting to verify this, found nothing in his dissertation that we could interpret as constituting a solution of this problem.

[4] P. Jordan, Zeits. f. Physik **40**, 809 (1927).

The symbols are the customary ones. $P_l^m(\cos\theta)$ is Ferrers' associated Legendre function of degree l and order m; and $L_{n+l}^{2l+1}(2\gamma r)$ is an associated Laguerre polynomial, defined by the identity[5]

$$\sum_{\beta=0}^{\infty} \frac{L_{\alpha+\beta}^{\alpha}(\xi)}{(\alpha+\beta)!} u^{\beta} \equiv (-)^{\alpha} \frac{e^{-\xi u/(1-u)}}{(1-u)^{\alpha+1}}. \tag{6}$$

3. Let

$$I_1 = \int_0^{2\pi} e^{\pm i m\phi + ib\cos(\Phi-\phi)} d\phi, \quad \text{with} \quad b = -(2\pi/h) rP \sin\theta \sin\Theta, \tag{7}$$

and

$$I_2 = \int_0^{\pi} e^{ic\cos\theta\cos\Theta} I_1 P_l^m(\cos\theta) \sin\theta d\theta, \quad \text{with} \quad c = -(2\pi/h) rP\,; \tag{8}$$

then

$$\Upsilon_{nlm}(P,\Theta,\Phi) = -\frac{h^{-3/2}}{(2\pi)^{1/2}} \left(\frac{(2l+1)(l-m)!}{2(l+m)!}\right)^{1/2} \frac{(2\gamma)^{l+1}}{(n+l)!} \left(\frac{\gamma(n-l-1)!}{n(n+l)!}\right)^{1/2} \int_0^{\infty} I_2 e^{-\gamma r} r^{l+2} L_{n+l}^{2l+1}(2\gamma r) dr. \tag{9}$$

The values of the first and second integrals are known. The transformation

$$\phi - \Phi = \omega \tag{10}$$

converts I_1 into Sommerfeld's integral,[6] which gives a Bessel function of order $\pm m$:

$$I_1 = e^{\pm i m\Phi} \int_0^{2\pi} e^{\pm i m\omega + ib\cos\omega} d\omega = 2\pi i^{\pm m} J_{\pm m}(b) e^{\pm i m\Phi}.$$

The relation

$$J_{-m}(b) = i^{2m} J_m(b)$$

permits this to be transformed into

$$I_1 = 2\pi i^m J_m(b) e^{\pm i m\Phi}. \tag{4}$$

We shall need the relation between the associated Legendre functions and the Gegenbauer C_k^{ν} functions,[7] which may be defined by the generating function[8]

[5] E. Schrödinger, Ann. d. Physik **80**, 484 (1926).

[6] A. Sommerfeld, Math. Ann. **47**, 335 (1896); see also Jahnke and Emde, "Funktionentafeln," p. 169.

[7] L. Gegenbauer, Wiener Sitzungsber. **70**, 6 (1874).

[8] An explicit expression for the C's is given in Whittaker and Watson, "Modern Analysis," p. 329.

$$Q_\nu \equiv (1-2ut+u^2)^{-\nu} \equiv \sum_{k=0}^{\infty} C_k^\nu(t) u^k. \tag{12}$$

When $\nu = \frac{1}{2}$ these functions reduce to the Legendre polynomials. On putting $\nu = \frac{1}{2}$ and differentiating m times with respect to t we obtain the relation

$$P_l^m(t) = 1 \cdot 3 \cdot 5 \cdot \cdots (2m-1)(1-t^2)^{m/2} C_{l-m}^{m+1/2}(t). \tag{13}$$

In 1877 Gegenbauer[9] evaluated the following definite integral

$$\int_0^\pi e^{iz\cos\theta\cos\psi} J_{\nu-1/2}(z \sin\theta \sin\psi) C_r^\nu(\cos\theta) \sin^{\nu+1/2}\theta d\theta$$

$$= \left(\frac{2\pi}{z}\right)^{1/2} i^r \sin^{\nu-1/2}\psi C_r^\nu(\cos\psi) J_{\nu+r}(z). \tag{14}$$

If we put $\nu = m+\frac{1}{2}$, $z=c$, $\psi = \Theta$, and $r = l-m$, this becomes, with the help of Eq. (13),

$$\int_0^\pi e^{ic\cos\theta\cos\Theta} J_m(c \sin\theta \sin\Theta) P_l^m(\cos\theta) \sin\theta d\theta$$

$$= \left(\frac{2\pi}{c}\right)^{1/2} i^{l-m} P_l^m(\cos\Theta) J_{l+1/2}(c). \tag{15}$$

On substitution for I_1 of its value given in Eq. (11) it is seen that I_2 is, except for a constant factor, equal to this integral, so that we may write

$$I_2 = 2\pi i^l e^{\pm im\Phi} P_l^m(\cos\Theta) \left(\frac{2\pi}{c}\right)^{1/2} J_{l+1/2}(c)$$

$$= -2\pi(-i)^l e^{\pm im\Phi} P_l^m(\cos\Theta) \left(\frac{h}{P}\right)^{1/2} r^{-1/2} J_{l+1/2}\left(\frac{2\pi r P}{h}\right). \tag{16}$$

Referring to Eqs. (9) and (16) we see that $\Upsilon_{nlm}(P, \Theta, \Phi)$ contains the integral

$$\int_0^\infty e^{-\gamma r} r^{l+3/2} \cdot \cdot \cdot \cdot \cdot \cdot /2\left(\frac{2\pi r P}{h}\right) L_{n+l}^{2l+1}(2\gamma r) dr, \tag{17}$$

which on substitution of

$$\xi = 2\gamma r \quad \text{and} \quad \zeta = 2\pi P/\gamma h \tag{18}$$

leads to

$$(2\gamma)^{-(l+5/2)} \int_0^\infty e^{-\xi/2} \xi^{l+3/2} J_{l+1/2}(\tfrac{1}{2}\zeta\xi) L_{n+l}^{2l+1}(\xi) d\xi. \tag{19}$$

[9] L. Gegenbauer, Wiener Sitzungsber. **75**, 221 (1877). The integral is also given in Watson, "Theory of Bessel Functions," p. 379.

4. Let

$$I_{nl}(\zeta) \equiv \int_0^\infty e^{-\xi/2}\xi^{l+3/2}J_{l+1/2}(\tfrac{1}{2}\zeta\xi)L_{n+l}^{2l+1}(\xi)d\xi. \tag{20}$$

In order to evaluate this integral we consider a function U defined by the following identity:

$$U \equiv U_l(\zeta, u) \equiv \sum_{n=l+1}^{\infty} \frac{I_{nl}(\zeta)}{(n+l)!}u^{n-l-1}. \tag{21}$$

It turns out that we can evaluate this function by using the generating function for the associated Laguerre polynomials (Eq. (6)), and thus obtain $I_{nl}(\zeta)$ as coefficients of the expansion of $U_l(\zeta, u)$ as a power series in u.

$$\begin{aligned} U &= \int_0^\infty e^{-\xi/2}\xi^{l+3/2}J_{l+1/2}(\tfrac{1}{2}\zeta\xi)\sum_{n=l+1}^{\infty}\frac{L_{n+l}^{2l+1}(\xi)}{(n+l)!}u^{n-l-1}d\xi, \text{ by 20,} \\ &= \int_0^\infty e^{-\xi/2}\xi^{l+3/2}J_{l+1/2}(\tfrac{1}{2}\zeta\xi)\frac{(-)^{2l+1}e^{-\xi u/(1-u)}}{(1-u)^{2l+2}}d\xi, \text{ by 6,} \\ &= (1-u)^{-2l-2}\int_0^\infty e^{-\xi(1+u)/2(1-u)}J_{l+1/2}(\tfrac{1}{2}\zeta\xi)\xi^{l+3/2}d\xi. \end{aligned} \tag{22}$$

Now the last integral is a special case of a more general integral which has been evaluated by Hankel[10] and Gegenbauer,[11] who obtained the result

$$\int_0^\infty e^{-a\xi}J_\nu(z\xi)\xi^{\mu-1}d\xi = \frac{(z/2a)^\nu\Gamma(\mu+\nu)}{a^\mu\Gamma(\nu+1)}F\left(\frac{\mu+\nu}{2}, \frac{\mu+\nu+1}{2}; \nu+1; -\frac{z^2}{a^2}\right). \tag{23}$$

Putting $z=\frac{1}{2}\zeta$, $\nu=l+\frac{1}{2}$, $\mu=l+5/2$, and $a=(1+u)/2(1-u)$, this gives

$$U = \frac{4\zeta^{l+1/2}(2l+2)!}{\Gamma(l+3/2)}\frac{(1-u)}{(1+u)^{2l+3}}F\left(l+\frac{3}{2}, l+2; l+\frac{3}{2}; -\frac{\zeta^2(1-u)^2}{(1+u)^2}\right).$$

The hypergeometric series F is a degenerate one, equal to

$$\left\{1+\frac{\zeta^2(1-u)^2}{(1+u)^2}\right\}^{-l-2},$$

so that U can be put in the form

$$U = A\frac{1-u^2}{(1-2xu+u^2)^{l+2}}, \tag{24}$$

in which

$$A = \frac{4(2l+2)!\zeta^{l+1/2}}{\Gamma(l+3/2)(\zeta^2+1)^{l+2}}, \quad \text{and} \quad x = \frac{\zeta^2-1}{\zeta^2+1}.$$

[10] H. Hankel, Math. Ann. **8**, 467 (1875).

[11] L. Gegenbauer, Wiener Sitzungsber. **72**, 343 (1876); see also Watson, "Theory of Bessel Functions," p. 384.

5. We now return to Eq. (12). Operating on both sides with $u^{-\nu+1}(\partial/\partial u)u^{\nu}$ we obtain

$$\frac{\nu(1-u^2)}{(1-2ut+u^2)^{\nu+1}} \equiv \sum_{k=0}^{\infty}(\nu+k)C_k^{\nu}(t)u^k. \tag{25}$$

Putting $\nu=l+1$ and $t=x$, we may rewrite Eq. (24) as

$$U=\frac{A}{l+1}\sum_{k=0}^{\infty}(l+k+1)C_k^{l+1}(x)u^k=\frac{A}{l+1}\sum_{n=l+1}^{\infty}nC_{n-l-1}^{l+1}(x)u^{n-l-1}. \tag{26}$$

Comparing Eqs. (26) and (21), we see that

$$I_{nl}(\zeta)=\frac{An(n+l)!}{l+1}C_{n-l-1}^{l+1}\left(\frac{\zeta^2-1}{\zeta^2+1}\right). \tag{27}$$

6. Thus the momentum eigenfunctions are found to be given by the expression

$$\Upsilon_{nlm}(P,\Theta,\Phi)=\left\{\frac{1}{(2\pi)^{1/2}}e^{\pm im\Phi}\right\}\left\{\left(\frac{(2l+1)(l-m)!}{2(l+m)!}\right)^{1/2}P_l^m(\cos\Theta)\right\}$$
$$\left\{-\frac{(-i)^l\pi 2^{2l+4}l!}{(\gamma h)^{3/2}}\left(\frac{n(n-l-1)!}{(n+l)!}\right)^{1/2}\frac{\zeta^l}{(\zeta^2+1)^{l+2}}C_{n-l-1}^{l+1}\left(\frac{\zeta^2-1}{\zeta^2+1}\right)\right\}, \tag{28}$$

in which $\zeta=2\pi P/\gamma h=nP/Zp_0=P/p_n$. p_0, which is equal to $2\pi\mu e^2/h$, is the momentum of the electron in a circular Bohr orbit with $n=1$ and $Z=1$, corresponding to a hydrogen atom in the normal state, and $p_n=Zp_0/n$ is the momentum of the electron in a circular Bohr orbit characterized by the total quantum number n and the nuclear charge Ze. The factor $-(-i)^l$ in Υ may be omitted, since its absolute value is unity.

Some of the Gegenbauer C functions which enter in this expression are given below. Others can be obtained from these by the application of the recursion formula

$$C_r^{\nu}(x)=\frac{2\nu}{r}\{xC_{r-1}^{\nu+1}(x)-C_{r-2}^{\nu+1}(x)\}.$$

	$l=0$	$l=1$	$l=2$	$l=3$	$l=4$
$n=1$	$C_0^1(x)=1$				
$n=2$	$C_1^1(x)=2x$	$C_0^2(x)=1$			
$n=3$	$C_2^1(x)=4x^2-1$	$C_1^2(x)=4x$	$C_0^3(x)=1$		
$n=4$	$C_3^1(x)=8x^3-4x$	$C_2^2(x)=12x^2-2$	$C_1^3(x)=6x$	$C_0^4(x)=1$	
$n=5$	$C_4^1(x)=16x^4-12x^2+1$	$C_3^2(x)=32x^3-12x$	$C_2^3(x)=24x^2-3$	$C_1^4(x)=8x$	$C_0^5(x)=1$
$n=6$	$C_5^1(x)=32x^5-32x^3+6x$	$C_4^2(x)=80x^4-48x^2+3$	$C_3^3(x)=80x^3-24x$	$C_2^4(x)=40x^2-4$	$C_1^5(x)=10x$

Gegenbauer[12] has shown that his $C_r^{\nu}(x)$ functions with a given upper index when multiplied by the factor $(1-x^2)^{\nu/2-1/4}$ form an orthogonal set, for they satisfy the equations

$$\int_{-1}^{+1}(1-x^2)^{\nu-1/2}C_r^{\nu}(x)C_{r'}^{\nu}(x)dx=\frac{2^{2\nu-1}\Gamma(r+2\nu)}{(r+\nu)\Gamma(r+1)}\left[\frac{\Gamma(\nu+1/2)}{\Gamma(2\nu)}\right]^2\delta_{rr'}. \tag{29}$$

[12] L. Gegenbauer, Wiener Sitzungsber. **70**, 6 (1874), Eq. (16).

The functions of P which occur in the momentum eigenfunctions with a given value of l also form an orthogonal set; but they are not the Gegenbauer orthogonal functions. Since the volume element involves P^2dP, the orthogonal functions are in this case

$$\frac{\pi 2^{2l+4}l!}{(\gamma h)^{3/2}}\left(\frac{n(n-l-1)!}{(n+l)!}\right)^{1/2}\frac{\zeta^l}{(\zeta^2+1)^{l+2}}C_{n-l-1}^{l+1}\left(\frac{\zeta^2-1}{\zeta^2+1}\right)P,$$

in which $\zeta=aP/np_0$ is different for different functions of the set, since it involves the quantum number n. That these functions are normalized can be shown with the aid of Gegenbauer's integral (29). The normalization integral

$$\left[\frac{\pi 2^{2l+4}l!}{(\gamma h)^{3/2}}\left(\frac{n(n-l-1)!}{(n+l)!}\right)^{1/2}\right]^2\int_0^\infty\left[\frac{\zeta^l}{(\zeta^2+1)^{l+2}}C_{n-l-1}^{l+1}\left(\frac{\zeta^2-1}{\zeta^2+1}\right)P\right]^2dP \qquad (30)$$

becomes on substituting x for $(\zeta^2-1)/(\zeta^2+1)$, and omitting the factor before the integral sign,

$$\int_{-1}^{+1}(1-x)(1-x^2)^{l+1/2}[C_{n-l-1}^{l+1}(x)]^2dx=\int_{-1}^{+1}(1-x^2)^{l+1/2}[C_{n-l-1}^{l+1}(x)]^2dx$$
$$-\int_{-1}^{+1}x(1-x^2)^{l+1/2}[C_{n-l-1}^{l+1}(x)]^2dx.$$

On substituting for $x\,C_{n-l-1}^{l+1}(x)$ its value given by the recursion formula

$$x\,C_r^\nu(x)=\frac{1}{2(r+\nu)}[(r+1)C_{r+1}^\nu(x)+(r+2\nu-1)C_{r-1}^\nu(x)]$$

the second integral is converted into two, each of which vanishes by Eq. (29). The value of the first integral as given by Eq. (29) is just that required to make (30) equal to unity.

7. The probability that the electron have a momentum lying in the range between P and $P+dP$ can be written as $\Xi_{nl}(P)dP$, in which $\Xi_{nl}(P)$, the momentum distribution function, is given by

$$\Xi_{nl}(P)=\int_0^\pi\int_0^{2\pi}|\,\Upsilon_{nlm}(P,\Theta,\Phi)\,|^2P^2\sin\Theta d\Theta d\Phi. \qquad (31)$$

On carrying out the integration this is found to become

$$\Xi_{nl}(P)=\frac{a_0}{Zh}\,\frac{2^{4l+6}n^2(l!)^2(n-l-1)!}{(n+l)!}\,\frac{\zeta^{2l+2}}{(\zeta^2+1)^{2l+4}}\left[C_{n-l-1}^{l+1}\left(\frac{\zeta^2-1}{\zeta^2+1}\right)\right]^2. \qquad (32)$$

8. It is of interest to evaluate the diagonal elements of the P^2 matrix, which are equal to the average values of the square of the momentum in the various quantum states:

$$\overline{P_n^2}=\int_0^\infty P^2\Xi_{nl}(P)dP. \qquad (33)$$

On substituting for P^2 its value $p_n^2(1+x)/(1-x)$, it is found that this integral, aside from the constant factor p_n^2, differs from the normalization integral only in having the factor $(1+x)$ in place of $(1-x)$; and since the integral involving x vanishes, and the normalization integral is equal to unity, we obtain

$$\overline{P_n^2} = p_n^2 = \left(\frac{2\pi\mu e^2 Z}{nh}\right)^2. \tag{34}$$

Now $\overline{p^2}_n$ is just the average value of the square of the momentum of the electron in a Bohr orbit with total quantum number n; so that the root mean square momentum for a hydrogen-like atom is the same in the quantum mechanics as in the old quantum theory, in each case depending only on the principal quantum number n.

MAXIMUM EXCURSION OF THE PHOTOELECTRIC LONG WAVE LIMIT OF THE ALKALI METALS

By Herbert E. Ives and A. R. Olpin
Bell Telephone Laboratories, New York

(Received March 28, 1929)

Abstract

Earlier experiments have shown that the long wave limit of photoelectric action in the case of thin films of the alkali metals varies with the thickness of the film. A maximum value is attained greater than that for the metal in bulk, which for the majority of the alkali metals lies in the infra-red. The wave-length of the maximum excursion of the long wave limit was first studied for Na, K, Rb and Cs. In each case it was found to coincide with the first line of the principal series, i.e. the resonance potential. If this relation holds for lithium, its maximum long wave limit should be greater than that of sodium. This was tested and confirmed by experiments in which red-sensitive lithium films were prepared, sensitive to 0.6708μ. It is suggested that photoelectric emission is caused when sufficient energy is given to the atom, to produce its first stage of excitation. The identity of photoelectric and thermionic work functions suggests that atomic excitation is the initial process in thermionic emission as well.

IN A previous publication,[1] the behavior of alkali metal films deposited slowly in high vacua has been described. The characteristic feature of such a film, as for instance one of sodium on platinum, is that as it accumulates, the photoelectric long wave limit moves from the blue end of the spectrum toward the red, reaches an extreme position and then recedes again to the final position characteristic of a thick layer. The curve showing the final relationship between photoelectric current and wave-length rises much more rapidly toward the short wave-lengths than does the curve with the same long wave limit during the building-up process.

The experimental procedure for studying these films as described in the earlier paper consisted first, of cleaning off a platinum plate in the photoelectric cell bulb by electronic bombardment and collecting the alkali metal on the cold walls of the cell; secondly, in allowing the alkali metal to slowly re-deposit on the platinum plate. In the case of sodium, the process of redeposition occurs quite slowly and the photoelectric behavior of the deposit may be studied over a period of many hours. With the metals potassium, rubidium and caesium, it is necessary to immerse the photoelectric cell in liquid air in order to hold the metal evaporated from the platinum plate on the walls long enough for the properties of the partially covered plate to be studied. The various thicknesses of film may be studied either while they increase in thickness as the bulb is allowed to warm or as they are decreased in thickness by successive warmings of the plate.

Another method of producing thin film cells is to allow the alkali metal to diffuse into the bulb through a side tube of small diameter. We have in

[1] Ives, Astrophys. J. **60**, 4 (1924).

this way prepared caesium cells with the caesium deposited on platinum, silver, magnesium, and other metals. The procedure is to allow the alkali metal to diffuse in while the cell is illuminated and connected with the galvanometer. When the maximum sensitiveness is reached, the side tube is sealed off. After sealing off, the sensitiveness is apt to continue to change somewhat but may be held more constant by admitting an inert gas such as argon. By properly choosing the time of sealing off the side tube, cells may be produced in which the long wave limit has made good approximation to its maximum position.

It has been a matter of interest to us to know how far the long wave limit travels in this excursion out to a maximum and then back. In the case of sodium, as is shown by Fig. 1, which is reproduced from the earlier paper,

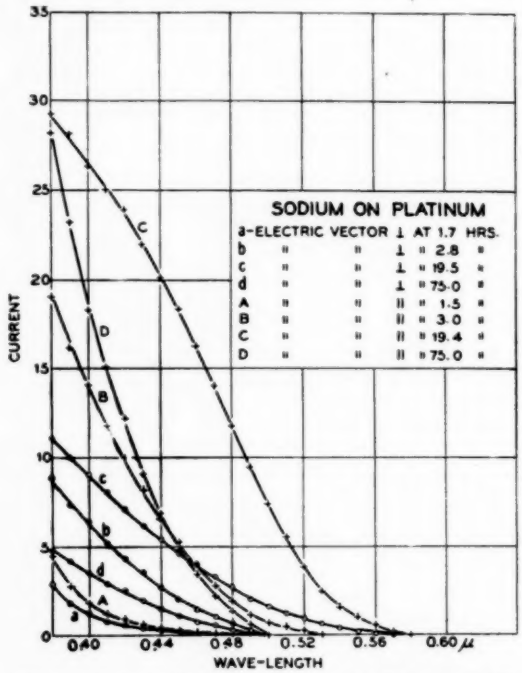

Fig. 1. Progress of photoelectric emission as Na film builds up on Pt plate; exciting light polarized; equal energy spectrum.

this maximum excursion is to a point still in the visible spectrum, somewhere between 0.57μ and 0.60μ. In the case of the other three metals which were studied, however, this maximum wave-length is in the infra-red, beyond the range of the spectrometer which was used in the earlier study. The determination of this maximum therefore awaited opportunity for securing a monochromatic illuminator suitable for near infra-red work.

Apparatus

As a monochromatic illuminator for working in the near infra-red, we have taken a Hilger spectrometer of the constant deviation type, and have extended its calibration beyond 1μ. This calibration was effected by the use

of a pair of partially silvered glass plates sealed together with a slight separation so as to produce interference bands in the spectrometer which were measured as to position in the visible spectrum, and followed out into the infra-red by means of a sensitive thalofide cell. Using the constant determined from the visual measurements the scale was extended and marked on an addition to the usual wave-length drum of the instrument.

As a light source we have used a coiled tungsten filament. The photoelectric currents were measured with an electrometer by the steady deflection method as described in earlier papers. For the present investigation, it has not been necessary in all cases to reduce the observations to equal energy values.

An adjunct which is absolutely essential to a study of this sort is a series of light filters, each of successively longer wave-length cut-off, to filter out the short wave end of the spectrum. The necessity for these filters arises from the fact that the long wave limit is approached very gradually, in fact, almost asymptotically, and that in all cases the amount of photoelectric action is so much greater from the short wave energy that an exceedingly small amount of scattered light will result in deflections beyond the true long wave limit. It is therefore necessary for the cut-off of the filters used to trail pretty closely behind the long wave limit as it moves out. To meet these requirements we have used a rather complete set of Wratten filters, which give progressively longer wave-length cut-offs from the blue end of the spectrum, well out into the infra-red. These have been employed both as adjuncts to the monochromatic illuminator, and also at times alone, directly in an unresolved beam of light, the wave-lengths transmitted being determined from the transmission data furnished by the makers of the filters.

The cells studied were mostly of the central cathode type. A polarizing voltage of 22.5 was used in all cases, as this produces practically complete saturation, and no shift of the threshold wave-length was found to occur with increased voltage.

Results on Sodium

In Fig. 2 are shown a series of curves for a thin film of sodium on platinum as it increases in thickness. Attention is called to the apparent extension of the long wave limit when no filter is used, and its recession toward the blue when such a filter is used that only the tail of the excitation region is exposed.

With the use of a filter, the long wave limit for sodium on platinum comes, at its maximum excursion, very nearly to 0.59μ. We have obtained exactly similar results with a sodium film on clean, thoroughly outgassed, tungsten.

The results with spectrally resolved light shown in the figure have been further confirmed by taking a sodium film on platinum through its complete life history while illuminated by the focussed image of a carbon arc crater, the light from which was passed through a series of Wratten yellow and orange-red filters. For this set of experiments a d'Arsonval galvanometer with a sensitivity of 10^{-10} amperes per mm deflection was used to

detect the currents. At the maximum excursion, a detectable current was found with the No. 26 filter (transmission 3.17 percent at 0.59μ) *and no current with filter No. 29 (transmission 0 at 0.59μ)*, showing that the long wave limit at 0.59μ is a real limit to photoelectric response.

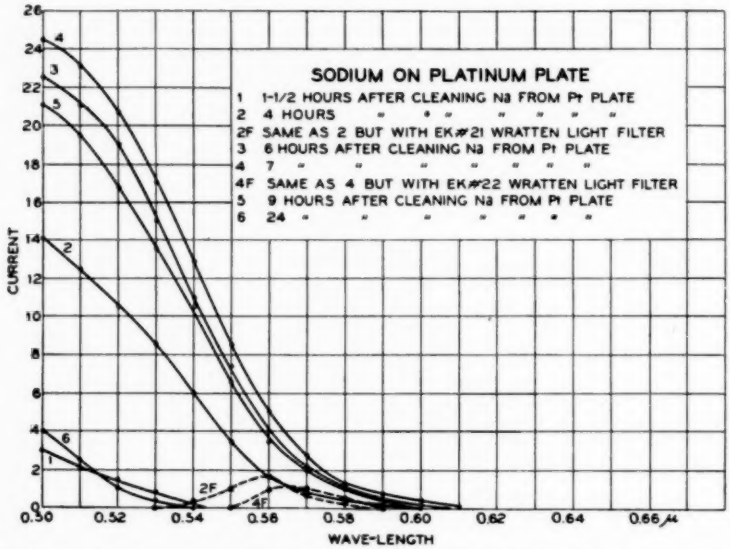
SODIUM ON PLATINUM PLATE
1 1-1/2 HOURS AFTER CLEANING Na FROM Pt PLATE
2 4 HOURS " " " " " " "
2F SAME AS 2 BUT WITH EK#21 WRATTEN LIGHT FILTER
3 6 HOURS AFTER CLEANING Na FROM Pt PLATE
4 7 " " " " " " "
4F SAME AS 4 BUT WITH EK#22 WRATTEN LIGHT FILTER
5 9 HOURS AFTER CLEANING Na FROM Pt PLATE
6 24 " " " " " " "
CURRENT
WAVE-LENGTH
0.50
0.52
0.54
0.56
0.58
0.60
0.62
0.64
0.66 μ

Fig. 2. Photoelectric current vs. wave-length of exciting light, showing excursion of long wave limit for Na film on Pt; critical maximum obtained accurately after eliminating light of short wave-lengths with suitable filters. Values not reduced to equal energy spectrum.

Results on Potassium, Rubidium and Caesium

Of these three metals, the maximum excursion has been determined for films on platinum, and, in the case of caesium, also on silver, as described more in detail below. The results may be summarized as follows: For potassium on platinum, with a Wratten No. 23 filter to cut out stray light, the extreme long wave limit found was 0.77μ. For rubidium, the extreme long wave limit found was 0.795μ. The complete series of curves for this metal are shown in Fig. 3. For caesium, with an extra dark, visually opaque Wratten filter (No. 87) for stray light elimination, the extreme long wave limit found was 0.895μ. Fig. 3 very conclusively illustrates the fact that the change in threshold value produced by varying the thickness of film was an actual shift in wave-length and could not possibly be explained as a general increase in sensitiveness resulting in a rotation of the spectral distribution curve about the maximum threshold as a pivot.

We have, in addition to the caesium-on-platinum, made measurements on two caesium-on-silver cells in which the caesium was deposited up to a maximum sensitiveness and the deposition then stopped somewhat in the manner described in the first part of this paper. Of these, one gave an extreme long wave limit of 0.86μ and the other 0.895μ. In view of the uncertainty of stopping the deposition process at exactly the right point, we believe that these cells confirm the value found in the controlled cells, the significance of which will now be discussed.

Discussion of Results on Sodium, Potassium, Rubidium and Caesium

Examination of the long wave limits for these four metals at their maximum value reveals at once, to the student of spectroscopy, a striking agreement with the wave-lengths of the first line of the principal series of each element, or the chief resonance line. The values of these are, in the several cases[2];—sodium 0.5896μ, potassium 0.7899μ, rubidium 0.7947μ and caesium 0.8943μ. The agreement, considering the difficulties of the experimental procedure, and the order of accuracy of the wave-length calibration, is so

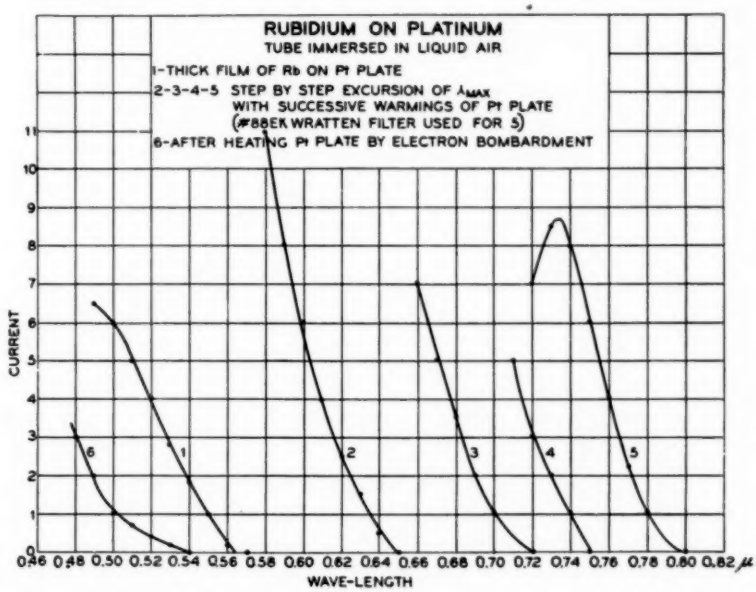
RUBIDIUM ON PLATINUM
TUBE IMMERSED IN LIQUID AIR
1-THICK FILM OF Rb ON Pt PLATE
2-3-4-5 STEP BY STEP EXCURSION OF λMAX WITH SUCCESSIVE WARMINGS OF Pt PLATE
(#88EK WRATTEN FILTER USED FOR 5)
6-AFTER HEATING Pt PLATE BY ELECTRON BOMBARDMENT
CURRENT
WAVE-LENGTH
0.46 0.48 0.50 0.52 0.54 0.56 0.58 0.60 0.62 0.64 0.66 0.68 0.70 0.72 0.74 0.76 0.78 0.80 0.82 μ

Fig. 3. Photoelectric current vs. wave-length of exciting light, showing excursion of long wave limit for Rb film on Pt; maximum value obtained after filtering our light of short wave-lengths. Values not reduced to equal energy spectrum.

close as to leave in our minds little doubt that this coincidence is actually exact. We shall leave until a later section the discussion of the significance of this agreement and confine ourselves for the moment to a discussion of further experiments which are suggested.

The most significant experiment in our opinion is a search for the same phenomenon with lithium, for although lithium is higher in the periodic table than sodium, the principal resonance line at 0.6708μ is considerably greater in wave-length than the corresponding sodium line. Another experiment or rather series of experiments would be a study of the same phenomena with the alkaline earth metals, of which magnesium, calcium, strontium and barium all have their first resonance lines in the spectroscopic region which is accessible to our apparatus.

[2] See "Critical Potentials," Bull. Nat. Res. Council **48**, 1924.

Experiments on Lithium

In view of the crucial test which lithium affords of the relationship found with the other alkali metals we have delayed publication of our findings with these until, by the development of a method of handling lithium its behavior could be satisfactorily studied. The technique of handling lithium has taken considerable time and effort to master, as it is in a different class, with respect to experimental difficulties, from the other alkali metals. It has considerably higher melting and boiling points, and is commonly believed to attack glass and platinum. The most serious obstacle to its manipulation is presented by the extreme toughness and hardness of the shell of oxide which forms on it in air, coupled with the extreme lightness of the metal. Attempts to melt and distill it in glass from the lump form in which it is obtained commercially have been quite unsuccessful, as the glass blackens and cracks before any lithium metal breaks through its oxide shell. There is reason to believe that the oxide sublimes at a temperature as low or lower[3] than the boiling point of the metal, and the common presence of carbide as an impurity offers a further obstacle to the melting and distilling processes.

The procedure which we have found successful for producing pure lithium metal is best described by reference to a figure showing the photoelectric cell design finally used. This (Fig. 4) consists of two Pyrex glass bulbs *A* and *B*, with a connecting tube *C*. Bulb *A* is provided with a central nickel cup, which stands directly below a long glass tube *T*, through which the lithium is to be introduced. The method of introducing the lithium is as follows: The bottom end of a thin-walled steel tube is turned down to a sharp edge. This tube is then driven down through a piece of lithium metal, [Kahlbaum], so that on withdrawing, the tube contains a cylindrical slug whose sides are protected from the air by the tube walls, and the only oxide present is on the comparatively small areas at top and bottom. The steel tube with its slug of lithium is placed in the glass tube *T*, which is so constructed as to hold the steel tube several centimeters above the nickel cup. Then a long steel rod, loosely fitting in the steel tube, is inserted, resting on top of the lithium, and the end of the glass tube is sealed off. The cell is then exhausted, all the metal parts in the bulb *B* are well baked out, and the cup in *A* is brought to a red heat by a high frequency field.

The next step consists in heating the steel tube, by a high frequency induction furnace, until the lithium melts. When it melts the weight of the steel rod suffices to break the oxide crust, and a globule of clean lithium metal appears at the end of the steel tube, where it may hang, or it may drop into the nickel cup. This globule is then held molten by the induction furnace and gives off metallic lithium which collects on the walls of the bulb *A*. By means of a bunsen flame this metal film is periodically redistilled off the walls and through the connecting tube into the bulb *B*. This bulb, the photoelectric cell proper, has as cathode, a metal plate (e.g. tungsten), behind which is a tungsten filament, to be used for heating the plate by electronic bombardment; and as anode, a nickel cylindrical can, open at

[3] Lebeau, Compte Rendus **136.** 1256 (1903).

the end toward *A*. As the distillation proceeds the metal parts of *B* become coated with lithium, which in appearance and behavior under the flame is very similar to the other alkali metals. The cathode plate is cleaned off by heating to a white heat several times, and allowed to re-coat. Meanwhile the bulb *A* becomes blackened by what appears to be at first partly carbon

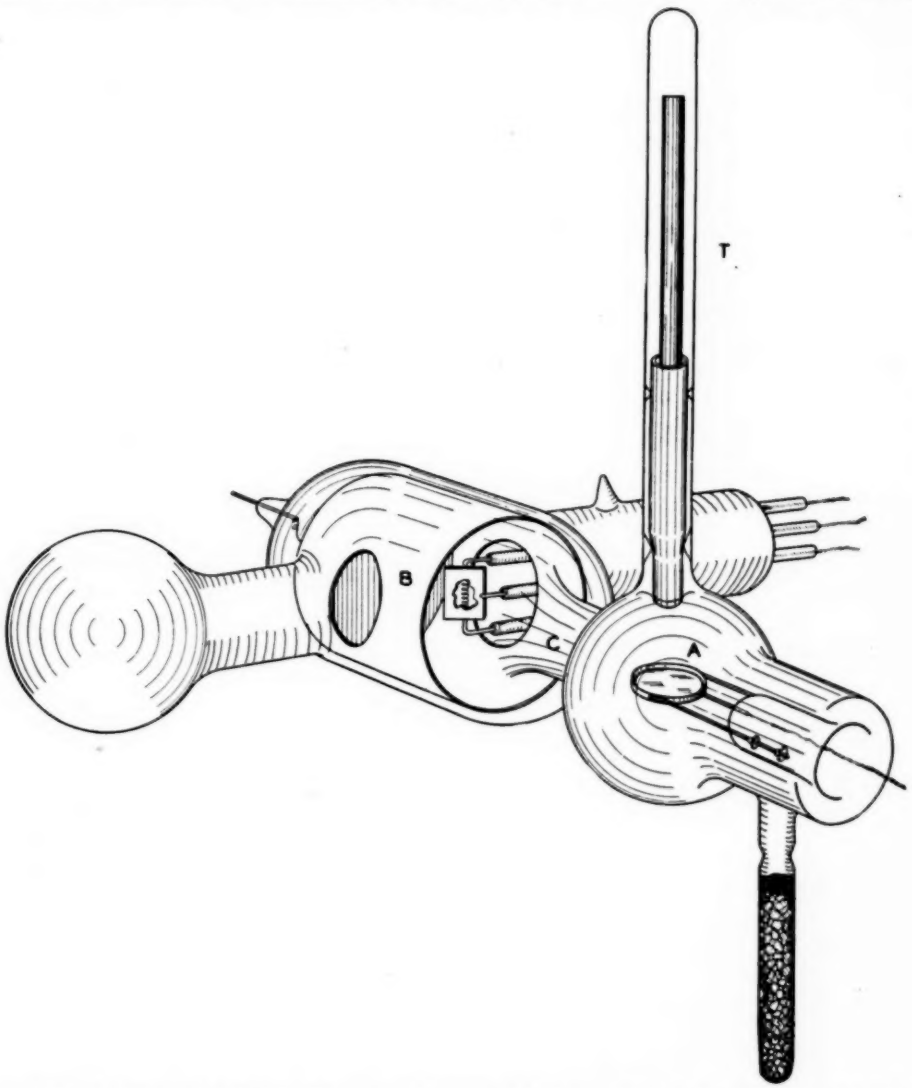

Fig. 4. Type of tube used in preparing pure Li films. Practically oxide-free Li metal dropped from tube *T* to cup of bulb *A*, then distilled into bulb *B* for measurement. (See text.)

from the carbide present in the original lithium and, later by a reaction between the lithium and the glass. When a good supply of lithium is obtained in *B*, the tube is pumped until a high vacuum is obtained, which is assisted by the charcoal tube, later to be placed in liquid air, and the whole cell is sealed off from the pump.

The cell thus prepared exhibits, as the tungsten plate is cleaned off, and then recoated, by gentle warming of the metal on the glass in *B*, *all the characteristic phenomena shown by the other alkali metals*. The cathode first became sensitive to blue light, then as the film increases in thickness, to green, yellow and red; on still further increasing its thickness the red and yellow sensitiveness disappear, and the final thick layer is sensitive only to blue light. *We believe this is the first time that red-sensitive lithium has been observed.*

Measurements through the spectrum of the lithium film on tungsten for all the characteristic stages are shown in Fig. 5. The value of the photo-

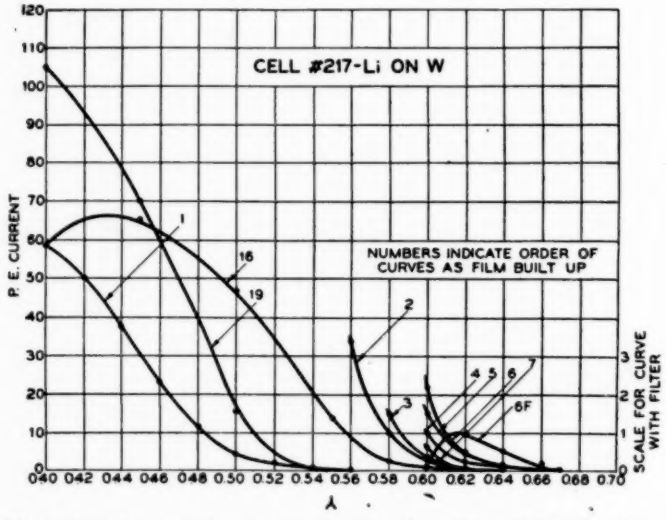

Fig. 5. Photoelectric current vs. wave-length of exciting light, showing maximum excursion to long wave-lengths for a Li film on W. Values not reduced to equal energy spectrum.

electric long wave limit for the thick film condition is shown to approach that given by Millikan[4] [0.526μ] and by Pohl and Pringsheim[5] [0.520μ] for lithium metal.[6] In the figure the maximum excursion is shown to a separate scale, as measured through a red filter to block out stray short-wave energy. *It is seen that the wave-length of maximum excursion is again that of the first line of the principal series* (*0.6708μ*) thus verifying the relationship found with the other alkali metals.

We have, by following substantially the procedure above outlined, made several lithium thin-film cells, sensitive to red light. These cells exhibit the characteristic phenomena only for a short time and the conditions for securing red sensitiveness have proved so critical that it is believed worth while to describe some of our experiments in detail. We have made successfully two cells with tungsten plates as the base for the thin films.

[4] Millikan, Phys. Rev. **7**, 355 (1916).

[5] Pohl and Pringsheim, Verb. D. Phys. Ges. **14**, 46 (1912).

[6] In our earlier attempts to prepare thin films of Li, contamination by the oxide and carbide was visibly evident. In that condition a constant value for λ_o for all thicknesses of film was found. This agreed closely with the long wave limits published by Pohl and Pringsheim and later by Millikan [0.520μ – 0.526μ].

An exactly similar platinum-plate cell failed to exhibit the characteristic thin-film life history, and red sensitiveness, although a section of platinum wire in a cell used in developing the technique of handling the lithium gave the typical long wave limit very definitely at its most sensitive part. In order to trace this discrepancy a cell was made containing two plates, one of tungsten and one of platinum, capable of illumination separately. This cell was studied on the pump, with color filters interposed before the light, with very interesting results. The first deposit of lithium made both plates sensitive to red light; the platinum plate being approximately three times as sensitive as the tungsten. Both plates were coated until the maximum was passed, and then bombarded until insensitive. On successive re-coatings with lithium the platinum plate became less and less sensitive and soon failed to go through the characteristic thin-film life history at all. The tungsten plate under the same treatment was many times more sensitive, but after several reheatings also failed to become red-sensitive.

Our observations suggest to us that the early failure of platinum as a base is to be ascribed to the alloying of the lithium with the platinum, after the first coating. Similarly the failure of tungsten after a few heatings suggests that it, in time, although more resistant, also takes up lithium to form an alloy, similar perhaps to the alloys of gold with the other alkali metals, which we have previously noted as forming an exception to the usual film-forming behavior. It is possible also that the lithium after having been in contact with the glass of the bulb and having been flamed about the cell is no longer pure enough to form true metallic films. The different behavior of tungsten and platinum plates in the same cell however points rather definitely to a reaction between the lithium and the metal of the plate as playing a predominant role in the character of the lithium film.

Much additional work will be necessary, with various metals as supports for the lithium, to establish the conditions necessary to produce the red-sensitive thin films easily and with assurance of success. For the purposes of the present paper however it is sufficient to have established that ithium films can be made, sensitive up to wave-length 0.6708μ.

Experiments on Barium

We have not as yet made any systematic experiments on the alkaline earth metals. We have, however, had available two Case barium cells[7] on which we have made measurements. In these cells, the barium is evaporated from a filament onto the silvered walls of the cell. Although this process is performed in a manner not known to us in detail, we understand that evaporation is continued until a maximum of sensitiveness is attained. The likelihood that these cells at least approximate to the characteristicl maximum long wave limit is reasonably high.

Measurements which we have made with diffused light on these cells so that their most sensitive spots wherever occurring would be operative gave for one of the cells a long wave limit of approximately 0.70μ and for the other, with a No. 88 Wratten filter, 0.79μ. The long wave limit of the

[7] Case, Phys. Rev. **17**, 398 (1921).

former lies farther toward the blue than the resonance line of barium (0.7911μ) while that for the latter agrees very closely with this wave-length. These measurements are, of course, not conclusive as we have no guarantee that if the deposition process were followed closely the significant wave-length might not be passed but we believe this to be a strong indication that the resonance frequency plays the same role here.

The Illumination Current Relationship

The idea that the long wave limit should correspond to the resonance frequency has been suggested before, in particular by Kirchner,[8] who in addition has tried to associate the "selective" maximum with the difference between the resonance and ionization potentials. Kirchner points out that if the incident light is responsible for the complete emission of the photoelectrons the process must be in two stages, and as a consequence the photoelectric current should be proportional to the square of the illumination. It is thus important to determine accurately the illumination current relation for the thin films of alkali metal, particularly as close to the long wave limit as possible.

We have made illumination current measurements with an electrometer for the current measuring instrument and with an inverse square law apparatus to vary the light. Illuminating the cells through color filters and taking a number of points we have obtained a close approximation to a rectilinear relation, with no indication of the second power law suggested by Kirchner. These measurements were, however, not entirely satisfactory because they consumed considerable time, in which the cell might change its sensitiveness. Especially does the sensitivity of the cell change when the illuminating source is the crater of an arc. Experiments show that an arc light focussed on a thick potassium film can change the galvanometer deflections for red light fifty-fold in less than ten minutes. We have therefore resorted to a simpler procedure, as follows:

The cells were illuminated by a tungsten lamp, the filament being focussed through a color filter on the cathode of the cell. To vary the illumination a metal plate perforated with many small holes was placed over the image-forming lens. The transmission of the plate was carefully measured in position by means of a potassium hydride cell which had previously been found to have an accurately linear response to illumination. The transmission found (0.38) is independent of the color of the light, as the holes in the plate (1 mm diameter) are too large to introduce any diffraction effects over the wave-length range in question. With this arrangement of apparatus the response of the extreme long wave region of sensitiveness was tested first of all with a sodium-on-platinum cell throughout its whole life history. At each stage such a color filter was selected that the galvanometer deflection was only four or five millimeters, which at the condition of maximum sensitiveness amounted to 1/1000 or less of the deflection with unfiltered light. The currents were then measured with and without the perforated plate. These measurements with the tungsten lamp were supplemented at the

[8] Kirchner, Phys. Zeits. **25**, 303 (1924).

extreme excursion of the long wave limit by measurements with the crater of a carbon arc, which because of its inferior steadiness and the danger of its heat quickly altering the emission would not alone have been wholly satisfactory.

For all positions of the long wave limit the illumination current relationship was found to be accurately rectilinear. The measurements of the transmission of the perforated plate all lie between 0.36 and 0.45, where the second power law would call for a value of 0.145.

Similar although less extensive measurements were made with a potassium cell immersed in liquid air, and on a caesium-on-silver cell of the permanent type. *The measurements as a group constitute a most perfect confirmation of the generality of the rectilinear illumination current relationship in the thin film cells of all types in all states of film thickness.*

Final Discussion

The coincidence of these wave-lengths of maximum excursion of the photoelectric long wave limit with the first line of the principal series, or with the resonance potential, of the various materials investigated points strikingly to the conclusion that when the film is in its most red-sensitive condition, *the process of photoelectric emission occurs when sufficient energy is given to the atom to produce its first stage of excitation.* In the Einstein equation $(1/2)\ mv^2 = h\nu - p$, as is well known, the term p is to be considered as consisting of two parts, $h\nu_a$ the energy necessary to release the electron from the atom and p', the energy necessary to carry the electron out through the surface of the metal. In the case of the thin films in their condition of maximum sensitiveness, the conclusion above-drawn implies that the photoelectron comes from the atom of alkali metal, that the energy necessary to bring the atom into resonance is sufficient to release the photoelectron, and finally that the term p' is zero.

If we assume that in all cases the photoelectron comes from the alkali metal atom, we may imagine the process of film deposition in general to be one in which up to the condition of maximum sensitiveness the alkali metal only partially covers the surface and the attractive force due to the supporting metal causes the return of the electrons of small energy into the surface. At the condition of maximum emission, the alkali metal is present as individual atoms sufficiently closely spaced so that the attractive action of the underlying metal is inhibited. As the film continues to thicken after the maximum excursion is reached, an alkali metal lattice is built up for which again the retarding forces are greater than for the individual atoms.

This picture of the process of deposition receives support from the differences in the photoelectric emission before and after the maximum is reached. The general slope of the current vs. wave-length curve is comparatively flat before the condition of maximum emission is reached, and steep afterward, indicating a different form of surface force.

Another significant observation is that, with a plane supporting surface, such as a polished platinum plate, the ratios of emissions for obliquely incident light polarized parallel to and perpendicular to the plane of incidence are quite different before and after the condition of maximum emis-

sion. In fact, in the earlier stages of film deposition this ratio, which finally may be as high as 20 or 30 to 1, is *unity*, indicating the absence of any regular orientation of the alkali metal atoms. Furthermore, we believe this means that the photoelectric emission must be entirely from the alkali metal atoms, since if the absorptive properties of the platinum entered in, this ratio would be considerably greater than unity. Another reason for believing that the photoelectrons come from the alkali metal atoms is the observation that the maximum long wave limit is the same with different supporting metals.

As already noted the idea that the long wave limit should correspond to the resonance frequency has been previously proposed by others, whose speculations have indicated that the process should consist of two stages, and that the photoelectric current should vary as the square of the illumination. The results of our study of the illumination current relation show this latter conclusion to be contrary to fact. We are therefore of the opinion that while the initial step toward release of the electron is the excitation of the atom by light, its further progress toward emission must be due to other processes, such as collisions. These processes must furthermore be peculiar to the solid, or at least to the thin film condition, as otherwise we would expect photoelectric emission at the resonance frequency from alkali metal vapors.

A matter of considerable interest in this connection is the bearing of this work on thermionic emission. It is very generally held and experimentally[9,10] well established that the photoelectric long wave limit coincides (when expressed in volts) with the thermionic work function. If then the photoelectric threshold is determined by the resonance potential of the atoms, it would appear to follow that thermionic emission is also dependent on the initiation of resonance in the atoms and the phenomenon of thermionic emission is to be associated with electrons belonging to the atoms and not with free electrons, as has been commonly held. As has been shown by Becker,[11] the thermionic work function for thin films of caesium on tungsten makes an excursion toward a low value and back, similar to that made by the photoelectric minimum frequency. It is of considerable significance in this connection that the value Becker finds, from Langmuir's data, for the minimum work function of caesium, is 1.36 volts, where the value from the resonance wave-length is 1.38 volts. The excursion of the work function in the case of barium in a thin film has been studied by Eglin,[12] who gives a minimum value of 1.66 volts, which is to be compared to the resonance potential value of 1.56 volts. It will be profitable to study the minimum thermionic work functions and maximum photoelectric long wave limits together, in the light of the relationship to spectroscopic data here indicated.

We wish to acknowledge our indebtedness to Mr. G. R. Stillwell for assistance in this work, particularly in connection with the method of handling lithium.

[9] Du Bridge, Phys. Rev. **31,** 236 (1928).
[10] Bridgman, Phys. Rev. **31,** 862 (1928).
[11] Becker, Phys. Rev. **28,** 341 (1926).
[12] Eglin, Phys. Rev. **31,** (1927) (Abstract).

CONTACT POTENTIAL MEASUREMENTS WITH ADSORBED FILMS

By Irving Langmuir and K. H. Kingdon
Research Laboratory, General Electric Company

(Received March 30, 1929)

Abstract

Measurements have been made of the contact potential differences between a clean unheated tungsten filament, and the same filament coated with an adsorbed film of thorium, caesium, oxygen, or a mixture of caesium and oxygen. The method used is well adapted to prevent accidental contamination of the filament surfaces. The values found for the contact potentials between cold surfaces are

Cs-O-W—W	3.1 volts
Cs-W—W	2.8
Th-W—W	1.46
W—OW	0.8

The surface on the left is positive to that on the right. These values of contact potential do not agree with those calculated from the thermionic emission constants. An example is given of the application of the method to the measurement of the changes in work function produced by heating a tungsten filament to various temperatures in presence of caesium vapor, thus changing the amount of adsorbed caesium.

THE measurement of the contact potential difference between two metallic surfaces has been a subject which has attracted the attention of experimenters for many years. Unfortunately the values obtained have been most inconsistent, chiefly on account of the great difficulty of keeping metal surfaces free from contaminating films. The great amount of experimental work with thermionic tubes during the last fifteen years has emphasized the difficulty of keeping hot filaments free from surface contamination. When the surfaces used are cold, as is usually the case in contact potential measurements, this difficulty is enhanced.

With this in mind we have made our contact potential measurements between filamentary electrodes, which can be easily cleaned by heating. Moreover, by working with adsorbed films, the surface of a single filament can be brought into different states, and the contact potential differences between these states determined. This makes the experimental tube very simple, so that good vacuum conditions are easily maintained.

The experimental method is illustrated in Fig. 1. The tube contains two cylinders *c*, *g*, and two loop filaments *a*, *b*. One of these filaments *b*, usually of thoriated tungsten, is maintained at a definite temperature and state of activation, and serves as a standard source of electrons. Cylinder *g* is fixed at a suitable negative potential with respect to *b*, so that no electrons can leave the part of *b* which is inside *g*. This serves to eliminate all effects occurring at the ends of the filaments, where conditions are not definite. Cylinder *c*, is fixed at about the same potential as the part of *b* which is inside *c*. Electrons can flow therefore from *b* to *c* or *a*. The surface of fila-

ment a is then put in some definite condition (for example, a complete film of thorium is formed on it[1]), and a characteristic is taken of the electron flow from b to a (i_{ba}) as a function of the potential of a with respect to b (V_{ab}). The surface of a is then changed (for example, by heating to a high enough temperature to drive the thorium completely off) and another characteristic taken of i_{ba} as a function of V_{ab}. The voltage displacement of these two characteristics from one another then measures the contact potential difference between the two states of the surface of a.

An alternative procedure is to find the values of V_{ab} for the two states of a, which are required to give the same value of i_{ba} (say 10^{-6} amp.) The difference between these two values of V_{ab} gives the contact potential.

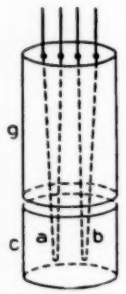

Fig. 1. Arrangement of filaments and cylinders.

It is advisable, however, to take the complete characteristics at first over a considerable voltage range, as lack of parallelism of the two characteristics is an indication of some wrong experimental condition.

Some necessary points in the experimental technique are as follows:—

(1) The vacuum must be good. The tube was immersed in liquid air during the measurements.

(2) If an alkali metal is present in the tube care must be taken to distill the metal from the surfaces of g and c, so that photoelectric currents caused by the light from the filaments will not vitiate the results. This distillation is conveniently done by warming the cylinders by radiation from one of the filaments after immersing the tube in liquid air.

(3) It is important to remove all easily volatile impurities from c and g even though the radiation from b does not cause appreciable photo-emission. If this has not been done, then when a is heated to change its surface condition, c is also heated enough to change its surface condition and a change in the electric field due to c ensues.

(4) Cylinder c must be negative to a so that secondary emission from a to c cannot occur.

(5) If very fine filaments (0.0025 cm diameter) are used the positions of the ends of the loops may change in an erratic manner when the filaments are heated to a high temperature. This change, of course, spoils the measurements.

[1] Langmuir, Phys. Rev. **22**, 357 (1923).

The measurements to be described[2] were made with two tubes—numbers 156 and 502.

In tube 156 cylinders c and g (Fig. 1) were of tungsten wire spirals, the idea being to insure that the caesium vapor pressure (for other experiments) inside the cylinders should be the same as that determined by the temperature of the bulb wall. Filaments a and b were of thoriated tungsten wire 0.0102 cm diameter, each containing 12.7 cm of wire. The area of the part of each filament inside c was 0.11 cm^2. The tube contained caesium. It was used on the pump and was immersed in liquid air during the measurements.

Tube 502 contained three filament loops—a and d were of thoriated tungsten wire (0.0102 cm diameter), and b was of pure tungsten (0.0051 cm diameter). The cylinders c and g were made of nickel sheet. This tube was

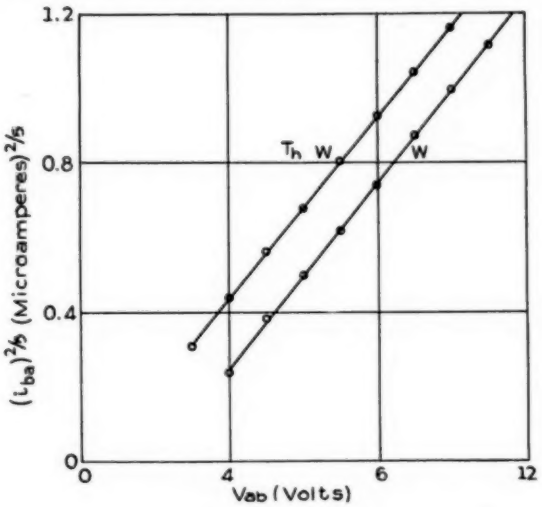

Fig. 2.

used on the pump, so that oxygen could be admitted. It was immersed in liquid air during measurements.

Measurements of the contact potential between tungsten and thoriated tungsten were made with tube 156. Filament b was thoriated and run at 1730°K as the standard source of electrons. The total potential drop over b was 5.5 volts, and that over the part of b inside c was 1.5 volts. The potential of the part of b inside c therefore ranged from +2.0 to 3.5 volts with respect to the negative end of b. The potential of c was +1.5 with respect to the negative end of b, so that c was negative to all parts of b inside it (apart from contact differences of potential). Therefore since the area of c was very large compared with that of a, the total field accelerating electrons away from b was small, even when a was 10 volts positive to b (negative end). As a result, the space charge limited current to a is proportional to the 5/2 power of the effective voltage accelerating electrons away from b. Ac-

[2] These measurements were made from two to four years ago. They are incomplete, and publication was delayed in the hope of doing further work. As opportunity for this has not occurred yet, it seems worthwhile to publish a description of the method and of the results obtained to date.

cordingly in Fig. 2 we plot $(i_{ba})^{2/5}$ as a function of V_{ab} in order to obtain a linear plot. Such characteristics were taken first with the surface of a completely coated with thorium, and then with the thorium removed. The other conditions were $E_g = -22.5$, $E_c = +1.5$, both with respect to the negative end of b. The two lines in Fig. 2 are parallel throughout their course and displaced from each other by 1.46 volts. This then is the contact potential difference between cold tungsten and thoriated tungsten surfaces, the ThW being positive to the W surface. The fact that the lines are parallel over the entire voltage range gives us confidence in the result. The same value for this contact potential difference was also obtained with tube 502.

Tube 502 was used chiefly to make measurements of the contact potential between tungsten surfaces, clean, or coated with oxygen, caesium, or both. Filament d was used as a thoriated electron source, while filament b was

Reference	Run	Cs OW Activated	Cs OW Unactivated	Cs W	W	OW Activated	OW	ΔV	V_c
1810	1,2		←	—	—	→		3.80	1.5
1810	2,3				←	→		0.70	1.5
			←	—	→			(3.10)	
1812	6,7				←	—	→	0.75	1.5
1814	21,22				←	→		0.75	1.5
1815	1			←	→			3.00	1.5
1815	2		←	—	—	→		4.24	1.5
1815	2				←	→		1.11	1.5
		←	—	—	→			(3.13)	
1816	3		←	—	—	→		3.78	1.5
1816	3				←	→		0.61	1.5
		←	—	—	→			(3.17)	
1817				←	→			2.72	0.5
1819	1			←	→			2.71	1.0
1819	2				←	—	→	0.90	1.0
1819	3		←	—	—	→		4.10	1.0
1819	3			→	←	→		1.00	1.0
			←	—	→			(3.10)	

Fig. 3

coated with various films. Filament a was heated to drive caesium off cylinders c and g before the measurements were started. Usually complete characteristics were not taken, but the potential of b necessary to take a certain electron current from d was found.

The measurements which were considered to have been made under satisfactory experimental conditions are listed in Fig. 3. The various kinds of surfaces are listed in separate columns, and the double arrow indicates between which pair of surfaces the measurement of contact potential difference (ΔV) was made. The values of ΔV in parentheses were obtained by subtracting the two preceding values. The cylinder potential V_c is given in the last column. V_g was kept at -22 volts throughout. The surfaces at the left of the table are positive to those at the right.

The method of preparation of the surfaces was as follows. The W surface was of course prepared by flashing filament b for a short time at a high temperature. This cleaning was always done before depositing an adsorbed

layer. The OW surface was prepared by letting oxygen come in contact with the cleaned, cold filament, the tube being immersed in liquid air to prevent rapid oxidation of the caesium in the tube. The CsW surface was similarly prepared by letting caesium vapor deposit on the cleaned, cold filament, the tube being subsequently immersed in liquid air. For the CsOW (unactivated) surface, an oxygen layer was first formed on the cleaned filament, sometimes by adsorption with the filament cold, and sometimes by heating the filament for 1 sec. at about 2000°K in a low pressure of oxygen (a few baryes). Caesium was then allowed to deposit on this surface. A surface prepared in this way is not an active thermionic electron emitter.[3] To obtain large emissions it is necessary first to activate the filament by heating for a few seconds at 1600 to 1800°K. The CsOW (activated) surfaces were prepared in this way.

Suppose we started with a CsOW (unactivated) surface, as in 1810 (1, 2) of Fig. 3, and measured the potential (V_{bd}) of b necessary to draw a certain electron current (i_{db}) from d. Filament b was then heated hot enough (up to 1600°K) to drive off all the caesium, but not to remove any large amount of oxygen. V_{bd} was then again determined for the same value of i_{db}. The difference between the values of V_{bd} then gave the contact potential difference between CsOW (unactivated) and OW (activated), since the heating to 1600°K was considered to have put the oxygen layer in nearly the same condition as that in an activated CsOW surface. The oxygen layer was then distilled off by heating to 2500 to 2800°K for a few seconds, giving a determination of the contact potential difference between OW (activated) and W. The procedure in the other cases of Fig. 3 was analogous.

The average values of contact potential taken from all the data are:—

CsOW-W: 3.1 volts	ThW-W: 1.46 volts
CsW-W: 2.8	W-OW: 0.8

In each case the surface on the left is positive to the one on the right. Most confidence is felt in the ThW-W result. The others should be regarded as provisional values, although no reason is known for suspecting serious error.

It will be noticed from Fig. 3 that the data are not accurate enough to distinguish between the different types of OW surfaces investigated. It is more surprising that there is also no distinction between activated and unactivated CsOW surfaces, as there is a large difference (of the order 10^5 fold) between the electron emissions from these surfaces.

The contact potential differences are connected with the thermionic emission constants for the various surfaces by the relation[4]

$$\Delta V = \phi_1 - \phi_2 + (T/11600)\ln(A_2/A_1) \qquad (1)$$

where ϕ_1 and ϕ_2 are the work functions of the two surfaces, expressed in volts, and A_1 and A_2 are the values of the A constant of the thermionic emission equation. The values of these constants are given in Table I, together with the temperature range over which the measurements on which the constants are based were made.

[3] Kingdon, Phys. Rev. **24**, 510 (1924).

[4] Richardson, Emission of Electricity from Hot Bodies (1921) p. 41.

TABLE I. *Thermionic constants of various surfaces.*

Surface	b degrees	ϕ volts	A amp/cm$^2T^2$	Temp. range °K
CsOW[5]	8300	0.71	0.003	600–700
ThW[6]	30500	2.63	3.0	1150–1600
W[7]	52600	4.52	60	1900–2300
OW[5]	107000	9.23	5×10^{11}	1500–1700

In Table II are shown the observed values of contact potential between various surfaces, together with the values calculated from Eq. (1) using the data of Table I. The contact potentials have been calculated for a temperature of 300°K in (1), since the filaments were not heated.

TABLE II. *Calculated and observed values of the contact potential for various surfaces.*

Surfaces	ΔV (calc.)	ΔV (obs.)
ThW–W	1.81	1.46
CsOW–W	3.55	3.1
W–OW	4.12	0.8

The agreement is not good. In no case was there any indication of a contact potential difference of 4 volts between tungsten and oxidized tungsten. It is believed that the differences between the observed and calculated values are well outside the experimental error in the contact potential measurements for the ThW-W and W-OW combinations. However it may not be justifiable to use electron emission constants determined at elevated temperatures to calculate contact potential differences between surfaces at room temperature. An attempt was made to measure contact potentials between hot surfaces, but the work was not completed.

In another experiment measurements were made of the changes in contact potential and electron emission when the temperature of a tungsten filament was varied, thereby changing the amount of caesium adsorbed on its surface. The experimental tube was similar to those described above, and had two filaments 15 cm long and 0.0102 cm diameter. One filament was of thoriated tungsten, and the other of pure tungsten. The area of that part of each of the filaments inside cylinder C (Fig. 1) was 0.30 cm^2. The thoriated filament was activated, and held at a constant temperature as the source of electrons. The caesium in the tube was kept at room temperature. Cylinder C was kept at -1.3 volts with respect to the negative ends of the filaments during the contact potential measurements.

The tungsten filament was heated to the temperatures shown in the first column of Table III. These temperatures are those calculated from the heating currents, and are subject to two large sources of error—cooling by the leads, and heating by radiation from the other filament. From rough calculations it appeared that these errors, although of the order of 100° at the lowest temperatures, approximately compensated each other in the center part of

[5] Kingdon, Phys. Rev. **24,** 510 (1924).
[6] Dushman and Ewald, Phys. Rev. **29,** 857 (1927).
[7] Dushman, Phys. Rev. **21,** 623 (1923); **25,** 338 (1925).

the filament, so that the original temperatures as determined from the heating current have been retained in the table.

TABLE III.

T °K	i_{obs} μa	V_f volts	ΔV volts	$\Delta\phi$ volts	ϕ volts	b degrees	i_{calc} μa
542	0.87	0.13	−0.565	−0.50	[1.38]	[16000]	[0.87]
607	7.39	0.21	−0.520	−0.42	1.46	16930	5.2
645	7.80	0.26	−0.465	−0.33	1.55	17980	6.2
678	5.80	0.31	−0.395	−0.24	1.64	19020	5.4
741	1.83	0.42	−0.190	+0.02	1.90	22030	1.3
794	0.41	0.55	0.000	0.27	2.15	24950	0.29
846	0.10	0.68	+0.190	0.53	2.41	27950	0.063
891	0.027	0.83	0.330	0.74	2.62	30400	0.023

The electron emission from the caesiated filament is given in the column headed i_{obs} (cylinder C was of course made positive for the emission measurement). The emission at first rose as the temperature was raised, but decreased at the higher temperatures, since some of the caesium coating had been driven off. At each temperature the rates of adsorption and evaporation of caesium were in equilibrium. V_f denotes the voltage drop over the caesiated filament due to the heating current. At each filament temperature the voltage ΔV was determined at which the caesiated filament must be held with respect to the thoriated filament in order that the former should receive 0.5 μa electron current from the latter. This current flow was also affected by the potential drop over the caesiated filament, and in order to correct approximately for this, $1/2\ V_f$ was added to ΔV, the sum being given in the column headed $\Delta\phi$. These values of $\Delta\phi$ then show the changes in the work function as the amount of caesium on the surface was varied, but do not fix its absolute value at any point. If the filament had been heated hot enough to keep its surface free of caesium, and thus fix ϕ from the value for tungsten, other complicating effects would have been introduced. The only available method for fixing the scale of ϕ was from the observed electron emission, using the emission equation

$$i = 60T^2 e^{-b/T} \text{ amps. per cm}^2. \qquad (2)$$

From this we find that at the 542°K point $b = 16000°$ and hence $\phi = 1.38$ volts. The other values of b and ϕ given in Table III were determined from this base value and the values of $\Delta\phi$. The last column of the table gives values of the emission from the caesiated filament calculated from Eq. (2) and the values of ϕ. The observed and calculated values of the emission agree fairly well.

Too much emphasis must not be placed on this agreement for the following reasons:—(1) the uncertainty in the temperature scale caused by lead cooling and radiation from the thoriated filament, (2) the approximate nature of the correction to ΔV involving V_f, and (3) the fact that the constant 60 in Eq. (2) is not correct for most adsorbed films. These inaccuracies are not inherent in the method, but could be overcome by changes in the construction of the tube so as to reduce the error in filament temperature; and by changes in the experimental procedure, so as to eliminate or correct for the effect of V_f, and to enable a direct calibration of the scale of ϕ to be made from the value for pure tungsten.

THE ATTENUATION OF ULTRA-VIOLET LIGHT BY THE LOWER ATMOSPHERE*

By L. H. Dawson, L. P. Granath and E. O. Hulburt
Naval Research Laboratory

(Received March 27, 1929)

Abstract

Measurements were made with a quartz mercury lamp, a quartz spectrograph and a recording densitometer of the attenuation of ultra-violet light from 3000 to 2050A by the atmosphere at sea level. For wave-lengths from 5000 to 3000A the absorption was too slight to be observed at distances up to 400 meters; for wave-lengths below 2800A there was pronounced absorption above that attributable to molecular scattering. The absorption was the same day and night, was unaffected by changes in the humidity, but increased with haze. The thicknesses of clear air necessary to reduce the light to 10^{-2} were about 22, 5, 0.57 and 0.20 km for 2800, 2500, 2200 and 2050A, respectively. The absorption in the lower atmosphere around 2800 to 2900A was not sufficient to account for the sharp cessation of the solar spectrum in this region. This result is in keeping with the fact that the ultra-violet limit of the solar spectrum is due to ozone in the high atmosphere. The absorption in the lower atmosphere at 2200 to 2050A, a spectrum region where ozone is relatively transparent, is great enough to prevent sunlight of these wave-lengths from penetrating to sea level.

THERE have been very few measurements of the attentuation of ultra-violet light by the lower atmosphere and no measurements at all for wave-lengths below 2600A. In the present investigation the absorption coefficients in the region 3000 to 2050A have been obtained for a clear and a hazy atmosphere. The absorption was found to increase with a decrease in wave-length and an increase in haze. Schaeffer[1] determined the atmospheric transmission on clear winter nights for the region 3300 to 2600A; his values are referred to in a later paragraph. Rayleigh[2] in connection with the investigations of atmospheric ozone by Fabry and Buisson[3] observed qualitatively that the absorption by several km of the atmosphere for wave-lengths around 2536A was greater than that given by the Rayleigh molecular scattering formula.

The present experiments were carried out on the edge of the Potomac River about five miles from the city of Washington. The source of ultra-violet light was placed at the focus of a metal mirror 24 inches in diameter, and the spectrum was photographed from a distance with a quartz spectrograph. For a specified region of the spectrum the distance was chosen so that the spectrum lines were weakened by absorption neither too much nor too little; this gave the most accurate results. A distance of 404 meters was used for the region 3000 to 2288A and in this case the source was an atmospheric pressure quartz mercury arc taking about 1.2 kw. Cadmium

* Published with the permission of the Navy Department.

[1] Schaeffer, Proc. Amer. Acad. of Arts and Sci. **57**, 365 (1922).

[2] Strutt, Proc. Roy. Soc. **A94**, 260 (1918).

[3] Fabry and Buisson, Journal de Phys. **3**, 196 (1913).

and zinc were put into the mercury to furnish some strong lines in regions of the spectrum where the mercury lines were faint. For wave-lengths 2288 to 2050A the distances were 30 to 50 meters and the source was a condensed spark between silver terminals with a current of about 15 amperes.

The method employed was one often used in ultra-violet photometry and has been described by Fabry[4] and others. It consisted in photographing the spectrum of the source at a distance, then bringing the spectrograph to within a meter of the source reflected from the mirror and impressing on the same plate with the same time of exposure a series of comparison spectra through screens which reduced the intensity of the light by known amounts. Wire gauze screens were used of transmissions 100 (i.e. no screen), 58, 32, 15 percent and sometimes of intermediate values. The transmissions of the screens were measured with a quartz monochromatic illuminator and a photoelectric cell, and tests showed the transmission of each screen was constant for wave-lengths in the visible and ultra-violet regions of the

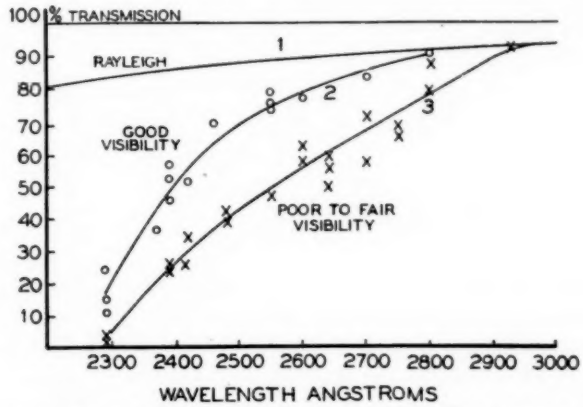

Fig. 1. Percentage of light of various wave-lengths transmitted through 404 meters of the of the atmosphere. Curve 1 calculated from Eq. (2); curve 2 and circles, values observed for a clear atmosphere, visibility greater than 15 km; curve 3 and crosses, values observed for a hazy atmosphere, visibility about 8 km.

spectrum. By means of a diaphragm the intensities of the comparison spectra were adjusted so that the strongest spectrum was stronger and the weakest weaker than the spectrum of the distance source. The width of the slit of the spectrograph was 0.1 mm and no lens was used in the front of the slit. Curves were taken with a recording densitometer of the spectra on each plate and from the measured heights of the curves the relative atmospheric transmission at each wave-length was determined. To get the absolute values of the transmission it was assumed that for wave-lengths where the absorption was too slight to be observed at the longest distance used, i.e. about 2800A for curve 2 and 2900A for curve 3, Fig. 1, the absorption was that given by the Rayleigh molecular scattering formula.

The percentage transmissions of wave-lengths down to 2288A through 404 meters of the atmosphere are given in curves 2 and 3, Fig. 1, for conditions of good visibility and poor to fair visibility, respectively. The

[4] Fabry, Proc. Phys. Soc. London **39**, 1 (1926).

visibility is defined as the distance beyond which a dark colored object could not be distinguished in daylight, good visibility referring to a distance greater than 15 km and poor to fair visibility to a distance about 8 km. The circles and crosses in Fig. 1 are plotted from some of the values of the various plates and indicate the experimental variations in the measurements. It is assumed that the transmission of the atmosphere is expressed by

$$I = I_0 10^{-\alpha x}, \tag{1}$$

where I_0 is the original intensity of the light, I is the intensity after passage through a distance x cm and α is the light absorption coefficient. The absorption coefficient due to molecular scattering given by Rayleigh[5] is

$$32\pi^3(\mu-1)^2/3N\lambda^4\times 2.3, \tag{2}$$

where μ is the refractive index of the air, N the number of molecules per cm^3 and λ is the wave-length of the light in cm. The factor 2.3 is in the denominator because we have written 10 in (1) instead of the Naperian base. Curve 1, Fig. 1, is the transmission through 404 meters of air calculated from Eqs. (1) and (2). It is seen that pronounced absorption above that attributable to molecular scattering set in at about 2800A. The absorption was found to be the same for day, night, summer and winter, and for conditions of high and low water vapor content, as long as the atmosphere was clear.

The values of α calculated by Eq. (1) from the smooth curves 2 and 3, Fig. 1, are given in curves 2 and 3, Fig. 2. Curve 2′ is the extension of curve 2 to wave-length 2050A, obtained from data similar to those of Fig. 1, but taken at shorter distances; for curve 2′ the ordinates of Fig. 2 should be multiplied by 10. The values of α calculated from the molecular scattering formula (2) are shown in curve 1. In curve 4 are given the values of α calculated by Eq. (1) from the atmospheric transmission percentages observed by Schaeffer for clear winter nights at a distance of 2300 meters. He joined his curve to the Rayleigh curve at 3400A. The measurements were made near Boston, Mass., and if it were assumed that the temperature was -10°C and that α is proportional to the density of the air and hence inversely proportional to the absolute temperature, the values of curve 4 should be reduced by about 10 percent to be compared with those of curve 2 which were for an average temperature of about 15°C. On the whole one would suppose that for wave-lengths longer than 2800A the values of curve 4 were more trustworthy than those of curve 2 and that below 2800A the reverse were true.

It is seen that the ultra-violet absorption of the atmosphere is made up of a permanent absorption due to the atmospheric gases and a variable absorption due to the particles which cause haze. From 2050 to 2100A the permanent absorption agrees with that to be expected from the oxygen in air according to the recent measurements of Granath (to be published soon). Although no measurements of the absorption coefficients are available for wave-lengths longer than 2100A, oxygen is known to possess absorption,

[5] Rayleigh, Phil. Mag. **47**, 375 (1899).

either continuous or in faint bands, in this region[6] and it seems probable that the air absorption is due mainly to the oxygen in the air.

From curve 2, Fig. 2, $\alpha = 0.9 \times 10^{-6}$ at 2800A, which shows that light of this wave-length is reduced to 10^{-2} of its original intensity by passage through 22 km of the atmosphere. Since the total vertical thickness of the atmosphere is equivalent to about 8 km at atmospheric pressure, the absorption from 2800 to 2900A by the lower atmosphere is not sufficient to account for the sharp cessation of the solar spectrum[3] at 2885A. This is in agreement with

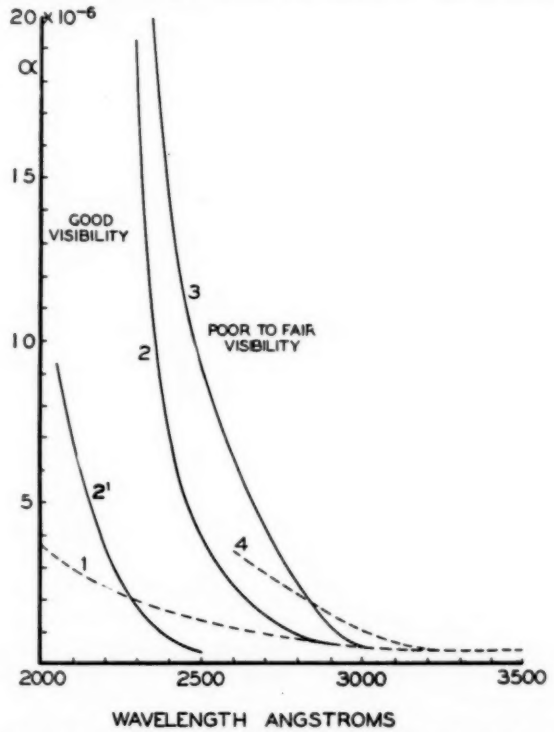

Fig. 2. Light absorption coefficient α of air. Curve 1, calculated from Eq. (2); curve 2, values observed for a clear atmosphere, visibility greater than 15 km; curve 2′, the extension of 2 to 2050A, the ordinates should be multiplied by 10 for 2′; curve 3, values observed for a hazy atmosphere, visibility about 8 km; curve 4, values observed by Schaeffer.

the fact that the ultra-violet limit of the solar spectrum is due to ozone in the high atmosphere. The ozone absorption band, however, which sets in at about 2900A extends only to about 2200A, and below this ozone is relatively transparent.[3] It has not been known why sunlight in the far ultra-violet region from 2200 to 2000A does not penetrate to the surface of the earth. The present measurements indicate that it is the lower atmosphere which stops these wave-lengths, for from the values of α of curve 2, Fig. 1, the thicknesses of clear atmosphere necessary to reduce the light to 10^{-2} of its original intensity were about 570, 350 and 200 meters for wave-lengths 2200, 2100 and 2050A, respectively.

[6] For references about the light absorption of oxygen, see Wulf, Proc. Nat. Acad. Sci. **14**, 609 (1928).

THE ABSORPTION OF LIGHT BY FOG*

By L. P. Granath and E. O. Hulburt
Naval Research Laboratory

(Received March 27, 1929)

Abstract

Measurements between two stations 0.4 km apart with a thermocouple and galvanometer and with spectrograms, properly calibrated, of the absorption of light by fog for wave-lengths from 0.4 to 3μ showed that the absorption increased slightly with decrease in wave-length, but hardly enough to indicate that red light is appreciably better than blue light for the purpose of penetrating fog. For a fairly dense fog, such that in daylight dark colored objects at about 0.6 km could barely be be seen, the distances necessary to reduce the light to 10^{-2} of its original value were about 710, 843, 910, 970, 980 and 980 meters for wave-lengths 0.4, 0.5, 0.6, 1.0, 2.0 and 3.0μ, respectively.

NO QUANTITATIVE data appear to be available for the absorption of various wave-lengths of light by fog. In the present experiments the absorption by fog was measured for light in the region of the spectrum from 0.4 to 3.0μ and was found to increase slightly with decrease of wave-length, but hardly enough to indicate that red light is appreciably better than blue light for the purpose of penetrating fog.

The apparatus consisted of a transmitter and a receiver, 0.4 km apart with a fairly open field between them, situated on the banks of the Potomac River about five miles below the city of Washington. Although taken on land the measurements are considered to apply to fogs at sea, for it is thought, although it is not known with certainty, that the fogs, mists and vapors of the valley of the Potomac River near Washington have roughly the same optical characteristics as the fogs at sea and along the coast, Washington and its surroundings being less smoky than some localities. The transmitter was in a small shed about 3 meters above the level of the river and the receiver was on the top of a building about 15 meters high. A small Nichrome heating coil operated at a temperature of 940°K and placed at the focus of a 24 inch metal mirror served as a transmitter of infra-red rays in a band around 3μ. The calculated spectral energy distribution curve of a black body at 940°K is given in curve 3, Fig. 1; the dots along curve 3 are the relative spectral energies of the Nichrome coil measured with a calibrated infra-red spectrograph. To obtain a transmitter of spectrum bands around 1.4μ and around 0.6μ the Nichrome coil was replaced by a 2 kw tungsten lamp with a heat transmitting screen of black glass and a heat absorbing screen of pale bluish green glass, respectively. The observed spectral energy curves of the tungsten lamp through the two screens are given in curves 2 and 1, Fig. 1, respectively. The bluish green glass was slightly transparent from 2.0 to 2.4μ but the amount of energy transmitted in these wave-lengths was too small to affect the present measurements and to be percepti-

* Published with the permission of the Navy Department.

ble on the scale of the drawing of curve 1. The transmitter was turned on and off by means of a shutter.

The receiver for measuring the 3μ, 1.4μ and 0.6μ bands was a 24 inch metal mirror at the focus of which was rigidly mounted a thermopile enclosed in a small metal box with a fluorite window transparent to about 8μ. The thermopile was connected to a galvanometer of moderate sensitivity with

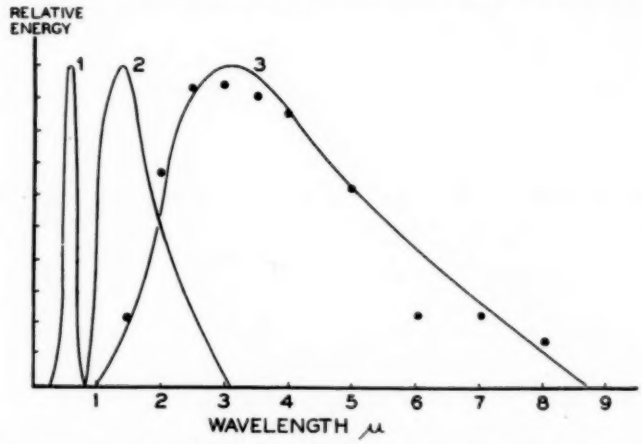

Fig. 1. Abscissas, wave-lenghts in μ; ordinates, relative energies in arbitrary units. Curve 1, tungsten lamp through bluish green heat absorbing glass; curve 2, tungsten lamp through black heat transmitting glass; curve 3, dots, Nichrome heating coil at 940°K, smooth curve, calculated black-body curve at 940°K.

a shunting resistance which could be varied to keep the deflections on the scale. For observing the intensities of wave-lengths in the visible spectrum a spectrograph was used. The transmitter and receiver were carefully focused at each other and the deflections for the 3, 1.4 and 0.6μ wave-length bands were observed on clear days, on days of fog and on clear days again.

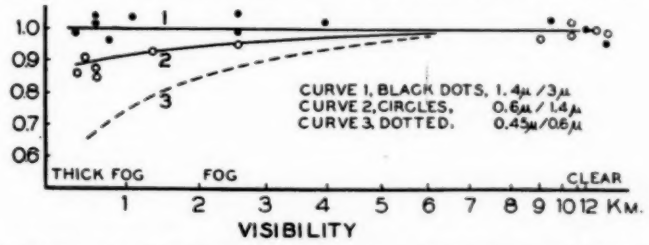

Fig. 2. Abscissas, the visibility defined as the maximum distance in km at which a dark object could be seen in the daytime; ordinates, the ratios of the intensity of one wave-length to another after transmission through 0.4 km of the atmosphere.

The deflections on clear days were reproducible within 10 percent for weeks at a time, and the ratios of the intensities 1.4μ/3μ, 0.6μ/1.4μ were reproducible within $\pm$3 percent. Thus the change in the ratios with fog could be observed quite accurately. The ratios for atmospheric conditions during daylight of the past few months varying from clear to dense fog are given in curves 1 and 2, Fig. 2. It is seen that the ratio of the intensities 1.4μ/3μ, shown by the dots and curve 1, remained constant when the atmosphere

changed from clear to thick fog. The ratio $0.6\mu/1.4\mu$, shown by the circles and curve 2, decreased slightly with decreasing visibility. During several different periods of fog the ratios were the same, within experimental error, for the same conditions of visibility. This experimental result was hardly expected, for there was no reason *a priori* to suppose that all fogs were alike; they did seem to be alike as far as the foregoing ratios were concerned. However, as described later, the intensity ratios for wave-lengths in the visible spectrum differed a little for the various fogs. The fractions of the transmitted energy in the 3, 1.4 and 0.6μ bands arriving at the receiver through a fairly dense fog are shown by the three circles of Fig. 3. The scale of the abscissas below 1μ is spread out.

The intensities of the wave-lengths in the visible spectrum were determined by photographing with a spectrograph the spectrum of the unscreened tungsten lamp search-light. By means of a 90° quartz prism, which could

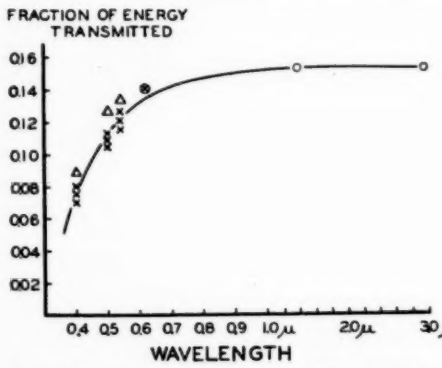

Fig. 3. Abscissas, wave-lengths in μ; ordinates, the fraction of the energy of a given wave-length transmitted through 0.4 km of the foggy atmosphere when the fog was so thick that in the daylight dark colored objects at 0.6 km could barely be seen. Crosses, triangles and circles are observed points, the smooth curve is a theoretical curve.

be swung into position in front of the slit, comparison spectra were photographed of a tungsten lamp 1 meter away through wire gauze screens. The transmission percentages of the screens were found to be independent of the wave-length of the light in the spectrum region under investigation and were 100 (i.e. no screen), 58, 32 and 15 percent. The procedure was to photograph on the same plate with the same time of exposure six spectra, namely, the spectrum of the search-light plus daylight, the spectrum of daylight alone, and spectra of the comparison lamp through the four screens. The intensity of the comparison lamp was adjusted so that its strongest spectrum was stronger and its weakest weaker than the spectrum of the search light. Curves with the recording densitometer were taken of these spectra, an example is shown in Fig. 4. Curves 1, 2, 3, 4, 5 and 6 are, respectively, from the spectrum of the search light plus the daylight, the spectrum of daylight alone, and the spectra of the comparison lamp through the 15, 32, 58 and 100 percent screens. In curve 2 it is interesting to note the *G*, *H* and *K* absorption lines at 4308, 3968 and 3934A, respectively, of the solar spectrum. The large maxima and minima in the tungsten lamp curves at the longer wave-lengths were due to the wave-length sensitivity

characteristics of the panchromatic plate; the spectral energy curve of the tungsten lamp is of course smooth in this region. In justice to the densitometer it should be pointed out that the curves of Fig. 4 were purposely made broad for reproduction, the curves made for measurement were very narrow and sharply defined.

Curves similar to those of Fig. 4 were made from spectra taken on clear days, and, omitting obvious and tedious details, the relative intensities of the various wave-lengths of the spectrum through fog, corrected for daylight, were derived from measurements of the heights of all the curves. The results for four different days of fog are given by the crosses and triangles of Fig. 3; these points were all relative to the cross at 0.6μ, the absolute value at 0.6μ being given by the galvanometer deflection with the 0.6μ transmitter observed at the same time that the spectra were photographed.

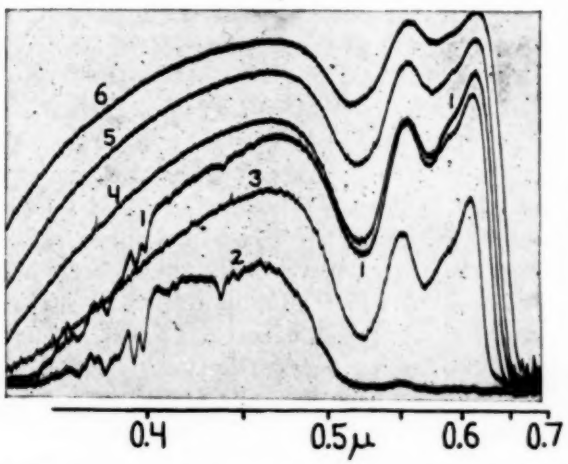

Fig. 4. Densitometer curves of spectra, Curve 1, tungsten search light (plus daylight) through 0.4 km of fog, visibility 0.6 km; curve 2, daylight spectrum; curves 3, 4, 5 and 6, the comparison lamp through 15, 32, 58 and 100 percent screens, respectively.

The triangles are a little higher than the crosses. It is thought that this represented a real difference between the fogs on the respective days because of the consistency of the measurements throughout the investigation. The variation of the ratio $0.45\mu/0.6\mu$ with the visibility is given in the dotted curve 3 of Fig. 2.

During days of clear weather and good visibility the intensity ratios for all the wave-lengths investigated did not vary appreciably with changes in the water vapor content and the temperature of the atmosphere. The data on the absorption coefficients of water vapor for wave-lengths from 0.5 to 5μ, which surprisingly enough are uncertain and incomplete,[1] indicate that the ratio of the intensities $1.4\mu/3\mu$ should have increased with the increase of water vapor content of the atmosphere. That this was not observed may have been due to the rather wide spectral regions, embraced in the transmitted bands, see Fig. 1, and to the relative narrowness of the water vapor

[1] Smithsonian Physical Tables, page 308 (1923); also see references in Lecompte, "Le Spectre Infrarouge," page 347 (1928).

bands. The question deserves a further investigation which will require a complete determination of the light absorption coefficients of water vapor from 0.4 to 5μ.

Discussions of the passage of light through a medium containing particles are usually based on Rayleigh's λ^{-4} scattering formula, where λ is the wave-length of the light. For example, King[2] has pointed out that the intensity of light passing through fog or smoke might be represented by the equation

$$I = I_0 e^{-(a+b/\lambda^{-4})x}, \qquad (1)$$

where I_o is the original intensity of the light, I the intensity after passage through a distance x in the medium, and a and b are constants. The formula neglects scattering back into the beam, probably a negligible effect in the present experiments. The a term represents an absorption or a blocking out of the energy which is independent of the wave-length. The b/λ^{-4} term was derived for scattering by particles small compared to the wave-length. Although fog probably contains many particles which are large compared with λ as well as small particles, we may never-the-less suppose that (1) represents the passage of light through fog, on the idea that the edge of a large particle is in effect a small particle as far as diffraction is concerned. The curve of Fig. 3 is plotted from Eq. (1) and was made to pass through the points at $\lambda 0.4$ and 3.0μ; a and b were 4.70 and 0.0459, respectively, for λ in μ and x in km. Although the theoretical curve fits the observations fairly well, we can hardly regard the theory as complete, for many equations with two arbitrary constants will fit equally well.

The present measurements indicate that a red light is practically no better than a blue light for fog penetration purposes. For example, from the data of Fig. 3 the distances through a fairly thick fog necessary to reduce the light to 10^{-3} of its original value were 1.40 and 1.20 km for red light $\lambda 0.65\mu$ and for blue light $\lambda 0.45\mu$, respectively, and the distances to reduce the light to 10^{-2} were 925 and 800 meters, respectively. It should be clearly understood, however, that the present measurements, which were concerned only with light intensity, do not in themselves yield a complete answer to the question whether a red light is better than a blue light in a fog. A complete answer about the visibility or recognizability of a particular light should probably consider in addition to light intensity such matters as the visibility curve of the eye, the contrast with the background, etc. In conclusion, it should be emphasized very strongly that the measurements of this paper on thick fogs over short distances can not be safely extrapolated to give information about mists, or haze due to moisture, smoke, dust, etc., over long distances. The facts that the sun is sometimes red at sunset, that distant lights are sometimes reddened, and that photography with light of the longer wave-lengths often gives pictures free from the veiling effects of haze[3] indicate that in haze the selective absorption, probably due to Rayleigh scattering, in the blue is often more pronounced than in the case of fog.

[2] King, Proc. Roy. Soc. **A88,** 83 (1913).

[3] Eastman Kodak Company, Monograph No. 4, "Aerial Haze and its Effect on Photography from the Air," page 15 (1923).

A PROBLEM IN BROWNIAN MOTION

By G. E. Uhlenbeck and S. Goudsmit
Department of Physics, University of Michigan

(Received April 26, 1929)

Abstract

Gerlach investigated the rotatorial Brownian motion of a small mirror suspended on a fine wire. It follows from the theorem of equipartition that the average square deviation of the mirror will depend on the temperature alone of the surrounding gas. Gerlach verified this for a large range of pressures (1 to 10^{-6} atm). The analogy which we found that exists between this problem and the well-known treatment of the shot effect by Schottky enables us to give a more detailed theory of this phenomenon. If the displacement, registered during a time, long compared with the characteristic period of the mirror, is developed into a Fourier series, we find the square of the amplitude of each Fourier component to be a function of the pressure and molecular weight of the surrounding gas as well as of its temperature, (formula 18). The sum of the squares, however, is a function of the temperature alone (proved in section 4). This explains why the curves registered by Gerlach at different pressures, though all giving the same mean square deviation, are quite different in appearance. To get the fluctuating torque on the mirror, the expression:

$$\overline{\delta_p^2} = \frac{16}{\pi} \cdot \frac{1}{n} \cdot \frac{1}{\bar{c}\,\Delta t \Delta o}$$

is obtained for the fluctuation in time of the pressure of a gas on the wall (section 5). In this n represents the number of molecules per cc, $\bar{c}$ is the mean velocity and Δo is the surface of the wall.

I. Introduction

INTERESTING experiments on Brownian motion around a position of equilibrium have been performed by Zeeman and Houdyk[1] in Amsterdam and by Gerlach[2] in Tübingen. The former registered the motion of the loose end of a suspended wire, the latter photographed by means of reflected light the rotational Brownian movement of a little mirror fixed on a very fine wire. The first experiment is theoretically more complicated, because one has to consider the many natural frequencies of the observed body. In the experiment of Gerlach on the other hand the observed system has only *one* characteristic frequency. We will restrict ourselves therefore in the following treatment to the latter case.

In both cases one can immediately predict by means of the equipartition theorem what the average square of the deflection will be. This will depend on the properties of the observed system and on *the temperature only* of the surrounding gas, *not* for instance on its pressure or molecular weight. The experiments however give *more* than merely the average square deviation; the registered curves show to some extent at least the time-dependence of

[1] P. Zeeman and A. Houdyk, Proc. Acad. Amsterdam, **28,** 52 (1925).
[2] W. Gerlach, Naturwiss. **15,** 15 (1927).

the irregular Brownian motion. As Professor Gerlach kindly communicated to us, the general appearance of these curves is quite different at different pressures of the surrounding gas, though the average square deviation remains the same for any given temperature. The problem is therefore to give a more detailed theory of these curves.

It has occurred to us that this problem may be treated in a manner quite analogous to the method employed by Schottky,[3] to describe the well-known shot-effect. In the experiments of Hull and Williams,[4] the fluctuating voltage in the shot-circuit is coupled inductively with the amplification-circuit, which possesses only one characteristic frequency. In the experiments of Gerlach the fluctuating moment of momentum around the mirror-axis of the gas-molecules, is coupled, by means of collisions, with the "amplifying" mirror, which has also only one characteristic frequency.

The analogy is complete only when *the surrounding gas is much rarefied*, because only then are the moments of momentum given by the gas-molecules to the mirror in successive time-elements independent of each other.[5]

By applying the method of Schottky, we will show in Sections II and III that for this case the amplitudes of the Fourier components of the motion depend on the pressure and the molecular weight of the surrounding gas. This will explain the different forms of the observed curves under various circumstances.

II. The Fourier-Analysis of the Brownian Motion

The equation of motion of the mirror is given by:

$$I\ddot{\phi}+f\dot{\phi}+D\phi=M(t), \tag{1}$$

where: I is the moment of inertia around the mirror-axis; ϕ is the angle of deflection; f the friction-coefficient; D the directional force; and $M(t)$ the fluctuating torque, caused by the collisions of the gas molecules. When we introduce the frequency in 2π sec:

$$\omega=(D/I)^{1/2} \tag{2}$$

and the angular acceleration:

$$T(t)=M(t)/I \tag{3}$$

and put:

$$r=f/I \tag{4}$$

Eq. (1) becomes:

$$\ddot{\phi}+r\dot{\phi}+\omega^2\phi=T(t). \tag{5}$$

For our further purposes it is essential to give now a more detailed discussion of the meaning of $M(t)$ or $T(t)$.

[3] W. Schottky, Ann. der Phys. **57**, 541 (1918); **68**, 157 (1922). Comp. also: J. Tinbergen, Physica, **5**, 361 (1925).

[4] A. W. Hull and N. H. Williams, Phys. Rev. **25**, 147 (1925). Comp. also N. H. Williams and H. B. Vincent, Phys. Rev. **28**, 1250 (1926).

[5] For higher pressures, the problem becomes analogous to the problem of the shot effect for high current densities. Because of the space charge the numbers of electrons hitting the anode in successive time elements are then not more independent of each other, and the fluctuations decrease. Comp. N. H. Williams and H. B. Vincent, ref.[4] p. 1262 and N. H. Williams and W. S. Huxford, Phys. Rev. **33**, 773 (1929).

The actual microscopic $M^*(t)$ consists of a large number of sharp peaks, each corresponding to the impulse moment transferred to the mirror by the collision of one (or a few) molecules. We introduce now a "physically infinitely small" time-element Δt,[6] very small compared with the characteristic period $2\pi/\omega$ of the mirror but within which many collisions occur.[7] Our function $M(t)$ consists of the averages of all $M^*(t)$ values included in each time-element Δt. The actual value of $M(t_i)$ for the time-element Δt_i is of course unknown *a priori*, but we can tell some of its properties:

(*a*) $M(t_i)$ will have equal chance of being positive or negative, so that the average over all the time-elements is zero.

(*b*) In our case, when the surrounding gas is rarefied, the $M(t_i)$ in the time-element Δt_i will be independent of the value $M(t_j)$ in the time-element Δt_j.

(*c*) In Section V we will show that the mean of $M^2(t_i)$ over all the time-elements is given by:

$$\overline{M^2(t_i)} = 4m\bar{c}pI/\rho\Delta t \tag{6}$$

where: m is the mass of the gas molecules; $\bar{c}$ their mean velocity; p the pressure of the surrounding gas, and ρ the mass of the mirror per square cm.

Let τ be the time of observation, which must be long compared with the period of the mirror, so that:

$$\Delta t \ll 2\pi/\omega \ll \tau. \tag{7}$$

Develop $T(t)$ within the interval $(0,\tau)$ in a Fourier series:

$$T(t) = \sum_{k=0}^{\infty}(A_k \cos \omega_k t + B_k \sin \omega_k t) \tag{8}$$

where:

$$\left.\begin{aligned} \omega_k &= 2\pi k/\tau \\ A_k &= \frac{2}{\tau}\int_0^{\tau} T(t)\cos\omega_k t \cdot dt \\ B_k &= \frac{2}{\tau}\int_0^{\tau} T(t)\sin\omega_k t \cdot dt \end{aligned}\right\} \tag{9}$$

We can now replace these integrals by the following sums:

$$\left.\begin{aligned} A_k &= \frac{2}{\tau}\sum_1^s T(t_i)\cos\omega_k t_i \cdot \Delta t_i \\ B_k &= \frac{2}{\tau}\sum_1^s T(t_i)\sin\omega_k t_i \cdot \Delta t_i \end{aligned}\right\} \tag{10}$$

where Δt_i are the successive, equal time-elements, and $T(t_i)$, $\cos \omega_k t_i$, $\sin \omega_k t_i$ are evaluated at a time t_i included within the i^{th} element Δt_i. Z

[6] We suppose them all equal.

[7] The introduction of such an "physically infinitely small" time element is characteristic in the kinetic theory of gases. Comp. e.g., P. and T. Ehrenfest, Enc. der Math. Wiss. Vol. IV, Art. 32, p. 39.

is the total number of time-elements. The motion of the mirror is then expressed by:

$$\phi(t)=\sum_k \phi_k(t)=\sum_k \frac{1}{(\omega^2-\omega_k^2)^2+r^2\omega_k^2}\left[\left\{A_k(\omega^2-\omega_k^2)-B_k r\omega_k\right\}\cos\omega_k t + \left\{A_k r\omega_k+B_k(\omega^2-\omega_k^2)\right\}\sin\omega_k t\right] \tag{11}$$

which is the solution of (5) under the conditions $\phi=\dot{\phi}=0$ for $t=0$. These conditions mean that we start our observations only when all external disturbances have been damped out, and the remaining motion is due only to collisions with the gas molecules, or in other words, we observe the Brownian motion around the position of equilibrium and not around an already existing vibration.

From this, we find for the time-average of ϕ_k^2:

$$\overline{\phi_k^2}=\frac{1}{2}\,\frac{A_k^2+B_k^2}{(\omega^2-\omega_k^2)^2+r^2\omega_k^2}\,. \tag{12}$$

In the case of very low pressure it is now possible to predict from the three properties (*a*), (*b*) and (*c*) of $M(t)$ (or $T(t)$) the value of A_k^2 and B_k^2. From (10) we have

$$A_k^2=\frac{4}{\tau^2}\sum_{i=1}^{Z}\sum_{j=1}^{Z}T(t_i)T(t_j)\cos\omega_k t_i\cos\omega_k t_j\cdot\Delta t_i\Delta t_j. \tag{13}$$

Consider first in this double sum the terms with $i\neq j$. As a consequence of property (*b*), in the case of low pressure $T(t_i)$ and $T(t_j)$ are completely independent; hence these terms will have equal chances of being positive or negative and for large Z their sum will vanish. Consider next the terms with $i=j$, which are all positive. Due to our choice of Δt_i, for all frequencies ω_k of the order of magnitude of ω (and only those give according to (12) an appreciable $\overline{\phi_k^2}$,) $2\pi/\omega_k$ will be very large with respect to Δt_i, so that $\cos^2\omega_k t$ changes very little over many time-elements Δt_i. We may therefore replace $T^2(t_i)$ by its average value and obtain:

$$A_k^2=\frac{4}{\tau^2}\overline{T^2(t)}\sum_{i=1}^{Z}\cos^2\omega_k t_i(\Delta t_i)^2. \tag{14}$$

Finally, replacing the sum once more by an integral, we have:

$$A_k^2=2/\tau\;\overline{T^2(t)}\cdot\Delta t \tag{15}$$

Obviously the value of B_k^2 is the same.

III. Discussion of the Final Formula

Formula (6), which will be developed in §5, together with equation (3) gives:

$$\overline{T^2(t)}=4m\bar{c}p/I\rho\Delta t. \tag{16}$$

In §6 we will prove, that for the case of low pressure, the friction-coefficient is given by:

$$f=2m\bar{c}p\rho I/kT. \tag{17}$$

Substituting (15), (16), (17) in (12), we get *the final formula:*

$$\overline{\phi_k{}^2}=\frac{\pi^{1/2}m^{1/2}(8kT)^{3/2}\cdot p}{\rho I\cdot\tau}\cdot\frac{1}{\pi kT(\omega^2-\omega_k{}^2)^2+32p^2\rho^2\omega_k{}^2} \tag{18}$$

in which the well-known relation is used that:

$$\bar{c}=(8kT/\pi m)^{1/2}.$$

From the analysis in Section II it is clear that this formula may be interpreted in the *two* following ways:

1. If we resolve into Fourier series *a great number of curves*, each observed over *a relatively short time* τ (which however must still fulfill the fundamental inequality (7)), the mean square of the amplitudes of the k^{th} components will be given by (18).

2. If we analyse *one curve*, observed over *a very long time* τ, then the square of the amplitudes of the k^{th} component will also be given by (18).

The formula (18) shows the noteworthy result, that $\overline{\phi_k{}^2}$ depends not only on the temperature, but also explicitly on *the pressure* and *the molecular weight* of the surrounding gas. As a test we must of course show, as we will do in §4, that *by summing over all values of* k, we obtain for the mean potential energy $\frac{1}{2}D\overline{\phi^2}$ the equipartition value $\frac{1}{2}kT$ which is *independent* of the pressure and the molecular weight of the surrounding gas.

The dependence on the pressure is rather complicated. For frequencies ω_k very near to ω, the $\overline{\phi_k{}^2}$ becomes inversely proportional to p, and for ω_k very large compared with ω, the $\overline{\phi_k{}^2}$ becomes almost directly proportional to p. These latter terms of course contribute very little to the total motion, the denominator being so large. When we plot therefore $\overline{\phi_k{}^2}$ against k, the resulting curve has a maximum in the neighborhood of ω, which rapidly becomes very sharp as the pressure decreases. The motion of the mirror than becomes more and more "monochromatic."

Appendix

IV. Proof of the Equipartition Theorem.

The average potential energy of the vibrating mirror is equal to:

$$\tfrac{1}{2}D\overline{\phi^2}=\tfrac{1}{2}D\sum_{k=0}^{\infty}\overline{\phi_k{}^2} \tag{19}$$

because the different Fourier components are independent of each other. Though we restricted ourselves to values of ω_k small with respect to $2\pi/\Delta t$, it is permissible to extend the summation to infinity, because the components with ω_k large compared to ω contribute very little to the sum.

Equation (15) shows, that $A_k{}^2$ and $B_k{}^2$ are independent of k; hence from (12) and (15):

$$\overline{\phi^2}=\sum_{k=0}^{\infty}\overline{\phi_k{}^2}=\frac{2}{\tau}\overline{I^2(t)}\cdot\Delta t\sum_{k=0}^{\infty}\frac{1}{(\omega^2-\omega_k{}^2)^2+r^2\omega_k{}^2}\cdot \tag{20}$$

The last sum we now replace by an integral, substituting:

$$x_k=\omega_k/\omega=2\pi k/\tau\omega$$

which gives:

$$\sum_{k=0}^{\infty}\frac{1}{(\omega^2-\omega_k{}^2)r^2+{}^2\omega_k{}^2}=\frac{\tau}{2\pi\omega^3}\int_0^{\infty}\frac{dx}{(1-x^2)^2+(r^2/\omega^2)x^2}$$

with very good approximation. The value of the integral is $\pi\omega/2r$,[8] so that we obtain:

$$\overline{\phi^2}=\overline{T^2(t)}\cdot\Delta t/2\omega^2 r. \tag{21}$$

Introducing the relations (16) and (17), and substituting from (2) and (4) the values of ω^2 and r, we obtain immediately:

$$\tfrac{1}{2}D\overline{\phi^2}=\tfrac{1}{2}kT. \tag{22}$$

V. Proof of the Fluctuation Formula (6) or (16).

This relation follows from a consideration of *the fluctuations in time* of the pressure exerted upon a wall by a rarefied gas. Using Maxwell's distribution law one easily derives an expression for the probability that a molecule of a gas within a volume V at the temperature T gives to a portion Δo of the wall a momentum normal to the wall lying between G and $G+\Delta G$ during the time Δt. It is:[9]

$$W\Delta t\Delta o\Delta G=\frac{\pi}{2}\cdot\frac{1}{(2\pi mkT)^{3/2}}\cdot\frac{kT}{V}\cdot Ge^{-G^2/8mkT}\Delta t\Delta o\Delta G. \tag{23}$$

Let n_{ij} be the number of molecules, which in the time-element Δt_i give a momentum lying between G_j and $G_j+\Delta G_j$ to the portion Δo of the wall. Then the total momentum given to Δo during Δt_i becomes:

$$G(t_i)=\sum_{j=0}^{\infty}G_jn_{ij}.$$

Using the bar to denote the average over all time-elements, we find easily:

$$\overline{G^2(t_i)}-\overline{G(t_i)}^2=\overline{(\Sigma_jG_jn_{ij})^2}-\overline{(\Sigma_jG_jn_{ij})}^2=\Sigma_jG_j^2(\overline{n_{ij}^2}-\overline{(n_{ij})}^2) \tag{24}$$

because the cross-terms cancel, and the average over the time-elements Δt_i extends only over the n_{ij}. In general the fluctuation formula holds:

$$\overline{n_{ij}^2}-(\overline{n_{ij}})^2=\overline{n}_{ij} \tag{25}$$

and $\overline{n_{ij}}$ follows immediately from (23), after multiplying by the total number of molecules N. Substituting then (25) in (24), and replacing the sum by an integral, we obtain:

$$\overline{G^2(t_i)}-\overline{G(t_i)}^2=\frac{\pi}{2}\cdot\frac{p}{(2\pi mkT)^{3/2}}\Delta o\Delta t\cdot\int_0^{\infty}G^3\exp[-G^2/8mkT]dG=2m\bar{c}p\Delta o\Delta t \tag{26}$$

for:

$$p=NkT/V.$$

[8] See W. Schottky, Ann. der Phys. **68**, 157 (1922).

[9] Integrating over G from 0 to ∞, we get for the probability that a molecule hits in the time Δt the surface element Δo:

$$w\Delta t\Delta o=\bar{c}\Delta t\Delta o/4V$$

corresponding to the well-known result for the mean number $\bar{n}$ striking 1 cm² of the wall per second:

$$\bar{n}=N\bar{c}/4V.$$

In the same way we find for the mean momentum given to the wall taken over all the molecules striking it:

$$\overline{G}=(2\pi mkT)^{1/2}$$

and for the mean square:

$$\overline{G^2}=8mkT.$$

This, divided by Δt^2, expresses the fluctuation in time of the pressure on the portion Δo of the wall.[10] From this it follows obviously that for a disc of surface o inside the gas, the mean of the square of *the force* $K(t_i)$ taken over all the time-elements Δt_i is given by:

$$\overline{K^2(t_i)} = 4m\bar{c}po/\Delta t \tag{27}$$

as for such a disc $\overline{K(t_i)} = 0$, and the fluctuations on the right and left side are independent of each other.

For a case like the experiment of Gerlach we must consider the moment of momentum around the mirror axis instead of the momentum. The analogous formula for *the torque* is then:

$$\overline{M^2(t_i)} = \frac{4m\bar{c}p}{\Delta t}\iint x^2 do = \frac{4m\bar{c}pI}{\rho\Delta t}$$

where x denotes the distance from the axis. This is equation (6).

VI. Proof of Formula (17) for the Friction Coefficient.[11]

Consider a portion Δo of the mirror, which moves, say to the right in the direction of the x-axis with the velocity u. The number of molecules per second, which strike this from the left, and which lie within a certain velocity-range $d\xi d\eta d\zeta$ is:

$$dN_1 = \left(\frac{m}{2\pi kT}\right)^{3/2}\frac{N}{V}(\xi - u)e^{-mc^2/2kT}\Delta o d\xi d\eta d\zeta \tag{28}$$

where we have used Maxwell's distribution law, because *in our case of very low pressure*, the mean free path is large with respect to the dimensions of the mirror, so that the motion of the mirror *does not disturb the velocity distribution* of the molecules. If x is the distance from Δo to the axis of the mirror, then the moment of momentum imparted per second by these molecules is:

$$dM_1 = \left(\frac{m}{2\pi kT}\right)^{3/2}\cdot\frac{2Nm}{V}\cdot(\xi - u)^2\cdot x\cdot e^{-mc^2/2kT}\Delta o d\xi d\eta d\zeta. \tag{29}$$

Neglecting the term with u^2 and integrating over η and ζ from $-\infty$ to $+\infty$, and over ξ from 0 to $+\infty$, we get:

$$M_1 = px\Delta o - m\bar{c}Nux\Delta oV^{-1}. \tag{30}$$

In the same way, we find for the moment of momentum given to Δo per second by molecules striking from the right:

$$M_2 = -px\Delta o - m\bar{c}Nux\Delta oV^{-1} \tag{31}$$

so that the total moment of momentum given to Δo per second is:

$$M_1 + M_2 = -2m\bar{c}pux\Delta o/kT. \tag{32}$$

Now $u = x\dot{\phi}$, so that we find for the friction coefficient:

$$f = \frac{2m\bar{c}p}{kT}\iint x^2 do = \frac{2m\bar{c}pI}{\rho kT}$$

which is formula (17).

[10] This can be written in the form:

$$\frac{\overline{p^2} - (\bar{p})^2}{(\bar{p})^2} = \overline{\delta_p^2} = \frac{16}{\pi}\cdot\frac{1}{n}\cdot\frac{1}{\bar{c}\Delta t\Delta o}$$

when n is the number of molecules per cc. It has then the same form as the expression for the fluctuation in pressure of a gas inside a volume element Δv (see R. Furth, Die Schwankungserscheinungen in der Physik, Vieweg, Braunschweig, 1920, p. 58):

$$\overline{\delta_p^2} = \frac{C_p}{C_v}\cdot\frac{1}{n}\cdot\frac{1}{\Delta v}$$

but it cannot be derived from it.

[11] Comp. H. A. Lorentz, Les theories statistiques en thermodynamique, Leipzig, 1916, p. 53.

THE CAPTURE OF ELECTRONS BY SWIFTLY MOVING ALPHA-PARTICLES

By Bergen Davis and A. H. Barnes
Physics Laboratories, Columbia University

(Received May 10, 1929)

Abstract

Relative velocities of an alpha particle and an electron which are favorable for the capture of the electron.—A stream of electrons from a thermionic source is superposed on a beam of α-particles from polonium. To determine the number of captures, the α-particle beam is subjected to a magnetic field and the number of deflected α-particles counted by the scintillation method. If an α-particle captures an electron before entering the magnetic field it will no longer be deflected to so great an extent. The number of scintillations for various velocities of the electrons, both greater and less than that of the α-particles, was observed. It was found that captures take place only at definite electron velocities. These velocities are related to velocities in the Bohr orbits of ionized helium as follows: $v=u-w$ and $v=w'-u$ where u is the velocity of the α-particle, w and w' are two velocities of the electron at which capture takes place and v is the velocity of an electron in any one of the circular Bohr orbits. A plot of the number of captures as a function of the voltage impressed on the electron stream gives a series of maxima on each side of the equivalent volt-velocity of the α-particles which correspond to the energy levels of ionized helium.

IT IS a matter of some surprise that an α-particle as it smashes its way through a gas and comes in contact with electrons should not attach one or more of them to itself. The approach is very close and the force is that due to a doubly charged nucleus. This matter was discussed by one of us (B. D.) in a letter to Nature (May 26, 1923). A possible explanation was given which agreed fairly well with the experimental facts. Experiments by Henderson[1] had shown that first capture took place when the velocity v_1 of the α-particle was reduced to 0.4 v_0, where v_0 is the normal velocity of the α-particle, which was given by him as 2.06×10^9 cm/sec. The second capture took place when $v_2=0.15v_0$ approximately. The point of view advanced in the letter was that the α-particle moved so swiftly that the chasing electron was not able to overtake it. If the α-particle were retarded and moved with a less velocity the electron would be able to catch up. This limiting velocity should be the parabolic velocity, or velocity of fall from infinity to the orbit or energy level in question under the action of the central forces. The computed velocity of fall to the energy level for quantum number one agreed very well with the value $v_1=0.4v_0$ as observed by Henderson.

The present experiments were undertaken to determine more precisely the way in which the chance of the capture of an electron by an α-particle varies with their relative velocity.

[1] Henderson, Proc. Roy. Soc. **A102**, 496–506 (1923).

It is difficult to retard the velocity of α-particles to a desired value. Since motions are relative the expedient was here adopted of increasing the velocity of the chasing electron by a suitable electric field. It was expected that as the velocity of the electron approached that of the α-particle it would unite with the nucleus and form an ionized helium atom. The striking results obtained in our present experiments might have been anticipated had we calculated the parabolic velocity for other energy levels as well as for the first one.

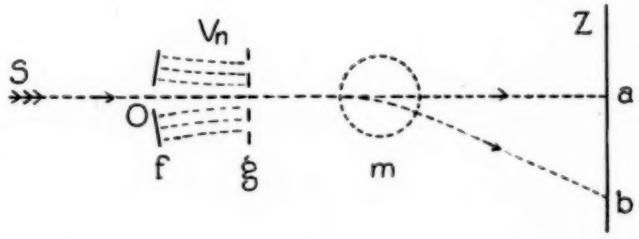

Fig. 1.

A schematic representation of the experimental arrangement is shown in Figure 1. The source of the α-particles is polonium deposited on the end of a pointed rod placed at S. The source of the electrons is a large oxide-coated filament f with a small aperature at O to permit the passage of the α-particles. The electrons are given the desired velocity by a suitable voltage V_n acting between filament and grid g. The α-particles are deflected by a magnetic

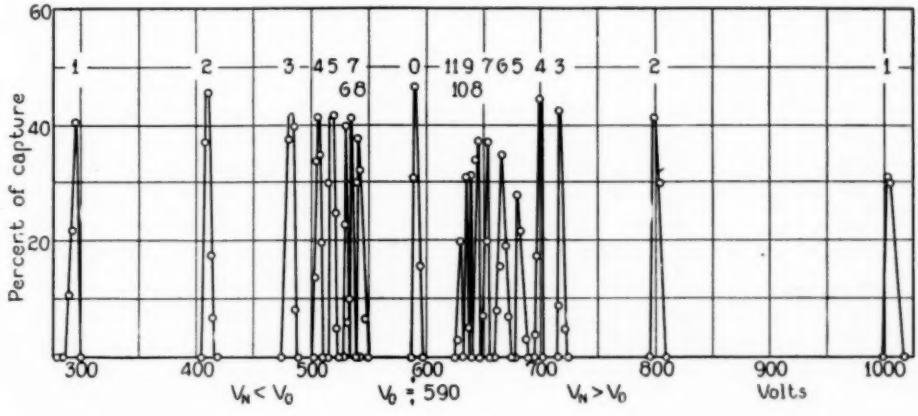

Fig. 2.

field at M and strike the zinc sulphide screen at b. The scintillations are counted in the usual manner. If an α-particle captures an electron between f and g it will not be deflected to b. The number of scintillations per minute will decrease. The experimental procedure was to count the scintillations without the electron stream, then to turn on the electron stream and progressively increase the electric field V_n by small steps. The decrease in scintillations gives at once the percent of captures.

The results of our experiment are given in Figure 2 and in the table. The ordinates are percent captures, and the abscissae are applied voltages, V_n. The voltage $V_0=590$ is the potential difference that gave the electrons a velocity equal to that of the α-particles. This velocity was 1.45×10^9 cm/sec. The velocity of the α-particles was diminished from their original one of 1.59×10^9 cm/sec by passing through a thin glass window that admitted them into the highly exhausted chamber. It was so arranged that the normal number of scintillations should be about 60 per minute. All observations were made with an electron current of 60 milliamperes excepting in the case of No. 1 on the low voltage side, namely, at $V_n=295$ volts. This curve was taken at 30 milliamperes.

The observed curves consist of two series of sharp maxima grouped on each side of the central line at V_0. They should correspond to the spectral series of the ionized helium atom.

In the figure the quantum number n is placed at the peak of the curves and V_n designates the potential at which the line of quantum number n is observed.

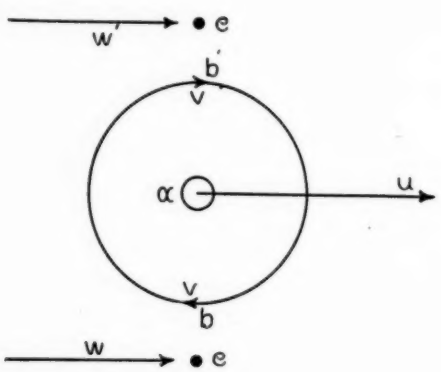

Fig. 3.

The kinematical relation of the chasing electron and the α-particle at the condition of capture is represented in Figure 3. The velocity of the α-particle is designated by u and that of the chasing electron by w. The circle about α represents a Bohr orbit and v is the velocity which an electron would have in this orbit. The condition of capture is that the electron e having velocity w or w' shall be at rest with respect to the hypothetical electron at b or at b'. This kinematical relation may be represented by $v=(u-w)$ and $v=(w'-u)$. This is the condition of capture in any orbit, and approximately represents the observed series of maxima.

The system of coordinates may be transferred to the α-particle. In this case the α-particle is at rest and the electron appears to approach from the right with a velocity v for the case for which V_n is less than V_0. It approaches from the left with velocity v for the case for which V_n is greater than V_0. In each case the velocity v is the relative velocity of α-particle and electron.

The velocities w and w′ are those acquired from the applied electric field V_n only. The velocity that the approaching electron may acquire from the doubly charged nucleus does not play a part in the process.

The energy relations may be directly written down;

$$\tfrac{1}{2}mv^2=\tfrac{1}{2}m(u-w)^2$$

and

$$\tfrac{1}{2}mv^2=\tfrac{1}{2}m(w'-u)^2.$$

By means of the relations:

$$E_ne=\tfrac{1}{2}mv^2;\ V_0e=\tfrac{1}{2}mu^2 \text{ and } V_ne=\tfrac{1}{2}mu^2$$

where E_n is the ionization potential of singly ionized helium from the energy-level characterized by the quantum number n, we derive at once the expression

$$E_n=(V_0^{1/2}-V_n^{1/2})^2$$

for the series of maxima when V_n is less than V_0 and to

$$E_n=(V_n^{1/2}-V_0^{1/2})^2$$

for the case when V_n is greater than V_0.

The series terms as calculated by the above expressions are given in Table I. The first column specifies the quantum number n of the energy level. The second and fourth columns show the applied potentials, and the

TABLE I.

n	$V_n<V_0$	E_n	$V_n>V_0$	E_n	$E_n=54.16/n^2$	Mean of E_n
1	295	50.6	1005	54.9	54.16	52.
2	410	16.7	800	15.6	13.54	16.2
3	483	5.33	720	6.45	6.01	5.67
4	505	3.29	700	4.71	3.38	4.00
5	519	2.28	681	3.27	2.16	2.77
6	531	1.56	667	2.41	1.50	1.98
7	535	1.34	653	1.59	1.10	1.46
8	538	1.19	645	1.23	.84	1.21
9	—	—	638	.96	.668	—
10	—	—	635	.88	.54	—

third and fifth columns give the energy levels as calculated from these potentials. The mean values are given in the last column. In the next to the last column are the energy levels as calculated by

$$E_n=4(13.54)/n^2 \text{ (volts)}$$

The ionized helium atom is a hydrogen-like structure with a double charge.

The agreement between the two last columns of the table is not good. Probably one should not expect a good agreement with the present arrangement of filament and grid. It is quite probable that a change in the potential V_n alters the distribution of the electrons. Also at these large electron currents (60 milliamperes), the space-charge effect must have been strongly present. This and other matters that may affect the results will be investigated.

The sharpness of the curves, together with the fact that there are no captures between the maxima indicate that the probability of recombination is very great when the relative velocity of an ion and an electron is that corresponding to an energy level. It is very small at all other velocities except for the special case when the relative velocity is zero, as indicated by the strong capture at $V_0 = 590$ volts.

A point of some interest also is the fact that there are no captures in a region about 40 volts wide on each side of the V_0 position. No decrease in the scintillations can be observed. The captures stop at about the tenth or eleventh energy level. This is far out from the nucleus from the point of view of the original Bohr model. The radius of the tenth orbit is about twenty-five times that of a normal hydrogen atom. The energy level is about 0.5 volts or less. It would appear that the nucleus is not able to retain an electron captured at a level of such small energy. Possibly also an atom may have actually a large radius when an electron is at large quantum number. If so the electron might be stripped off by collisions with the molecules of the residual gas in the vessel. The distance from the grid g to the magnetic field M was 25 centimeters.

The electron is captured only when its relative velocity due to the accelerating field V_n is that of the electron in its orbit. The velocity of fall into an energy level due to mutual attraction of the charges does not appear to be involved. If, however, the electron is subject to the central forces it does not start from rest at infinity as in the Bohr theory. It has an initial energy already equal to the energy level at which it is captured. It arrives with twice the normal energy for that level. This energy must be radiated. Is it radiated in two quanta of normal frequency or in a single quantum of twice that frequency?

This is a preliminary announcement and details and descriptions of apparatus have been purposely omitted. The investigation will be continued by one of us (A. H. B.) and a complete description given in a later paper.

A NEW METHOD OF POSITIVE RAY ANALYSIS AND ITS APPLICATION TO THE MEASUREMENT OF IONIZATION POTENTIALS IN MERCURY VAPOR

By Walker Bleakney
Physics Laboratory, University of Minnesota,

(Received June 8, 1929).

Abstract

A new method of positive ray analysis is described which lends itself particularly well to the study of the nature of the ions formed by single electron impact in gases, the efficiency of their production, and the measurement of their ionization potentials. The novel feature of the method is the use of the uniform magnetic field of a large solenoid so to concentrate a beam of electrons as to provide a linear source of positive ions. The ions are then pulled across the magnetic field and subjected to an e/m analysis by a suitably designed analyser.

Some preliminary results are given for mercury vapor in which the ionization potentials of Hg^{2+}, Hg^{3+}, and Hg^{4+} are found at 30, 71, and 143 volts respectively.

THE object of this paper is to describe a new method of positive ray analysis[1] which may be quite generally applied to the study of (1) the nature of the ions formed by single electron impact in gases, (2) the efficiencies of the production of these ions, and (3) the accurate measurement of their ionization potentials. Some preliminary results are given on the values of the first, second, third, and fourth ionization potentials in mercury vapor.

The Method

The essential feature of the new scheme is the use of a uniform magnetic field to confine a narrow beam of electrons to a straight path of considerable length and, at the same time, to effect the separation of the ions having different values of e/m. The electrons from the filament F, Fig. 1, are accelerated by the field V_1 through the system of slits S into the region between the plates A and B where the positive ions formed are drawn out by the small field V_2. The strong magnetic field H restricts the electrons to a very narrow beam. The pressure of the gas is such that only a small fraction of the electrons collide with molecules along the way. The beam is collected in the trap T where secondaries may be prevented from returning along the beam by applying a holding-on potential to the plate P. This beam of electrons provides a linear source of positive ions of practically uniform density. The ions are pulled out of the beam by applying between plates A and B a suitable cross field. This cross field will not, because of the magnetic field, appreciably affect either the velocity of the electrons in the beam or the position of the beam. A long narrow slit, parallel to the electron beam is cut in the plate B, and there emerges therefore behind B a wide ribbon of positive ions which may be subjected to an e/m analysis. The design of this analyzer will depend

[1] For a list of references on positive ray analysis see Phys. Rev. **33**, 789 (1929).

upon the particular problem in hand. In what follows there will be described a particular form of analyser which was used to determine the first four ionization potentials of the mercury atom.

The type of analyzer chosen was one which seemed to fit best the dimensions of the tube available. It is illustrated by the diagram in Fig. 2. The magnetic field, furnished by a long solenoid, is now perpendicular to the paper. The electron beam shown by the dots is seen to be in the form of a

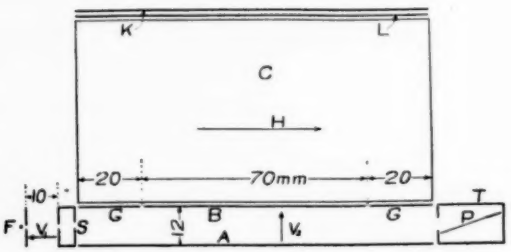

Fig. 1. Side view of apparatus.

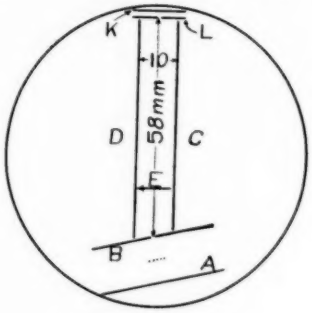

Fig. 2. End view.

ribbon. This configuration was secured by stretching a tungsten filament wire lengthwise before the first slit (Fig. 1), this slit having dimensions 1×4 mm. The slit in plate B, Fig. 2, has the dimensions 0.25×60 mm. Hence a wide sheet of ions is shot up between the condenser plates CD. Here an electric field E is applied of a strength sufficient just to balance the force of the magnetic field on a particular type of ion. This selected ion will then travel in a straight line up through the slit in the plate L where it will be collected on the plate K. Any ion having a different value of e/m will be deflected from this path. The plates A and B are set at a slight angle to the horizontal to allow for the curvature of the ion-path before it reaches the slit in the plate B.

In Fig. 2 let x be a horizontal axis and let y be the vertical. If a particle of charge e and mass m passes vertically through the slit in B with a velocity v_0 the equations of its path in the condenser will be

$$x=(mc/eH)(v_0-Ec/H)[1-\cos\ (eHt/mc)]$$
$$y=Ect/H+(mc/eH)(v_0-Ec/H)\ \sin\ (eHt/mc)$$

where E and H are the electric and magnetic fields respectively and c is the velocity of light. For a particular ion to be collected on the plate K, x must vanish identically. This can only happen when $v_0=Ec/H$. But $v_0=(2Ve/m)^{1/2}$ where V is the potential through which the ion has fallen before entering the region. Hence it follows that

$$e/m=E^2c^2/2VH^2.$$

The apparatus was constructed entirely of copper with Pyrex glass insulation. The principal dimensions are shown in the figures. All the parts were baked out at red heat before assembling in a Pyrex tube of 9.5 cm diameter where the whole apparatus was again baked out at 400°C. One end of the tube was sealed off except for two small tubes, one leading to the pumps and the other containing the filament. The other end was closed by a

large metal plate sealed in with wax. Care was always taken to keep the wax cool. This end of the tube may be sealed off if future work demands it. It has been found possible to keep the pressure of foreign gases below 10^{-6} mm of mercury as read on the McLeod gauge while the tube was in operation.

The procedure is to fix the magnetic field and the potentials V_1 and V_2, and then analyze the ions produced by varying the electric field E. The total ionization for a given length of path is measured by the current to the plate B and the analyzer gives the relative numbers of different kinds of ions formed.

The advantages of this method over other methods of positive ray analysis are: (1) The electron velocity is uniform and well defined, (2) the design lends itself to the study of ionization at very low pressures and very low current densities, i.e., to the study of the result of a single impact, (3) the different ions are examined by varying an electric field, all other conditions

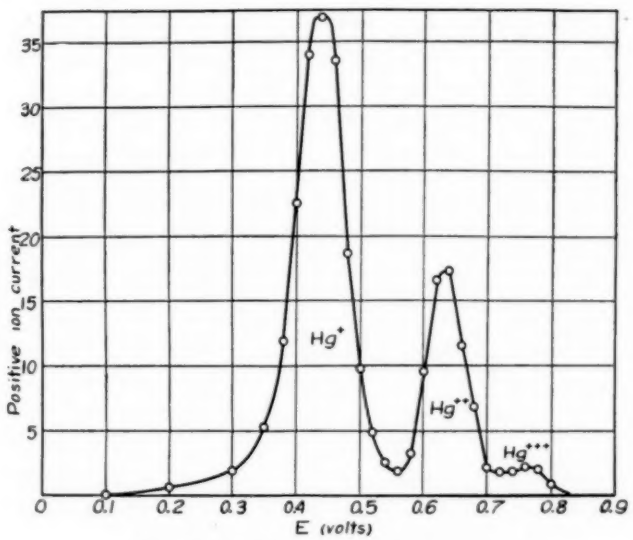

Fig. 3. A typical e/m analysis curve.

in the tube remaining constant, a feature which conduces toward great stability in operation, (4) the gas pressure throughout the tube is in equilibrium and hence may be accurately measured, (5) at the low current densities used the effect of space charge and positive ion sheaths is negligible, (6) the apparatus may be sealed up in a glass tube and thoroughly baked out. While the resolving power of the analyzer is not particularly high, yet it has proved to be excellent for the purposes for which it was designed.

Ionization Potentials in Mercury Vapor

T. J. Jones[2] in his work on the efficiency of ionization in mercury vapor pointed out that before a satisfactory analysis of his own results or of those of Compton and Van Voorhis or of Hughes and Klein could be made it would be necessary to determine for each electron speed the relative number

[2] T. J. Jones, Phys. Rev. **29**, 822 (1927).

of ions having one, two, three, etc., charges. The analyzing system just described was designed to give information on this point and preliminary results have fixed the critical potentials for the formation of Hg^{2+}, Hg^{3+}, and Hg^{4+}.

Figure 3 is a typical example of many curves obtained at different electron velocities and different pressures. In this particular case $V_1 = 100$ volts, $V_2 = 1.2$ volts, and $H = 400$ gauss. The pressure was that corresponding to saturated mercury vapor at $-8°C$. The electron current used was approximately 3×10^{-7} amperes. The current to the plate K was measured with a Dolezalek electrometer having a sensitivity of 1500 mm/volt. The curve shows a large number of singly and doubly charged ions and also a slight peak corresponding to the triply charged ion. Ions corresponding to Hg^{+}, Hg^{2+}, Hg^{3+}, Hg^{4+} and Hg^{5+} have been found below 300 volts. It is believed that all these ions are the result of a single impact since the relative numbers have not been found to depend on the current density of the electrons. The chance that a single ion will be struck a second time before escaping from the beam is of the order of one in a million.

The ionization potentials of the first four ions have been measured by extrapolating to zero the curves, Fig. 4, representing the areas under the peaks as functions of the electron velocity. The first one was assumed to be at 10.4 volts in order to fix the voltage scale. The points lying on the zero

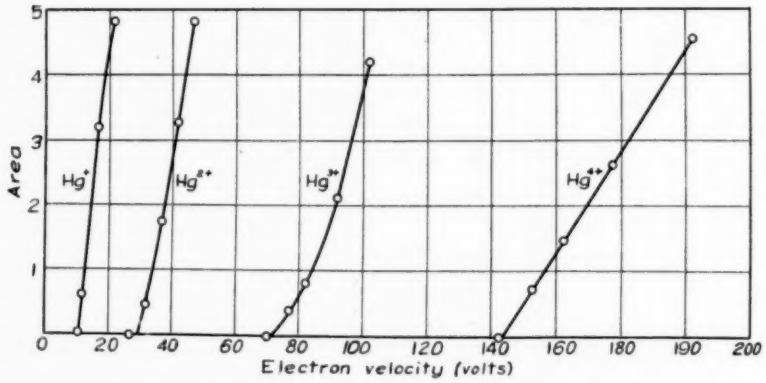

Fig. 4. Curves showing the ionization potentials of four Hg ions.

axis are not points on the curves necessarily, but merely represent runs in which no ions could be detected. The results obtained for Hg^{2+}, Hg^{3+} and Hg^{4+} are 30, 71 and 143 volts respectively. The value of Hg^{2+} is in agreement with that obtained by Smyth[3] (20 volts) for a double collision.

A quantitative study of efficiencies of ionization in mercury vapor is in progress. The same type of work will then be carried out for many other gases.

It is a pleasure to acknowledge the many helpful discussions with Professor John T. Tate during the course of this work. The author is also indebted to Mr. Wm. B. Haliday for his suggestions and aid in constructing the apparatus.

[3] H. D. Smyth, Proc. Roy. Soc. **A102**, 283 (1922).

LETTERS TO THE EDITOR

Prompt publication of brief reports of important discoveries in physics may be secured by addressing them to this department. Closing dates for this department are, for the first issue of the month, the twenty-eight of the preceding month; for the second issue, the thirteenth of the month. The Board of Editors does not hold itself responsible for the opinions expressed by the correspondents.

Wind Mixing and Diffusion in the Upper Atmosphere

Progress in theories of the high atmosphere of the earth, as described in recent papers from this laboratory, has depended in no small part upon the paper by H. B. Maris dealing with gaseous diffusion, winds, temperatures and pressures in the upper atmosphere. A summary appeared in Nature, December, 1927 and the complete paper in Terr. Mag. and Atmos. Elect., December, 1928. Until Maris worked out the effects of wind mixing and diffusion the theories were almost at a stand-still. Thus it was that the present writer guided by the results of Maris was able to show (Phys. Rev., June, 1928) that the ultra-violet light of the sun might be expected to cause the ionization of the high atmosphere inferred from the behavior of wireless waves. Earlier writers, referred to in the reference just cited, had concluded that ultra-violet light, solar α or β particles and penetrating radiation were each apparently able to produce the inoization, although to be sure the ionization which they calculated did not decrease at night in such a way as to agree with the indications from the wireless waves.

In a recent paper (Proc. Roy. Soc., February, 1929) on the diurnal variations of terrestrial magnetism, Professor S. Chapman discussed the question of diffusion and wind mixing. He followed closely but added nothing to the results of Maris, quoted the same facts about the drift of meteor trails, adopted Maris' values of the temperatures and diffusion level, etc., with no reference to the source of the ideas. A copy of Maris' paper was received by Professor Chapman in May, 1928, six months in advance of publication. To avoid possible future confusion, it has been thought advisable to point out the true origin of the ideas. Further, Professor Chapman offered certain objections to the diamagnetic theory of the diurnal variations of the earth's magnetism of Gunn (Phys. Rev., July, 1928) partly on the basis that there were not enough ions for the purpose of the theory. To reach this conclusion he quoted Pederson's estimates of ion densities. In this he was inconsistent, for Pederson ("The Propagation of Radio Waves," Copenhagen, 1927) arrived at the estimates on the assumption of no wind mixing and no diffusion in the high atmosphere, whereas with these influences ion densities great enough for the diamagnetic theory seem possible.

Finally, the diffusion of ions enters into Professor Chapman's suggestions towards a theory, as given in his paper, in an interesting way. The question will be discussed in a forthcoming paper.

E. O. HULBURT.
Naval Research Laboratory,
Washington, D.C.,
May 7, 1929.

A Phenomenon Observed in a Rotary Spark Gap

While working with a rotary spark gap the writer observed a phenomenon which, so far as he has been able to ascertain, has not been described heretofore.

The gap was formed by two fixed aluminum electrodes with a rotor composed of a moulded disk carrying twelve aluminum electrodes between them. The potential across the gap was about 10,000 volts and a large condenser was in parallel with the gap. When the discharge occurred the ends of the rotating electrodes were observed to describe a green luminous

path. The rotor was turning at a rate of 6500 r.p.m. and the green path extended from one fixed electrode to another (one-half a revolution), representing a time interval of about 0.0045 sec. Over this distance the intensity dropped by about one-half (a visual estimate) of its value at the starting point of the path.

By cleaning (scraping) the ends of the electrodes the luminescence described above disappears but returns after the discharge passes for a few minutes and finally builds up to its former intensity. At the same time the ends of the electrodes show a marked degree of corrosion. By substituting iron for the aluminum of the fixed electrodes the phenomenon disappears and does not reappear until the aluminum is replaced. Increasing the capacity across the gap increases the intensity of the green radiation. The above treatment of the electrodes seems to indicate that aluminum oxide is the emitter of this radiation. The intensity of radiation given off by the ends of the rotating electrodes is so low as to make it difficult to photograph its spectrum with high dispersion; although it can be observed with a direct vision spectroscope which shows it to extend from around 4800Å to 5300Å. Examination of the spark indicates that a green "flame" "follows" the rotating electrodes out of the white spark for a distance of about one-quarter of an inch. This "flame" is much more intense than the radiation emitted from the arc described by the rotating electrodes but in the direct vision spectroscope it appears identical in structure (a series of unresolved bands in the blue-green and green). This "flame" has been photographed with a grating spectrograph of about 4Å per millimeter dispersion. From the position of the heads of the bands and the structure of two of them they have been identified as the bands of aluminum oxide which were described by Pomeroy.[1] An effort is being made to photograph the spectral structure of this radiation at a point along the arc 90° from the spark.

The observations recorded above indicate that during the discharge aluminum oxide is formed and that this molecule is raised to some particular energy state in which it can remain, without radiating the excess energy, for at least four thousandths of a second. Work now in progress will determine the maximum life of this condition and probably the life of the aluminum oxide molecule.

R. E. BURROUGHS
Kodak Research Laboratories,
Rochester, New York.
June 7, 1929.

[1] W. C. Pomeroy, Phys. Rev. **29**, 59 (1927).

Electron Scattering in Hydrogen

The experiments on the angular scattering of electrons described in an article in the PHYSICAL REVIEW (Vol. 33, page 559, 1929) have been extended both in angular range and accuracy. The scattering gas most extensively used in this recent work has been hydrogen.

The apparatus, though new, was essentially the same as that described in the article referred to. The changes consisted in refinements, such as narrower slits, and more accurate methods of measuring the angles and potentials. The hydrogen was admitted to the scattering chamber from the center of a Wood's tube. The distance from the Wood's tube to the region where the scattering occurred was made as small as possible. The flow of hydrogen was as rapid as the conditions allowed in order to favor the presence of a large percentage of atomic hydrogen in the scattering chamber. The actual amount of atomic hydrogen present in this region when the discharge was in operation could not be determined accurately, but from the work of Wood, Bonhoeffer, Kaplan, and others probably in excess of 75 percent of the hydrogen was in the atomic condition.

A further check on the presence of atomic hydrogen in the scattering chamber was afforded by the scattering curves themselves. Several differences were apparent between the curves obtained when the discharge was on and when it was not. The magnitude of the peak due to elastic impacts dropped slightly in the presence of the discharge. The peak representing those electrons which had suffered an inelastic collision with a loss of approximately 12.5 volts shifted over till the peak occurred between 10.5 and 11 volts. This has been taken to indicate the presence of those lower energy losses due to collisions with atomic hydrogen. In addition, another peak, representing an energy loss of from 8 to 9

volts dropped very greatly in magnitude though it never completely disappeared. This critical potential has been previously observed by Jones and Whiddington (Phil. Mag. **6**, 889, 1928). The conditions under which they observed it were quite different from those existing in the present apparatus but the behavior of the peak was quite similar. They attributed it to an energy loss characteristic of the hydrogen molecule and this hypothesis seems to gain additional support from the present work. Unfortunately the most recent theoretical work on the hydrogen molecule contains no explanation for an energy loss of this value. However, it is not contrary to any experimental work as hydrogen has not previously been investigated under the conditions necessary to bring the effect into evidence.

Accurate data has been obtained for the angular distribution of scattered electrons with from one hundred to two hundred volts energy in both atomic and molecular hydrogen. The experimental points obtained for elastically scattered electrons in atomic hydrogen lie within the limits of experimental error on the theoretical curve predicted by the new quantum mechanics. This is of a different order of magnitude from the scattering which would be expected classically. The scattering in molecular hydrogen is somewhat greater than in atomic hydrogen. This is in general what would be expected from theoretical considerations. No accurate comparison with the theory is possible, however, for molecular hydrogen, as the scattering to be expected has not been calculated for this case.

The inelastic scattering in hydrogen has also yielded some very interesting results which will be discussed more fully in a forthcoming article. But one point should be mentioned here in as much as one statement made in the PHYSICAL REVIEW article previously referred to has been found to be in error. The decrease in the number of electrons scattered inelastically as one proceeds from small to large angles is more rapid than the similar decrease in the number of elastically scattered electrons. The reason for this is not clear, but the same thing has been observed by Dymond (Proc. Roy. Soc. **122**, 571, 1929) for electrons scattered in helium.

These results will be reported in full in an article to appear shortly in the PHYSICAL REVIEW.

GAYLORD P. HARNWELL

Palmer Physical Laboratory,
June 15, 1929.

The Uncertainty Principle

The uncertainty principle is one of the most characteristic and important consequences of the new quantum mechanics. This principle, as formulated by Heisenberg for two conjugate quantum-mechanical variables, states that the accuracy with which two such variables can be measured simultaneously is subject to the restriction that the product of the uncertainties in the two measurements is at least of order h (Planck's constant). Condon* has remarked that an uncertainty relation of this type can not hold in the general case where the two variables under consideration are not conjugate, and has stressed the desirability of obtaining a general formulation of the principle. It is the purpose of the present letter to give such a general formulation, and to apply it in particular to the case of angular momentum.

We define the "mean value" A_0 of an (Hermitean) operator A in a system whose state is described by the (normal) function ψ as

$$A_0 = \int \bar{\psi} A \psi d\tau$$

where the integral is extended over the entire coordinate space. The Hermitean character of A (i.e.

$$\int \bar{\phi} A \psi d\tau = \int \bar{\psi} A \phi d\tau$$

for arbitrary ϕ, ψ) insures the reality of A_0. The "uncertainty" ΔA in the value of A is then defined, in accordance with statistical usage, as the root mean square of the deviation of A from this mean, i.e.

$$(\Delta A)^2 = \int \bar{\psi} (A - A_0)^2 \psi d\tau.$$

The uncertainty principle for [illegible] variables A, B, whose commutator $AB - [illegible] 2\pi i$, is expressed by

$$\Delta A \cdot \Delta B \geqq h \left| C_0 \right| / 4\pi$$

i.e. the product of the uncertainties in A, B is not less than half the absolute value of the mean of their commutator.

* E. U. Condon "Remarks on Uncertainty Principles" Science LXIX, p. 573 (May 31, 1929), and in conversations with the writer on this topic.

We here confine ourselves to sketching the proof of this principle for a one-particle system and for quantum mechanical variables $A(q, p)$, $B(q, p)$ which are linear in the momenta (p_x, p_y, p_z).[1] (The proof for the general case in which the operators can be expanded in powers of the momenta can be made along exactly the same lines.) Writing

$$A = a + a_x p_x + a_y p_y + a_z p_z$$

where $p_x = (h/2\pi i)\partial/\partial x$, etc. and the a's are functions of position, the Hermitean character of A requires that these functions be real and that div $(a_x, a_y, a_z) = 0$. The expression for $(\Delta A)^2$ may be written, on integrating once by parts, using the fact that div $(a) = 0$ and discarding the resulting surface integral, in the form

$$(\Delta A)^2 = \int |(A - A_0)\psi|^2 d\tau.$$

We are now in a position to apply the Schwarzian inequality[2]

$$[\int (f_1\bar{f}_1 + f_2\bar{f}_2)d\tau][\int (g_1\bar{g}_1 + g_2\bar{g}_2)d\tau] \geqq |\int (f_1 g_1 + f_2 g_2)d\tau|^2$$

Taking

$$\bar{f}_1 = (A - A_0)\psi = f_2, \; g_1 = (B - B_0)\psi = -\bar{g}_2$$

and reducing the integral on the right hand side by integration by parts we find

$$\Delta A \cdot \Delta B \geqq \tfrac{1}{2}|\int \bar{\psi}(AB - BA)\psi d\tau|,$$

the required result.

[1] Cf. proof of special case $A = p$, $B = q$ in H. Weyl "Gruppentheorie und Quantenmechanik" pp. 66, 272.

[2] Weyl, l. c. p. 272.

We obviously obtain Heisenberg's result if the two variables are conjugate, for then C, and consequently C_0, are ± 1. As a further illustration of the principle, we apply it to the case of angular momentum. Here we have

$$M_x = yp_z - zp_y, \; M_x M_y - M_y M_x = -hM_z/2\pi i$$

so *the product of the uncertainties in two of the components of angular momentum is not less than $h/4\pi$ times the mean value of the third component in the state under consideration.* Consider in particular the state, treated by Condon, defined by

$$\psi = f(r)e^{im\phi}P_l^m(\cos\theta)$$

where the pole of the spherical coordinates lies on the z-axis. Then M_z, $M^2 (= M_x^2 + M_y^2 + M_z^2)$ have the definite values

$$M_z = M_{z0} = mh/2\pi, \; M^2 = l(l+1)(h/2\pi)^2$$

the mean values of M_x, M_y are zero and the uncertainties are given by

$$(\Delta M_x)^2 = (\Delta M_y)^2 = \tfrac{1}{2}[l(l+1) - m^2](h/2\pi)^2, \quad \Delta M_z = 0.$$

Now from the uncertainty principle for M_x, M_y we find

$$l(l+1) \geqq m(m+1)$$

which is in fact the case. This example shows that for $m = l$ the equality holds; the inequality is consequently the most restrictive one that can be deduced for angular momenta, for we have here a case in which the ultimate limit has (in principle) been reached.

H. P. ROBERTSON
Palmer Physical Laboratory,
Princeton, N. J.,
June 18, 1929.

The Emission of Positive Ions from Metals

During an investigation of the critical potentials in metallic vapors the writer observed that considerable positive ion currents were obtained when the metals were heated. A study of these currents by positive ray analysis has yielded the following results. Fe, Ni, Cu, Zr, Pt, Pd give alkaline ions which persist for a considerable time when the metals are heated. The persistence in iron was most [illegible]t, as a sample of electrolytic iron sh[illegible]rable potassium ion emission a[illegible]been heated for 200 hours in a vacuum of 10^{-3} mm and at a temperature of 850°C.

W, Mo, Ta, and Rh gave alkaline ions initially but these disappeared after a few minutes' heating. When the temperature of the metals was increased to the point where vaporization became appreciable, positive ion emissions were again observed. The atomic weights of these ions check within the limits of error with the atomic weights of the respective metals.

It is hoped to extend these results to other metals as well as to study the emission as a function of the temperature.

H. B. WAHLIN
University of Wisconsin,
June 24, 1929.

Excitation of the β Bands of Nitric Oxide

Henri and Wolff, in the Journal de Physique et le Radium of March 1929, have discussed in considerable detail the formation, predissociation and dissociation of molecules, by studying the spectrum of SO, as obtained by the decomposition of SO_2 in an electric discharge. Since their results are very similar to those obtained by the writer in NO_2 it seems of some interest briefly to report the results obtained. The NO_2 was obtained by passing an uncondensed discharge through mixtures of nitrogen and oxygen at 0.5 mm. A commonly observed afterglow results, possessing a continuous spectrum in the visible, and ascribed to the decomposition of NO_2. It was observed that on passing a weak discharge through this glow the β bands of nitric oxide were very strongly excited. These bands possess several very interesting properties. They correspond to a transition from the B to the X level of the molecule and the transition B_0-X_0 is very improbable because of the large difference in nuclear separation. These bands have never been reported as being intense in electric discharges and they have been obtained with considerable intensity only in active nitrogen. This present experiment is therefore the first one in which these bands have been observed with great intensity in an electric discharge.

The β bands, as observed in the present experiments, correspond to transitions only from the B_0 to the various X vibrational levels, whereas in the afterglow of active nitrogen they correspond to transitions from several B levels to the various X levels. This difference indicates that there are at least two possible methods for exciting these unusual bands and two of these methods have been discussed in brief by Kinsey and the author. They are excitation by recombination, and excitation by collisions of the second kind. They may, however, arise by a method, similar to that proposed by Henri and Wolff, for SO, namely the formation of excited NO by the decomposition of NO_2. This will be discussed in full elsewhere.

JOSEPH KAPLAN

University of California at Los Angeles,
Los Angeles, California,
June 24, 1929.

BOOK REVIEWS

Polarisation Diélectrique. J. ERRERA, Professor of Physical Chemistry in the University of Brussels. 172 pp., 35 figs. Les Presses Universitaires de France, 49 Boulevard Saint-Michel, Paris, France, 1928. Price 35 Fr.

Occasional summaries in the recent periodical literature dealing with the field of dielectric polarization have treated largely that part of the polarization which is due to the presence of electric doublets in the molecule. The polarization induced within the molecule, that is, the molecular refraction, was discussed so often a generation and more ago that it is now commonly regarded as an outworn subject and dismissed with a cursory treatment as a necessary preliminary to the discussion of the dipole polarization. Professor Errera, on the other hand, takes up the classical theory of polarization in an alternating electric field throughout the range of electromagnetic waves from X-rays to Hertzian waves and, by this comprehensive treatment, gives the reader an unusually coherent account of the field as a whole. The theory of polarization for the region of short waves is, of course, available in many hand-books and larger text-books and the relation of refraction to chemical composition was for years the theme of many papers, but it is helpful to have this material summarized together with that on dipoles.

The brief account of experimental procedure is useful in showing what methods are available and, through literature references, where the details of technique may be found. A few of these are described rather fully, and some experimental results are presented, usually as illustrations of general behavior. Of course, a reader can always find details to criticize and may cavil over matters of inclusion and exclusion. The physicist may inquire why the application of the wave mechanics to the theory of dielectrics is not discussed and the chemist may wonder at the very small space allotted to the relation between electric moment and molecular structure. The inclusion of an adequate treatment of these subjects would, however, so expand the book as possibly to interfere with the admirable logic and clarity with which its material is presented.

CHARLES P. SMYTH

Künstliche Verwandlung der Elemente. HANS PETTERSSON. Translated from the Swedish by ELISABETH KIRSCH. Pp. VIII+151. Figs. 59. Walter de Gruyter and Co. Berlin and Leipzig, 1929. Price Rm 9.

The book is a presentation of the subject of atomic disintegration for the general public. It is profusely illustrated. After an historical introduction to the subject, leading through radioactivity, it gives the history of the artificial disintegration of atoms, stressing the work in Cambridge and in Vienna and follows this by a description of the various methods of observation. Considerable space is also devoted to the description of the ways and means of preparing the radioactive material used as the source of the alpha-particles which are to bombard and disintegrate the atoms. This is followed by a discussion of the fundamental (building) units in the structure of all matter, of the nucleus of an atom, of the possibility of transmutation and of annihilation of matter and finally of the radiation from stars and of the inner structure of stars. The scope and method of presentation may perhaps be gleaned from one of the concluding sentences in the book: "Der Weg des Forschers, welchen ich dem Leser hiermit gezeigt habe, führt vom Laboratorium des Alchimisten bis nach demjenigen des Astrophysikers, Milliarden von Erdradien entfernt von dem Stäubchen im Weltraum, welches wir bewohnen."

ALOIS F. KOVARIK